

Diss. ETH No. 17083

Sorption of Organic Compounds to
Humic and Fulvic Acids:
Development of a Unifying Model Covering
Sorbate and Sorbent Variability

A dissertation submitted to the

SWISS FEDERAL INSTITUTE OF TECHNOLOGY ZURICH

For the degree of

DOCTOR OF SCIENCES

Presented by

Christian Niederer

Dipl. Umwelt-Natw. ETH

Born June 19, 1976

Citizen of Walzenhausen (AR)

Accepted on the recommendation of

Prof. Dr. René P. Schwarzenbach, examiner

Prof. Dr. Michael H. Abraham, co-examiner

PD Dr. Kai-Uwe Goss, co-examiner

Zurich 2007

FAUST. Werd ich beruhigt je mich auf ein Faulbett legen,
So sei es gleich um mich getan!
Kannst du mich schmeichelnd je belügen,
Dass ich mir selbst gefallen mag,
Kannst du mich mit Genuss betrügen –
Das sei für mich der letzte Tag!
Die Wette biet ich!

MEPHISTOPHELES. Topp!

FAUST. Und Schlag auf Schlag!
Werd ich zum Augenblicke sagen:
Verweile doch! du bist so schön!
Dann magst du mich in Fesseln schlagen,
Dann will ich gern zugrunde gehen!
(..) Die Uhr mag stehn, der Zeiger fallen,
Es sei die Zeit für mich vorbei!

Johann Wolfgang Goethe, FAUST I

Dank

Ich möchte mich herzlich bei den Betreuern meiner Arbeit, Kai Goss und René Schwarzenbach, bedanken. Durch einen kritischen Blickwinkel sowie kreativen Ideen haben sie die Arbeit wesentlich mitgeprägt und weitergebracht. Ganz herzlich danken möchte ich Kai für seine kompetente Betreuung und die Zeit, die er sich jederzeit für Diskussionen nahm. Michael Abraham möchte ich für sein Interesse an meiner Arbeit sowie für seine Bereitschaft, das Koreferat zu übernehmen, danken.

Ebenfalls herzlich bedanken möchte ich mich bei meinen Kolleginnen und Kollegen im Labor für die angenehme und freundschaftliche Arbeitsatmosphäre: Sandra Endres, Ireen Kamprad, Andrea Ciani, Hans Peter Arp, Guido Bronner und Michael Madliger. Vor allem möchte mich bei Chris Roth für ihre grosse Hilfe bei der Einarbeitung in die IGC bedanken. Weiter bedanken möchte ich mich bei allen Mitgliedern der Umweltchemie-Gruppe, die den (Labor-)Alltag spannender und abwechslungsreicher gemacht haben, insbesondere bei Anke Neumann, Akané Hartenbach, Kov Bolotin, Michael Sander, Andi Peter, Thomas Hofstetter, Luc Zwank, Dieter Diem, Werner Angst und Béatrice Schwertfeger. Für ihre grosse Hilfsbereitschaft und ihre aufstellenden Worte möchte ich mir vor allem bei Nicole Tobler bedanken. Gérard Mohler hat mit grossem Einsatz dafür gesorgt, dass das COSMOtherm System immer funktionierte. Ebenfalls bedanken möchte ich mich bei meinen ehemaligen MitarbeiterInnen an der EAWAG, im speziellen bei Sibylle Kaiser, Beate Escher, Brian Sinnet, Philippe Périsset, Zach Schreiber und Christoph Aeppli.

Von Herzen bedanken möchte ich mich bei Franziska Morganti, die mich bei Tiefs während der Arbeit immer aufgestellt und unterstützt hat; sowie bei meinen Eltern, die mir das Studium ermöglicht haben und mich jederzeit in jeder Form unterstützen.

This Ph.D. project was conducted at ETH Zurich and at the Swiss Federal Institute of Aquatic Science and Technology, EAWAG, Dübendorf and financially supported by the Swiss National Science Foundation (project-no. 200020-111753/1).

Table of Contents

Summary	v
Zusammenfassung	ix
Introduction	1
References Introduction	6
 Chapter 1: Sorption Equilibrium of a Wide Spectrum of Organic Vapors in Leonardite Humic Acid: Experimental Setup and Experimental Data	 9
Introduction	11
Materials and Methods	12
Results and Discussion	15
Evaluation of the Sorption Equilibrium	15
Reproducibility	16
Linearity of the Sorption Isotherm	16
Influence of the Support on the Observed Sorption	17
Outliers	17
Sorption Coefficients	17
Comparison with Literature Data	20
Temperature Dependence	22
Influence of the Relative Humidity	22
References Chapter 1	26
Appendix Chapter 1	31
 Chapter 2: Sorption Equilibrium of a Wide Spectrum of Organic Vapors in Leonardite Humic Acid: Modeling of Experimental Data	 55
Introduction	57
Methods	58

Results and Discussion.....	59
Single Parameter Model: Octanol/Air Approach.....	59
EPI-Suite – PcKocWIN: A Model based on MCIs.....	61
Polyparameter Model: Linear Free Energy Relationship.....	63
Temperature-Dependence of the Sorption Process.....	66
Prediction of $\Delta_{\text{abs}}H_i$ using the Sorption Coefficient $K_{i\text{HA,air}}$	67
Prediction of the Temperature Dependence.....	67
Comparison with Partition Data from the Literature.....	68
References Chapter 2.....	73
Appendix Chapter 2.....	77
 Chapter 3: Quantum Chemical Modeling of Humic Acid/Air	
Equilibrium Partitioning of Organic Vapors.....	115
Introduction.....	117
Method.....	120
COSMOtherm (COSMO-RS).....	120
Input Structures.....	121
Results and Discussion.....	124
Performance of Monomer M1.....	127
Variations between the Monomers M1-M4.....	128
Conformers.....	129
Simulation of the Influence of the Relative Humidity.....	130
Simulation of Temperature Dependence.....	131
SPARC.....	131
References Chapter 3.....	135
Appendix Chapter 3.....	139
 Chapter 4: Variations in the Sorption Properties of Nine	
Humic and Fulvic Acids from Different Origins.....	187
Introduction.....	189
Materials and Methods.....	191
Experimental.....	191
Natural Organic Matter.....	192

Results and Discussion.....	193
Exp. Partition Coefficients: Scatter and Sorption Variability.....	193
Modeling Sorption Coefficients with a pp-LFER.....	197
Influence of the Relative Humidity.....	199
Mechanistical Interpretation.....	201
Predicting the Different Sorption Capacities of Various Humic and Fulvic Acids.....	203
References Chapter 4.....	205
Appendix Chapter 4.....	209
 Conclusions and Outlook.....	 249
References Conclusions and Outlook.....	255
 Curriculum Vitae.....	 257

Summary

Sorption in natural organic matter (NOM) is a key process in determining the transport as well as the bioavailability of organic pollutants in the environment. A dataset containing more than 1000 NOM/air partition coefficients of nonionic organic chemicals measured in 10 different NOM from terrestrial and aquatic origins at different temperatures and different relative humidities is presented in this work. The conclusions that can be drawn from this extended sorption dataset provide a deeper understanding of the mechanisms involved in the sorption of organic compounds in NOM. In addition, this dataset allows the evaluation as well as the development of predictive models for NOM sorption.

Relative humidity had a rather small influence (less than a factor of three) on the experimental partition coefficients. However, these results provided interesting mechanistical insights into the sorption process in dry NOM compared to completely hydrated NOM. Polar compounds generally sorbed more strongly than nonpolar compounds due to H-bonds (electron donor/acceptor interactions) with the NOM. No glass transitions in the range of 5 to 75 °C that would be relevant in respect to the sorption properties of Leonardite humic acid were observed.

We found differences of more than one order of magnitude in the sorption coefficients of a given compound measured in NOM from different origins. The terrestrial HA exhibited substantially higher sorption coefficients compared to aquatic HA and FA. The difference between any two types of NOM is mainly reflected by a constant shift in the partition coefficients that applies to all compounds in the same way. This indicates that it is the number of available sorption sites per mass of sorbents rather than the types of intermolecular interactions between the sorbate and the sorbent that governs the major differences between the sorption properties of various types of NOM. An empirical correlation

between the aromaticity and the differences in the sorption capacities of each NOM compared to Leonardite HA was found.

While several models for the prediction of sorption coefficients of different compounds in a given NOM system have been published, no systematic approach has yet been developed for modeling of the natural variability in the sorption properties of NOM from different origins. The former models were evaluated using a subset of 200 experimental Leonardite HA/air partition coefficients. This evaluation revealed that none of the regression models based on partitioning into octanol yielded satisfactory fits for polar compounds although the octanol-based Karickhoff model showed good performance for nonpolar compounds. For PcKocWIN, a model based on molecular connectivity indices, some major shortcomings became apparent. SPARC, another increment method, predicted the experimental Leonardite HA partition coefficients with good accuracy. However, like other increment methods, SPARC suffers from the general disadvantage that its application domain is limited by its calibration dataset that is unknown to the user. A good description of the whole dataset is achieved with a polyparameter linear free energy relationship (pp-LFER) that explicitly accounts for cavity formation, nonpolar (van der Waals) and polar (electron donor/acceptor) interactions between the sorbate molecule and the sorbent phase. With this pp-LFER model, most of the Leonardite HA/air partition coefficients could be predicted within a factor of 2. The quantum chemical model COSMOtherm predicted the experimental Leonardite HA partition coefficients within a factor of 3 to 5 using a suggested 3-dimensional structure of Leonardite HA. COSMOtherm can be expected to be very robust with respect to new and complex structures because its calculations are based on a fundamental assessment of the underlying intermolecular forces; calibrations with experimental compound descriptors are not required.

The pp-LFER model evaluated with the big experimental dataset for Leonardite HA was successfully applied to all other NOM. These pp-LFER equations provide for the first time a tool that allows including the variability in the sorption properties of NOM in environmental fate

models. The pp-LFER model also successfully predicted organic-C/water partition coefficients collected from the literature when it was combined with experimental air/water partition coefficients. This expands the applicability of the results of this study because NOM/water sorption processes are of equal or even higher importance compared to NOM/air partitioning.

Zusammenfassung

Sorption in natürliches organisches Material (NOM) ist ein fundamentaler Prozess für den Transport und die Bioverfügbarkeit von organischen Schadstoffen in der Umwelt. In dieser Arbeit wird ein Sorptionsdatensatz vorgestellt, der mehr als 1000 NOM/Luft Verteilungskoeffizienten nicht-ionischer organischer Substanzen enthält, die in 10 unterschiedlichen NOM (aquatischen und terrestrischen Ursprungs) bei verschiedenen relativen Luftfeuchtigkeiten und unterschiedlichen Temperaturen gemessen wurden. Die aus diesem ausgedehnten Datensatz abgeleiteten Schlussfolgerungen tragen zu einem verbesserten mechanistischen Verständnis der Sorption organischer Substanzen in NOM bei. Zudem erlaubt dieser Sorptionsdatensatz sowohl die Evaluation als auch die Entwicklung von Voraussagemodellen für Verteilungskoeffizienten in NOM.

Die relative Luftfeuchtigkeit zeigte einen moderaten Einfluss auf die experimentellen Verteilungskoeffizienten (kleiner als einen Faktor 3). Diese Resultate geben jedoch interessante Einblicke in die Sorptionseigenschaften von trockenem NOM im Vergleich zu vollständig hydratisiertem natürlichem Material.

Aufgrund von Wasserstoffbrückenbindungen (Elektronen Donor/Akzeptor Interaktionen) mit dem NOM sorbierten die polaren Substanzen aus dem Datensatz im Allgemeinen stärker als die unpolaren Substanzen. Es wurden keine Glassübergänge zwischen 5 bis 75 °C in Leonardite HA beobachtet, welche relevant in bezug auf die Sorptionseigenschaften dieser HA sind.

Die NOM unterschiedlicher Herkunft zeigten bis zu einer Größenordnung unterschiedliche Verteilungskoeffizienten. Dabei wiesen die drei boden-extrahierten Huminsäuren deutlich höhere Verteilungskoeffizienten auf im Vergleich zu terrestrischen/aquatischen Fulvinsäuren sowie aquatischen Huminsäuren. Der Unterschied

zwischen zwei beliebigen NOM manifestiert sich vor allem in einer konstanten Verschiebung der Verteilungskoeffizienten, die für alle Substanzen in gleicher Weise gilt. Das weist darauf hin, dass die Unterschiede in den Sorptionseigenschaften, die zwischen den NOM gefunden wurden, durch die Anzahl verfügbarer Sorptionsplätze und weniger durch intermolekulare Interaktionen zwischen dem Sorbat und dem Sorbenten verursacht werden. Die Aromatizität der einzelnen NOM korrelierte mit den Unterschieden in den Sorptionskapazitäten der einzelnen NOM im Vergleich zu Leonardite HA.

Währenddem mehrere Modelle für die Voraussage von Sorptionskoeffizienten unterschiedlicher Substanzen in ein gegebenes NOM publiziert sind, fehlen systematische Ansätze, die die natürliche Variabilität in den Sorptionseigenschaften von NOM unterschiedlichen Ursprungs modellieren können. Erstere Modelle wurden hier mithilfe von 200 experimentellen Leonardite HA/Luft Verteilungskoeffizienten evaluiert. Die experimentellen Daten zeigten, dass kein Regressionsmodell basierend auf Oktanol-Verteilungskoeffizienten zuverlässige Voraussagen für polare Substanzen liefert, obwohl das oktanol-basierte Karickhoff Modell gute Resultate für unpolare Substanzen lieferte. PcKocWIN, ein Modell, das Verteilungskoeffizienten zwischen organischem Kohlenstoff und Wasser basierend auf molekularen Konnektivitätsindizes berechnet, sagt die experimentellen Daten nur ungenügend voraus. Mehrere prinzipielle Probleme im Berechnungsverfahren von PcKocWIN wurden identifiziert. SPARC, eine weitere Inkrementmethode, sagte die experimentellen Leonardite HA/Luft Verteilungskoeffizienten mit relativ hoher Genauigkeit voraus. Wie andere Inkrementmethoden weist jedoch SPARC den Nachteil auf, dass der Applikationsbereich durch den Kalibrationsdatensatz des Modells limitiert ist, welcher dem Benutzer nicht bekannt ist. Eine Polyparameter Lineare Freie Energiebeziehung (pp-LFER), welche Kavitätsbildung, unpolare (van der Waals) sowie polare (Elektron Donor/Akzeptor) Interaktionen zwischen den Substanzen und dem NOM berücksichtigt, konnte hingegen alle Verteilungskoeffizienten des Datensatzes innerhalb eines Faktors 2 voraussagen. Das

quantenchemische Modell COSMOtherm konnte mit einer hier vorgeschlagenen 3-dimensionalen Struktur von Leonardite HA als Input die experimentellen Verteilungskoeffizienten innerhalb eines Faktors 3 bis 5 voraussagen. Wir erwarten, dass COSMOtherm bei der Voraussage von komplexeren chemischen Strukturen robuste Resultate liefern wird, da die COSMOtherm Berechnungen auf fundamentalen intermolekularen Wechselwirkungen basiert und keine Kalibration mit experimentellen Substanzdeskriptoren und experimentellen Verteilungskoeffizienten nötig ist.

Das pp-LFER Model, das für Leonardite HA evaluiert wurde, konnte erfolgreich auf alle anderen NOM angewendet werden. Diese zehn pp-LFER Gleichungen erlauben zum ersten Mal, in Risikoanalysen chemischer Substanzen die Variabilität in den Sorptionseigenschaften von NOM zu berücksichtigen. Die pp-LFER sagten ebenfalls erfolgreich NOM/Wasser Verteilungskoeffizienten aus der Literatur voraus, nachdem die NOM/Luft Gleichungen mit experimentellen Wasser/Luft-Verteilungskoeffizienten umgerechnet wurden. Dadurch wird der Anwendungsbereich der Resultate dieser Studie enorm vergrössert, da Sorptionsprozesse zwischen natürlichem organischem Material und Wasser von ähnlicher oder grösserer Bedeutung sind im Vergleich zu Sorptionsprozessen zwischen NOM und Luft.

Introduction

Organic pollutants can undergo various transport and degradation processes in the environment. These processes must be understood in order to predict the transport behavior as well as the bioavailability of those pollutants in the environment. Sorption to natural organic matter (NOM) in soils, sediments, and aquatic systems controls the freely dissolved or gaseous concentration of a pollutant. This fraction is directly bioavailable and therefore relevant for toxic effects on the one hand but it is also subject to degradation and transport processes on the other hand. In general, soil organic matter is the most important sorbent phase for organic pollutants because a significant part of the global natural organic matter is contained in soils and sediments (1).

Natural organic matter (soil and sediment organic matter; dissolved organic matter in terrestrial and aquatic systems) is a very complex matrix consisting of humic acids (HA), fulvic acids (FA), and humin. The chemical structures of these materials vary depending on their phase of origin, i.e., aquatic or terrestrial origin, and environmental parameters such as vegetation or climatological parameters (e.g., temperature and precipitation). The chemical variability of these materials likely causes variability in the sorption properties of these humic and fulvic acids. Indeed, several studies reported differences in partition coefficients of up to an order of magnitude or even more for single compounds measured in humic- and fulvic acids from different origins (2-5). Despite this considerable variance that has been found for sorption to different types of NOM, it is still common practice in environmental fate modeling to use a single K_{ioc} -value (i.e., organic carbon/water partition coefficient) for a given compound in all kinds of NOM. This is because none of the studies conducted so far allow generalizable conclusions for all types of chemicals and for humic material that is considered as representative of NOM. Traditionally, research in environmental chemistry has focused on

the partitioning of nonpolar compounds such as polycyclic aromatic hydrocarbons (PAHs) or polychlorinated biphenyls (PCBs). However, compounds of actual environmental concern such as pesticides, pharmaceuticals, or plasticizers are much more polar compounds exhibiting one or several functional groups.

Therefore, for a comprehensive understanding of the variability in the sorption properties of NOM as well as the variability in the sorption of different organic compounds it is necessary to conduct an extended study involving different types of NOM as well as a broad spectrum of compounds exhibiting different functionalities. This work presents an extended dataset containing more than 1000 experimental partition coefficients measured in NOM from different origins (i.e, aquatic and terrestrial humic and fulvic acids) for 80-200 polar and nonpolar organic compounds in each material. This dataset allows investigating both the variability in the sorption of compounds from different chemical families as well as the variability of the sorption properties of NOM.

Modeling of the Compound Variability

Experimental determinations of NOM/air or NOM/water partition coefficients of organic compounds are often tedious and time-consuming. In view of a daily increasing number of new compounds, reliable predictive models for these sorption data are needed. Traditionally, sorption models like the octanol-based models have been used for the predicting of soil organic matter partition coefficients in environmental fate assessments. The experimental data are usually evaluated by a double logarithmic linear regression with the octanol/air or octanol/water partition constant of the respective compounds. In this approach, octanol serves as a model phase for NOM. However, NOM is a complex phase that is unlikely to resemble octanol in its sorption properties. It is neither possible to extrapolate results from such a regression with nonpolar compounds to more polar pollutants (e.g., many pesticides or pharmaceuticals) nor to understand the variability of the sorption properties of natural phases (6). In addition, literature data of octanol/water or octanol/air partition coefficients can vary

significantly (more than one order of magnitude), particularly for substances such as DDT or DDE as shown in (7).

Polyparameter Linear Free Energy Relationships (pp-LFER) that describe nonspecific interactions (van der Waals forces) and specific interactions (electron donor/acceptor interactions including H-bonds) between the sorbates and the sorbent phases by separate terms (6) are able to overcome the discussed shortcomings of the octanol approach. Each interaction term contains the property of the sorbate as well as the complementary property of the sorbent phase. These equations have successfully been applied to the sorption of organic vapors on/in different ambient phases (e.g., minerals, snow, aerosols) in previous work (8-12). As we will show in this study, the pp-LFER approach is also applicable to a large dataset of experimental Leonardite HA/air partition coefficients.

However, the polyparameter approach is limited in its applicability because for every sorbate of interest its van-der-Waals (vdW) and electron donor/acceptor descriptors have to be known. These descriptors are tabulated for many compounds in the literature (13, 14) but for many other compounds they have yet to be determined experimentally. Hence, the screening of large and diverse compound sets or the estimation of the sorption behavior of new compounds that have not yet been synthesized will require different approaches based on the molecular structures of the compound alone. Tools such as PckocWIN (15) or the model published by Schüürmann et al. (16), calculate K_{ioc} partition coefficients from the molecular structure of the sorbate molecules based on group contribution or incremental methods and principally fulfil these requirements. However, these methods have the disadvantage that their applicability domain is limited by the used training compound set and that they completely ignore the variability in the sorption properties of NOM.

It would therefore be very desirable to have a tool that predicts NOM partition coefficients only based on the molecular structures of the sorbates and the sorbent phases without preliminary calibration. Several studies have already been performed using molecular modeling

approaches to study sorbate/sorbent interactions (17-20). However, the approaches published so far are not able to predict quantitative NOM partition constants. In this work we are going to evaluate the performance of the commercial quantum-chemical software COSMOtherm for the prediction of Leonardite HA/air partition coefficients. COSMOtherm combines the calculation of intermolecular interactions with statistical thermodynamics and can thus provide partition coefficients of organic molecules in various partition systems if the molecular structures of the sorbate and the sorbent phases are known. For this purpose a 3-dimensional structure of Leonardite HA based on published ^{13}C -NMR and elemental analysis data has been postulated. As will be demonstrated in this study, COSMOtherm is a promising tool for the prediction of NOM partition coefficients.

Modeling the Variability in the Sorption Properties of NOM

Another important aspect besides the compound variability is the expected variability in the sorption properties of various natural organic materials. So far little attempt has been made in environmental chemistry to either systematically measure the variance in the sorption properties of NOM or to set up models for the prediction of partition coefficients in different natural organic materials. Some researchers have suggested a correlation between NOM-specific descriptors such as elemental analysis data (e.g., O/H ratio) and ^{13}C -NMR data (e.g., aromaticity) and the sorption properties of NOM. In some cases such an approach could indeed describe the experimental data (3). However, this approach does not really comply with our general concept of partitioning as a result of various intermolecular interactions between the sorbate and the sorbent.

The established models for the prediction of NOM partitioning such as the octanol approach or fragment method such as PckocWIN completely ignore the variability in the sorption properties of NOM from different origins and chemical composition. In contrast, the polyparameter approach can account for the variability in NOM. Therefore, we have also tested the performance of our pp-LFER equations on experimental

partition coefficients for diverse compound datasets measured in various humic acids and fulvic acids from different origins.

Chapter Overview

In a first step an experimental procedure had to be set up for an efficient and reproducible measurement of NOM/air partition coefficients. In Chapter 1, experimental partition coefficients of more than 200 compounds from very different compound classes in Leonardite HA are presented and compared to literature data. We have investigated whether glassy regions in Leonardite HA, if present, have an influence on the partition coefficients. In addition, the influence of the hydration state of the humic acid on its sorption properties has been studied.

In Chapter 2 we evaluate the performance of different prediction models for NOM partitioning coefficients using our diverse compound dataset for Leonardite HA gained in Chapter 1: an approach based on octanol, the fragment method P_cKocWIN, and a polyparameter linear free energy relationship. In Chapter 3, we evaluate the quantum chemical model COSMOtherm for the prediction of about 200 experimental Leonardite Humic Acid/air partition coefficients without calibration or experimental compound descriptors, but simply based on molecular structures. For this purpose, we had to postulate a 3D structure for Leonardite HA.

Chapter 4 finally investigates differences in the sorption properties of HA and FA from aquatic and terrestrial origin based on a big experimental dataset. A mechanistical interpretation of the observed differences is provided and the applicability of the pp-LFER approach evaluated for Leonardite HA in Chapter 2 is tested for all HA and FA.

Scientific and Practical Contribution of this Research

This research intends to make a significant contribution to a better mechanistic understanding of the influence of sorbate and sorbent properties on the respective sorption constant in NOM. This allows a more precise modeling of the environmental fate of organic pollutants. The ultimate goal is to develop an improved conceptual and

mechanistical understanding of the partitioning of organic pollutants in the environment.

Currently, all guidelines for the testing of chemicals (e.g., OECD guidelines) strongly rely on the $\log(K_{ioa})$ or $\log(K_{iow})$ values of a substance in order to predict its environmental fate. However, these approaches have the shortcomings discussed above. The practical contribution of this work is to overcome traditional approaches and to use new concepts like the pp-LFER approach or quantum chemical modeling that can successfully describe the partitioning of organic pollutants in the environment based on parameters that can be determined accurately with reasonable effort or only based on the molecular structures.

References

- (1) Lal, R. Soil carbon sequestration impacts on global climate change and food security *Science* **2004**, *304*, 1623-1627.
- (2) Gauthier, T. D., Seitz, W.R., Grant, C.L. Effects of structural and compositional variations of dissolved humic materials on pyrene K_{oc} values *Environ. Sci. Technol.* **1987**, *21*, 243-248.
- (3) Kopinke, F. D., Georgi, A., Mackenzie, K. Sorption of pyrene to dissolved humic substances and related model polymers. 1. Structure-property correlation *Environ. Sci. Technol.* **2001**, *35*, 2536-2542.
- (4) Grathwohl, P. Influence of organic matter from soils and sediments from various origins on the sorption of some chlorinated aliphatic hydrocarbons: Implications on K_{oc} correlations *Environ. Sci. Technol.* **1990**, *24*, 1687-1693.
- (5) Brannon, J. M., Pennington, J.C., Davis, W.M., Hayes, C. Fluoranthene KDOC in sediment pore waters *Chemosphere* **1995**, *30*, 419-428.

- (6) Goss, K.-U.; Schwarzenbach, R. P. Linear free energy relationships used to evaluate equilibrium partitioning of organic compounds *Environ. Sci. Technol.* **2001**, 35, 1-9.
- (7) Pontolillo, J., Eganhouse, R.P. "The search for reliable aqueous solubility (Sw) and octanol-water partitioning coefficient (Kow) data for hydrophobic organic compounds: DDT and DDE as a case study," U.S. Geological Survey, 2001.
- (8) Goss, K.-U., Buschmann, J., Schwarzenbach, R.P. Adsorption of organic vapors to air-dry soils: model predictions and experimental validation *Environ. Sci. Technol.* **2004**, 38, 3667-3673.
- (9) Goss, K.-U. The role of air/surface adsorption equilibrium for the environmental partitioning of organic compounds *Cri. Rev. Environ. Sci. Technol.* **2004**, 34, 339-389.
- (10) Roth, C. M., Goss, K.-U., Schwarzenbach, R.P. Adsorption of a diverse set of organic vapors on the bulk water surface *J. Coll. Interf. Sci.* **2002**, 252.
- (11) Roth, C. M., Goss, K.-U., Schwarzenbach, R.P. Sorption of diverse organic vapors to snow *Environ. Sci. Technol.* **2004**, 38, 4078-4084.
- (12) Roth, C. M., Goss, K.-U., Schwarzenbach, R.P. Sorption of a diverse set of organic vapors to diesel soot and road tunnel aerosols *Environ. Sci. Technol.* **2005**, 39.
- (13) Abraham, M. H., Chadha, H.S., Whiting, G.S., Mitchell, R.C. Hydrogen bonding. 32. An analysis of water-octanol and water-alkane partitioning and the Dlog P parameter of Seiler *J. Pharm. Sci.* **1994**, 83, 1085-1100.
- (14) Abraham, M. H., Andonian-Haftvan, J., Whiting, G.S., Leo, A., Taft, R.S. Hydrogen bonding. Part 34. The factors that influence the solubility of gases and vapors in water at 298 K, and a new method for its determination *J. Chem. Soc. Perkin Trans. 2* **1994**, 1777-1791.
- (15) US-EPA, 2004.
- (16) Schüürmann, G., Ebert, R.-U., Kühne, R. Prediction of the sorption of organic compounds into soil organic matter from molecular structure *Environ. Sci. Technol.* **2006**.

- (17) Kubicki, J. D., Trout, C.C. Molecular modeling of fulvic and humic acids: charging effects and interactions with Al^{3+} , benzene, and pyridine. In *Geochemical and hydrological reactivity of heavy metals in soils*; Kingery, W. L., Selim, H.M., Ed.; CRC Press, 2003; pp 113-143.
- (18) Kubicki, J., Apitz, S.E. Models of natural organic matter and interactions with organic contaminants *Org. Geochem.* **1999**, 30, 911-927.
- (19) Diallo, M. S., Faulon, J.L., Goddard, W.A., III., Johnson, J.H., Jr. Binding of hydrophobic organic compounds to dissolved humic substances: a predictive approach based on computer assisted structure elucidation, atomistic simulations and flory-huggins solution theory. In *Humic Substances: Structures, Models and Functions*; Ghabbour, E. A., Davies, G., Ed.; The Royal Chemical Society: Cambridge, UK, 2001; pp 221-237.
- (20) Schulten, H.-R., Thomsen, M., Calsen, L. Humic complexes of diethyl phthalate: molecular modelling of the sorption process *Chemosphere* **2001**, 45, 357-369.

Sorption Equilibrium of a Wide Spectrum
of Organic Vapors in Leonardite
Humic Acid: Experimental Setup
and Experimental Data

reproduced from
Environmental Science and Technology, 2006, 40, 5368-5373.
Copyright 2006 American Chemical Society

Abstract

The environmental fate of volatile and semi-volatile organic compounds is determined by their partitioning between air and soil constituents, in particular soil organic matter (SOM). While there are many studies on the partitioning of nonpolar compounds between water and SOM, data on sorption of polar compounds and data for sorption from the gas phase are rather limited. In this study, Leonardite humic acid/air partition coefficients for 188 polar and nonpolar organic compounds at temperatures between 5 and 75 °C and relative humidities between <0.01% and 98% have been determined using a dynamic flow-through technique. To the best of our knowledge, this is by far the largest and most diverse and consistent dataset for sorption into humic material published so far. The major results are as follows: the relative humidity affected the experimental partition coefficients by up to a factor of 3; polar compounds generally sorbed more strongly than nonpolar compounds due to H-bonding (electron donor/acceptor interactions) with the humic acid; no glass transitions in the range of 5–75 °C that would be relevant with respect to the sorption behavior of hydrated Leonardite humic acid were observed; our experimental data agree well with experimental partition coefficients from various literature sources.

Introduction

Organic pollutants can undergo various transport and degradation processes in the environment. Air constitutes a major transport medium for volatile and semi-volatile pollutants on a microscopic (porescale) as well as on a macroscopic (regional, global) scale. This transport is strongly governed by the partitioning of the pollutants between air and condensed phases including aerosols, plants, and soils as well as water, snow, and ice. In general, organic compartments such as soil organic matter (SOM) or plants are considered to be the primary sorbents of organic pollutants. A large number of papers have been published about the sorption of organic compounds to SOM; however, with the exception of a few studies (1-3), most of the studies focused on a few, rather nonpolar compounds (e.g., polycyclic aromatic hydrocarbons, polychlorinated biphenyls) and disregarded polar compounds (4-7). Data for larger and more diverse sets of organic compounds measured with a consistent method are lacking, except for the studies of Borisover and Graber (8, 9). Furthermore, most of the available studies have focused on the partitioning between SOM and water and not between SOM and air (10). It is not clear whether SOM/air partitioning can readily be estimated via the thermodynamic cycle using SOM/water and air/water partitioning coefficients, particularly because the hydration states of SOM are different in air-dry soils (i.e., in equilibrium with less than 100% relative humidity) as compared to moist soils.

For a comprehensive understanding of sorption in SOM, it is necessary to have a large experimental data set covering all relevant functional groups in the sorbates as well as all variability in SOM. In this paper we do the first step in this direction by presenting experimental sorption data on a specific humic acid for a large variety of organic chemicals. Our future work will focus on variability of the sorption properties of various types of SOM.

The major goals of this study (presented in this article and a companion paper (11)) are as follows:

(a) to develop and evaluate an experimental system for the measurement of a large number of equilibrium sorption constants from the gas phase to humic material; (b) to determine a large number of sorption coefficients for a diverse set of organic compounds representing all major functional groups including compounds of environmental concern such as polychlorinated benzenes, phenols, nitro aromatic compounds, or pesticides; (c) to determine the influence of humidity and temperature on this sorption process; (d) to check the influence of the hydration state on the sorption properties of the studied humic acid; and (e) to elucidate the intermolecular interactions that are responsible for the sorption process.

Materials and Methods

Materials. A standard humic acid (Leonardite HA, Cat. No. 1S104H, standard from the International Humic Substances Society IHSS) was used as received. Leonardite humic acid is the product of the natural oxidation of exposed lignite, a low-grade coal, and originates from the Gascoyne Mine in Bowman County, North Dakota, U.S.A ((12), (<http://www.ihss.gatech.edu>)). One hundred eighty-eight substances from different substance classes were used (see Table 1) that cover a wide variability in the physicochemical properties, i.e., a wide range in their van der Waals and electron donor/acceptor-interaction (EDA-interactions; including H-bondings) parameters. Compounds (from Fluka, Buchs, Switzerland and Merck, Dietikon, Switzerland) were used as received and had a purity of at least 96%. Compounds within this data set that are of special environmental concern are two pesticides (*p*-nitroanisole, lindane [γ -hexachlorocyclohexane]), two phthalates, nitro aromatic compounds, chlorobenzenes, and several chlorophenols.

Method. The humic acid/air partition coefficients $K_{iHA,air}$ [L/kg_{HA}] were determined by inverse gas chromatography (IGC) (13, 14) in which the sorbent serves as stationary phase in a gas chromatography system. When the substance *i* is injected onto the column under isothermal

conditions, the retention observed is a measure of its tendency to sorb. $K_{iHA,air}$ values (in mL/g_{HA} or L/kg_{HA}) are calculated using eq (1):

$$K_{iHA,air} = \frac{V_i - V_{ibkgnd}}{M_{HA}} \quad (1)$$

where M_{HA} is the total humic acid (HA) mass [g_{HA}] in the column, V_i is the retention volume of compound i [mL], and V_{bkgnd} is the retention volume of the system without humic acid [mL]. V_{ibkgnd} accounts for the dead volume of the system, potential sorption to the stainless steel system (capillaries, frit), and the uncoated support of the humic acid (Alltech glassbeads, see below). The retention caused by the background was only $12.2 \pm 11.6\%$ compared to the retention caused by the humic acid. The volumes V_i and V_{ibkgnd} are determined from the retention time of the respective peaks, which are calculated using the peak center (first moment) and the volumetric flow rate of the carrier gas while accounting for the pressure drop in the IGC system. Typical peak shapes are shown in Supporting Information (SI)-1. Equation 1 requires that the organic compounds are present at low concentrations (i.e., in the linear range of the sorption isotherm) and that the sorption kinetics is fast enough to guarantee sorption equilibrium during the chromatographic process. The rate determining step is the diffusion of the compound i into the humic acid. Obtaining equilibrium is a challenging task because of the high carrier gas velocities applied in gas chromatography. Equilibrium conditions are generally reached in analytical applications of gas chromatography in which typical carrier gas flows of $0.5 \text{ m}\cdot\text{s}^{-1}$ and sorbent layer thicknesses of $1 \text{ }\mu\text{m}$ or below are used. For that reason we developed a method to coat humic acid on a support with a layer thickness $<2 \text{ }\mu\text{m}$. The support were deactivated (silanized) glass beads (Alltech glass beads, DMCS-treated, 100/120 mesh, Alltech, Deerfield, IL) with an average diameter of $125 \text{ }\mu\text{m}$. The Leonardite HA was dissolved in a 2:3 mixture (volume-based) of pentan-1-ol and N,N -dimethylformamide. The glass beads were mixed with this solution and the solvents were subsequently evaporated under an air-stream under constant stirring. Scanning Electron Microscope (SEM) images show

coating layer thicknesses $< 2\ \mu\text{m}$ throughout the entire sample (images available in SI-2). The amount of humic acid coated on the glassbeads was determined by redissolving the coated HA of a defined amount of glassbeads in *N,N*-dimethylformamide. The absorption intensity of the HA solution was measured with a UV-vis spectrophotometer (Uvikon 860, Kontron Instruments) at the wavelengths $\lambda = 300, 350, 400,$ and $450\ \text{nm}$ and quantified with respect to standard solutions. The coatings were found to be completely removable because the Leonardite HA coating adhered by physisorption on the support. By contrast, in many other studies (15, 16), the humic acids were coated by formation of covalent bonds between the humic acid and the support (chemisorption). The UV spectra of the original dissolved humic acid and of the humic acid from the coated glass beads were identical. Therefore, we conclude that the experiments did not show a fractionation effect, i.e., no specific fractions of the humic acid adhered to the support more favorably than others.

The coated glass beads were packed into stainless steel high-pressure liquid chromatography columns (1.0 cm length, 0.3 cm inner diameter) and installed in a gas chromatograph (Carlo Erba 4160, Milan, Italy) equipped with a flame ionization detector (FID). To obtain the desired relative humidities (rh; 45%, 70%, 98%), the carrier gas (N_2) was passed through a water saturator in a water bath before it entered the IGC system. The temperature of the water saturator was selected according to the column temperature and the pressure drop between the water saturator and the column. The humic acid column was equilibrated for at least 48 h at the chosen rh at a carrier gas flow of $20\ \text{mL}\cdot\text{min}^{-1}$. In a long-term experiment, the humic acid column was equilibrated for 80 days at 98% rh. The partition coefficients after 48 h and 80 days agreed within 12%. Gas flow rates were between 5 and $30\ \text{mL}\cdot\text{min}^{-1}$ corresponding to a linear velocity in the range of $0.02\ \text{m}\cdot\text{s}^{-1}$ to $0.14\ \text{m}\cdot\text{s}^{-1}$ which is notably smaller than that in standard GC ($0.5\ \text{m}\cdot\text{s}^{-1}$). Flow rates were measured with a mass flow meter (F-111C-HAD-11-V, Bronkhorst, Reinach, Switzerland). The whole system exhibited a dead volume of $0.25\ \text{mL}$ (capillary system, column, frit). Only substances with a net-retention volume $> 0.25\ \text{mL}$ were considered. For some substances exhibiting

particularly low vapor pressures and low detectabilities, solid-phase microextraction (SPME) needles (7 μm PDMS needle, Supelco, Bellefonte, PA) were used to collect the sorbate and to inject it into the system.

Results and Discussion

Evaluation of the Sorption Equilibrium. Realization of sorption equilibrium in the IGC system is a fundamental condition for the correct determination of sorption coefficients. Therefore, we evaluated our experimental approach by the following three steps:

1) Diffusion Calculations with AQUASIM

Diffusion calculations with the transport model AQUASIM 2.0 (17) were conducted under the following conditions that represent our experimental system: humic acid coating thickness of 1 and 2 μm ; a volume flow rate of 20 $\text{mL}\cdot\text{min}^{-1}$ (linear velocity = 0.1 $\text{m}\cdot\text{s}^{-1}$); and diffusion coefficient of the sorbate $10^{-9} \text{ cm}^2\cdot\text{s}^{-1}$ (18, 19). The results show that we are close to equilibrium conditions. Furthermore, evaluation of the peaks using the peak center (first moment) instead of the peak maximum is not very susceptible to nonequilibrium conditions (for more details see SI-3 and ref (20); for typical peak shapes see SI-1). It must be noted that we would not have achieved equilibrium with our experimental setup if diffusion coefficients in the humic acid had been much smaller than $10^{-9} \text{ cm}^2\cdot\text{s}^{-1}$. However, such small diffusion coefficients are only expected for glassy polymers. Our results discussed below indicate that glassy domains are not prevalent to a degree that would have affected sorption.

2) Coating Thicknesses

Images recorded by the SEM indicate that the coatings are not absolutely homogeneous. However, even the thickest humic acid regions on the support are still thinner than 2 μm (images available in SI-2).

3) Variation of Humic Acid Layer Thicknesses on the Support

The humic acid/air partition coefficients were determined at coating thicknesses varying by a factor of about five. The retention volumes increased proportionally to the total amount of humic acid in the column providing compelling evidence that sorption equilibrium is obtained as

otherwise thicker coatings would exhibit a lower relative sorption. In addition, this result indicates that the observed sorption mechanism is dominated by sorption into the inner material of the humic acid (adsorption to internal surfaces of pores in the coating or absorption) rather than adsorption to the outer surface of the coating.

Reproducibility. Various error sources in the experimental procedure had to be considered. These include the following: variations between different coatings; errors in the quantification of the coated amount of humic acid; and variations in column packing. Therefore, we determined humic acid/air partition coefficients on five, separately prepared coatings at 15 °C and 98% rh. Measurements of 48 substances from different substance classes were obtained from these five columns (see SI-4). The average standard deviation was 38% in the nonlogarithmic sorption coefficients. Most of this error is due to deviations between different columns (SI-4). The reproducibility of the retention volume of the same substance on a given column was better than 5%. In the following, this relative precision of 5% applies to all results that have been measured on a single column, i.e., for the experiments on the influence of humidity, temperature and the relative difference for various compound classes.

Linearity of the Sorption Isotherms. From various literature studies it is known that humic acids exhibit an expanded range of sorption linearity (1, 10, 21-23). We tested these findings by varying the gas-phase concentrations of 10 substances within a factor of 20 in our experimental system. We found no significant deviation in the retention volumes as a function of the sorbate concentration in the gas phase. This result implies that the used sorbate concentrations for both headspace and SPME injection lied in the linear range of the sorption isotherm. According to the current consensus concerning sorption isotherms in humic materials, a nonlinear sorption isotherm goes along with the occurrence of glassy (rigid) polymeric structure in the humic matrix (1, 24-26). Typical glass transition temperatures for these glassy regions in humic substances have been found in the range of 50 °C to 75 °C (26, 27). LeBoeuf et al. (28) found a glass transition at 70–73 °C in the dry Leonardite HA as well as a substantial decrease (e.g., 20 °C) in the glass transition temperatures in

water-wet humic acid compared to the dry material. Here, we did not observe glass transitions in the range of 5 °C to 75 °C (98% rh) that would have been relevant with respect to the sorption properties of wet Leonardite humic acid (see below: Temperature Dependence and SI-5).

Influence of the Support on the Observed Sorption. Strong interactions between the support and the humic acid can change the structure of the sorbed humic acid and influence its sorption properties. Such an effect would be particularly strong for the first molecular layer of the humic acid on the support and would decrease with increasing coating thicknesses. But as already mentioned above, the sorption coefficients did not alter with increasing layer thicknesses. In addition, we conducted experiments with a completely different support (quartz sand, SiO₂; will be published elsewhere) that showed identical sorption coefficients for the coated humic acid.

Outliers. Aliphatic amines (e.g., diethylamine, triethylamine) and short-chained acids (formic acid, acetic acid) caused problems in the measurement and the evaluation of the peaks. We assume that acid-base reactions with the numerous carboxylic groups of the humic acids cause the abnormal behavior of the amines. Furthermore, the acids and some aliphatic amines can form dimers in the gas phase (29, 30) which might be responsible for the irreproducible retention volumes. Consequently, these substances were not considered in our data set (for more details see SI-1b).

Sorption Coefficients

Table 1 gives an overview of the experimental Leonardite HA/air partition coefficients measured for 188 nonionic compounds at 98% rh and 15 °C. An extensive table with all partition coefficients determined at 98% rh and different temperatures (5–75 °C) as well as experimental sorption enthalpies can be found in SI-7. To our knowledge, this is by far the largest data set of partition coefficients ever measured for a humic material with one consistent method. The partition coefficients of substances from a large variety of different nonpolar and polar substance classes extend almost over 7 orders of magnitude.

Compound classes	number of compounds measured	range of $\log(K_{HA,air}/[L/kg_{HA}])$ 15 °C, 98% rh
alkanes and alkenes	14	2.08 – 5.43
alcohols	22	3.42 – 8.20
phenolic compounds including chlorophenols	11	5.44 – 8.20
ketones and acetates	24	2.39 – 5.74
ethers and aldehydes	11	1.94 – 5.80
alkyl benzenes and PAHs	19	2.18 – 9.49
halogenated benzenes	17	2.21 – 6.50
halogenated alkanes and alkenes	8	2.50 – 4.67
N-compounds (including anilines and nitrobenzenes)	27	3.02 – 7.10
organic acids	5	5.51 – 6.17
bifunctional compounds (including dioles, diones, dinitrobenzenes)	20	3.75 – 8.30
S-compounds, lactones, phosphates, siloxanes	6	2.55 – 7.06
compounds of high environmental relevance: lindane (γ -HCH), two phthalates, 4-nitroaniso	4	6.55 – 7.68

Table 1 Overview of the experimental Leonardite HA/air partition coefficients (15 °C, 98% rh). An extensive table containing all experimental $K_{iHA,air}$ values as well as experimental sorption enthalpies can be found in the SI-7.

The partitioning of an organic compound between two phases depends on the molecular interactions between the compound and the molecules of the corresponding phases. Only interactions of the compounds with the humic acid have to be considered for their humic acid/air partitioning because the gas phase can be approximated as ideal. The relevant interactions comprise the cavity energy (i.e., the energy that is required to form a cavity of the size of the sorbate in the sorbent) and van der Waals interactions as well as specific EDA-interactions (including H-bonding interactions). The logarithm of the hexadecane ($C_{16}H_{34}$)/air partitioning coefficient of a compound can be used as a

descriptor that is proportional to the nonspecific interactions (cavity and van der Waals) that occur for any sorbate. Therefore, a plot of the measured humic acid/air partition coefficients of various compounds against their hexadecane/air partition coefficient makes it possible to identify those compounds that additionally interact by specific EDA-interactions with the humic acid (see also ref (8)). Figure 1 clearly shows that the alkanes and halogenated alkanes exhibit the lowest sorption coefficients because they interact only via van der Waals forces which are always present.

These compounds define a line that may be referred to as “baseline sorption”, as no compound can lie below that line (indicated by the trendline in Figure 1). Every compound that lies above this line must exhibit specific EDA-interactions with the humic acid. In fact, the vertical distance to the baseline sorption is a direct measure for the strength of these specific interactions. They are highest for compounds that form strong H-bonds with the humic acid (like alcohols and acids) and they are lowest for the alkyl aromatic compounds which are only weak electron donors (i.e., H-bond acceptors). The line for “baseline sorption” reveals a much higher affinity of nonspecific interacting molecules to hexadecane than to the humic acid (almost two log units). This indicates a much higher cohesive energy in the humic acid which is likely caused by intramolecular hydrogen bonds.

Figure 1 shows that specific interactions have a huge influence on the sorption of monopolar (either electron donor or electron acceptor) and bipolar (electron donor and electron acceptor) compounds in Leonardite humic acid. The alcohols and phenols sorb more strongly by a factor of 50-30000 than would be predicted by the baseline sorption. Therefore, the sorption of organic compounds in Leonardite humic acid can only be predicted correctly if the sorption process is understood on a mechanistic basis including the discrimination of specific and nonspecific molecular interactions. The octanol model that is often used as a surrogate for soil humic matter is not able to reproduce this situation correctly as we will show in ref (11). Instead, a polyparameter model is required in order to cover all types of interactions properly (11, 31).

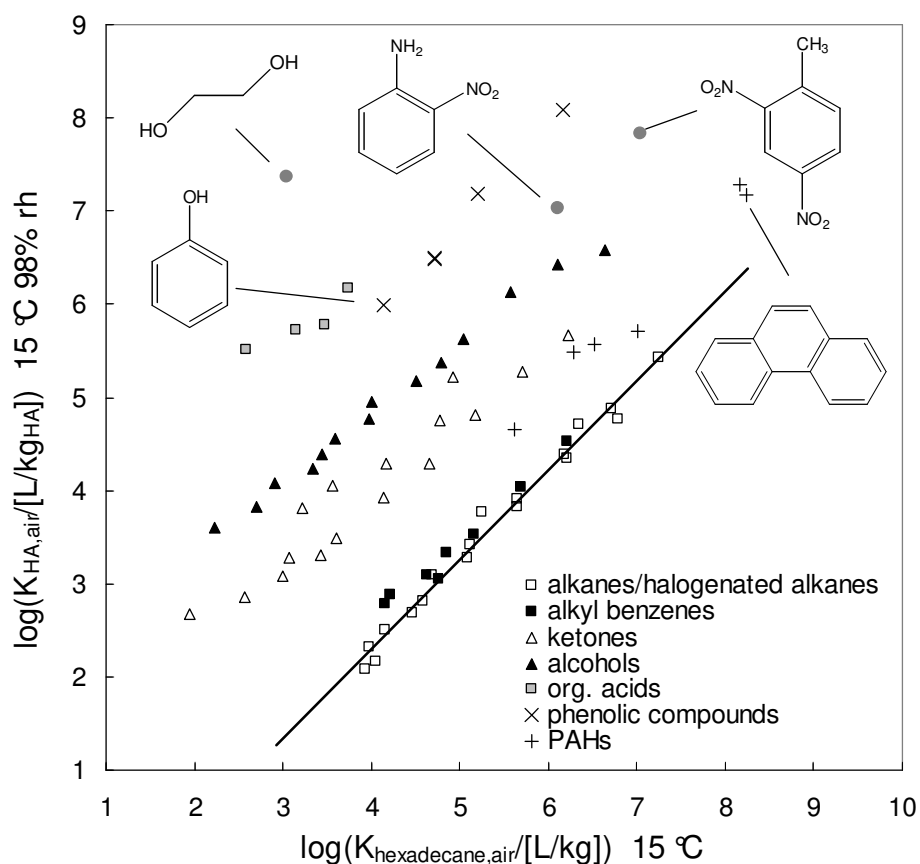


Figure 1. Comparison of HA/air partition coefficients (15 °C, 98% rh) with the corresponding hexadecane ($C_{16}H_{34}$)/air partition coefficients. Compounds that do not belong to a substance class indicated in the legend are represented by their chemical structure.

Comparison with Literature Data. Only a few humic acid/air partition coefficients (and not for Leonardite) can be found in the literature (10). Data on Leonardite HA/water partition coefficients or humic acid/water partition coefficient for other humic acids are also limited. Comparison with the latter is only possible when converting our data into humic acid/water partition coefficients using the water/air partition coefficient. The thermodynamic cycle should be valid here because we use data for the highly hydrated form of the humic acid (at 98% rh) and because the relevant sorption process can be assumed to be absorption (see ref (32) for the incorrectness of applying the thermodynamic cycle to adsorption data). The comparison shows that the converted data agree in all cases within experimental error to those reported in the literature (Table 2). Leonardite humic acid values of Lee et al. (33) and our data differ by

only a factor of three. The difference between our data and the values of Kang and Xing (23) and Schlautman and Morgan (34) do not exceed a factor of 2. Our data correspond especially well with the humic acid data by Poerschmann et al. (35), who also used a coal derived humic acid. The related origin should imply that the humic materials have similar structural properties which likely give rise to comparable sorption properties.

The good agreement of our data with literature data confirms again the suitability of our experimental method and suggests that the thermodynamic cycle in the wet HA/water/air system is indeed applicable. It also suggests that there is relatively low variability of sorption properties for different humic acid fractions. To provide more

Sorbate	Source	Literature material	$\log K_{iOC,water}$ [L/kg _{OC}]	this study $\log(K_{iHA-OC,water})$ [L/kg _{OC}]
Phenanthrene	(33)	Leonardite HA	4.56	4.05 ¹
Phenanthrene	(23)	various HA fractions	4.15-4.38	4.05 ¹
Phenanthrene	(35)	HA from highly polluted coal wastewater (East Germany)*	3.85 ($\log K_{HA,water}$)	3.85 ($\log K_{HA,water}$)
Anthracene	(34)	IHSS Suwannee River HA	4.42	4.11 ²
Anthracene	(35)	*material: see above	3.97 ($\log K_{HA,water}$)	3.92 ($\log K_{HA,water}$)
Naphthalene	(36)	Aldrich HA	3.02	2.91 ³
Naphthalene	(35)	*material: see above	3.05 ($\log K_{HA,water}$)	2.74 ($\log K_{HA,water}$)
Acenaphthene	(35)	*material: see above	3.38 ($\log K_{HA,water}$)	2.99 ⁴ ($\log K_{HA,water}$)

¹ $\log K_{water,air} = 2.85$; ² $\log K_{water,air} = 2.90$; ³ $\log K_{water,air} = 1.76$; ⁴ $\log K_{water,air} = 2.31$; all water/air partition coefficients are from (37).

Table 2: Comparison of humic acid/water partition coefficients from the literature with Leonardite HA/water partition coefficients from this study; data from this study were converted to humic acid organic carbon/water partition coefficients $K_{iHA-OC,water}$ using water/air partition coefficients and C-org = 63.8% for Leonardite HA. All data are at 25 °C.

support to this hypothesis, more experiments with various humic and fulvic acids are presently being conducted.

Temperature Dependence. The temperature dependence of the partition equilibrium between air and Leonardite HA was investigated by measuring the sorption coefficients of 180 compounds at three to five different temperatures ranging from 5 to 75 °C at 98% rh. The sorption enthalpies, $\Delta_{\text{abs}}H_i$, were calculated from van't Hoff plots which exhibited very good linearity over the studied temperature range (for 90% of the compounds $r^2 \geq 0.98$; see SI-7 for $\Delta_{\text{abs}}H_i$ values and SI-5 for representative van't Hoff plots). In ref (11) we investigate various methods to predict the temperature effect on sorption.

When sorption in glassy polymers is studied as a function of temperature, an increase of sorption with temperature (instead of the expected decrease) is observed when the glass transition temperature is exceeded (13, 38, 39). This is because glassy domains are converted to rubbery domains and become kinetically available for sorption. We did not see such an effect for hydrated Leonardite HA in the studied temperature range (for details see SI-5). Therefore, we conclude that below 75 °C there were no glass transitions that had an effect on the sorption properties of the humic acid.

Influence of the Relative Humidity. Soil organic matter in equilibrium with water-saturated air can take up a significant amount of water (e.g., up to 24 mass-% (on a dry basis) has been reported for peat (27)). Due to the incorporation of water molecules into the humic acid, its polymeric structure can undergo changes. Water molecules can break up internal EDA-interactions and establish their own EDA-interactions with functional groups of the matrix (9). This causes the matrix to change its flexibility, polarity, and conformation. Acid-base reactions with the carboxylic groups of the humic acid, involving changes in the ionic state, are also possible. Additionally, the water molecules are in competition with the organic sorbates for sorption sites in the humic acid. All these

effects could possibly influence the sorption capacity of the humic acid, and the extent of this effect would be a function of rh.

Figure 2 compares Leonardite HA/air partition coefficients at <0.01% rh with the partition coefficients at 98% rh. For experimental data see SI-7.

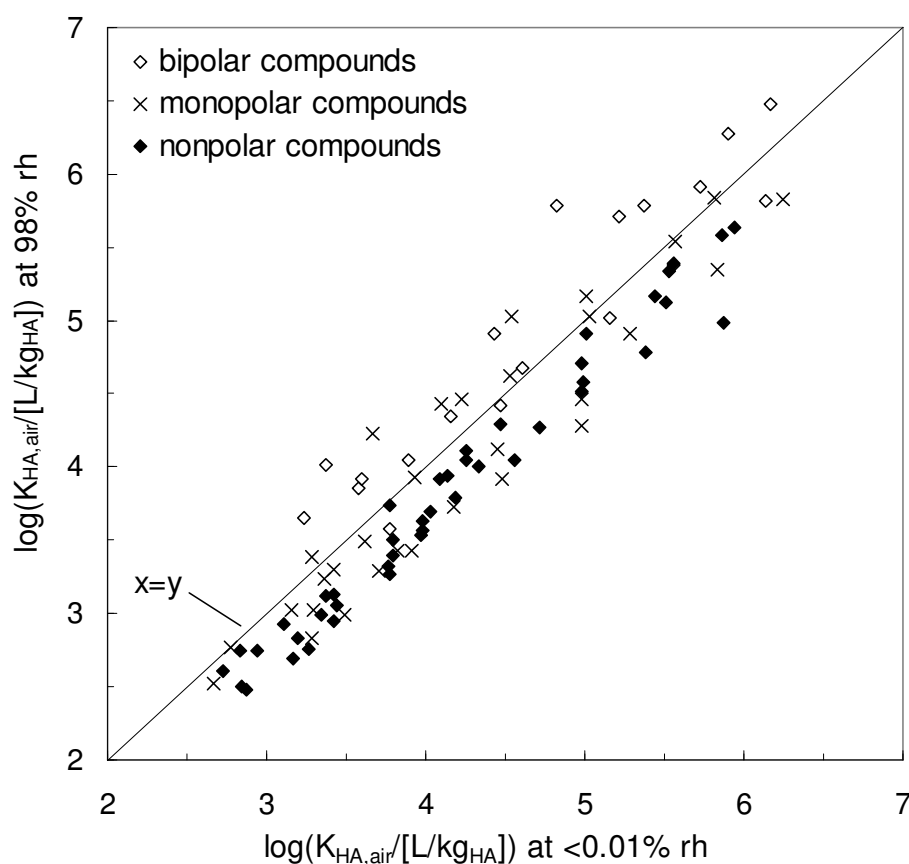


Figure 2. Leonardite HA/air partition coefficients for dry humic acid and hydrated humic acid at 15 °C. The plot indicates that the nonpolar compounds prefer dry humic acid, while the bipolar compounds (alcohols, caboxylic acids) prefer hydrated HA. No consistent behavior can be observed for the monopolar compounds (acetates, ethers, ketones).

The plot shows the influence of rh on the sorption of bipolar substances (electron donor and electron acceptor: alcohols, carboxylic acids), monopolar compounds (electron donors: ketones, ethers, acetates, nitro aromatic compounds) and nonpolar substances (weak or no electron donors: alkyl benzenes, alkanes, alkenes, halogen alkanes, halogenated aromatics). The comparison reveals that rh influences the sorption generally by less than a factor of 3 for all substance classes tested.

The relative sorption behavior of the tested substance classes as a function of rh is instructive regarding sorbent/sorbate interactions. Most aliphatic alcohols sorb more strongly into the hydrated humic acid than into the dry humic acid (up to a factor of 3). In contrast, all nonpolar substances sorb strongest into the humic acid that is in equilibrium with <0.01% rh. The monopolar substances do not show any uniform pattern: the sorption of about half of the substances is similar at <0.01% and 98% rh (short-chained ethers and ketones, nitrobenzenes), the other half shows preferential sorption to dry humic acid (acetates, long-chained ketones). In comparison with short-chained alcohols and ketones, the long-chained members of these substance classes in the dataset prefer the dry humic acid (for more details see SI-6). All polar aromatic compounds (e.g., phenol, benzyl alcohol, nitrobenzene) sorb more strongly at 98% rh. The interpretation we give here mainly follows the arguments given by Borisover and Graber (9, 40, 41): An increasing water content in the humic acid causes the number of EDA-interactions in the matrix to increase because the water molecules are excellent electron donors/acceptors that act as bridges between functional sites in the humic acid that are too far apart for direct interactions. This causes an increase in the cohesive energy of the humic acid matrix. As a consequence, sorption of the nonpolar compounds decreases with increasing rh because the energy required for cavity formation has increased. In contrast, the polar compounds can undergo more EDA-interactions in the hydrated matrix, which compensates the increased cavity energy (alcohols, ketones, polar aromatic compounds). The bipolar alcohols are even able to over-compensate the increased cavity energy leading to an increase in the sorption coefficients with increasing rh. In good agreement with this hypothesis, we observed that with increasing chain length the polar aliphatic compounds tend to prefer the dry humic acid to the wetted humic acid because with rising chain length the cavity energy increases, while the gain of energy by the specific interactions remains constant (see SI-6).

Borisover and Graber (9) investigated the influence of rh on the sorption capacities of a peat humic acid fraction and on the peat itself for benzyl

alcohol, acetophenone, nitrobenzene, and *m*-nitrophenol. Rutherford et al. (42) analyzed the influence of water saturation on the sorption capacity of Florida peat (IHSS standard) for benzene and trichloroethene. Table 3 compares these data with our results. Borisover and Graber as well as Rutherford et al. also found a change in sorption by factor 2-5 depending on humidity, which is in good agreement with our results for Leonardite HA. Except for nitrobenzene, the substances exhibit a similar behavior in the four SOM systems. We have no explanation why the trend that Borisover and Graber observed for nitrobenzene is opposite to and much stronger than what we saw in our experiments.

Sorbate	Leonardite HA ¹	Peat humic acid ²	Peat ²	Florida peat ³
Nitrobenzene	factor 1.4	factor 0.2-0.35	similar	<i>n.d.</i>
Acetophenone	factor 0.95	<i>n.d.</i>	similar	<i>n.d.</i>
Benzyl alcohol	factor 2.1	<i>n.d.</i>	factor 4.0	<i>n.d.</i>
Benzene	factor 0.8	<i>n.d.</i>	<i>n.d.</i>	factor 0.55
Trichloroethene	factor 0.75	<i>n.d.</i>	<i>n.d.</i>	factor 0.45

¹ this study; ² (9); ³ (42); *n.d.*: no data

Table 3: Comparison to dry humic material and to hydrated humic material displayed as $K_{\text{wet-HA}}/K_{\text{dry-HA}}$.

In summary, our data demonstrate that the influence of rh on the observed sorption is moderate compared to the large differences that we observed for various sorbates due to influence of various functional groups. The presented dataset allows for a much more comprehensive evaluation of existing sorption models than has been possible so far (see ref (11)). However, this evaluation must be completed in future with experimental sorption data that reveal the differences in the sorption properties of humic and fulvic acids. This is the focus of our ongoing work.

Acknowledgements

We thank Brian Sinnet for his support at the Scanning Electron Microscope and Christine Roth, Hans Peter Arp, Thorsten Schmidt, Guido Bronner, Tom Gallé, Satoshi Endo, and two anonymous reviewers for critical comments on the manuscript. This research was financially supported by the Swiss National Science Foundation (project-no. 200020-111753/1) and partly by the European Union (European Commission, FP6 Contract No. 003956).

References Chapter 1

- (1) Xing, B., Pignatello, J.J. Dual-mode sorption of low polarity compounds in glassy poly(vinyl chloride) and soil organic matter *Environ. Sci. Technol.* **1997**, 31, 792-799.
- (2) Xing, B., McGill, W.B., Dudas, M.J. Sorption of alpha-naphthol onto organic sorbents varying in polarity and aromaticity *Chemosphere* **1994**, 28, 145-153.
- (3) Chiou, C. T., Kile, D.E. Effects of polar and nonpolar groups on the solubility of organic compounds in soil organic matter *Environ. Sci. Technol.* **1994**, 28, 1139-1144.
- (4) Kile, D. E., Chiou, C.T. Partition of nonpolar organic pollutants from water to soil and sediment organic matters *Environ. Sci. Technol.* **1995**, 29, 1401-1406.
- (5) Grathwohl, P. Influence of organic matter from soils and sediments from various origins on the sorption of some chlorinated aliphatic hydrocarbons: Implications on K_{oc} correlations *Environ. Sci. Technol.* **1990**, 24, 1687-1693.
- (6) Kopinke, F. D., Poerschmann, J., Stottmeister, U. Sorption of organic pollutants on anthropogenic humic matter *Environ. Sci. Technol.* **1995**, 29, 941-950.
- (7) Xia, C., Ball, W.P. Adsorption-partitioning uptake of nine low-polarity organic chemicals on a natural sorbent *Environ. Sci. Technol.* **1999**, 33, 262-269.

- (8) Borisover, M., Graber, E.R. Specific interactions of organic compounds with soil organic carbon *Chemosphere* **1997**, 34, 1761-1776.
- (9) Borisover, M., Graber, E.R. Hydration of natural organic matter: effect on sorption of organic compounds by humin and humic acid fractions vs original peat material *Environ. Sci. Technol.* **2004**, 38, 4120-4129.
- (10) Chiou, C. T., Kile, D.E., Malcom, R.L. Sorption of vapors of some organic liquids on soil humic acid and its relation to partitioning of organic compounds in soil organic matter *Environ. Sci. Technol.* **1988**, 22, 298-303.
- (11) Niederer, C., Goss, K.U., Schwarzenbach, R.P. Sorption equilibrium of a wide spectrum of organic vapors in Leonardite humic acid: Modeling of experimental data *Environ. Sci. Technol.* **2006**, 40, 5374-5379.
- (12) Mao, J. D., Hu, W.G., Schmidt-Rohr, K., Davies, G., Ghabbour, E.A., Xing, B. Quantitative characterization of humic substances by solid-state carbon-13 nuclear magnetic resonance *Soil Sci. Soc. Am. J.* **2000**, 64, 873-883.
- (13) Conder, J. R., Young, C.L. *Physicochemical measurement by gas chromatography*; Wiley: New York, 1979.
- (14) Voelkel, A. Inverse gas chromatography: characterization of polymers, fibers, modified silicas, and surfactants *Crit. Rev. Anal. Chem.* **1991**, 22, 411-439.
- (15) Yang, Y. H., Koopal, L.K. Immobilisation of humic acids and binding of nitrophenol to immobilised humics *Colloid Surfaces* **1999**, 151, 201-212.
- (16) Nielsen, T., Siigur, K., Helweg, C., Jorgensen, O., Hansen, P.E., Kirso, U. Sorption of polycyclic aromatic compounds to humic acid as studied by high-performance liquid chromatography *Environ. Sci. Technol.* **1997**, 31, 1102-1108.
- (17) Reichert, P.; Aquasim. Computer Program for the Identification and Simulation of Aquatic Systems. Swiss Federal Institute for Environmental Science and Technology (EAWAG): Duebendorf, 1998.
- (18) Chang, M. L., Wu, S.C., Chen, C.Y. Diffusion of volatile organic compounds in pressed humic acid disks *Environ. Sci. Technol.* **1997**, 31, 2307-2312.

- (19) Piatt, J. J., Brusseau, M.L. Rate-limited sorption of hydrophobic organic compounds by soils with well-characterized organic matter *Environ. Sci. Technol.* **1998**, 32, 1604-1608.
- (20) Valocchi, A. J. Validity of the local equilibrium assumption for modeling sorbing solute transport through homogeneous soils *Water Resour. Res.* **1985**, 21, 808-820.
- (21) Kopinke, F. D., Georgi, A., Mackenzie, K. Sorption of pyrene to dissolved humic substances and related model polymers. 1. Structure-property correlation *Environ. Sci. Technol.* **2001**, 35, 2536-2542.
- (22) Allaire, S. E., Yates, S.R., Ernst, F.F., Gan, J. A dynamic two-dimensional system for measuring volatile organic compound volatilization and movement in soils *J. Environ. Qual.* **2002**, 31, 1079-1087.
- (23) Kang, S., Xing, B. Phenanthrene sorption to sequentially extracted soil humic acids and humins *Environ. Sci. Technol.* **2005**, 39, 134-140.
- (24) Xing, B., Pignatello, J.J. Time-dependent isotherm shape of organic compounds in soil organic matter: implications for sorption mechanism *Environ. Toxicol. Chem.* **1996**, 15, 1282-1288.
- (25) Xing, B., Pignatello, J.J., Gigliotti, B. Competitive sorption between atrazine and other organic compounds in soils and model sorbents *Environ. Sci. Technol.* **1996**, 30, 2432-2440.
- (26) LeBoeuf, E. J., Weber, W.J. A distributed reactivity model for sorption by soils and sediments *Environ. Sci. Technol.* **1997**, 31, 1697-1702.
- (27) Schaumann, G. E., LeBoeuf, E.J. Glass transitions in peat: their relevance and the impact of water *Environ. Sci. Technol.* **2005**, 39, 800-806.
- (28) LeBoeuf, E. J., Weber, W.J. Jr. Macromolecular characteristics of natural organic matter. 1. Insights from glass transition and enthalpic relaxation behavior *Environ. Sci. Technol.* **2000**, 34, 3623-3631.
- (29) Weckwerth, J. D., Carr, P.W., Vitha, M.F., Nasehzadeh, A. A comparison of gas-hexadecane and gas-apolane partition coefficients *Anal. Chem.* **1998**, 70, 3712-3716.
- (30) Hierlemann, A., Zellers, E.T., Ricco, A.J. Use of linear solvation energy relationships for modeling responses from polymer-coated acoustic-wave vapor sensors *Anal. Chem.* **2001**, 73, 3458-3466.
- (31) Goss, K.-U.; Schwarzenbach, R. P. Linear free energy relationships used to evaluate equilibrium partitioning of organic compounds *Environ. Sci. Technol.* **2001**, 35, 1-9.

- (32) Goss, K.-U. Comment on 'Influence of soot carbon on the soil-air partitioning of polycyclic aromatic hydrocarbon' *Environ. Sci. Technol.* **2004**, 38, 1622-1623.
- (33) Lee, C. L., Kuo, L.J., Wang, H.L., Hsieh, P.C. Effects of ionic strength on the binding of phenanthrene and pyrene to humic substances: three-stage variation model *Water Res.* **2003**, 37, 4250-4258.
- (34) Schlautman, M. A., Morgan, J.J. Effects of aqueous chemistry on the binding of polycyclic aromatic hydrocarbons by dissolved humic materials *Environ. Sci. Technol.* **1993**, 27, 961-969.
- (35) Poerschmann, J., Kopinke, F.D., Plugge, J., Gorecki, T. Interaction of organic chemicals (PAH, PCB, triazines, nitroaromatics and organotin compounds) with dissolved humic organic matter. In *Understanding humic substances: Advanced methods, properties, applications*; Davies, G., Ghabbour, E.A., Ed.; The Royal Society of Chemistry, 1999.
- (36) McCarthy, J. F., Jimenez, B.D. Interactions between polycyclic aromatic hydrocarbons and dissolved humic material: binding and dissociation *Environ. Sci. Technol.* **1985**, 19, 1072-1076.
- (37) Abraham, M. H., Andonian-Haftvan, J., Whiting, G.S., Leo, A., Taft, R.S. Hydrogen bonding. Part 34. The factors that influence the solubility of gases and vapors in water at 298 K, and a new method for its determination *J. Chem. Soc., Perkin Trans. 2* **1994**, 1777-1791.
- (38) Braun, J.-M., Guillet, J.E. Studies of polystyrene in the region of the glass transition temperature by inverse gas chromatography *Macromolecules* **1975**, 8, 882-888.
- (39) Hamdi, S., Hamdi, B., Kessaissia, Z., Barthel, H., Balard, H., Donnet, J. B. Influence of poly(methyl methacrylate) impregnation ratio on the surface properties of fumed silica and on the glassy temperature of poly(methyl methacrylate) using inverse gas chromatographic analysis *J. Chromatogr., A* **2002**, 969, 143-151.
- (40) Borisover, M., Graber, E.R. Simplified link solvation model (LSM) for sorption in natural organic matter *Langmuir* **2002**, 18, 4775-4782.
- (41) Borisover, M., Graber, E.R. Relationship between strength of organic sorbate interactions in NOM and hydration effect on sorption *Environ. Sci. Technol.* **2002**, 36, 4570-4577.
- (42) Rutherford, D. W., Chiou, C.T. Effect of water saturation in soil organic matter on the partition of organic compounds *Environ. Sci. Technol.* **1992**, 26, 965-970.

Appendix 1

Experimental Setup and Experimental Data

Content

SI-1 Chromatograms and outliers

SI-2 Humic acid coatings on Alltech glass beads: SEM images

SI-3 Diffusion calculations with AQUASIM

SI-4 Statistical variations between different columns and packings

SI-5 Glass transitions and van't Hoff plots

SI-6 Influence of the relative humidity

SI-7 Detailed experimental results: humic acid/air partition coefficients at all relative humidities (<0.01%, 45%, 70%, 98%; Table SI-2) and at all temperatures (5 °C – 75 °C; Table SI-3)

SI-1 Chromatograms and Outliers

a) Chromatograms

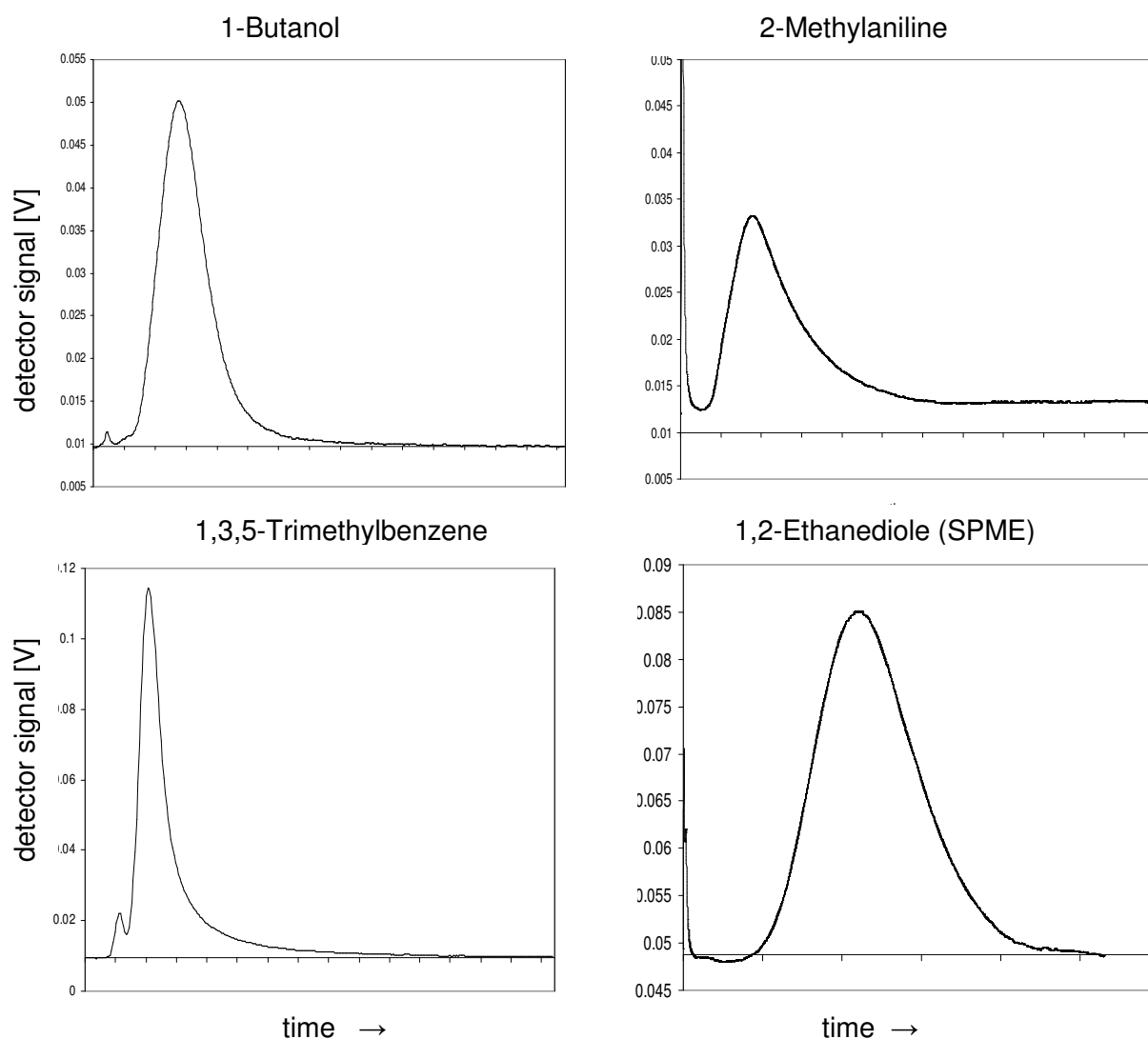
Figure SI-1 (below) shows four typical chromatograms determined in the IGC system. Generally, the peaks show slight tailing and peak broadening caused by diffusion and dispersion in the packed column. Besides the main peak, in all four chromatographs at least one additional peak is visible. These peaks result from contaminations in the pure compounds that were shipped in purities between 95% and 99.9%. However, in most cases it was easy to identify the main peak.

1-Butanol: 15 °C, injected volume: 10 µl headspace

2-Methylaniline: 15 °C, injected volume: 2500 µl headspace

1,3,5-Trimethylbenzene: 15 °C, injected volume: 10 µl headspace

1,2-Ethanediole: 45 °C, SPME injection (sorption to SPME fiber: 5 min; desorption in GC-injector: 5 sec)



b) Outliers

Aliphatic amines (methyl amine, diethyl amine, triethyl amine) and short-chained acids (formic acid, acetic acid) caused problems in the measurement and the evaluation of the peaks. Characteristic for the amines were abnormal peak forms and irreproducible retention volumes. Figure SI-2 shows the chromatogram of triethyl amine. The peak exhibits an extensive tailing. In addition, the retention volumes were irreproducible.

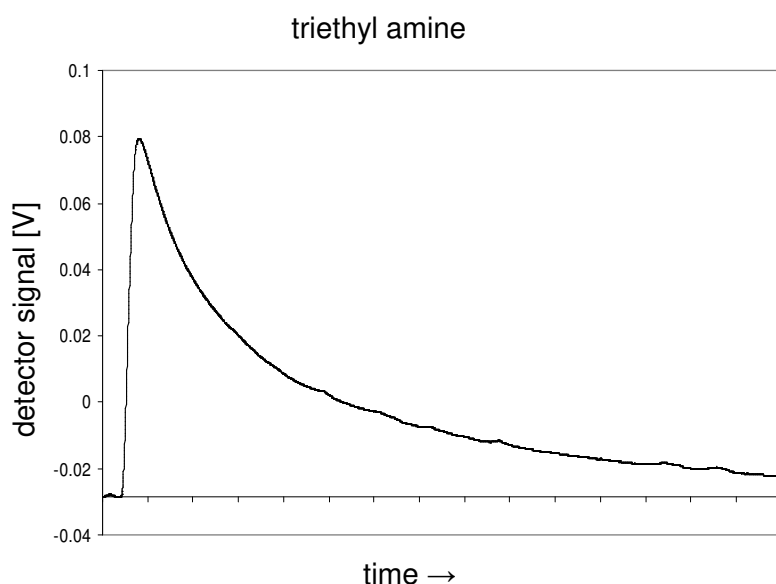


Figure SI-2 Peak shape of triethyl amine

Aliphatic amines are relatively strong organic bases with pK_a values of around 10.7 at 25 °C (methylamine: 10.66; ethylamine: 10.65; diethylamine: 10.60; triethylamine: 10.75 (1) in contrast to aromatic amines (aniline: 4.87; 2-methylaniline: 4.45; N,N-dimethylaniline: 5.12; 2,6-dimethylaniline: 3.89) or to pyridine ($pK_a = 5.23$) that showed normal behavior. We assume that acid-base reactions with the numerous carboxylic groups of the humic acids cause the abnormal behaviour of the amines. Carboxylic acids and some aliphatic amines can form dimers in the gas phase (2, 3) which might be responsible for the irreproducible retention volumes. Consequently, these substances were not considered in our dataset.

SI-2 Humic Acid Coatings on Glass Beads: SEM Images

Humic acid coated and uncoated Alltech glass beads were recorded by a scanning electron microscope SEM (Philips XL-30 with a LaB6 filament, Philips Electronics, Netherlands). The samples were coated with carbon using an evaporative coating device (Balzers CED 010, Balzers, FL) in order to increase the conductivity of the sample surface.

Figure SI-3A shows an Alltech glass bead without humic acid coating. The images SI-3 B-D show humic acid coatings on glass beads at different enlargements. In images SI-3 B-D the dark areas are uncoated glass bead surfaces. As indicated by image SI-3B, the coatings are relatively homogeneous, the layer thicknesses are everywhere $< 2\ \mu\text{m}$ according to images SI-3C, and SI-3D.

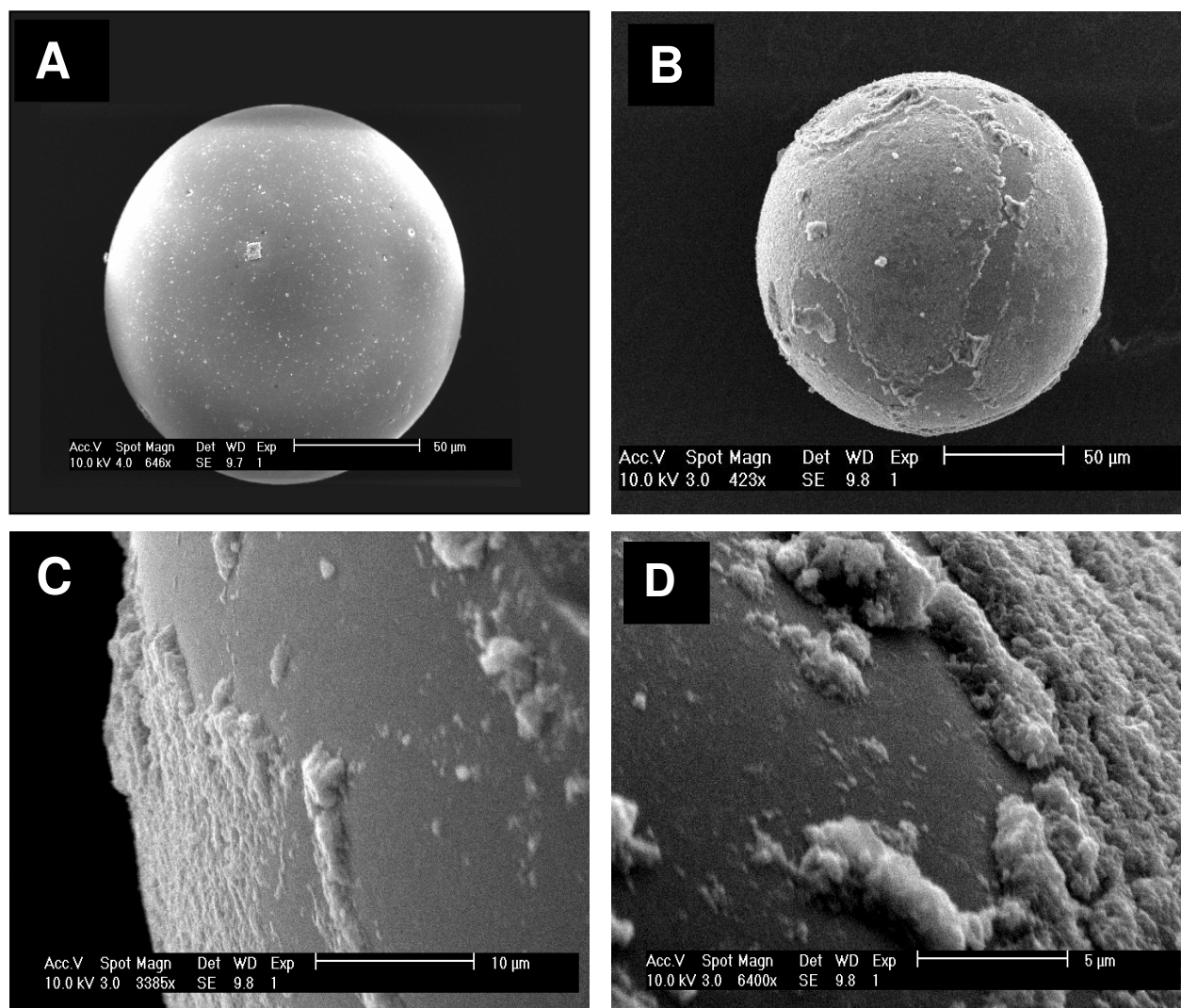


Figure SI-3: Scanning Electron Microscope images of Leonardite humic acid coatings on Alltech glassbeads

SI-3 Diffusion Calculations with AQUASIM

Realisation of sorption equilibrium in the IGC system is a fundamental requirement for the correct determination of sorption coefficients. The transport model AQUASIM (4) provides a tool to estimate whether a sorption equilibrium between sorbent and sorbate can theoretically be realized under given conditions. We performed the simulations with the following parameters that correspond to the conditions in our experimental system:

- volume flow rate: $20 \text{ ml} \cdot \text{min}^{-1}$ (linear velocity = $0.1 \text{ m} \cdot \text{s}^{-1}$)
- diffusion coefficient: $1 \cdot 10^{-9} \text{ cm}^2 \cdot \text{s}^{-1}$ (5, 6) conservative assumption for rubbery polymers
- diffusion length I: $1 \text{ } \mu\text{m}$
- diffusion length II: $2 \text{ } \mu\text{m}$

These conditions can be approximated by the following first-order rate constants:

$$1 \text{ } \mu\text{m} \rightarrow k = 7 \cdot 10^{-2} \text{ s}^{-1}$$

$$2 \text{ } \mu\text{m} \rightarrow k = 2.5 \cdot 10^{-1} \text{ s}^{-1}$$

Note: Doubling the diffusion length does not double the amount of humic acid in the model system because the total amount of humic acid in the system is set to be constant.

Figure SI-4 depicts the results for calculation of diffusion for a hypothetical compound under the mentioned conditions. Table 1 shows the evaluation of the peaks calculated by the model.

The peak maximum shifted significantly to shorter retention times for $2 \text{ } \mu\text{m}$ diffusion length compared to equilibrium conditions (-10%). However, the corresponding peak centres (which are the basis for our retention time analysis) do not change substantially.

These calculations confirm that our experimental data are at least a good approximation of the real equilibrium data for absorption into humic acid.

	diffusion length		
	equilibrium	1 μm	2 μm
peak maximum [ml]	62.27	61.85	56.28
peak centre [ml] (first moment)	61.80	62.67	62.99

Table SI-1: model outputs; for both diffusion length the amount of humic acid in the system is identical.

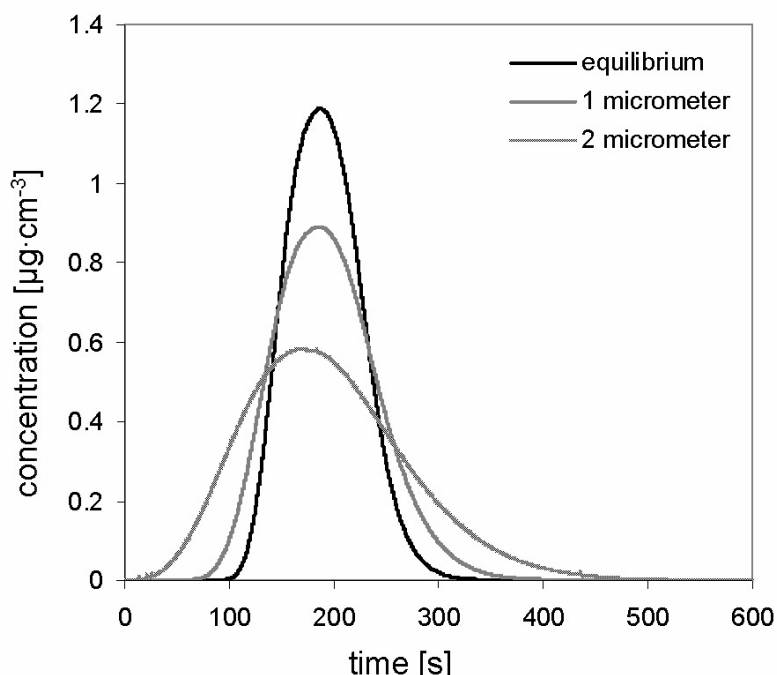


Figure SI-4: Breakthrough curves at equilibrium conditions, at 1 μm and at 2 μm diffusion length.

The AQUASIM calculations (for 2 μm thickness) further show that we would encounter significant non-equilibrium conditions for diffusion coefficients of $1\text{--}3 \cdot 10^{-10} \text{ cm}^2 \cdot \text{s}^{-1}$ which would become obvious when flow velocity is altered from 20 to 2 $\text{ml} \cdot \text{min}^{-1}$ (graph not shown). In our experiments variations of flow velocities in this range were without visible effect. For diffusion coefficients $\leq 3 \cdot 10^{-11} \text{ cm}^2 \cdot \text{s}^{-1}$ no sorption at all and no hint on non-equilibrium conditions would be visible in our experimental setup. However, such small diffusion coefficients appear to be not realistic. **Pulse-width correction:** The injected volume was always very small compared to the peak width of the compound and a correction of the pulse width was not necessary.

SI-4 Statistical variations between different columns and packings

Figure SI-5 shows experimental humic acid/air partition coefficients measured at equal experimental conditions (15 °C, 98% relative humidity; $n = 48$) using five different columns prepared separately. The total mass of coated Leonardite HA normalized to the surface area of the support material (glassbeads) in the five columns were: 0.09 g/m², 0.10 g/m², 0.10 g/m², 0.12 g/m², 0.15 g/m², and 0.41 g/m². Average standard deviation of non-logarithmic $K_{iHA,air}$: $\pm 38\%$.

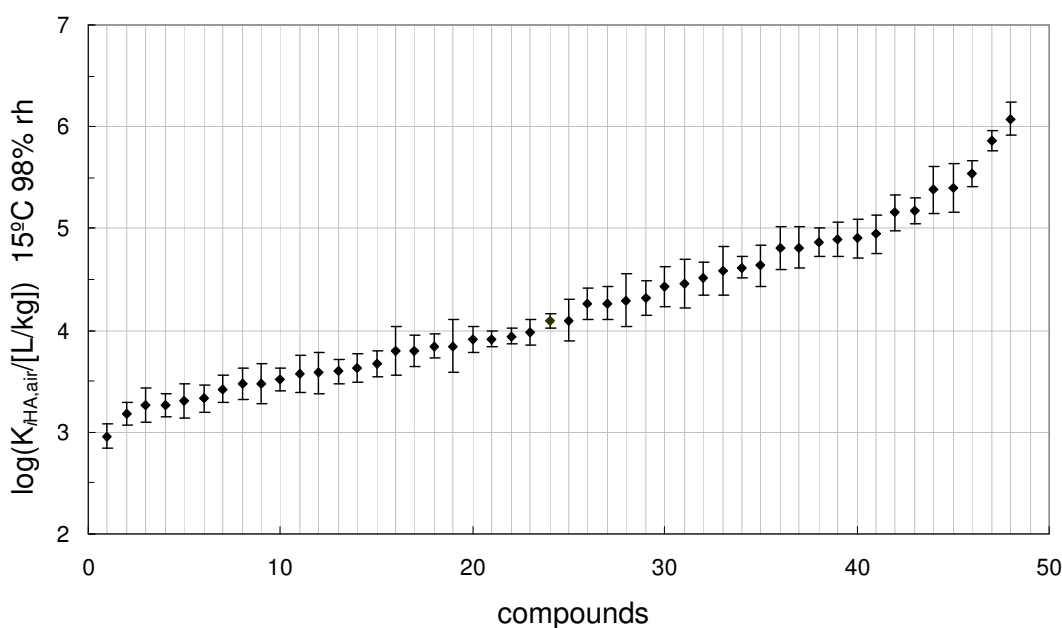


Figure SI-5. Humic acid/air partition coefficients measured at equal experimental conditions (15 °C, 98% relative humidity; $n = 48$) using five different columns prepared separately and varying only in coating thicknesses. Average standard deviation of non-logarithmic $K_{iHA,air}$: $\pm 38\%$.

As discussed in the text, the relative humidity had only a moderate influence on the sorption process. Because the systematic variations between different columns were almost in the same order of magnitude than the differences between partition coefficients determined at different rh, all rh-dependence measurements had to be conducted on the same column (Table SI-2). Therefore, our extensive dataset determined at 98% rh (Table SI-3) on a different column could not be used for the evaluation of the rh-dependence. This explains why two datasets at 15 °C/98% rh are presented in this paper that deviate

according to the reproducibility discussed above. The two datasets are compared in Figure SI-6. The relative precision is high while a slight systematic error can be observed.

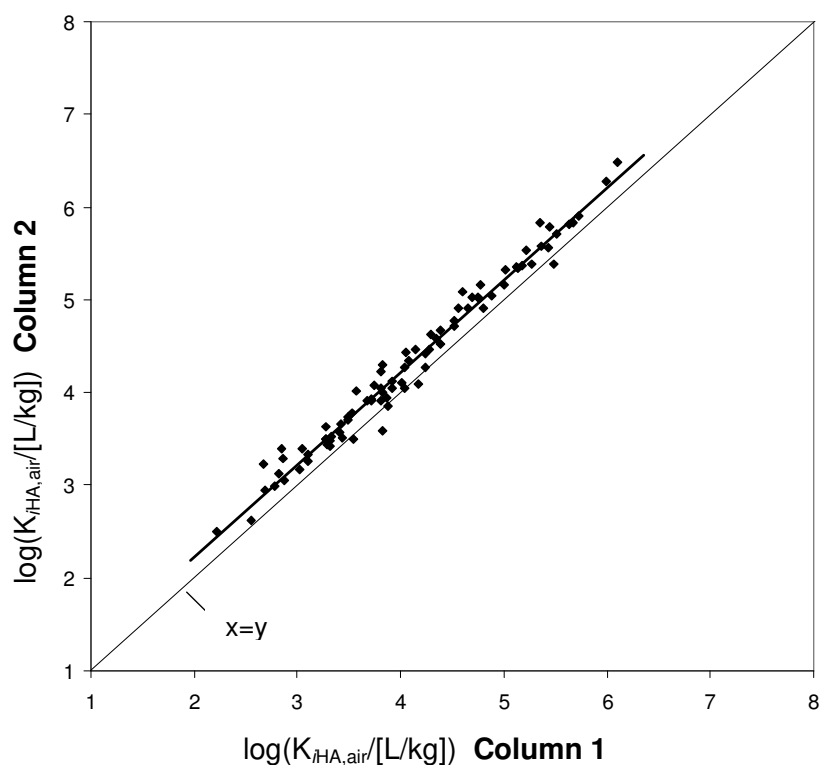


Figure SI-6 Column 1: dataset Table SI-3 (extensive dataset at 98% rh); Column 2: dataset Table SI-2 (influence of rh: dataset at 98%). Statistics: $r^2=0.98$, $n=86$, absolute error=0.22.

SI-5 Glass Transitions and van't Hoff Plots

Figure SI-7 shows the van't Hoff plot of an organic compound that sorbs into a rubbery polymer. As expected, a linear relationship is found. **Figure SI-8** shows the sorption of an organic compound into a polymer that exhibits glassy regions: the van't Hoff plot shows a linear shape up to the glass transition temperature (t_{glass}). At this temperature glassy regions are converted to rubbery domains. These rubberized domains become kinetically available for sorption (whereas the glassy regions are kinetically not available in terms of the conditions in IGC). This results in an enhanced sorption capacity (i.e., sorption sites that become available under the kinetic conditions in the IGC system) of the polymer causing an increase of the partition coefficient instead of a decrease (see also (7, 8)).

We measured humic acid/air partition coefficients for various compounds between 15°C and 75°C at 98% rh. We observed linear van't Hoff plots for all compounds indicating that Leonardite HA does not feature glass transitions that are relevant for the sorption capacity of this humic acid. All glass transitions that have so far been reported for hydrated humic material occurred at temperatures well below 75 °C (9-11). We therefore conclude that the Leonardite humic acid used in this study does not possess glassy domains that would have any significant impact on the sorption of organic compounds.

Figure SI-7

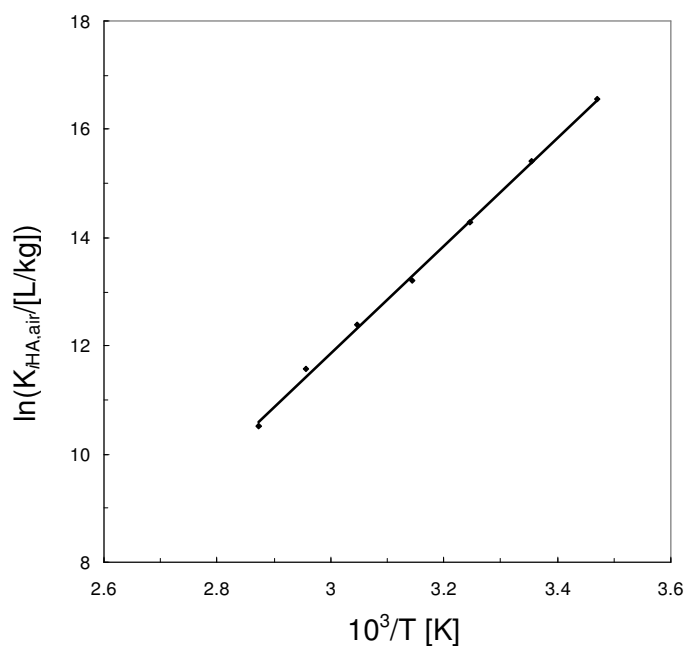


Figure SI-8

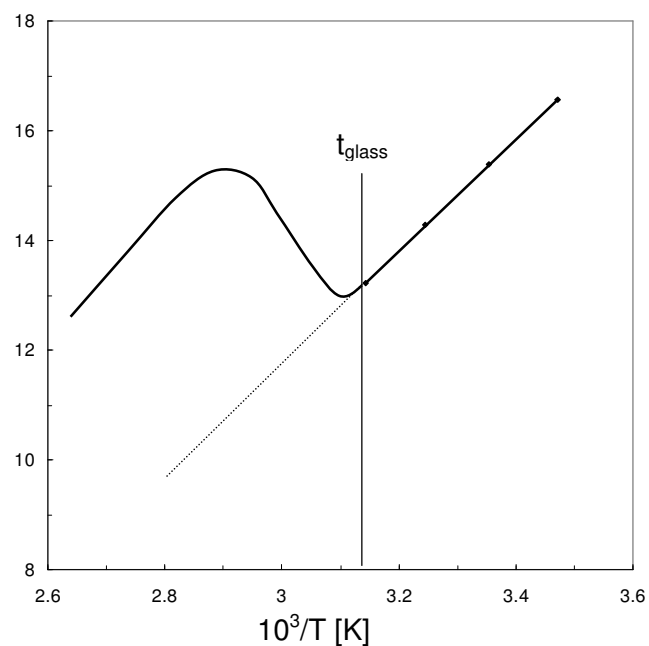
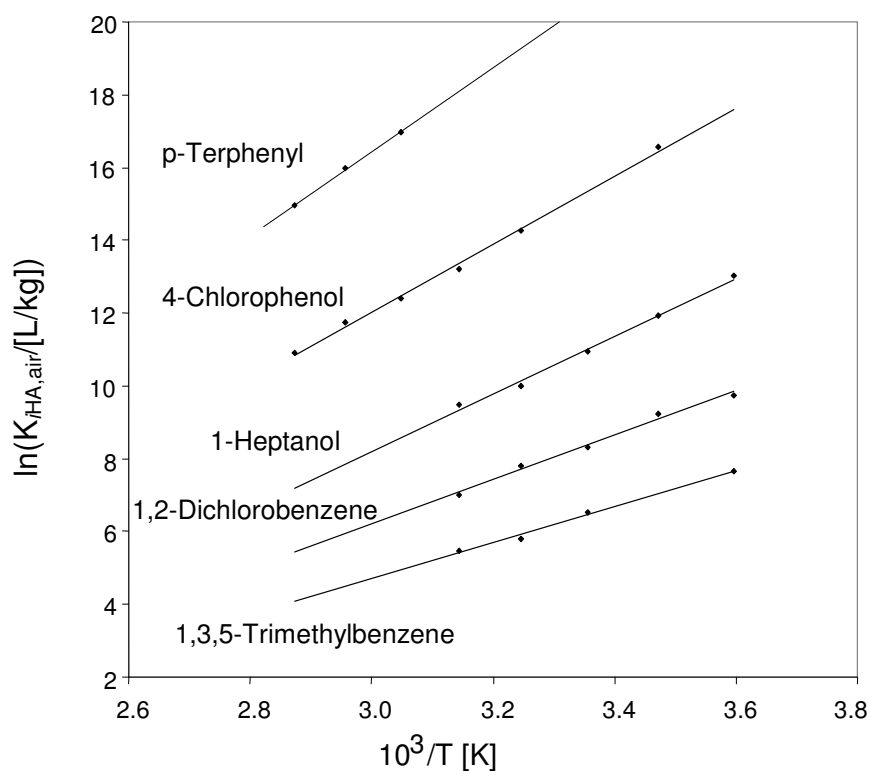


Figure SI-9 shows representative van't Hoff plots of five compounds from our dataset. As discussed in the main text, the plots are linear in the temperature range 15-75 °C. Please find experimental sorption enthalpies in Table SI-3.

Figure SI-9



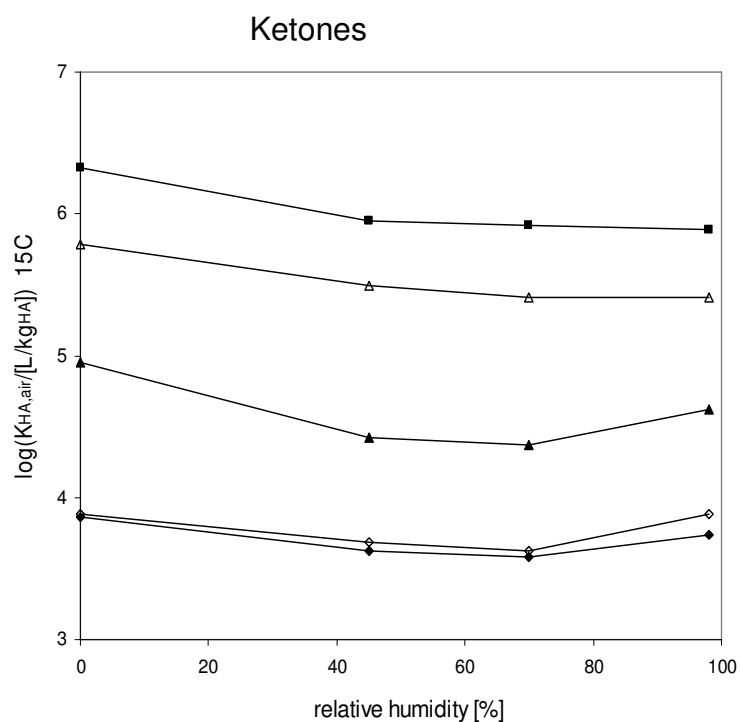
SI-6 Partition Coefficients as a Function of Relative Humidity

Figure SI-10, SI-11, and SI-12 show humic acid/air partition coefficients of ketones (Fig. SI-10), alcohols (Fig. SI-11) and alkanes (Fig. SI-12) as a function of relative humidity. All partition coefficients at <0.01%, 45%, 70% and 98% rh have been determined on one single column. This guarantees very low relative errors between the partition coefficients of one compound at different rh (<5% in the non-logarithmic partition coefficient).

Figure SI-10 indicates that the short-chain ketones (2-propanone, 2-butanone) exhibit comparable partition coefficients at <0.01% and 98% rh, while the partition coefficients at 45% and 70% rh are lower than at <0.01% and 98% (explanation see below). The long-chain ketones (2-heptanone, 2-nonanone, 2-decanone) show substantially lower partition coefficients at 98% than at <0.01% → with rising chain length the cavity energy increases while the gain of energy by the specific interactions remains constant.

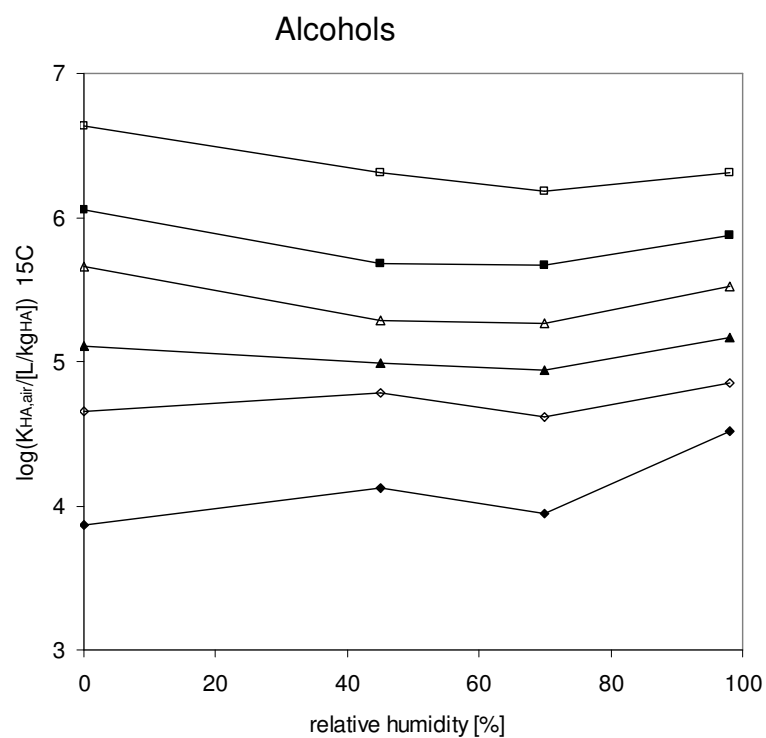
Figure SI-11: The short-chained alcohols (isopropanol, 1-butanol, 1-pentanol) exhibit higher partition coefficients at 98% rh than at <0.01% rh. These compounds are able to over-compensate the increased cavity energy in the wet humic by more electron donor/acceptor interactions in the hydrated matrix. The long-chained alcohols (1-hexanol, 1-heptanol and 1-octanol) sorb stronger in the dry humic acid than in the wet humic acid. This effect is more prominent the longer the C-chains are as already observed for the ketones. The sorption intensity for 1-pentanol, 1-hexanol, 1-heptanol and 1-octanol decreases from <0.01% to 45% rh, remains almost constant from 45% to 70% rh and increases again from 70% to 98% rh. This can be explained by the increasing cavity energy (at increasing rh) that negatively affects sorption; but with increasing water content of the humic acid its polarity increases favouring electron donor/acceptor interactions of the alcohols with the phase. This effect can also be observed for the short-chained ketones.

Figure SI-10



(◆) Propanone (◇) 2-Butanone (▲) 2-Heptanone (△) 2-Nonanone (■) 2-Decanone

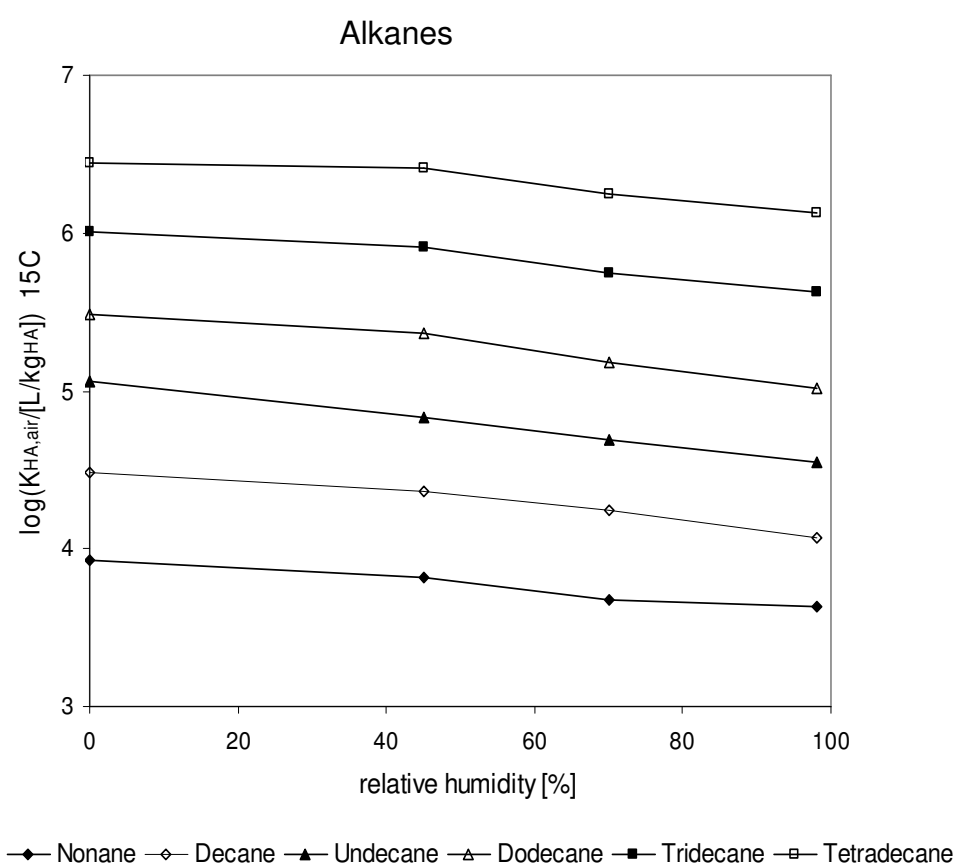
Figure SI-11



(◇) 1-Butanol (▲) 1-Pentanol (△) 1-Hexanol (■) 1-Heptanol (◆) Isopropanol (□) 1-Octanol

Figure SI-12: All alkanes exhibit higher partition coefficients in the dry humic acid than in the wet humic acid. In addition, with increasing rh that goes along with increasing cavity energy the partition coefficients of all alkanes decrease. Alkanes only interact nonspecifically with the humic acid (i.e., no electron donor/acceptor interactions) and the increasing cavity energy requirements at increasing rh cannot be compensated with more EDA-interactions in the hydrated matrix.

Figure SI-12



SI-7 Extended Tables

Please note: Table SI-2 and SI-3 overlap in the dataset for $K_{iHA,air}$ values at 15 °C and 98% rh (as discussed in SI-4). Nevertheless, the two datasets are not identical because they have not been measured with the same column. Such differences between separately prepared columns and column packings typically amounted to an average standard deviation of 0.17 log units.

Table SI-2: Leonardite humic acid/air partition coefficients at 15 °C and various relative humidities

CAS	Compound	$K_{iHA,air}$ [L/kg _{HA}] <0.01% rh 15 °C	$K_{iHA,air}$ [L/kg _{HA}] 45% rh 15 °C	$K_{iHA,air}$ [L/kg _{HA}] 70% rh 15 °C	$K_{iHA,air}$ [L/kg _{HA}] 98% rh 15 °C
111-84-2	n-Nonane	2.64E+03	2.06E+03	1.48E+03	1.35E+03
124-18-5	n-Decane	9.60E+03	7.21E+03	5.47E+03	3.73E+03
1120-21-4	n-Undecane	3.64E+04	2.12E+04	1.56E+04	1.12E+04
112-40-3	n-Dodecane	9.61E+04	7.37E+04	4.84E+04	3.32E+04
629-50-5	n-Tridecane	2.94E+05	2.26E+05	1.59E+05	1.11E+05
629-59-4	n-Tetradecane	8.79E+05	8.05E+05	5.62E+05	3.65E+05
293-96-9	Cyclodecane	7.54E+02	3.54E+02	3.34E+02	3.02E+02
292-64-8	Cyclooctane	1.46E+03	1.14E+03	1.14E+03	4.93E+02
124-11-8	1-Nonene	2.63E+03	1.34E+03	1.79E+03	8.91E+02
872-05-9	1-Decene	9.62E+03	7.94E+03	6.00E+03	4.32E+03
821-95-4	1-Undecene	2.97E+04	2.42E+04	1.84E+04	1.97E+04
112-41-4	1-Dodecene	9.68E+04	6.98E+04	5.23E+04	3.79E+04
2437-56-1	1-Tridecene	2.74E+05	2.00E+05	1.95E+05	1.47E+05
64-17-5	Ethanol	4.00E+03	1.15E+04	5.55E+03	8.20E+03
71-23-8	Propan-1-ol	7.86E+03	1.32E+04	8.18E+03	1.11E+04
71-36-3	Butan-1-ol	1.44E+04	1.91E+04	1.29E+04	2.23E+04
71-41-0	Pentan-1-ol	4.06E+04	3.06E+04	2.75E+04	4.69E+04
111-27-3	Hexan-1-ol	1.45E+05	6.08E+04	5.89E+04	1.04E+05
111-70-6	Heptan-1-ol	3.60E+05	1.51E+05	1.49E+05	2.37E+05
111-87-5	Octan-1-ol	1.38E+06	6.52E+05	4.80E+05	6.52E+05
67-63-0	Propan-2-ol	2.34E+03	4.21E+03	2.79E+03	1.04E+04
78-83-1	2-Methylpropan-1-ol	6.01E+03	3.56E+03	3.88E+03	3.82E+03
123-51-3	3-Methylbutan-1-ol	2.93E+04	1.07E+04	1.06E+04	2.62E+04
100-51-6	Benzyl alcohol	1.46E+06	2.14E+06	2.02E+06	3.00E+06
96-41-3	Cyclopentanol	2.70E+04	3.60E+04	2.71E+04	8.23E+04
75-89-8	2,2,2-Trifluoroethanol	1.73E+03	1.53E+03	1.14E+03	4.50E+03
920-66-1	Hexafluoropropan-2-ol	3.81E+03	3.36E+03	4.26E+03	7.10E+03
108-95-2	Phenol	7.97E+05	1.77E+06	9.67E+05	1.92E+06
95-57-8	2-Chlorophenol	2.37E+05	1.34E+05	2.23E+05	6.12E+05
67-64-1	2-Propanone	2.30E+03	1.33E+03	1.20E+03	1.72E+03
78-93-3	2-Butanone	2.40E+03	1.73E+03	1.34E+03	2.44E+03

CAS	Compound	$K_{iHA,air}$ [L/kg _{HA}] <0.01% rh 15 °C	$K_{iHA,air}$ [L/kg _{HA}] 45% rh 15 °C	$K_{iHA,air}$ [L/kg _{HA}] 70% rh 15 °C	$K_{iHA,air}$ [L/kg _{HA}] 98% rh 15 °C
107-87-9	2-Pentanone	4.15E+03	1.09E+03	1.47E+03	3.09E+03
591-78-6	2-Hexanone	1.50E+04	3.47E+03	2.38E+03	5.35E+03
110-43-0	2-Heptanone	2.84E+04	8.41E+03	7.38E+03	1.32E+04
111-13-7	2-Octanone	9.60E+04	2.48E+04	1.70E+04	2.93E+04
821-55-6	2-Nonanone	1.93E+05	9.89E+04	8.13E+04	8.13E+04
693-54-9	2-Decanone	6.74E+05	2.84E+05	2.63E+05	2.45E+05
112-12-9	2-Undecanone	1.77E+06	1.29E+06	5.81E+05	6.69E+05
108-10-1	4-Methylpentan-2-one	6.69E+03	1.24E+03	1.05E+03	2.66E+03
120-92-3	Cyclopentanone	1.25E+04	1.43E+04	1.23E+04	2.67E+04
108-94-1	Cyclohexanone	3.38E+04	1.52E+04	1.14E+04	4.23E+04
502-42-1	Cycloheptanone	1.06E+05	5.00E+04	4.76E+04	1.06E+05
98-86-2	Acetophenone	3.67E+05	1.86E+05	1.91E+05	3.46E+05
109-60-4	n-Propyl acetate	5.03E+03	1.22E+03	1.48E+03	1.93E+03
123-86-4	n-Butyl acetate	8.18E+03	2.18E+03	2.69E+03	2.69E+03
628-63-7	n-Pentyl acetate	2.95E+04	9.77E+03	7.32E+03	8.28E+03
93-58-3	Methyl benzoate	1.03E+05	6.96E+04	7.93E+04	1.46E+05
693-65-2	Di-n-pentylether	9.46E+04	3.19E+04	2.70E+04	1.89E+04
108-20-3	Isopropylether	5.99E+02	3.35E+02	2.89E+02	5.93E+02
123-91-1	1,4-Dioxane	4.68E+03	1.22E+04	7.00E+03	1.69E+04
100-66-3	Methyl phenyl ether	8.62E+03	5.13E+03	4.62E+03	8.49E+03
106-42-3	p-Xylene	2.76E+03	1.27E+03	1.47E+03	1.14E+03
100-41-4	Ethylbenzene	2.20E+03	1.23E+03	1.16E+03	9.69E+02
103-65-1	n-Propylbenzene	5.97E+03	3.13E+03	2.75E+03	1.84E+03
104-51-8	n-Butylbenzene	1.55E+04	9.98E+03	8.04E+03	6.11E+03
538-68-1	n-Pentylbenzene	5.21E+04	3.03E+04	2.94E+04	1.88E+04
1077-16-3	n-Hexylbenzene	2.41E+05	1.17E+05	1.68E+05	6.01E+04
95-63-6	1,2,4-Trimethylbenzene	9.35E+03	5.80E+03	5.47E+03	3.41E+03
108-67-8	1,3,5-Trimethylbenzene	6.23E+03	4.42E+03	3.64E+03	2.48E+03
496-11-7	Indane	1.07E+04	7.25E+03	5.64E+03	4.99E+03
91-20-3	Naphthalene	1.02E+05	6.52E+04	6.53E+04	8.06E+04
90-12-0	1-Methylnaphthalene	3.60E+05	2.20E+05	1.97E+05	2.43E+05
95-50-1	1,2-Dichlorobenzene	1.81E+04	1.12E+04	1.03E+04	1.28E+04
541-73-1	1,3-Dichlorobenzene	1.24E+04	8.51E+03	7.61E+03	8.32E+03
106-46-7	1,4-Dichlorobenzene	1.36E+04	8.86E+03	7.57E+03	8.67E+03
120-82-1	1,2,4-Trichlorobenzene	9.46E+04	5.53E+04	5.74E+04	5.16E+04
634-66-2	1,2,3,4-Tetrachlorobenz.	7.28E+05	3.15E+05	4.25E+05	3.84E+05
634-90-2	1,2,3,5-Tetrachlorobenz.	3.35E+05	2.27E+05	2.11E+05	2.17E+05
462-06-6	Fluorobenzene	7.01E+02	4.23E+02	3.00E+02	3.13E+02
108-90-7	Chlorobenzene	2.38E+03	1.20E+03	1.32E+03	1.32E+03
108-86-1	Bromobenzene	6.16E+03	3.39E+03	2.68E+03	3.19E+03
591-50-4	Iodobenzene	1.81E+04	1.08E+04	8.56E+03	1.11E+04
629-06-1	1-Chloroheptane	5.86E+03	3.99E+03	3.41E+03	2.12E+03
111-85-3	1-Chlorooctane	2.17E+04	1.72E+04	1.14E+04	1.00E+04

CAS	Compound	$K_{iHA,air}$ [L/kg _{HA}] <0.01% rh 15 °C	$K_{iHA,air}$ [L/kg _{HA}] 45% rh 15 °C	$K_{iHA,air}$ [L/kg _{HA}] 70% rh 15 °C	$K_{iHA,air}$ [L/kg _{HA}] 98% rh 15 °C
100-52-7	Benzaldehyde	3.45E+04	4.67E+04	4.54E+04	1.07E+05
109-74-0	1-Cyanopropane	3.71E+03	2.10E+03	2.68E+03	3.26E+03
98-95-3	Nitrobenzene	1.43E+05	9.84E+04	1.28E+05	2.08E+05
88-72-2	2-Nitrotoluene	2.09E+05	1.05E+05	1.36E+05	2.29E+05
100-47-0	Benzonitrile	5.30E+04	4.53E+04	6.35E+04	1.20E+05
75-52-5	Nitromethane	1.56E+03	4.27E+03	2.65E+03	3.11E+03
79-24-3	Nitroethane	2.39E+03	3.36E+03	3.43E+03	3.04E+03
108-03-2	1-Nitropropane	2.03E+03	1.51E+03	2.03E+03	2.99E+03
79-46-9	2-Nitropropane	8.98E+02	5.10E+02	1.16E+03	1.48E+03
79-09-4	Propanoic acid	1.64E+05	3.92E+05	5.17E+05	5.18E+05
107-92-6	Butanoic acid	5.31E+05	9.41E+05	7.48E+05	8.13E+05
110-02-1	Thiophene	5.02E+02	3.08E+02	5.02E+02	4.18E+02
108-98-5	Thiophenol	9.31E+03	1.03E+04	8.80E+03	1.24E+04
123-54-6	2,4-Pentanedione	1.68E+04	2.85E+04	1.79E+04	2.93E+04
78-95-5	Chloroacetone	5.42E+03	1.40E+04	8.84E+03	1.17E+04
106-65-0	Dimethyl succinate	6.58E+05	1.05E+06	5.40E+05	6.83E+05

Table SI-3 Leonardite humic acid/air partition coefficients at 98% rh and various temperatures; values in bold are extrapolated to 15 °C using $\Delta_{\text{abs}}H_i$ (experimental sorption enthalpy); n: amount of data points for Van't Hoff plots; r^2 : correlation coefficient for Van't Hoff plot; n.d.: not determined; $K_{i\text{HA,air}}$ are in [L/kg_{HA}]

CAS	Compound	<i>exp.</i> $K_{\text{HA,air}}$ 5 °C	<i>exp.</i> $K_{\text{HA,air}}$ 15 °C	<i>exp.</i> $K_{\text{HA,air}}$ 25 °C	<i>exp.</i> $K_{\text{HA,air}}$ 35 °C	<i>exp.</i> $K_{\text{HA,air}}$ 45 °C	<i>exp.</i> $K_{\text{HA,air}}$ 55 °C	<i>exp.</i> $K_{\text{HA,air}}$ 65 °C	<i>exp.</i> $K_{\text{HA,air}}$ 75 °C	n	<i>exp.</i> $\Delta_{\text{abs}}H$ [kJ/mol]	r^2
111-65-9	n-Octane	5.17E+02	1.46E+02								<i>n.d.</i>	
111-84-2	n-Nonane	1.61E+02	6.61E+02	6.50E+02							<i>n.d.</i>	
124-18-5	n-Decane	4.64E+03	2.59E+03	1.15E+03	7.79E+02					4	-46.4	0.988
1120-21-4	n-Undecane	1.75E+04	8.18E+03	3.67E+03	1.17E+03	7.65E+02				5	-62.8	0.987
112-40-3	n-Dodecane	5.68E+04	2.41E+04	1.09E+04	4.11E+03					4	-64.1	0.996
629-50-5	n-Tridecane	1.74E+05	7.55E+04	3.60E+04	1.69E+04	7.57E+03				5	-59.6	0.999
629-59-4	n-Tetradecane		2.69E+05	1.17E+05	3.23E+04	1.49E+04				4	-78.4	0.990
293-96-9	Cyclodecane	9.67E+03	4.86E+03	2.64E+03	1.20E+03					4	-51.2	0.995
111-66-0	1-Octene	7.67E+02	1.19E+02								<i>n.d.</i>	
124-11-8	1-Nonene	1.43E+03	4.87E+02	6.41E+02							<i>n.d.</i>	
872-05-9	1-Decene	3.65E+03	1.90E+03	1.04E+03	6.46E+02	3.86E+02				5	-43.5	0.999
821-95-4	1-Undecene	1.53E+04	6.77E+03	3.33E+03	1.72E+03					4	-54.2	1.000
112-41-4	1-Dodecene	4.17E+04	2.25E+04	1.11E+04	4.20E+03	1.86E+03				5	-60.3	0.986
2437-56-1	1-Tridecene	1.71E+05	5.87E+04	3.08E+04	1.14E+04	4.74E+03				5	-67.2	0.995
64-17-5	Ethanol	1.08E+04	4.81E+03		1.96E+03	1.13E+03				4	-42.3	0.991
71-23-8	Propan-1-ol	1.43E+04	6.56E+03		2.27E+03	1.54E+03				4	-43.2	0.993
71-36-3	Butan-1-ol	2.82E+04	1.21E+04	5.26E+03	2.32E+03	1.45E+03				5	-58.4	0.996
71-41-0	Pentan-1-ol	5.90E+04	2.45E+04	1.10E+04	4.67E+03	2.51E+03				5	-61.2	0.999
111-27-3	Hexan-1-ol	1.49E+05	5.78E+04	2.59E+04	9.32E+03	5.18E+03				5	-65.3	0.997
111-70-6	Heptan-1-ol	4.47E+05	1.50E+05	5.67E+04	2.23E+04	1.31E+04				5	-68.6	0.994
111-87-5	Octan-1-ol		4.27E+05	1.62E+05	5.53E+04	2.47E+04				4	-75.8	0.998
143-08-8	Nonan-1-ol		1.37E+06	4.00E+05	1.45E+05	5.55E+04				4	-83.5	0.999
112-30-1	Decan-1-ol		2.66E+06		3.76E+05	1.25E+05				3	-79.2	0.997

CAS	Compound	<i>exp.</i> $K_{HA,air}$ 5 °C	<i>exp.</i> $K_{HA,air}$ 15 °C	<i>exp.</i> $K_{HA,air}$ 25 °C	<i>exp.</i> $K_{HA,air}$ 35 °C	<i>exp.</i> $K_{HA,air}$ 45 °C	<i>exp.</i> $K_{HA,air}$ 55 °C	<i>exp.</i> $K_{HA,air}$ 65 °C	<i>exp.</i> $K_{HA,air}$ 75 °C	n	<i>exp.</i> $\Delta_{abs}H$ [kJ/mol]	r^2
112-42-5	Undecan-1-ol		3.86E+06				1.00E+05	5.38E+04	2.21E+04	3	-73.8	0.985
67-63-0	Propan-2-ol	9.09E+03	3.66E+03	1.95E+03	1.04E+03					4	-53.3	0.995
78-83-1	2-Methylpropan-1-ol	1.45E+04	6.64E+03	2.60E+03	1.31E+03	6.49E+02				5	-60.1	0.999
75-65-0	2-Methylpropan-2-ol	8.51E+03	3.98E+03	2.71E+03	1.33E+03					4	-44.9	0.986
123-51-3	3-Methylbutan-1-ol	4.25E+04	1.71E+04	7.76E+03	3.20E+03	1.55E+03				5	-63.5	0.999
104-76-7	2-Ethyl-1-hexanol		2.37E+05	8.30E+04	3.13E+04	1.19E+04				4	-78.2	1.000
821-41-0	5-Hexen-1-ol	2.26E+05	8.89E+04	4.09E+04	1.70E+04	6.80E+03				5	-66.1	0.997
100-51-6	Benzyl alcohol		1.26E+06	5.02E+05	2.02E+05	9.37E+04				4	-68.9	1.000
90-15-3	1-Naphthol		1.57E+08		1.41E+07		1.74E+06	6.21E+05		3	-92.1	1.000
96-41-3	Cyclopentanol	9.20E+04	3.65E+04	1.62E+04	8.20E+03	4.69E+03				5	-57.4	0.997
108-93-0	Cyclohexanol	2.51E+05	8.30E+04	4.19E+04	1.81E+04	9.39E+03				5	-62.1	0.996
75-89-8	2,2,2-Trifluoroethanol		2.64E+03	1.46E+03	9.35E+02					3	-40.8	0.997
920-66-1	Hexafluoropropan-2-ol	1.90E+04	7.62E+03	3.29E+03	1.52E+03	7.96E+02				4	-61.2	0.999
108-95-2	Phenol	2.08E+06	9.90E+05	4.16E+05		7.12E+04				4	-65.1	0.994
95-48-7	o-Cresol (2-Methylphenol)		9.04E+05	3.17E+05	1.43E+05	6.47E+04	3.34E+04			5	-67.0	0.998
108-39-4	m-Cresol (3-Methylphenol)		3.18E+06	6.99E+05	3.16E+05		7.35E+04			4	-74.4	0.978
106-44-5	p-Cresol (4-Methylphenol)		3.01E+06	7.63E+05	3.35E+05	1.38E+05	7.10E+04			5	-75.1	0.990
95-57-8	2-Chlorophenol	5.90E+05	2.77E+05	1.34E+05	5.01E+04	2.60E+04				5	-60.9	0.995
106-48-9	4-Chlorophenol		1.55E+07		1.59E+06	5.47E+05	2.40E+05	1.26E+05	3.67E+04	6	-83.9	0.999
6640-27-3	2-Chloro-4-methylphenol		4.44E+05	2.51E+05	1.20E+05	6.09E+04				4	-53.4	0.994
576-24-9	2,3-Dichlorophenol		2.28E+06	7.47E+05	3.51E+05	2.08E+05				4	-63.2	0.981
87-65-0	2,6-Dichlorophenol		7.43E+05	4.65E+05	2.20E+05	1.28E+05				4	-48.2	0.991
95-95-4	2,4,5-Trichlorophenol		1.21E+08		5.64E+06	1.14E+06	2.13E+05		2.70E+04	4	-121.7	0.999
88-06-2	2,4,6-Trichlorophenol		1.60E+08			2.44E+06	1.19E+06	2.39E+05		3	-105.6	0.947
67-64-1	2-Propanone	1.87E+03	4.76E+02								<i>n.d.</i>	
78-93-3	2-Butanone	2.43E+03	7.08E+02	7.59E+02							<i>n.d.</i>	
107-87-9	2-Pentanone	3.69E+03	1.89E+03	1.04E+03	5.42E+02	4.34E+02				4	-43.3	0.984
591-78-6	2-Hexanone	5.84E+03	3.10E+03		8.12E+02					3	-49.6	0.998

CAS	Compound	<i>exp.</i> $K_{HA,air}$ 5 °C	<i>exp.</i> $K_{HA,air}$ 15 °C	<i>exp.</i> $K_{HA,air}$ 25 °C	<i>exp.</i> $K_{HA,air}$ 35 °C	<i>exp.</i> $K_{HA,air}$ 45 °C	<i>exp.</i> $K_{HA,air}$ 55 °C	<i>exp.</i> $K_{HA,air}$ 65 °C	<i>exp.</i> $K_{HA,air}$ 75 °C	n	<i>exp.</i> $\Delta_{abs}H$ [kJ/mol]	r^2
108-88-3	Toluene	3.70E+02	1.94E+02								<i>n.d.</i>	
106-42-3	p-Xylene	6.58E+02	7.58E+02								<i>n.d.</i>	
100-41-4	Ethylbenzene	5.89E+02	6.09E+02	3.82E+02							<i>n.d.</i>	
103-65-1	n-Propylbenzene		1.25E+03	8.84E+02	3.29E+02					3	-51.3	0.917
104-51-8	n-Butylbenzene	5.86E+03	3.41E+03	1.64E+03	8.78E+02					4	-48.1	0.994
538-68-1	n-Pentylbenzene	2.00E+04	1.08E+04	4.27E+03	2.14E+03					4	-56.7	0.992
1077-16-3	n-Hexylbenzene	8.67E+04	3.36E+04	1.80E+04	6.03E+03	2.69E+03				5	-66.1	0.992
95-63-6	1,2,4-Trimethylbenzene	3.08E+03	2.14E+03		4.72E+02	3.14E+02				4	-47.1	0.983
108-67-8	1,3,5-Trimethylbenzene	2.11E+03	1.13E+03	6.72E+02	3.28E+02	2.40E+02				4	-43.7	0.992
100-42-5	Styrene	3.03E+03	2.18E+03		8.36E+02	7.48E+02				4	-30.2	0.978
496-11-7	Indane	5.20E+03	3.07E+03	1.74E+03	1.37E+03	9.95E+02				4	-32.9	0.980
91-20-3	Naphthalene	1.05E+05	4.58E+04	2.99E+04	1.32E+04	5.58E+03				5	-54.7	0.984
90-12-0	1-Methylnaphthalene		3.01E+05	8.97E+04	3.63E+04	1.35E+04	6.92E+03			5	-76.9	0.996
83-32-9	Acenaphthene		5.62E+05	1.99E+05	1.21E+05					3	-59.3	0.967
120-12-7	Anthracene		1.93E+07		1.91E+06	9.31E+05	4.20E+05	1.79E+05	7.06E+04	5	-79.6	0.997
85-01-8	Phenanthrene		1.48E+07		1.71E+06	6.62E+05	3.03E+05	1.35E+05	6.32E+04	5	-79.0	0.996
92-52-4	Biphenyl		3.76E+05	1.50E+05	7.80E+04	3.45E+04	1.13E+04			5	-68.9	0.987
92-94-4	p-Terphenyl		3.11E+09				2.37E+07	8.59E+06	3.10E+06	3	-98.7	0.999
108-90-7	Chlorobenzene	1.68E+03	1.13E+03	8.13E+02						3	-27.4	0.999
95-50-1	1,2-Dichlorobenzene	1.70E+04	1.02E+04	4.11E+03	2.45E+03	1.08E+03				5	-53.3	0.989
541-73-1	1,3-Dichlorobenzene	1.06E+04	6.46E+03	2.87E+03	1.65E+03	7.24E+02				5	-51.8	0.988
106-46-7	1,4-Dichlorobenzene		7.37E+03	3.43E+03	2.18E+03	9.19E+02				4	-53.5	0.985
106-37-6	1,4-Dibromobenzene	1.10E+05	4.86E+04	2.40E+04	1.23E+04	5.37E+03				5	-56.9	0.997
615-42-9	1,2-Diiodobenzene		7.66E+05	3.78E+05	1.71E+05	5.77E+04				4	-67.4	0.983
624-38-4	1,4-Diiodobenzene		2.79E+06	6.55E+05	1.71E+05	4.65E+04				3	-106.7	1.000
120-82-1	1,2,4-Trichlorobenzene	5.75E+04	3.27E+04	1.73E+04	7.87E+03	3.65E+03				5	-53.3	0.988
634-66-2	1,2,3,4-Tetrachlorobenzene	3.90E+05	2.31E+05	8.64E+04	3.86E+04					4	-58.6	0.982
634-90-2	1,2,3,5-Tetrachlorobenzene	1.84E+05	1.39E+05	6.02E+04	3.18E+04					4	-45.6	0.960
95-94-3	1,2,4,5-Tetrachlorobenzene	1.60E+06	6.14E+05	2.49E+05						3	-66.3	1.000

CAS	Compound	exp. $K_{HA,air}$ 5 °C	exp. $K_{HA,air}$ 15 °C	exp. $K_{HA,air}$ 25 °C	exp. $K_{HA,air}$ 35 °C	exp. $K_{HA,air}$ 45 °C	exp. $K_{HA,air}$ 55 °C	exp. $K_{HA,air}$ 65 °C	exp. $K_{HA,air}$ 75 °C	n	exp. $\Delta_{abs}H$ [kJ/mol]	r^2
608-93-5	Pentachlorobenzene		1.13E+06		1.40E+05	7.96E+04				3	-71.3	0.989
118-74-1	Hexachlorobenzene		3.19E+06	1.62E+06		2.09E+05	3.31E+04			4	-89.9	0.961
462-06-6	Fluorobenzene	1.87E+02	1.63E+02								<i>n.d.</i>	
108-86-1	Bromobenzene		3.45E+03	1.86E+03	1.17E+03	6.26E+02				4	-45.0	0.995
591-50-4	Iodobenzene		1.08E+04	5.20E+03	2.15E+03					4	-61.9	0.995
352-32-9	4-Fluorotoluene	3.35E+02	3.96E+02	2.23E+02							<i>n.d.</i>	
98-56-6	4-Chlorobenzotrifluoride	1.73E+03	1.00E+03	5.69E+02						3	-40.7	0.996
630-20-6	1,1,1,2-Tetrachloroethane	1.49E+03	1.02E+03		4.97E+02	4.20E+02				3	-26.4	0.991
79-34-5	1,1,2,2-Tetrachloroethane	9.25E+03	5.06E+03	2.27E+03	9.83E+02	5.76E+02				5	-55.3	0.994
544-10-5	1-Chlorohexane	4.68E+02	3.19E+02								<i>n.d.</i>	
629-06-1	1-Chloroheptane	1.95E+03	1.26E+03	7.90E+02	4.27E+02					4	-38.2	0.987
111-85-3	1-Chlorooctane	1.19E+04	6.63E+03	2.93E+03	1.45E+03	1.15E+03				5	-48.1	0.982
1002-69-3	1-Chlorodecane	1.33E+05	4.72E+04	2.34E+04	1.08E+04	5.86E+03				5	-59.4	0.997
110-53-2	1-Bromopentane	9.22E+01	2.09E+02								<i>n.d.</i>	
123-72-8	Butanal/Butyraldehyde	4.89E+02	2.57E+02	1.87E+02						3	-35.5	0.970
110-62-3	Pentanal	1.08E+03	3.92E+02								<i>n.d.</i>	
100-52-7	Benzaldehyde	9.81E+04	4.97E+04	2.93E+04	1.22E+04	7.85E+03				5	-49.9	0.992
109-74-0	1-Cyanopropane	3.71E+03	2.74E+03	1.43E+03		6.01E+02				4	-37.1	0.987
62-53-3	Aniline		6.49E+05	2.36E+05	1.11E+05	4.59E+04	1.76E+04			5	-72.0	0.997
95-53-4	o-Toluidine (2-Methylaniline)		6.58E+05	2.83E+05	1.16E+05	5.74E+04				4	-65.0	0.999
106-49-0	p-Toluidine (4-Methylaniline)		4.28E+06	1.06E+06	4.29E+05	1.51E+05				4	-85.9	0.995
87-62-7	2,6-Dimethylaniline		5.73E+05	2.56E+05	9.30E+04	4.59E+04				4	-67.9	0.996
121-69-7	N,N-Dimethylaniline	2.42E+05	1.31E+05	5.11E+04	1.69E+04	9.52E+03				5	-65.0	0.987
615-43-0	2-Iodoaniline		2.83E+06		2.55E+05	1.05E+05	3.18E+04			3	-89.9	0.999
540-37-4	4-Iodoaniline		1.26E+07		1.93E+06	1.03E+06	3.88E+05			3	-69.9	0.980
98-95-3	Nitrobenzene	1.58E+05	1.04E+05	5.09E+04	2.22E+04	1.34E+04				5	-50.0	0.985
88-72-2	2-Nitrotoluene	2.40E+05	1.31E+05	5.35E+04	3.01E+04	1.72E+04				5	-52.1	0.995
88-73-3	2-Chlornitrobenzene		3.85E+05	2.39E+05	9.90E+04	4.20E+04	2.10E+04			5	-61.7	0.987
100-47-0	Benzonitrile	9.45E+04	4.02E+04	2.54E+04	1.27E+04	8.58E+03				5	-46.3	0.991

[illegible]

CAS	Compound	<i>exp.</i> $K_{HA,air}$ 5 °C	<i>exp.</i> $K_{HA,air}$ 15 °C	<i>exp.</i> $K_{HA,air}$ 25 °C	<i>exp.</i> $K_{HA,air}$ 35 °C	<i>exp.</i> $K_{HA,air}$ 45 °C	<i>exp.</i> $K_{HA,air}$ 55 °C	<i>exp.</i> $K_{HA,air}$ 65 °C	<i>exp.</i> $K_{HA,air}$ 75 °C	n	<i>exp.</i> $\Delta_{abs}H$ [kJ/mol]	r^2
108-98-5	Thiophenol	2.91E+04	1.50E+04	6.78E+03	3.82E+03					4	-51.5	0.997
67-68-5	Dimethylsulfoxide		1.06E+06	4.09E+05	9.91E+04	4.45E+04				4	-85.7	0.990
123-54-6	2,4-Pentanedione	2.35E+04	1.39E+04	9.23E+03	5.46E+03	3.54E+03				5	-37.2	0.998
107-21-1	1,2-Ethanediol		2.35E+07		3.15E+06	1.07E+06	5.13E+05			3	-79.0	0.992
78-95-5	Chloroacetone	1.05E+04	5.58E+03	2.92E+03	1.68E+03	9.37E+02				5	-46.9	1.000
98-88-4	Benzoylchloride	6.50E+04	2.91E+04	1.76E+04	7.01E+03					4	-53.6	0.986
116-09-6	Hydroxyacetone	5.93E+05	2.20E+05	1.31E+05	6.18E+04	3.13E+04				5	-55.1	0.994
106-65-0	Dimethyl succinate	4.47E+05	2.24E+05	1.01E+05	4.87E+04	2.82E+04				5	-54.3	0.998
58-89-9	Lindane (gamma-HCH)		1.88E+07		1.87E+06	6.12E+05	2.40E+05			3	-89.0	0.999
109-86-4	2-Methoxyethanol	2.84E+05	1.00E+05	5.13E+04	2.85E+04	1.44E+04				5	-55.7	0.993
110-80-5	2-Ethoxyethanol	2.78E+05	8.77E+04	4.76E+04	2.45E+04	1.14E+04				5	-58.9	0.991
541-05-9	Hexamethylcyclotrisiloxane	2.70E+03	1.33E+03	9.73E+02	5.91E+02					4	-37.2	0.981
524-42-5	1,2-Naphthoquinone		3.94E+07	1.10E+07	2.78E+06	1.31E+06	3.10E+05			4	-95.8	0.986
130-15-4	1,4-Naphthoquinone		3.19E+06		6.87E+05	3.50E+05	2.02E+05			4	-57.2	0.999
88-74-4	2-Nitroaniline		1.08E+07		9.38E+05	3.68E+05	1.13E+05			3	-91.4	0.993
591-31-1	3-Methoxybenzaldehyde		1.60E+06	4.61E+05	1.92E+05	1.08E+05	4.06E+04			5	-71.8	0.990
150-78-7	1,4-Dimethoxybenzene	3.88E+05	2.65E+05	1.16E+05	5.20E+04	3.63E+04				5	-49.2	0.980
873-62-1	3-Hydroxybenzonitrile		2.01E+08			1.82E+07	1.05E+07	4.71E+06		3	-62.8	0.985
1885-29-6	2-Aminobenzonitrile		1.92E+07		1.63E+06	5.14E+05	1.82E+05			3	-94.6	1.000
873-74-5	4-Aminobenzonitrile		1.08E+08		1.66E+07	9.14E+06	4.94E+06	1.63E+06		4	-67.7	0.966
103-33-3	Azobenzene		2.83E+06		4.39E+05	2.30E+05	9.53E+04	4.52E+04	2.31E+04	5	-69.4	0.997

REFERENCES APPENDIX 1

- (1) Lide, D.R. Handbook of Chemistry and Physics; 82nd Edition ed.; CRC press: Florida, **2001**.
- (2) Weckwerth, J.D.; Carr, P.W.; Vitha, M.F.; Nasehzadeh, A. A. comparison of gas-hexadecane and gas-apolane partition coefficients. *Anal. Chem.* **1998**, *70*, 3712-3716.
- (3) Hierlemann, A.; Zellers, E.T.; Rocco, A.J. Use of linear solvation energy relationships for modeling responses from polymer-coated acoustic-wave vapor sensors. *Anal. Chem.* **2001**, *74*, 4250-4258.
- (4) Reichert, P. **1998**. Aquasim. Duebendorf, Swiss Federal Institute for Environmental Science and Technology (EAWAG).
- (5) Chang, ML; Wu, SC; Chen, CY. Diffusion of volatile organic compounds in pressed humic acid disks. *Environ. Sci. Technol.* **1997**, *31*, 2307-2312.
- (6) Piatt, JJ; Brusseau, ML. Rate-limited sorption of hydrophobic organic compounds by soils with well-characterized organic matter. *Environ. Sci. Technol.* **1998**, *32*, 1604-1608.
- (7) Braun, JM; Guillet, JE. Studies of polystyrene in the region of the glass transition temperature by inverse gas chromatography. *Macromolecules.* **1975**, *8*, 882-888.
- (8) Hamdi, S; Hamdi, B; Kessaissia, Z; Barthel, H; Balard, H; Donnet, JB. Influence of poly(methyl methacrylate) impregnation ratio on the surface properties of fumed silica and on the glassy temperature of poly(methyl methacrylate) using inverse gas chromatographic analysis. *Journal of Chromatography A.* **2002**, *969*, 143-151.
- (9) LeBoeuf, E.J.; Weber, W.J. A distributed reactivity model for sorption by soils and sediments. *Environ. Sci. Technol.* **1997**, *31*, 1697-1702.
- (10) LeBoeuf, E.J.; Weber, W.J. Jr. Macromolecular characteristics of natural organic matter. 1. Insights from glass transition and enthalpic relaxation behavior. *Environ. Sci. Technol.* **2000**, *34*, 3623-3631.
- (11) Schaumann, G.E.; LeBoeuf, E.J. Glass transitions in peat: their relevance and the impact of water. *Environ. Sci. Technol.* **2005**, *39*, 800-806.

2

Sorption Equilibrium of a Wide Spectrum of Organic Vapors in Leonardite Humic Acid: Modeling of Experimental Data

reproduced from
Environmental Science and Technology, 2006, 40, 5374-5379.
Copyright 2006 American Chemical Society

Abstract

In a recent publication we presented experimental Leonardite humic acid/air partition coefficients for about 190 polar and nonpolar organic compounds measured with one consistent method. In this paper these experimental data are evaluated with various model predictions. For the PCKocWIN model some major shortcomings become apparent. The octanol-based Karickhoff-model exhibits a good performance for the nonpolar compounds but not for the polar ones.

A good description of the whole dataset is achieved with a polyparameter Linear Free Energy Relationship (pp-LFER) that explicitly accounts for the nonpolar (van der Waals and cavity formation) and polar (electron donor/acceptor) interactions between the sorbate molecule and the sorbent phase. With this pp-LFER model, most of the humic acid/air partition coefficients could be predicted within a factor of 2. The pp-LFER model also successfully predicts organic-C/water partition coefficients (K_{ioc}) collected from the literature when it is combined with a pp-LFER for air/water partition coefficients. This supports our earlier conclusion that the thermodynamic cycle is applicable in the humic acid/water/air system. Based on our experimental data, we present a pp-LFER-model for humic acid/air and humic acid/water partitioning at any ambient temperatures.

Introduction

Sorption in soil organic matter (SOM) is a key process in determining the transport as well as the bioavailability of organic pollutants in the environment. For practical applications in environmental chemistry, the availability of reliable soil organic matter sorption coefficients is of critical importance. The measurement of equilibrium sorption coefficients, however, is often tedious. Therefore, there has always been a demand for predictive models. The first and still most widely used approach is based on a log-linear correlation between sorption in SOM and partitioning in octanol. In an earlier paper we have shown that, on theoretical grounds, such correlations are principally restricted to single compound classes and cannot be expected to work for compound classes for which they have not been calibrated (1). In addition, existing models for the prediction of sorption in SOM have been calibrated and evaluated mainly with nonpolar compounds, and it can be shown that they are not suitable for polar compounds (1, 2). This shortcoming stands in contrast to an increasing number of polar chemicals that are of environmental concern. We have also pointed out that alternative models, based on so called poly-parameter Linear Free Energy Relationships (pp-LFERs), are able to predict the partitioning of both nonpolar compound classes and polar classes, because these models use descriptors to account for both nonspecific and polar interactions. In ref (3) we present a consistent set of experimental Leonardite humic acid/air (IHSS standard humic acid) equilibrium sorption coefficients for 190 polar and nonpolar compounds spanning a range of 7 orders of magnitude. To our knowledge, this is by far the largest and most diverse dataset for sorption in a humic acid. This data set allows carrying out a very comprehensive evaluation of various sorption models, particularly for polar compounds. Such an evaluation is of great interest because there are continuously more emerging chemicals of environmental concern exhibiting one or several polar functional groups, e.g., pharmaceuticals, pesticides, or plasticizers.

Methods

Most of the published prediction models for sorption in SOM have been developed for partitioning from water. For comparison, we calculated humic acid/water ($K_{i\text{HA},\text{water}}$) or humic acid organic carbon/water ($K_{i\text{HA-oc},\text{water}}$) partition coefficients (organic-C content of Leonardite humic acid: 63.8%) using our experimental humic acid/air partition coefficients and the respective water/air partitioning (please note the difference between HA and HA org-C in the text). Although this thermodynamic cycle is not generally applicable (4), there are several reasons to believe that it is valid for sorption processes in humic acid:

(1) Our data for sorption to humic acid coatings of various thicknesses suggested that absorption rather than adsorption is the dominating sorption process (3). Unlike for surface adsorption, the thermodynamic cycle is applicable for absorption mechanisms (4).

(2) A humic acid in aqueous solution is completely hydrated. The thermodynamic cycle therefore requires the humic acid in the humic acid/air sorption experiments also to be completely hydrated. Therefore, we use partition coefficients determined at 98% relative humidity (rh) which is close enough to 100% rh to represent sorption in an almost completely hydrated humic acid.

(3) As shown in ref (3), we found good agreement between humic acid/water partition coefficients from various literature sources and our experimental humic acid partition coefficients after conversion through the thermodynamic cycle. In this article, the converted humic acid/water partition coefficients will be compared to experimental $K_{i\text{oc}}$ values from the literature for various soils and sediments (see below).

To convert the experimental $K_{i\text{HA},\text{air}}$ partition coefficients into $K_{i\text{HA},\text{water}}$ partition coefficients, we mostly used $K_{i\text{water},\text{air}}$ partition coefficients for which pp-LFERs show high internal consistency (5) (see Supporting Information SI-1 for data). Most of the models for the prediction of partitioning of organic compounds in SOM that we evaluate in this study are calibrated at 25 °C. For the evaluation we therefore used our experimental dataset for 25 °C which is somewhat smaller than the one at 15 °C.

Results and Discussion

Evaluation of Models for the Prediction of Soil Organic Matter Partitioning

Single-Parameter Model: Octanol/Air Approach

In environmental chemistry sorption processes between organic phases and air or water are often modeled using octanol/air or octanol/water partition coefficients (K_{ioa} ; K_{iow}) as a predictor. However, this approach is problematic for the following reasons:

- (1) Published octanol/water partition coefficients are often unreliable. For example for DDT, DDE, and PCBs the K_{iow} -values can scatter over more than 2 orders of magnitude (6, 7). This uncertainty is transferred into model predictions of SOM partitioning processes.
- (2) Models that rely on a single predictor variable are inadequate to predict partition coefficients of polar and nonpolar compound classes because it is impossible to describe all intramolecular interactions with a single variable like $\log(K_{ioa})$ (1).
- 3) These models do not contain any descriptors of the sorption properties of the organic phase. Instead, this information is implicitly contained in the regression coefficients. Therefore, changes in the sorption properties would always require a new calibration of the model. There are indications that there is only a small variability of the sorption properties of soil organic matter (2); however, this is somewhat of a contradiction to other studies that report substantial differences in the sorption properties of various humic and fulvic acids (8).

Figure 1 compares our experimental humic acid/air partition coefficients at 25 °C and 98% rh with octanol/air partition coefficients, K_{ioa} , at 25 °C. The K_{ioa} partition coefficients were calculated from K_{iow} and K_{iaw} values. Most of the K_{iow} values are from ref (9) and most of the K_{iaw} values are from ref (5). These data are consistent and can be assumed to be reliable. Only a few K_{iow} and K_{iaw} partition coefficients have been estimated (for extended tables see SI-1). Hence, this comparison gives direct evidence of the performance of the model itself and is not influenced by the quality of the model input data.

The polar compounds scatter substantially ($r^2 = 0.82$) indicating that no regression model with octanol as a predictor will yield satisfactory fits for the polar compounds (Figure 1). In contrast, the nonpolar compounds scatter only slightly ($r^2 = 0.95$). In this context it is interesting to check the performance of models based on K_{iow} or K_{ioa} that have already been calibrated before with other experimental data: In environmental fate assessments of organic chemicals the empirical model $K_{ioc} = 0.41 \cdot K_{iow}$ published by Karickhoff (10) is often used to predict soil organic carbon/water partition coefficients.

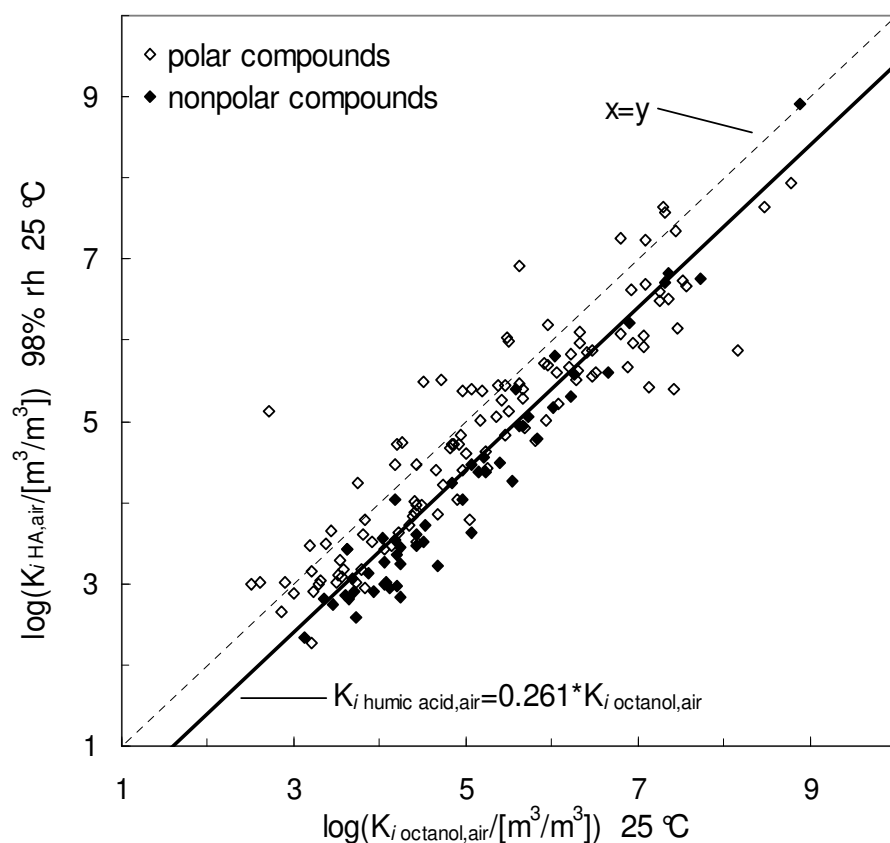


Figure 1. Plot of experimental $K_{iHA,air}$ values against $K_{ioctanol,air}$ partition coefficients. $K_{iHA,air}$ values are normalized to the volume of the humic acid assuming a density of $1 \text{ g}\cdot\text{cm}^{-3}$. The bold line ($\log K_{i \text{ humic acid, air}} = 0.261 \cdot K_{ioctanol, air}$) represents the model proposed by Karickhoff (10). Nonpolar compounds are as follows: Alkanes, alkenes, alkyl benzenes, polycyclic aromatic hydrocarbons, halogenated alkanes/alkenes, and halogenated benzenes. $r^2 = 0.83$ (all compounds); $r^2 = 0.95$ (nonpolar compounds).

A transformation of this model to HA/air partitioning ($C_{org} = 63.8\%$) leads to the model $K_{iHA,air} = 0.26 \cdot K_{ioa}$ that is plotted in Figure 1 (solid line). The

Karickhoff model succeeds at describing our experimental data for nonpolar compounds (Figure 1; for the logarithmic values: root-mean-square error (rmse) = 0.40; r^2 = 0.95; |absolute error| = 0.24; percentage of data that deviate more than a factor of 10 (R_{10}) = 0%). This suggests that Leonardite HA partition coefficients for nonpolar compounds can be predicted with satisfactory precision using the Karickhoff model. However, it should be emphasized that reliable K_{ioa} values are essential for the application of this model (see above). As expected, sorption of the polar compounds cannot be predicted well with the Karickhoff model that generally underestimates the sorption of the polar compounds (for the logarithmic values: rmse = 0.71; r^2 = 0.82; R_{10} = 13.2%, |absolute error| = 0.35).

EPI Suite – PcKocWIN: A Model based on Molecular Connectivity Indices

The EPI (Estimation Programs Interface) Suite (Version 3.12) is a computer based suite of physical/chemical property and environmental fate estimation models made available on the World Wide Web by the US-EPA (United States Environmental Protection Agency (11)). PcKocWIN, as part of the EPI Suite package, estimates organic-C/water partition coefficients (K_{ioc}) of organic compounds based on “first-order connectivity indices” (1-MCI) (12) and was developed by the Syracuse Research Corporation. The model was adapted by Meylan and Howard (13) by adding improved fragment contribution factors for polar compounds. Molecular connectivity indices are topological descriptors of molecular structure based on a count of skeletal atom grouping (14). Hence, the partition coefficients are simply derived from the chemical structure of the compound. For the functional groups of polar compounds, fragment correction factors are applied (for tabulated correction factors see ref (13)). Figure 2 compares K_{ioc} -values calculated by PcKocWIN (Version 1.66) at 25 °C with our Leonardite $K_{iHA-oc,water}$ partition coefficients that were converted from our experimental $K_{iHA,air}$ values with experimental water/air partition coefficients (see SI-2). The agreement is rather poor (r^2 = 0.68; rmse = 1.04; R_{10} = 26.5%). Some

substance classes, in particular alkanes, alkenes, aliphatic alcohols, and phenols, show big deviations (up to a factor of 4000) from the experimental $K_{i\text{HA-oc,water}}$ -values. A number of problems can be identified in the PcKocWIN model that contribute to this failure.

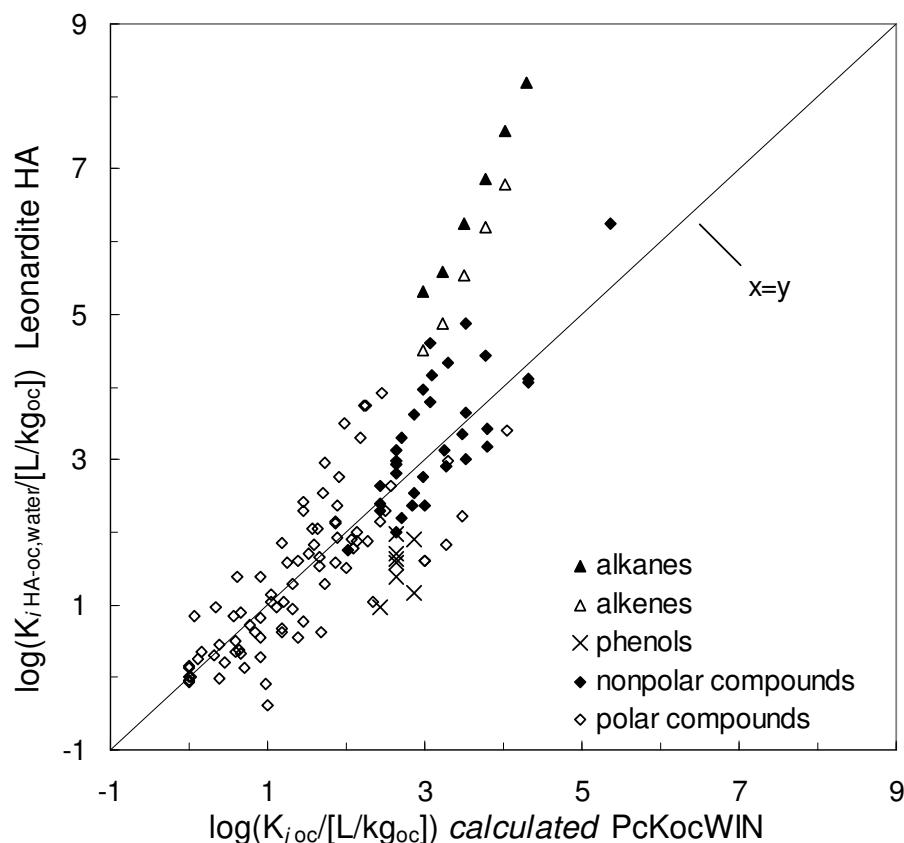


Figure 2. Comparison of experimental $\log(K_{i\text{HA-oc,water}})$ values (Leonardite, 25 °C) with $\log(K_{ioc})$ values predicted by PcKocWIN.

For highly polar compounds such as aliphatic dioles and diones, methanol and ethanol, and 2-ethoxyethanol and 2-methoxyethanol, PcKocWIN calculates negative $\log K_{ioc}$ values, but in the output file the program deliberately sets all negative values equal to zero. This procedure is highly questionable on theoretical grounds because negative $\log K_{ioc}$ -values are thermodynamically reasonable for highly polar compounds. In our dataset, negative experimental $\log K_{ioc}$ -values were measured for dimethyl sulfoxide, 2-methoxyethanol, and dimethyl succinate.

Furthermore, as an example, Figure 2 shows for the alkanes/alkenes a higher increase of the partition coefficients per additional $-\text{CH}_2-$ group for the experimental humic acid data than for the values calculated by PcKocWIN (increase in $\log K_{ioc}$ for every additional $-\text{CH}_2-$ unit: PcKocWIN model: 0.26; experimental HA-data (this study): 0.53). This causes an increasing divergence of the experimental and calculated partition coefficients with increasing molecular size. The same problem can be found for all other substance classes (not shown). In the expanded MCI model developed by Meylan and Howard (13) phenolic compounds were included in the calibration dataset for nonpolar compounds although they are strong electron donors/acceptors. Consequently, the PcKocWIN model lacks a fragment correction for aromatic hydroxy groups so that the predicted values for phenol and naphthol are close to those of benzene and naphthene, respectively. This results in an overestimation of soil organic matter/water partition coefficients of phenols and naphthols of at least 1 order of magnitude compared to our experimental data (Figure 2). In conclusion, the comparison of the PcKocWIN predictions with our experimental partition coefficients shows that the MCI-based prediction model does not provide reliable and consistent K_{ioc} values, neither for polar nor for nonpolar compounds.

Poly-Parameter Model: Linear Free Energy Relationship (pp-LFER)

The evaluation of the K_{ioa} -based model showed that Leonardite humic acid/air partition coefficients cannot adequately be predicted with a one-parameter model. Therefore, we propose the use of poly-parameter Linear Free Energy Relationships (pp-LFER) that describe nonspecific interactions (van der Waals forces) and specific interactions (EDA-interactions including H-bonds) by different terms (1). These equations have already been successfully applied to the sorption of organic vapors on/in different ambient phases in previous work (15-19). The pp-LFER in eq 1 describes partition processes of compound i between any two phases 1 and 2 and should be applicable to the partitioning of i between humic acid and air:

$$\log K_{i12} = l_{12} \cdot L_i + v_{12} \cdot V_i + b_{12} \cdot B_i + a_{12} \cdot A_i + s_{12} \cdot S_i + c_{12} \quad (1)$$

L_i , V_i , B_i , A_i and S_i are sorbate-specific descriptors. The McGowan volume of the compound i V_i [$\text{cm}^3 \cdot \text{mol}^{-1}$]/100] and the logarithm of the compound's hexadecane/air partition coefficient (L_i) describe the nonspecific interactions of the compound i (i.e., cavity formation and van der Waals interactions), while the other descriptors stand for specific EDA-interactions (A_i : electron acceptor property; B_i : electron donor property; S_i : solvent's dipolarity/polarizability). These substance-specific descriptors are tabulated for hundreds of substances and have been shown to describe their respective partition behavior in very diverse partition systems (5, 9, 20). If a partition process between the gas phase and humic acid is considered (phase 1 = humic acid, phase 2 = gas phase), the coefficients $a_{\text{HA,air}}$, $b_{\text{HA,air}}$, $l_{\text{HA,air}}$, $s_{\text{HA,air}}$, and $v_{\text{HA,air}}$ in eq 1 are the complementary interaction descriptors of the condensed phase (here: humic acid). For example, the sorbent descriptor $b_{\text{HA,air}}$ is related to the electron-acceptor property of the sorbent. Using multi-parameter linear regression, the coefficients $a_{\text{HA,air}}$, $b_{\text{HA,air}}$, $l_{\text{HA,air}}$, $s_{\text{HA,air}}$, and $v_{\text{HA,air}}$ can be fitted by applying eq 1 to our large dataset of logarithmic experimental Leonardite HA/air partition coefficients. Note that in most references slightly different combinations of descriptors are used: For gas phase/organic phase partitioning the excess molar refractivity E_i instead of V_i is used in combination with L_i to describe nonspecific interactions, while for water/organic phase partitioning E_i instead of L_i is used in combination with V_i (21). This slightly different type of pp-LFER is usually known as Linear Solvation Energy Relationship (LSER). The form of the pp-LFER equation used here (eq 1) has the advantage that a single equation can be used for gas phase and water phase partitioning, and the respective conversion can be performed with the thermodynamic cycle (see ref (22)).

The pp-LFER model in eq 1 was applied to 158 of our Leonardite humic acid/air partition coefficients (eq 2) measured at 15 °C and 98% rh. For about 30 measured compounds no or no complete sets of descriptors were available.

$$\log(K_{i\text{HA},\text{air}}/[L/\text{kg}_{\text{HA}}]) = 0.81(\pm 0.07) \cdot L_i - 0.08(\pm 0.27) \cdot V_i + 1.88(\pm 0.15) \cdot B_i + 3.62(\pm 0.13) \cdot A_i + 1.14(\pm 0.17) \cdot S_i - 0.65(\pm 0.15) \quad (2)$$

$n = 158$; $r^2 = 0.96$; $\text{rmse} = 0.32$; $R_{10} = 0.63\%$

Figure 3 compares the *experimental* $K_{i\text{HA},\text{air}}$ partition coefficients with those *fitted* by the pp-LFER in eq 2. For 16 of the substances, $K_{i\text{HA},\text{air}}$ partition coefficients have been extrapolated to 15 °C from higher temperatures using the experimental sorption enthalpies $\Delta_{\text{abs}}H_i$ (see SI in ref (3)). These substances are marked in the plot. According to Figure 3, the pp-LFER model in eq 2 is well suited to describe the experimental $K_{i\text{HA},\text{air}}$ partition coefficients of 158 compounds in our dataset (for details see SI-3) within a factor of about 2. Systematic deviations of specific substance classes (e.g., different behavior of the polar/nonpolar compounds) are not evident. The 158 compounds used for the model fit represent a very diverse dataset: a wide range in the physical-chemical descriptors is covered by these substances ($0 \leq A_i \leq 0.83$; $0 \leq B_i \leq 1.06$; $0 \leq S_i \leq 1.55$; $0.31 \leq V_i \leq 2.08$; $0.97 \leq L_i \leq 9.69$; see SI-3).

The nitrogen-containing compound 2-methylpyridine was an outlier in the pp-LFER and was excluded from the model.

In a sensitivity analysis 57 substances were removed from the dataset and the pp-LFER model was recalculated with the truncated dataset. The removed substances were chosen randomly, but proportionally to the number of compounds within one compound class to ensure the required diversity in the dataset. The pp-LFER based on the limited dataset is close to the original pp-LFER (for more details see SI-4). The experimental $K_{i\text{HA},\text{air}}$ values of the removed substances can successfully be predicted by the limited pp-LFER ($r^2 = 0.95$; $\text{rmse} = 0.36$).

It must be noted that the comparisons conducted in this article are based on compounds for which reliable substance-specific descriptors ($K_{i\text{ow}}/K_{i\text{oa}}$ as well as A_i , B_i , L_i , V_i and S_i) were available. The descriptors A_i , B_i , L_i , V_i and S_i are typically determined from various types of partition data such that an over-determined system of linear equations is solved (23-25). This allows the identification of experimental outliers so that these descriptors can principally be determined with a higher reliability than a single value like $K_{i\text{ow}}$.

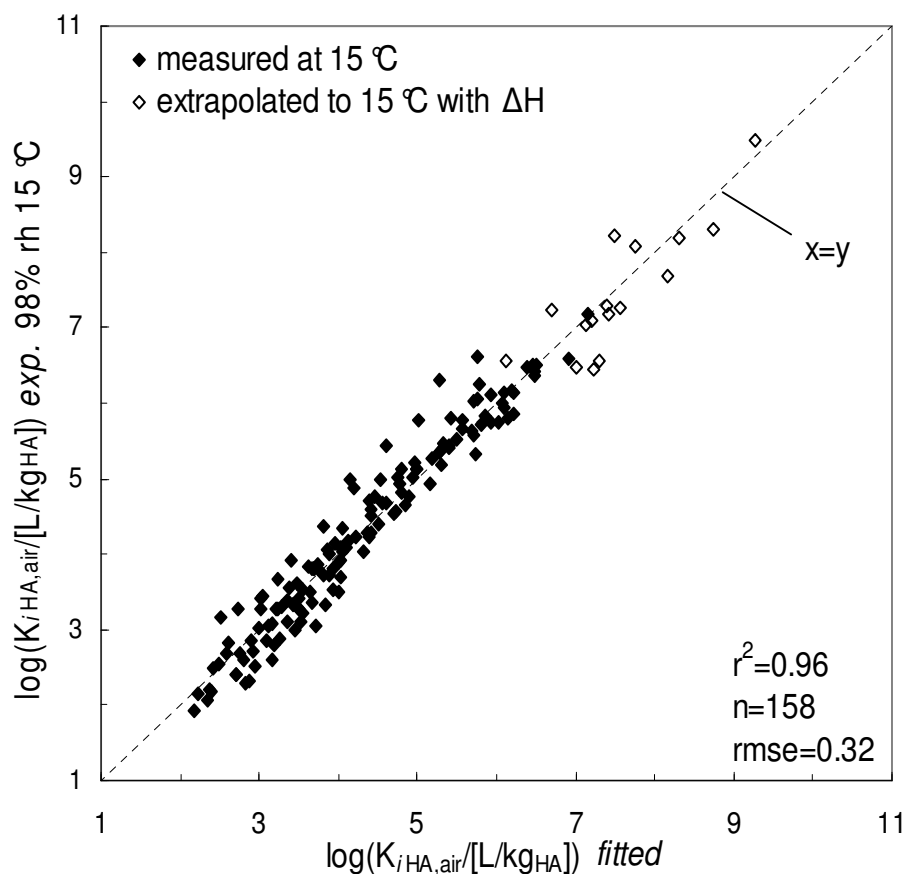


Figure 3. Experimental $\log(K_{i\text{HA,air}})$ partition coefficients (15 °C) are plotted against $\log(K_{i\text{HA,air}})$ partition coefficients fitted by the pp-LFER in eq 2. Compounds represented by empty symbols have been extrapolated to 15 °C using the experimental data at higher temperatures and experimental sorption enthalpies.

We conclude that the pp-LFER presented here describes sorption of polar and nonpolar compounds equally well and with very satisfactory precision.

Temperature-Dependence of the Sorption Process

Practical environmental applications demand partition coefficients at various temperatures. The sorption enthalpies that are required for a temperature extrapolation are often approximated by the respective heat of vaporization $\Delta_{\text{vap}}H_i$ for partition processes between air and an organic sorbent. However, the sorption enthalpy $\Delta_{\text{abs}}H_i$ derived from our experimental data between 5 and 75 °C correlate only poorly with $\Delta_{\text{vap}}H_i$ (plot in SI-5; $r^2 = 0.58$; $\text{rmse} = 12.2$). Therefore, we evaluated other

approaches to estimate the temperature dependence of the humic acid/air sorption process.

Prediction of $\Delta_{\text{abs}}H_i$ using the Sorption Coefficient $K_{i\text{HA},\text{air}}$

We have shown before (26) that the sorption enthalpy $\Delta_{12}H_i$ of various sorption processes correlate with the respective sorption entropy $\Delta_{12}S_i$. In such a case, the Gibbs free energy $\Delta_{12}G_i$ and thus the logarithmic partition coefficients $\ln(K_{i12})$ at a given temperature also correlates with the sorption enthalpy and can be used for its prediction (i.e., $\Delta_{12}H_i = \text{slope} \cdot (-R \cdot T \cdot \ln(K_{i12})) + \text{intercept}$). As an example, for hexadecane/air partitioning the following correlation can be found: $\Delta_{12}H_i = 1.68 \cdot (-R \cdot T \cdot \ln(K_{i12})) - 6.75 \text{ [kJ} \cdot \text{mol}^{-1}]$, $r^2 = 0.98$ (27). However, recently Kuhne et al. (28) have found that such a simple relationship does not exist for air/water partitioning. Similarly, we found a poor correlation here between the experimental sorption enthalpies $\Delta_{\text{abs}}H_i$ for humic acid and the $\ln(K_{i\text{HA},\text{air}})$ values at 15 °C ($r^2 = 0.67$; $\text{rmse} = 9.82$; plot in SI-5). It appears that a correlation between $\Delta_{12}H_i$ and $\Delta_{12}G_i$ works best if nonpolar interactions are dominating as it is the case in hexadecane. In humic acid, polar interactions are quite important (see also ref (3)). These specific interactions show stronger temperature dependencies than nonspecific interactions (see below).

Prediction of the Temperature Dependence using a pp-LFER Approach

Poole et al. found linear relationships between pp-LFER sorbent-descriptors (i.e., a_{12} , b_{12} , c_{12} , l_{12} , s_{12} , and v_{12} in eqs 1 and 2) and the temperature, T , for stationary GC-phases (29). We determined $K_{i\text{HA},\text{air}}$ partition coefficients for about 165 compounds over a temperature range of 5–75 °C (see ref (3)). Thus, it is possible to test whether such a relationship can be found for the sorption process studied here. The statistics of the fitted pp-LFERs at the four temperatures are similar and indicate that the pp-LFER approach works equally well at all temperatures. We found reasonably good linear relationships for all system coefficients (i.e., sorbent descriptors) as a function of temperature (see Table 1).

sorbent descriptor	288K	298K	308K	318K	slope 1/[K]	intercept	r ²
l _{HA,air}	0.81	0.75	0.72	0.71	-0.0031	1.693	0.91
v _{HA,air}	-0.08	-0.17	-0.40	-0.44	-0.0131	3.705	0.93
c _{HA,air}	-0.65	-0.44	-0.19	-0.24	0.015	-4.918	0.83
b _{HA,air}	1.88	1.86	1.72	1.62	-0.0094	4.610	0.95
a _{HA,air}	3.62	3.18	2.90	2.73	-0.0296	12.06	0.96
s _{HA,air}	1.14	1.01	0.81	0.76	-0.0135	5.030	0.96

Table 1. pp-LFER-sorbent descriptors (sd; see eq 1) as a function of temperature sd(T) = $\text{slope} \cdot T/[K] + \text{intercept}$. The pp-LFERs calculate HA/air partition coefficients in [L/kg_{HA}]. Note that the equations require temperatures in Kelvin units. The pp-LFERs for every temperature are based on 122-158 compounds. At least 95 compounds are included in all four pp-LFERs.

Table 1 in combination with eq 1 provides the possibility to set up pp-LFERs for any temperature between 0 °C and 50 °C. For an evaluation we predicted the pp-LFER parameters for 5 °C (the pp-LFER for 5 °C was not part of the calibration dataset). A comparison of the *calculated* pp-LFER descriptors for 5 °C with the pp-LFER *fitted* from the experimental sorption coefficients at 5 °C show good agreement ($r^2 = 0.99$; slope = 1.05; intercept = -0.06; plot shown in SI-6). In contrast, we did not find a pp-LFER that was capable of predicting $\Delta_{\text{abs}}H_i$ directly from the compound descriptors. The linear relationship between the sorbent descriptors and the temperature is based on empirical observations and can serve as a valuable practical tool. We cannot provide a mechanistical explanation for these findings; it is likely that the relationship between the temperature and the sorbent descriptors is much more complex.

Comparison with Partition Data from the Literature

Comparison based on the Dataset collected by Nguyen et al.

Nguyen et al. collected 356 published K_{ioc} (organic-C/water) partition coefficients for 75 compounds derived from batch experiments with different soils and sediments (2). These literature data have carefully been selected with respect to the experimental setup, linearity of the sorption isotherm, constitution of soils, and sediments and equilibrium

conditions at the measurement. The dataset is diverse and contains polar compounds (e.g., phenols, anilines, amides, ureas) as well as nonpolar compounds (e.g., aromatic hydrocarbons, halogenated hydrocarbons, polycyclic aromatic hydrocarbons). To compare our humic acid/air pp-LFER for 25 °C with these data, our pp-LFER was converted to a humic acid organic carbon/water $K_{i\text{HA-oc,water}}$ pp-LFER using a pp-LFER for water/air partitioning (see ref (22)) and the organic-C content of Leonardite humic acid (C-org = 63.8%). The applicability of the thermodynamic cycle is discussed above. With this $K_{i\text{HA-oc,water}}$ pp-LFER we predict $K_{i\text{HA-oc,water}}$ partition coefficients for the substances in Nguyen's dataset (all relevant data and equations are reported in SI-7 and SI-11) and compare these estimated values with the experimental $K_{i\text{oc}}$ values (Figure 4). The plot shows neither systematic deviations of any substance class nor large absolute deviations ($r^2 = 0.83$; $\text{rmse} = 0.44$; $R_{10} = 1.96\%$) although the correlation coefficient is only moderate.

The consistency between our pp-LFER model and the literature data is taken as corroborative evidence that: (a) the sorption properties of a humic acid in equilibrium with 98% relative humidity correspond to a completely hydrated humic acid; and that (b) the tested Leonardite humic acid seems to be representative for typical humic materials found in soils and sediments with respect to sorption properties. This suggests that our pp-LFER model can generally be used for the prediction of partition coefficients within the linear part of the sorption isotherm in soils and sediments. Currently, we are conducting experimental work to further elucidate differences in the sorption properties of various humic and fulvic acids. Note that soils and sediments whose sorption properties are dominated by black carbon must be excluded from this conclusion.

In the publication of Nguyen et al. the collected experimental $K_{i\text{oc}}$ partition coefficients (75 compounds) are compared with the $K_{i\text{oc}}$ values predicted by the PckocWIN model (plot shown in SI-9 of this article). At first glance the correlation is quite good ($r^2 = 0.93$, $\text{rmse} = 0.48$). But this is not surprising because 75% of the compounds in Nguyen's dataset are part of the dataset that had been used by Meylan et al. (13) to calibrate the PckocWIN model. However, the trendline through the alkyl

benzenes homologue series in the plot indicates a slope of 1.87 instead of unity. This already indicates a problem in the predictions similar to the findings from the comparison of our experimental data with PcKocWIN (Figure 2).

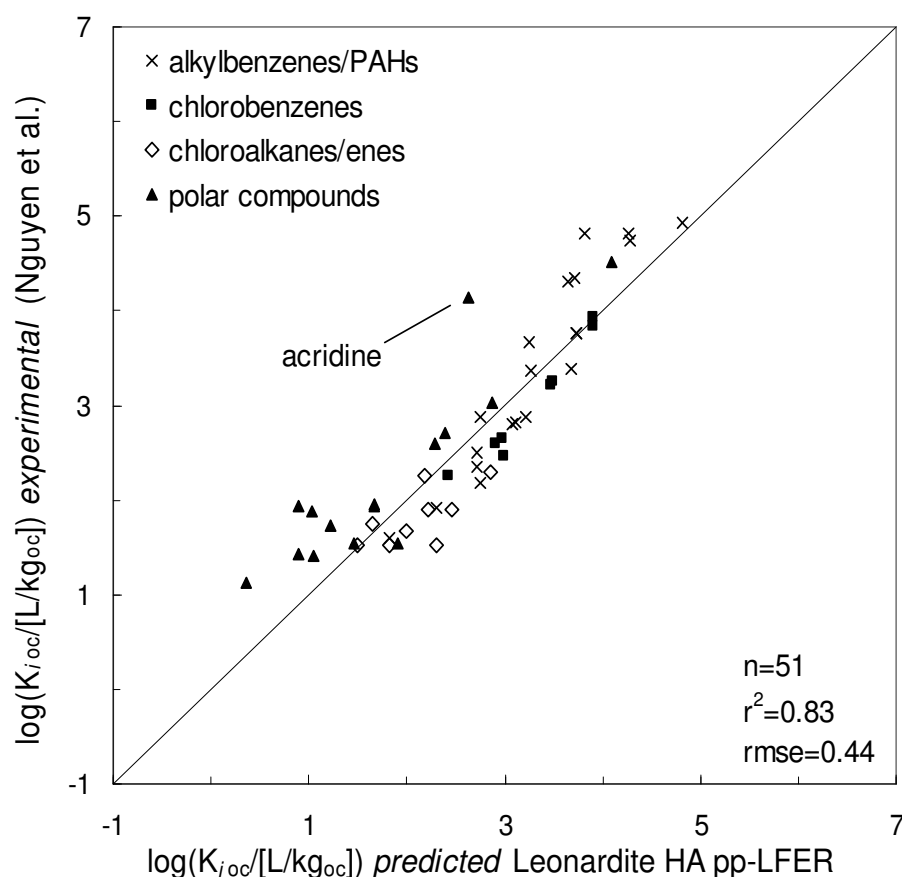


Figure 4. Comparison of $\log(K_{ioc})$ values predicted by the pp-LFER from this study (transformed to an org-C/water partition pp-LFER, see text for details) with experimental $\log(K_{ioc})$ values collected from literature sources (2). Outlier: Acridine (also outlier in ref (2) ; not considered for statistics).

Nguyen et al. also proposed a pp-LFER based on the literature K_{ioc} values. In analogy to the procedure in the last paragraph, we converted Nguyen's pp-LFER via the water/air partitioning to an org-C/air pp-LFER. Nguyen's pp-LFER contains the excess molar refraction (R_i) instead of L_i . Therefore, we recalculated the Nguyen's pp-LFER with L_i and without R_i (for details see SI-7). Using this pp-LFER, we predicted $K_{iorg-C,air}$ partition coefficients for the compounds in our dataset. The experimental and predicted partition coefficients correlate also

satisfactorily ($r^2 = 0.85$, $rmse = 0.47$; Figure in SI-8). However, the alkanes show larger deviations of a factor of 10–20. The same deviation can also be observed in a comparable pp-LFER equation published by Poole et al. (30) (plot shown in SI-8). This shortcoming in the previously published pp-LFER model predictions can be ascribed to deficient calibration datasets that lack any alkanes or alkenes. It is indeed extremely difficult to get accurate experimental data for the partitioning of alkanes and halogenated alkanes in aqueous solution due to their very low solubility. The only experimental data that we could find in the literature (31) agree within experimental error (0.5 log units) with our results. However, in contrast to measuring partition coefficients of alkanes from the aqueous phase, measuring the same compounds from the gas phase as in our experimental system (IGC) does not cause any problems. Hence, the pp-LFER presented here appears to be more robust and more precise than other pp-LFERs published previously because of a more diverse calibration dataset.

Practical applications in environmental chemistry demand SOM/water partition coefficients in addition to SOM/air partition coefficients. Therefore, it is advantageous to have a pp-LFER model not only for partitioning between humic acid and air at various temperatures but also for humic acid/water partitioning. The latter can be derived from the former and the air/water partitioning in ref (32) at various temperatures using the thermodynamic cycle (see above). With eq 3, $K_{iHA-oc,water}$ partition coefficients at 15 °C can be calculated (please note: the equation is normalized on humic acid org-C).

$$\log(K_{iHA-oc,water}/[L/kg_{HA-oc}]) = 0.29(\pm 0.07) \cdot L_i + 2.50(\pm 0.28) \cdot V_i - 3.29(\pm 0.16) \cdot B_i - 0.21(\pm 0.14) \cdot A_i - 0.79(\pm 0.18) \cdot S_i + 0.01(\pm 0.15) \quad (3)$$

SI-10 provides further HA-oc/water pp-LFER equations for other temperatures as well as linear correlations for calculating HA-oc/water pp-LFERs at any temperature (according to Table 1). Based on the evaluation that we have performed above (see Figure 4), we do expect that these equations work just as well as those for humic acid/air partitioning. With this system of pp-LFERs we are able to predict

partitioning between Leonardite humic acid and air or water for any nonionic organic compound at any ambient temperature. In a follow-up paper we will evaluate a completely different type of model for the prediction of humic acid/air partitioning that is based on a molecular modeling approach. This approach has the big advantage that it does not require any other input parameter than the molecular structures of the sorbates and the sorbent.

Acknowledgements

We thank Christine Roth, Torsten Schmidt, Hans Peter Arp, and Michael Sander for critical comments on the manuscript. This research was financially supported by the Swiss National Science Foundation (project-no. 200020-111753/1) and partly by the European Union (European Commission, FP6 Contract No. 003956)

References Chapter 2

- (1) Goss, K.-U.; Schwarzenbach, R. P. Linear free energy relationships used to evaluate equilibrium partitioning of organic compounds *Environ. Sci. Technol.* **2001**, 35, 1-9.
- (2) Nguyen, T., Goss, K.U., Ball, W.P. Polyparameter linear free energy relationships for estimating the equilibrium partition of organic compounds between water and the natural organic matter in soils and sediments *Environ. Sci. Technol.* **2005**, 39, 913-923.
- (3) Niederer, C., Goss, K.U., Schwarzenbach, R.P. Sorption equilibrium of a wide spectrum of organic vapors in Leonardite humic acid: Experimental setup and experimental data *Environ. Sci. Technol.* **2006**, 40, 5368-5373.
- (4) Goss, K.-U. Comment on "influence of soot carbon on the soil-air partitioning of polycyclic aromatic hydrocarbon *Environ. Sci. Technol.* **2004**, 38, 1622-1623.
- (5) Abraham, M. H., Andonian-Haftvan, J., Whiting, G.S., Leo, A., Taft, R.S. Hydrogen bonding. Part 34. The factors that influence the solubility of gases and vapors in water at 298 K, and a new method for its determination *J. Chem. Soc., Perkin Trans. 2* **1994**, 1777-1791.
- (6) Pontolillo, J., Eganhouse, R.P. "The search for reliable aqueous solubility (S_w) and octanol-water partitioning coefficient (K_{ow}) data for hydrophobic organic compounds: DDT and DDE as a case study," U.S. Geological Survey, 2001.
- (7) Linkov, I., Ames, M.R., Crouch, E.A.C., Satterstrom F.K. Uncertainty in octanol-water partition coefficients: Implications for risk assessment and remedial costs *Environ. Sci. Technol.* **2005**, 39.
- (8) Kopinke, F. D., Georgi, A., Mackenzie, K. Sorption of pyrene to dissolved humic substances and related model polymers. 1. Structure-property correlation *Environ. Sci. Technol.* **2001**, 35, 2536-2542.
- (9) Abraham, M. H., Chadha, H.S., Whiting, G.S., Mitchell, R.C. Hydrogen bonding. 32. An analysis of water-octanol and water-alkane partitioning and the Dlog P parameter of Seiler *J. Pharm. Sci.* **1994**, 83, 1085-1100.
- (10) Karickhoff, S. W. Semi-empirical estimation of sorption of hydrophobic pollutants on natural sediments and soils *Chemosphere* **1981**, 10, 833-846.

- (11) US-EPA EPI Suite V3.12;
<http://www.epa.gov/opptintr/exposure/pubs/episuite.htm> **2004**.
- (12) Sabljic, A. Predictions of the nature and strength of soil sorption of organic pollutants by molecular topology *J. Agric. Food Chem.* **1984**, 32, 243-246.
- (13) Meylan, W., Howard, P.H. Molecular topology/fragment contribution method for predicting soil sorption coefficients *Environ. Sci. Technol.* **1992**, 26, 1560-1567.
- (14) Murray, W. J., Hall, L.H., Kier, L.B. Molecular connectivity 3: Relationship to partition-coefficients *J. Pharm. Sci.* **1975**, 64, 1978-1981.
- (15) Goss, K.-U., Buschmann, J., Schwarzenbach, R.P. Adsorption of organic vapors to air-dry soils: model predictions and experimental validation *Environ. Sci. Technol.* **2004**, 38, 3667-3673.
- (16) Goss, K.-U. The role of air/surface adsorption equilibrium for the environmental partitioning of organic compounds *Cri. Rev. Environ. Sci. Technol.* **2004**, 34, 339-389.
- (17) Roth, C. M., Goss, K.-U., Schwarzenbach, R.P. Adsorption of a diverse set of organic vapors on the bulk water surface *J. Coll. Interface Sci.* **2002**, 252.
- (18) Roth, C. M., Goss, K.-U., Schwarzenbach, R.P. Sorption of diverse organic vapors to snow *Environ. Sci. Technol.* **2004**, 38, 4078-4084.
- (19) Roth, C. M., Goss, K.-U., Schwarzenbach, R.P. Sorption of a diverse set of organic vapors to diesel soot and road tunnel aerosols *Environ. Sci. Technol.* **2005**, 39.
- (20) Abraham, M. H. Hydrogen Bonding, XXVII. Solvation parameters for functionally substituted aromatic compounds and heterocyclic compounds, from gas-liquid chromatographic data *J. Chromatogr.* **1993**, 644, 95-139.
- (21) Acree, W. E. J., Abraham, M.H. Solubility predictions for crystalline polycyclic aromatic hydrocarbons (PAHs) dissolved in organic solvents based upon the Abraham general solvation model *Fluid Phase Equilibria* **2002**, 201, 245-258.
- (22) Goss, K.-U. Predicting the equilibrium partitioning of organic compounds using just one linear solvation energy relationship (LSER) *Fluid Phase Equilib.* **2005**, 233, 19-22.
- (23) Zissimos, A. M., Abraham, M.H., Du, C. M., Valko, K., Bevan, C., Reynolds, D., Wood, J., Tam, K.Y. Calculation of Abraham descriptors

from experimental data from seven HPLC systems; evaluation of different methods of calculation *J. Chem. Soc., Perkin Trans. 2* **2002**, 2001-2010.

(24) Zissimos, A. M., Abraham, M.H., Barker, M.C., Box, K., Tam, Y.K. Calculation of Abraham descriptors from solvent-water partition coefficients in four different systems; evaluation of different methods of calculation *J. Chem Soc. Perkin Trans. 2* **2002**, 470-477.

(25) Abraham, M. H., Ibrahim, A., Zissimos, A. M. Determination of sets of solute descriptors from chromatographic measurements *J. Chromatogr., A* **2004**, 1037, 29-47.

(26) Goss, K.-U., Schwarzenbach, R.P. Empirical prediction of heats of vaporization and heats of adsorption of organic compounds *Environ. Sci. Technol.* **1999**, 33, 3390-3393.

(27) Abraham, M. H., Whiting, G.S., Fuchs, R., Chambers, E.J. Thermodynamics of solute transfer from water to hexadecane *J. Chem. Soc. Perkin Trans. 2* **1990**, 291-300.

(28) Kuhne, R., Ebert, R.U., Schuurmann, G. Prediction of the temperature dependency of Henry's law constant from chemical structure *Environ. Sci. Technol.* **2005**, 39, 6705-6711.

(29) Poole, C. F., Li, Q., Kiridena, W., Koziol, W.W. Selectivity assessment of popular stationary phases for open-tubular column gas chromatography *J. Chromatogr. A* **2001**, 912, 107-117.

(30) Poole, S. K., Poole, C.F. Chromatographic models for the sorption of neutral organic compounds by soil from water and air *J. Chromatogr., A* **1999**, 845, 381-400.

(31) Georgi, A., Kopinke, F.-D. Validation of a modified Flory-Huggins concept for description of hydrophobic organic compound sorption on dissolved humic substances *Environ. Toxicol. Chem.* **2002**, 21, 1766-1774.

(32) Goss, K.-U. Prediction of the temperature dependency of Henry's law constant using poly-parameter linear free energy relationships *Chemosphere* **2006**, 64, 1369-1374.

Appendix 2

Modeling of Experimental Data

Content

- SI-1** Octanol/water, water/air and octanol/air partition coefficients
- SI-2** K_{ioc} partition coefficients calculated by PcKocWIN™ and experimental $K_{iHA-oc,water}$ partition coefficients
- SI-3** pp-LFER model: fitted values and sorbate-specific descriptors
- SI-4** Sensitivity analysis: limited pp-LFER
- SI-5** Exp. $\Delta_{abs}H_i$ compared to $\Delta_{vap}H_i$; correlation of exp. $\Delta_{abs}H_i$ with $\ln(K_{iHA,air})$
- SI-6** pp-LFER parameters as a function of temperature
- SI-7** Comparison with data from Nguyen et al. (2005)
- SI-8** Comparison of exp. $K_{iHA-oc,water}$ with K_{ioc} partition coefficients predicted by pp-LFER from literature sources (Nguyen et al. (2005); Poole and Poole (1999)).
- SI-9** Comparison of the PcKocWIN™ model with literature K_{ioc} partition coefficients collected by Nguyen et al. (2005)
- SI-10** Sorbent descriptors for HA org-C/water pp-LFERs at different temperatures
- SI-11** All relevant pp-LFER equations for the comparison of our experimental data with literature data

SI-1: Octanol/air and water/air partition coefficients

Table SI-1 contains octanol/water and water/air partition coefficients collected from the literature. K_{iow} values are in $[m^3/m^3]$, K_{iwa} values are in $[(mol/l)/(mol/l)]$. Octanol/air partition coefficients are calculated from K_{iaw} and K_{iow} . All coefficients are at 25 °C.

CAS-Nr.	Compound	$\log K_{i\text{octanol,water}}$ [m ³ /m ³] 25 °C	Ref	$\log K_{i\text{water,air}}$ [(mol/l)/(mol/l)] 25 °C	Ref	^{d)} $\log K_{i\text{octanol,air}}$ [m ³ /m ³] 25 °C
111-65-9	n-Octane	5.15	[21]	-2.11	[1]	3.04
111-84-2	n-Nonane	5.65	[21]	-2.30	[1]	3.35
124-18-5	n-Decane	6.01	a)	-2.32	[1]	3.69
1120-21-4	n-Undecane	6.54	[21]	-2.50	a)	4.04
112-40-3	n-Dodecane	6.80	[21]	-2.63	a)	4.17
629-50-5	n-Tridecane	8.00	[21]	-2.78	a)	5.22
629-59-4	n-Tetradecane	8.64	[21]	-2.92	a)	5.72
293-96-9	Cyclodecane	5.14	[24]	-1.51	[9] ^{b)}	3.63
111-66-0	1-Octene	4.57	[26]	-1.41	[1]	3.16
124-11-8	1-Nonene	5.15	[21]	-1.51	[1]	3.64
872-05-9	1-Decene	5.74	a)	-1.67	a)	4.07
821-95-4	1-Undecene	6.33	a)	-1.82	a)	4.52
112-41-4	1-Dodecene	6.92	a)	-1.96	a)	4.96
2437-56-1	1-Tridecene	7.51	a)	-2.11	a)	5.40
64-17-5	Ethanol	-0.30	[21]	3.67	[1]	3.37
71-23-8	Propan-1-ol	0.25	[21]	3.56	[1]	3.81
71-36-3	Butan-1-ol	0.88	[21]	3.46	[1]	4.34
71-41-0	Pentan-1-ol	1.56	[21]	3.35	[1]	4.91
111-27-3	Hexan-1-ol	2.03	[21]	3.23	[1]	5.26
111-70-6	Heptan-1-ol	2.72	[21]	3.09	[1]	5.81
111-87-5	Octan-1-ol	3.07	[21]	3.00	[1]	6.07
143-08-8	Nonan-1-ol	3.67	[21]	2.85	[1]	6.52
112-30-1	Decan-1-ol	4.28	a)	2.67	[1]	6.95
112-42-5	Undecan-1-ol	4.84	a)	2.62	a)	7.46
67-63-0	Propan-2-ol	0.05	[21]	3.48	[1]	3.53
78-83-1	2-Methylpropan-1-ol	0.76	[21]	3.30	[1]	4.06
75-65-0	2-Methylpropan-2-ol	0.35	[21]	3.28	[1]	3.63
123-51-3	3-Methylbutan-1-ol	1.16	[21]	3.24	[1]	4.40
104-76-7	2-Ethyl-1-hexanol	2.73	[24]	2.97	[3], [5] ^{c)}	5.70
100-51-6	Benzyl alcohol	1.10	[21]	4.86	[1]	5.96
90-15-3	1-Naphthol	2.84	[22]	5.63	[1]	8.47
96-41-3	Cyclopentanol	0.71	[21]	4.03	[1]	4.74
108-93-0	Cyclohexanol	1.23	[21]	4.01	[1]	5.24
75-89-8	2,2,2-Trifluoroethanol	0.41	[21]	3.16	[1]	3.57
920-66-1	Hexafluoropropan-2-ol	1.66	[21]	2.76	[1]	4.42
108-95-2	Phenol	1.46	[21]	4.85	[1]	6.31
95-48-7	o-Cresol (2-Methylphenol)	1.98	[21]	4.31	[1]	6.29

CAS-Nr.	Compound	$\log K_{i\text{octanol,water}}$ [m ³ /m ³] 25 °C	Ref	$\log K_{i\text{water,air}}$ [(mol/l)/(mol/l)] 25 °C	Ref	^{d)} $\log K_{i\text{octanol,air}}$ [m ³ /m ³] 25 °C
108-39-4	m-Cresol (3-Methylphenol)	1.98	[21]	4.42	[17]	6.40
106-44-5	p-Cresol (4-Methylphenol)	1.97	[21]	4.50	[1]	6.47
95-57-8	2-Chlorophenol	2.15	[21]	3.34	[1]	5.49
106-48-9	4-Chlorophenol	2.40	[21]	5.16	[1]	7.56
6640-27-3	2-Chloro-4-methylphenol	2.70	[24]	4.73	[9] ^{b)}	7.43
576-24-9	2,3-Dichlorophenol	3.26	[27]	4.90	[9] ^{b)}	8.16
87-65-0	2,6-Dichlorophenol	2.92	[27]	3.96	[14] ^{c)}	6.88
95-95-4	2,4,5-Trichlorophenol	3.90	[17]	3.55	[17]	7.45
88-06-2	2,4,6-Trichlorophenol	3.67	[17]	3.65	[17]	7.32
67-64-1	2-Propanone	-0.24	[21]	2.79	[1]	2.55
78-93-3	2-Butanone	0.29	[21]	2.72	[1]	3.01
107-87-9	2-Pentanone	0.91	[21]	2.58	[1]	3.49
591-78-6	2-Hexanone	1.38	[21]	2.41	[1]	3.79
110-43-0	2-Heptanone	1.98	[21]	2.23	[1]	4.21
111-13-7	2-Octanone	2.37	[21]	2.11	[1]	4.48
821-55-6	2-Nonanone	3.14	[21]	1.83	[1]	4.97
693-54-9	2-Decanone	3.73	[21]	1.72	[1]	5.45
112-12-9	2-Undecanone	4.09	[21]	1.58	[1]	5.67
563-80-4	3-Methylbutan-2-one	0.84	[21]	2.38	[1]	3.22
108-10-1	4-Methylpentan-2-one	1.31	[21]	2.24	[1]	3.55
120-92-3	Cyclopentanone	0.38	[21]	3.45	[1]	3.83
108-94-1	Cyclohexanone	0.81	[21]	3.60	[1]	4.41
502-42-1	Cycloheptanone	1.62	[24]	2.56	[9] ^{b)}	4.18
98-86-2	Acetophenone	1.58	[21]	3.36	[1]	4.94
79-20-9	Methyl acetate	0.18	[21]	2.30	[1]	2.48
141-78-6	Ethyl acetate	0.73	[21]	2.16	[1]	2.89
109-60-4	n-Propyl acetate	1.24	[21]	2.05	[1]	3.29
123-86-4	n-Butyl acetate	1.78	[21]	1.94	[1]	3.72
110-19-0	Isobutyl acetate	1.78	[21]	1.73	[1]	3.51
628-63-7	n-Pentyl acetate	2.30	[21]	1.84	[1]	4.14
93-58-3	Methyl benzoate	2.12	[21]	2.88	[1]	5.00
140-11-4	Benzyl acetate	1.83	[21]	3.34	[4], [14] ^{c)}	5.17
103-45-7	2-Phenylethylacetate	2.30	[25]	3.11	[9] ^{b)}	5.41
142-96-1	Di-n-butyl ether	3.21	[21]	0.61	[1]	3.82
693-65-2	Di-n-pentylether	4.36	a)	0.32	a)	4.68
1634-04-4	Methyl tert-butyl ether	0.94	[26]	0.03	[16]	0.97
109-99-9	Tetrahydrofuran	0.46	[21]	2.55	[1]	3.01
123-91-1	1,4-Dioxane	-0.27	[21]	3.71	[1]	3.44
271-89-6	Benzofuran	2.67	[21]	2.38	[9] ^{b)}	5.05
132-64-9	Dibenzofuran	4.12	[21]	2.36	[14]	6.48
100-66-3	Methyl phenyl ether	2.11	[21]	1.80	[1]	3.91
71-43-2	Benzene	2.13	[21]	0.63	[1]	2.76
108-88-3	Toluene	2.73	[21]	0.65	[1]	3.38
106-42-3	p-Xylene	3.15	[21]	0.59	[1]	3.74

CAS-Nr.	Compound	$\log K_{\text{ioctanol,water}}$ [m ³ /m ³] 25 °C	Ref	$\log K_{\text{iwater,air}}$ [(mol/l)/(mol/l)] 25 °C	Ref	^{d)} $\log K_{\text{ioctanol,air}}$ [m ³ /m ³] 25 °C
100-41-4	Ethylbenzene	3.15	[21]	0.58	[1]	3.73
103-65-1	n-Propylbenzene	3.72	[21]	0.39	[1]	4.11
104-51-8	n-Butylbenzene	4.38	[21]	0.29	[1]	4.67
538-68-1	n-Pentylbenzene	4.90	[21]	0.17	[1]	5.07
1077-16-3	n-Hexylbenzene	5.52	[21]	0.03	[1]	5.55
95-63-6	1,2,4-Trimethylbenzene	3.56	[21]	0.63	[1]	4.19
108-67-8	1,3,5-Trimethylbenzene	3.59	[21]	0.66	[1]	4.25
100-42-5	Styrene	2.95	[21]	0.91	[1]	3.86
496-11-7	Indane	3.18	[21]	1.07	[1]	4.25
91-20-3	Naphthalene	3.30	[21]	1.76	[1]	5.06
90-12-0	1-Methylnaphthalene	3.87	[21]	1.79	[1]	5.66
83-32-9	Acenaphthene	3.92	[21]	2.31	[1]	6.23
120-12-7	Anthracene	4.45	[21]	2.90	[1]	7.35
85-01-8	Phenanthrene	4.46	[21]	2.85	[1]	7.31
92-52-4	Biphenyl	4.06	[21]	1.95	[1]	6.01
92-94-4	p-Terphenyl	6.03	[21]	2.86	[2], [20] ^{c)}	8.89
108-90-7	Chlorobenzene	2.89	[21]	0.82	[1]	3.71
95-50-1	1,2-Dichlorobenzene	3.43	[21]	1.00	[1]	4.43
541-73-1	1,3-Dichlorobenzene	3.53	[21]	0.72	[1]	4.25
106-46-7	1,4-Dichlorobenzene	3.44	[21]	0.74	[1]	4.18
106-37-6	1,4-Dibromobenzene	3.79	[21]	1.44	[2], [6] ^{c)}	5.23
615-42-9	1,2-Diiodobenzene	4.33	[24]	1.93	[9] ^{b)}	6.26
624-38-4	1,4-Diiodobenzene	4.11	[25]	1.93	[9] ^{b)}	6.04
120-82-1	1,2,4-Trichlorobenzene	4.02	[21]	0.82	[1]	4.84
634-66-2	1,2,3,4-Tetrachlorobenzene	4.64	[21]	0.98	[1]	5.62
634-90-2	1,2,3,5-Tetrachlorobenzene	4.65	[21]	1.19	[1]	5.84
95-94-3	1,2,4,5-Tetrachlorobenzene	4.60	[21]	0.98	[1]	5.58
608-93-5	Pentachlorobenzene	5.18	[21]	1.47	[17]	6.65
118-74-1	Hexachlorobenzene	5.37	[21]	1.54	[17]	6.91
462-06-6	Fluorobenzene	2.27	[21]	0.59	[1]	2.86
108-86-1	Bromobenzene	2.99	[21]	1.07	[1]	4.06
591-50-4	Iodobenzene	3.25	[21]	1.28	[1]	4.53
352-32-9	4-Fluorotoluene	2.58	[14]	0.55	[9] ^{b)}	3.13
98-56-6	4-Chlorobenzotrifluoride	3.60	[24]	-0.15	[9] ^{b)}	3.45
630-20-6	1,1,1,2-Tetrachloroethane	2.66	[21]	0.94	[1]	3.60
79-34-5	1,1,2,2-Tetrachloroethane	2.39	[21]	1.81	[1]	4.20
544-10-5	1-Chlorohexane	3.66	[21]	0.00	[1]	3.66
629-06-1	1-Chloroheptane	4.15	[21]	-0.21	[1]	3.94
111-85-3	1-Chlorooctane	4.73	[21]	-0.31	a)	4.42
1002-69-3	1-Chlorodecane	5.72	a)	-0.57	a)	5.15
110-53-2	1-Bromopentane	3.37	[21]	0.07	[1]	3.44
123-72-8	Butanal/Butyraldehyde	0.88	[25]	2.33	[1]	3.21
110-62-3	Pentanal	1.31	[24]	2.22	[1]	3.53
100-52-7	Benzaldehyde	1.48	[21]	2.95	[1]	4.43

CAS-Nr.	Compound	$\log K_{\text{ioctanol,water}}$ [m ³ /m ³] 25 °C	Ref	$\log K_{\text{iwater,air}}$ [(mol/l)/(mol/l)] 25 °C	Ref	^{d)} $\log K_{\text{ioctanol,air}}$ [m ³ /m ³] 25 °C
109-74-0	1-Cyanopropane	0.53	[21]	2.67	[1]	3.20
62-53-3	Aniline	0.94	[22]	4.03	[17]	4.97
95-53-4	2-Methylaniline	1.32	[26]	4.06	[1]	5.38
106-49-0	4-Methylaniline	1.39	[22]	4.09	[1]	5.48
87-62-7	2,6-Dimethylaniline	1.84	[26]	3.82	[1]	5.66
121-69-7	N,N-Dimethylaniline	2.31	[22]	2.53	[1]	4.84
615-43-0	2-Iodoaniline	2.32	[25]	4.74	[9] ^{b)}	7.06
540-37-4	4-Iodoaniline	2.34	[23]	4.74	[9] ^{b)}	7.08
98-95-3	Nitrobenzene	1.85	[21]	3.02	[1]	4.87
88-72-2	2-Nitrotoluene	2.30	[21]	2.63	[1]	4.93
88-73-3	2-Chloronitrobenzene	2.45	[17]	2.74	[17]	5.19
100-47-0	Benzonitrile	1.56	[21]	3.09	[1]	4.65
75-05-8	Acetonitrile	-0.34	[21]	2.85	[1]	2.51
75-52-5	Nitromethane	-0.35	[21]	2.95	[1]	2.60
79-24-3	Nitroethane	0.18	[21]	2.72	[1]	2.90
108-03-2	1-Nitropropane	0.87	[21]	2.45	[1]	3.32
79-46-9	2-Nitropropane	0.55	[21]	2.30	[1]	2.85
110-86-1	Pyridine	0.65	[26]	3.44	[1]	4.09
109-06-8	2-Methylpyridine	1.11	[25]	3.40	[1]	4.51
1122-62-9	2-Acetylpyridine	0.85	[25]	6.28	[9] ^{b)}	7.13
109-08-0	2-Methylpyrazine	0.23	[21]	4.04	[1]	4.27
74-89-5	Methylamine	-0.57	[21]	3.34	[1]	2.77
68-12-2	N,N-Dimethylformamide	-1.01	[21]	5.73	[1]	4.72
127-19-5	N,N-Dimethylacetamide	-0.77	[21]	6.27	[12]	5.50
120-72-9	Indole (1H-Indole)	2.14	[25]	4.67	[2], [14] ^{c)}	6.81
91-22-5	Chinoline	2.03	[25]	4.20	[1]	6.23
79-09-4	Propanoic acid	0.33	[21]	4.74	[1]	5.07
107-92-6	Butanoic acid	0.79	[21]	4.66	[1]	5.45
109-52-4	Pentanoic acid	1.39	[21]	4.52	[1]	5.91
503-74-2	3-Methylbutanoic acid	1.16	[21]	4.47	[1]	5.63
528-29-0	1,2-Dinitrobenzene	1.69	[25]	5.66	[2], [14] ^{c)}	7.35
99-65-0	1,3-Dinitrobenzene	1.49	[17]	5.77	[17]	7.26
100-25-4	1,4-Dinitrobenzene	1.46	[25]	5.47	[9] ^{b)}	6.93
121-14-2	2,4-Dinitrotoluene	2.00	[17]	4.80	[17]	6.80
100-17-4	4-Nitroanisole	2.03	[25]	4.29	[9] ^{b)}	6.32
131-11-3	Dimethylphthalate	1.60	[23]	4.35	[17]	5.95
84-66-2	Diethylphthalate	2.47	[21]	4.61	[14]	7.08
78-40-0	Triethylphosphate	0.80	[21]	5.53	[1]	6.33
110-02-1	Thiophene	1.81	[21]	1.04	[1]	2.85
108-98-5	Thiophenol	2.52	[21]	1.87	[1]	4.39
67-68-5	Dimethylsulfoxide	-1.35	[25]	7.41	[1]	6.06
123-54-6	2,4-Pentanedione	0.40	[25]	4.02	[4], [14] ^{c)}	4.42
107-21-1	1,2-Ethanediole	-1.36	[25]	6.99	[15]	5.63
78-95-5	Chloroacetone	0.02	[24]	3.17	[10]	3.19

CAS-Nr.	Compound	$\log K_{i\text{octanol,water}}$ [m ³ /m ³] 25 °C	Ref	$\log K_{i\text{water,air}}$ [(mol/l)/(mol/l)] 25 °C	Ref	^{d)} $\log K_{i\text{octanol,air}}$ [m ³ /m ³] 25 °C
98-88-4	Benzoylchloride	1.44	[24]	2.30	[9] ^{b)}	3.74
116-09-6	Hydroxyacetone	-0.78	[24]	3.50	[9] ^{b)}	2.72
553-90-2	Dimethyl succinate	0.35	[25]	5.58	[9] ^{b)}	5.93
58-89-9	Lindane (gamma-HCH)	3.78	[17]	3.94	[17], [19]	7.72
109-86-4	2-Methoxyethanol	-0.77	[21]	4.96	[1]	4.19
110-80-5	2-Ethoxyethanol	-0.10	[21]	4.91	[1]	4.81
541-05-9	Hexamethylcyclotrisiloxane	4.47	[24]	-0.41	[9] ^{b)}	4.06
88-74-4	2-Nitroaniline	1.85	[21]	5.41	[1]	7.26
591-31-1	3-Methoxybenzaldehyde	1.71	[14]	4.49	[9] ^{b)}	6.20
150-78-7	1,4-Dimethoxybenzene	2.03	[21]	3.32	[14] ^{c)}	5.35
873-62-1	3-Hydroxybenzonitrile	1.70	[21]	7.08	[1]	8.78
1885-29-6	2-Aminobenzonitrile	1.40	[25]	6.12	[9] ^{b)}	7.52
873-74-5	4-Aminobenzonitrile	1.17	[24]	6.12	[9] ^{b)}	7.29
103-33-3	Azobenzene	3.82	[21]	3.26	[14] ^{c)}	7.08

a) extrapolated from homologue series, based on it's proportionality to the number of carbons

b) estimated by the method published in [9]

c) estimated with vapor pressure p_{iL} and water solubility $C_{iw,sat}$

d) $K_{ioa} = K_{iow} \cdot K_{iwa}$

[1] Abraham, M.H.; Andonian-Haftvan, J.; Whiting, G.S.; Leo, A.; Taft, R.S. Hydrogen Bonding. Part 34. The factors that influence the solubility of gases and vapours in water at 298K, and a new method for its determination. *J. Chem. Soc. Perkin Trans. 2*. **1994**. 8: 1777-1791.

[2] Myrdal, P.; Ward, G.H.; Dannenfelser, R.M.; Mishra, D.; Yalkowsky, S.H. Aquafac 1 - Aqueous functional-group activity-coefficients – application to hydrocarbons. *Chemosphere*. **1992**. 24(8): 1047-1061.

[3] Amidon, G.L.; Yalkowsky, S.H.; Leung, S. Solubility of nonelectrolytes in polar-solvents. 2. Solubility of aliphatic-alcohols in water. *J. Pharm. Sci.* **1974**. 63(12): 1858-1866.

[4] Daubert, T.E.; Danner, R.P. (eds). Design Institute for Physical Property Data. Physical and thermodynamic properties of pure chemicals: data compilation. American Institute of Chemical Engineers; NSRDS, National Standard Reference Data System. Hemisphere Publishing cop. **1989**. New York.

[5] Daubert, T.E.; Danner, R.P. (eds.) Design Institute for Physical Property Data - American Institute of Chemical Design and National Standard. Reference Data System and AIChE. Data compilation tables of properties of pure compounds. University Park - Pa.: Department of Chemical Engineering - Pennsylvania State University. **1985**.

- [6] Walsh, P.N.; Smith, N.O. Sublimation pressure of solid solutions. 2. Systems p-dichlorobenzene-p-dibromobenzene, p-dichlorobenzene-p-bromochlorobenzene and p-dibromobenzene-p-bromochlorobenzene at 50 degrees. *J. Phys. Chem.* **1961**. 65(5): 718.
- [7] Bidleman, T.F.; Renberg, L. Determination of vapor-pressures for chloroguaiacols, chloroveratroles, and nonylphenol by gas-chromatography. *Chemosphere*. **1985**. 14(10): 1475-1481.
- [8] Leuenberger, C.; Ligocki, M.P.; Pankow, J.F. Trace organic-compounds in rain. 4. Identities, concentrations, and scavenging mechanisms for phenols in urban air and rain. *Environ. Sci. Technol.* **1985**. 19(11): 1053-1058.
- [9] Meylan, W.M.; Howard, P.H. Bond contribution method for estimating Henry's law constants. *Environ. Toxicol. Chem.* **1991**. 10(10): 1283-1293.
- [10] Betterton, E.A. The partitioning of ketones between the gas and aqueous phases. *Atmos. Environ. A*. **1991**. 25(8): 1473-1477.
- [11] Altschuh, J.; Bruggemann, R.; Santl, H.; Eichinger, G.; Piringer, O.G.; Henry's law constants for a diverse set of organic chemicals: experimental determination and comparison of estimation methods. *Chemosphere*. **1999**. 39(11): 1871-1887.
- [12] Taft, R.W.; Abraham, M.H.; Doherty, R.M.; Kamlet, M.J. The molecular properties governing solubilities of organic nonelectrolytes in water. *Nature*. **1985**. 6001: 384-386.
- [13] Kochetkov A.; Smith, J.S.; Ravikrishna, R.; Valsaraj, K.T.; Thibodeaux, L.J. Air-water partition constants for volatile methyl siloxanes. *Environ. Toxicol. Chem.* **2001**. 20(10): 2184-2188.
- [14] SRC Syracuse Research Corporation: Physical Properties Database (PHYSPROP). <http://www.syrres.com/esc/physprop.htm> accessed September 30 2005.
- [15] Bone, R.; Cullis, P.; Wolfenden, R. Solvent effects on equilibria of addition of nucleophiles to acetaldehyde and the hydrophilic character of diols. *J. Am. Chem. Soc.* **1983**. 105: 1339-1343.
- [16] Arp, H.P.H.; Schmidt, T.C. Air-water transfer of MTBE, its degradation products, and alternative fuel oxygenates: The role of temperature. *Environ. Sci. Technol.* **2004**. 38(20): 5405-5412.
- [17] Schwarzenbach, R.P.; Gschwend, P.M.; Imboden, D.M. Environmental Organic Chemistry. 2nd Edition, **2003**, Wiley Interscience, Hoboken, New Jersey.
- [18] Daubert, T.E.; Danner, R.P. DIPPR Data Compilation, Version 13. New York. **1995**.

- [19] Xiao, H.; Li, N.; Wania, F. Compilation, evaluation, and selection of physical-chemical property data for alpha-,beta-, and gamma-hexachlorocyclohexane. *J. Chem. Eng. Data.* **2004.** 173-175.
- [20] Lide, D.R. (ed.). CRC Handbook of Chemistry and Physics. 84th Edition. **2003.** CRC Press, Boca Ration, Florida.
- [21] Abraham, M.H.; Chadha, H.S.; Whiting, G.S.; Mitchell, R.C. Hydrogen bonding. 32. An analysis of water-octanol and water-alkane partitioning and the $\Delta\log P$ parameter of Seiler. *J. Pharmaceut. Sci.* **1994.** 83(8): 1085-1100.
- [22] Poole, S.K.; Poole, C.F. Chromatographic models for the sorption of neutral organic compounds by soil from water and air. *J. Chromatogr. A.* **1999.** 845: 381-400.
- [23] Torres-Lapasio, J.R.; Garcia-Alvarez-Coque, M.C.; Roses, M.; Bosch, E.; Zissimos, A.M.; Abraham, M.H. Analysis of a solute polarity parameter in reversed-phase liquid chromatography on a linear solvation relationship basis. *Anal. Chim. Acta.* **2004.** 515: 209-227.
- [24] Data estimated by the method of: Meylan, W.M.; Howard, P.H. Atom/fragment contribution method for estimating octanol-water partition coefficients. *J. Pharm. Sci.* **1995.** 84: 83-92.
- [25] Hansch, C.; Leo, A.; Hoekman, D. Exploring QSAR. Heller, S.R. (Ed.). American Chemical Society. **1995.** Washington.
- [26] Kamlet, M.J.; Doherty, R.M.; Abraham, M.H.; Marcus, Y.; Taft, R.W. Linear solvation energy relationships. 46. An improved equation for correlation and prediction of octanol/water partition coefficients of organic nonelectrolytes (including strong hydrogen bond donor solutes). *J. Phys. Chem.* **1988.** 92: 5244-5255.
- [27] Kishino, T.; Kobayashi, K. Relation between the chemical structures of chlorophenols and their dissociation constants and partitioning coefficients in several solvent/water systems. *Wat. Res.* **1994.** 28(7): 1547-1552.

SI-2: K_{ioc} partition coefficients calculated by PcKocWIN

Table SI-2 contains K_{ioc} values *predicted* by PcKocWIN and Leonardite humic acid org-carbon/water partition coefficients $K_{iHA-oc,water}$ (25 °C). The $K_{iHA-oc,water}$ partition coefficients are calculated from experimental humic acid/air partition coefficients, the organic-C content of Leonardite HA (63.81%) and experimental water/air partition coefficients (SI-1).

Compound	$\log(K_{ioc}/[L/kg_{oc}])$ PcKocWIN™	$\log(K_{HA-oc,water})$ [L/kg _{oc}] <i>experimental</i>	Compound	$\log(K_{ioc}/[L/kg_{oc}])$ PcKocWIN™	$\log(K_{HA-oc,water})$ [L/kg _{oc}] <i>experimental</i>
n-Nonane	2.97	5.31	n-Hexylbenzene	3.78	4.42
n-Decane	3.24	5.58	1,2,4-Trimethylbenzene	2.86	2.54
n-Undecane	3.50	6.26	1,3,5-Trimethylbenzene	2.85	2.36
n-Dodecane	3.77	6.86	Indane	3.00	2.37
n-Tridecane	4.03	7.53	Naphthalene	3.26	2.91
n-Tetradecane	4.30	8.18	1-Methylnaphthalene	3.48	3.36
1-Nonene	2.97	4.51	Acenaphthene	3.79	3.18
1-Decene	3.24	4.88	Anthracene	4.31	4.11
1-Undecene	3.50	5.53	Phenanthrene	4.32	4.05
1-Dodecene	3.77	6.20	Biphenyl	3.80	3.42
1-Tridecene	4.03	6.79	p-Terphenyl	5.37	6.25
Ethanol	0.00	0.02	Chlorobenzene	2.43	2.29
Propan-1-ol	0.12	0.24	1,2-Dichlorobenzene	2.65	2.81
Butan-1-ol	0.39	0.46	1,3-Dichlorobenzene	2.64	2.93
Pentan-1-ol	0.65	0.89	1,4-Dichlorobenzene	2.64	2.99
Hexan-1-ol	0.92	1.38	1,4-Dibromobenzene	2.64	3.14
Heptan-1-ol	1.19	1.86	1,2,4-Trichlorobenzene	2.86	3.61

Compound	$\log(K_{ioc}/[L/kg_{oc}])$ PcKocWIN™	$\log(K_{HA-oc,water})$ [L/kg _{oc}] <i>experimental</i>	Compound	$\log(K_{ioc}/[L/kg_{oc}])$ PcKocWIN™	$\log(K_{HA-oc,water})$ [L/kg _{oc}] <i>experimental</i>
Octan-1-ol	1.45	2.40	1,2,3,4-Tetrachlorobenzene	3.08	4.15
Nonan-1-ol	1.72	2.95	1,2,3,5-Tetrachlorobenzene	3.07	3.78
Decan-1-ol	1.98	3.49	1,2,4,5-Tetrachlorobenzene	3.07	4.61
Undecan-1-ol	2.25	3.74	Pentachlorobenzene	3.30	4.33
Propan-2-ol	0.03	0.01	Hexachlorobenzene	3.53	4.86
2-Methylpropan-1-ol	0.31	0.31	Bromobenzene	2.43	2.39
2-Methylpropan-2-ol	0.17	0.35	Iodobenzene	2.43	2.63
3-Methylbutan-1-ol	0.58	0.85	4-Fluorotoluene	2.64	2.00
Benzyl alcohol	1.19	1.04	1,1,2,2-Tetrachloroethane	2.03	1.74
1-Napthol	3.48	2.22	1-Chloroheptane	2.70	3.30
Cyclopentanol	0.64	0.37	1-Chlorooctane	2.97	3.98
Cyclohexanol	0.91	0.81	Butanal/Butyraldehyde	0.71	0.14
2,2,2-Trifluoroethanol	0.47	0.20	Benzaldehyde	1.51	1.71
Hexafluoropropan-2-ol	1.31	0.95	1-Cyanopropane	1.18	0.68
Phenol	2.43	0.96	Aniline	1.65	1.54
o-Cresol	2.65	1.39	o-Toluidine (2-Methylaniline)	1.87	1.59
m-Cresol	2.64	1.62	p-Toluidine (4-Methylaniline)	1.86	2.13
p-Cresol	2.64	1.58	2,6-Dimethylaniline	2.09	1.78
2-Chlorophenol	2.65	1.98	N,N-Dimethylaniline	1.89	2.37
4-Chlorophenol	2.64	1.71	4-Iodoaniline	1.86	2.14
2,3-Dichlorophenol	2.86	1.17	Nitrobenzene	2.28	1.88
2,6-Dichlorophenol	2.86	1.90	2-Nitrotoluene	2.50	2.29
2-Butanone	0.58	0.36	Benzonitrile	1.99	1.51

Compound	$\log(K_{ioc}/[L/kg_{oc}])$ PcKocWIN™	$\log(K_{HA-oc,water})$ [L/kg _{oc}] <i>experimental</i>	Compound	$\log(K_{ioc}/[L/kg_{oc}])$ PcKocWIN™	$\log(K_{HA-oc,water})$ [L/kg _{oc}] <i>experimental</i>
2-Pentanone	0.85	0.63	Acetonitrile	0.65	0.34
2-Hexanone	1.11	0.97	Nitromethane	0.91	0.27
2-Heptanone	1.38	1.60	1-Nitropropane	1.46	0.78
2-Octanone	1.65	2.05	2-Nitropropane	1.40	0.55
2-Nonanone	1.91	2.76	2-Methylpyridine	1.46	2.29
2-Decanone	2.18	3.31	N,N-Dimethylformamide	0.38	-0.02
2-Undecanone	2.44	3.91	N,N-Dimethylacetamide	0.97	-0.10
3-Methylbutan-2-one	0.78	0.72	Indole (1H-Indole)	3.00	1.61
4-Methylpentan-2-one	1.04	1.05	Chinoline	3.26	1.83
Cyclopentanone	0.91	0.54	Propanoic acid	0.08	0.85
Cyclohexanone	1.18	0.61	Butanoic acid	0.35	0.97
Acetophenone	1.66	1.66	Pentanoic acid	0.61	1.40
n-Propyl acetate	1.05	1.13	1,3-Dinitrobenzene	2.34	1.03
n-Butyl acetate	1.32	1.27	2,4-Dinitrotoluene	2.56	2.65
Isobutyl acetate	1.24	1.58	4-Nitroanisole	2.13	2.00
n-Pentyl acetate	1.59	1.82	Dimethylphthalate	1.57	2.05
Methyl benzoate	1.89	1.93	Triethylphosphate	1.68	0.63
Benzyl acetate	2.13	1.86	Thiophenol	2.43	2.16
Di-n-butyl ether	1.71	2.53	Dimethylsulfoxide	0.64	-1.60
Di-n-pentylether	2.24	3.74	2,4-Pentanedione	0.00	0.14
1,4-Dioxane	0.00	0.13	Chloroacetone	0.58	0.49
Benzofurane	3.00	1.60	Dimethyl succinate	1.00	-0.38
Dibenzofuran	4.05	3.40	Lindane (gamma-HCH)	3.53	3.00

Compound	$\log(K_{ioc}/[L/kg_{oc}])$ PcKocWIN™	$\log(K_{HA-oc,water})$ [L/kg _{oc}] <i>experimental</i>	Compound	$\log(K_{ioc}/[L/kg_{oc}])$ PcKocWIN™	$\log(K_{HA-oc,water})$ [L/kg _{oc}] <i>experimental</i>
Methyl phenyl ether	2.07	1.91	2-Methoxyethanol	0.00	-0.05
Ethylbenzene	2.71	2.20	2-Ethoxyethanol	0.00	-0.04
n-Propylbenzene	2.98	2.75	2-Nitroaniline	1.72	1.28
n-Butylbenzene	3.25	3.12	Azobenzene	3.29	2.98
n-Pentylbenzene	3.51	3.66			

SI-3: pp-LFER model

Table SI-3: sorbate-specific descriptors, *experimental* Leonardite humic acid/air partition coefficients at 15 °C and humic acid partition coefficients *fitted* by the pp-LFER in Equation 2 (Equation 2 in the article for 15 °C).

Compound	$\log(K_{\text{HA,air}}/[\text{L/kg}_{\text{HA}}])$ 15°C <i>measured</i>	$K_{\text{HA,air}}/[\text{L/kg}_{\text{HA}}]$ 15°C <i>measured</i>	A_i	B_i	V_i [10 ⁻⁴ m ³ /mol]	L_i [m ³ /m ³]	S_i	$\log(K_{\text{HA,air}}/[\text{L/kg}_{\text{HA}}])$ 15°C <i>fitted</i> by pp-LFER	$K_{\text{HA,air}}/[\text{L/kg}_{\text{HA}}]$ 15°C <i>fitted</i> by pp-LFER	<i>fitted /</i> <i>measured</i>	Ref $A_i, B_i,$ $V_i,$ L_i, S_i
n-Octane	2.16	1.46E+02	0.00	0.00	1.24	3.677	0.00	2.22	1.64E+02	1.13	[1]
n-Nonane	2.82	6.61E+02	0.00	0.00	1.38	4.182	0.00	2.61	4.10E+02	0.62	[1]
n-Decane	3.41	2.57E+03	0.00	0.00	1.52	4.686	0.00	3.01	1.02E+03	0.40	[1]
n-Undecane	3.91	8.18E+03	0.00	0.00	1.66	5.191	0.00	3.40	2.54E+03	0.31	[3,4]
n-Dodecane	4.38	2.41E+04	0.00	0.00	1.80	5.696	0.00	3.80	6.33E+03	0.26	[3,4]
n-Tridecane	4.87	7.41E+04	0.00	0.00	1.96	6.200	0.00	4.20	1.57E+04	0.21	[3,4]
n-Tetradecane	5.43	2.69E+05	0.00	0.00	2.08	6.705 ^{a)}	0.00	4.59	3.92E+04	0.15	[3,4]
1-Octene	2.08	1.19E+02	0.00	0.07	1.19	3.568	0.08	2.35	2.26E+02	1.89	[1]
1-Nonene	2.69	4.87E+02	0.00	0.07	1.33	4.073	0.08	2.75	5.64E+02	1.16	[1]
1-Decene	3.28	1.90E+03	0.00 ^{a)}	0.07 ^{a)}	1.47	4.658 ^{a)}	0.08 ^{a)}	3.21	1.63E+03	0.86	[1]
1-Undecene	3.83	6.77E+03	0.00 ^{a)}	0.07 ^{a)}	1.62	5.192 ^{a)}	0.08 ^{a)}	3.63	4.29E+03	0.63	[3]
1-Dodecene	4.35	2.25E+04	0.00 ^{a)}	0.07 ^{a)}	1.76	5.726 ^{a)}	0.08 ^{a)}	4.05	1.13E+04	0.50	[3]
1-Tridecene	4.77	5.87E+04	0.00 ^{a)}	0.07 ^{a)}	1.90	6.260 ^{a)}	0.08 ^{a)}	4.47	2.97E+04	0.50	[3]
Ethanol	3.68	4.81E+03	0.37	0.48	0.45	1.485	0.42	3.23	1.70E+03	0.35	[1]
Propan-1-ol	3.82	6.56E+03	0.37	0.48	0.59	2.031	0.42	3.66	4.57E+03	0.70	[1]
Butan-1-ol	4.08	1.21E+04	0.37	0.48	0.73	2.601	0.42	4.11	1.29E+04	1.07	[1]
Pentan-1-ol	4.39	2.45E+04	0.37	0.48	0.87	3.106	0.42	4.51	3.21E+04	1.31	[1]
Hexan-1-ol	4.76	5.78E+04	0.37	0.48	1.01	3.610	0.42	4.90	7.97E+04	1.38	[1]
Heptan-1-ol	5.18	1.50E+05	0.37	0.48	1.15	4.115	0.42	5.30	1.99E+05	1.33	[1]
Octan-1-ol	5.63	4.27E+05	0.37	0.48	1.30	4.619	0.42	5.69	4.94E+05	1.16	[1]
Nonan-1-ol	6.14	1.37E+06	0.37	0.48	1.44	5.124	0.42	6.09	1.23E+06	0.90	[1]

Compound	$\log(K_{HA,air}/[L/kg_{HA}])$ 15°C <i>measured</i>	$K_{HA,air}/[L/kg_{HA}]$ 15°C <i>measured</i>	A_i	B_i	V_i [10 ⁻⁴ m ³ /mol]	L_i [m ³ /m ³]	S_i	$\log(K_{HA,air}/[L/kg_{HA}])$ 15°C <i>fitted</i> by pp-LFER	$K_{HA,air}/[L/kg_{HA}]$ 15°C <i>fitted</i> by pp-LFER	<i>fitted /</i> <i>measured</i>	Ref $A_i, B_i,$ $V_i,$ L_i, S_i
Decan-1-ol	6.42	2.66E+06	0.37	0.48	1.58	5.628	0.42	6.49	3.06E+06	1.15	[1]
Undecan-1-ol	6.59	3.86E+06	0.37	0.48	1.72	6.175 ^{a)}	0.42	6.92	8.26E+06	2.14	[3]
Propan-2-ol	3.56	3.66E+03	0.33	0.56	0.59	1.764	0.36	3.38	2.41E+03	0.66	[1]
2-Methylpropan-1-ol	3.82	6.64E+03	0.37	0.48	0.73	2.413	0.39	3.92	8.38E+03	1.26	[1]
2-Methylpropan-2-ol	3.60	3.98E+03	0.31	0.60	0.73	1.963	0.30	3.47	2.93E+03	0.73	[1,3]
3-Methylbutan-1-ol	4.23	1.71E+04	0.37	0.48	0.87	3.011	0.39	4.40	2.48E+04	1.45	[1]
Benzyl alcohol	6.10	1.26E+06	0.33	0.56	0.92	4.221	0.87	5.92	8.35E+05	0.66	[1]
1-Naphthol	8.20	1.57E+08	0.61	0.37	1.14	6.130	1.05	8.31	2.02E+08	1.28	[1]
Cyclopentanol	4.56	3.65E+04	0.32	0.56	0.76	3.241	0.54	4.73	5.37E+04	1.47	[1]
Cyclohexanol	4.92	8.30E+04	0.32	0.57	0.90	3.758	0.54	5.16	1.43E+05	1.72	[1]
2,2,2-Trifluoroethanol	3.42	2.64E+03	0.57	0.25	0.50	1.224	0.60	3.51	3.25E+03	1.23	[1]
Hexafluoropropan-2-ol	3.88	7.62E+03	0.77	0.10	0.70	1.390	0.55	4.02	1.04E+04	1.36	[1]
Phenol	6.00	9.90E+05	0.60	0.30	0.78	3.766	0.89	6.08	1.19E+06	1.20	[2,8]
o-Cresol	5.96	9.04E+05	0.52	0.30	0.92	4.218	0.86	6.11	1.28E+06	1.41	[2,8]
m-Cresol	6.50	3.18E+06	0.57	0.34	0.92	4.310	0.88	6.46	2.88E+06	0.91	[2,8]
p-Cresol	6.48	3.01E+06	0.57	0.31	0.92	4.312	0.87	6.39	2.47E+06	0.82	[2,8]
2-Chlorophenol	5.44	2.77E+05	0.32	0.31	0.90	4.178	0.88	5.39	2.47E+05	0.89	[2,5]
4-Chlorophenol	7.19	1.55E+07	0.67	0.20	0.90	4.775	1.08	7.16	1.45E+07	0.94	[2,8]
2,3-Dichlorophenol	6.36	2.28E+06	0.48	0.20	1.02	4.989	0.94	6.48	3.01E+06	1.32	[2,5]
2,6-Dichlorophenol	5.87	7.43E+05	0.38	0.24	1.02	5.086	0.90	6.22	1.68E+06	2.26	[2,8]
2,4,5-Trichlorophenol	8.08	1.21E+08	0.73	0.10	1.14	5.725	0.92	7.76	5.71E+07	0.47	[2,8]
2,4,6-Trichlorophenol	8.21	1.61E+08	0.68	0.15	1.14	5.664	0.80	7.48	3.05E+07	0.19	[2,8]
2-Propanone	2.68	4.76E+02	0.04	0.51	0.55	1.696	0.70	2.57	3.76E+02	0.79	[1]
2-Butanone	2.85	7.08E+02	0.00	0.51	0.69	2.287	0.70	2.90	7.87E+02	1.11	[1]
2-Pentanone	3.28	1.89E+03	0.00	0.51	0.83	2.755	0.68	3.24	1.74E+03	0.92	[1]
2-Hexanone	3.49	3.10E+03	0.00	0.51	0.97	3.262	0.68	3.64	4.35E+03	1.40	[1]

Compound	$\log(K_{HA,air}/[L/kg_{HA}])$ 15°C <i>measured</i>	$K_{HA,air}/[L/kg_{HA}]$ 15°C <i>measured</i>	A_i	B_i	V_i [10 ⁻⁴ m ³ /mol]	L_i [m ³ /m ³]	S_i	$\log(K_{HA,air}/[L/kg_{HA}])$ 15°C <i>fitted</i> by pp-LFER	$K_{HA,air}/[L/kg_{HA}]$ 15°C <i>fitted</i> by pp-LFER	<i>fitted /</i> <i>measured</i>	Ref $A_i, B_i,$ $V_i,$ L_i, S_i
2-Heptanone	3.92	8.36E+03	0.00	0.51	1.11	3.760	0.68	4.03	1.07E+04	1.28	[1]
2-Octanone	4.29	1.93E+04	0.00	0.51	1.25	4.257	0.68	4.42	2.62E+04	1.36	[1]
2-Nonanone	4.81	6.42E+04	0.00	0.51	1.39	4.735	0.68	4.79	6.22E+04	0.97	[1]
2-Decanone	5.27	1.86E+05	0.00	0.51	1.53	5.245	0.68	5.19	1.56E+05	0.84	[1]
2-Undecanone	5.67	4.66E+05	0.00	0.51	1.67	5.732	0.68	5.58	3.77E+05	0.81	[1]
3-Methylbutan-2-one	3.08	1.21E+03	0.00	0.51	0.83	2.692	0.65	3.15	1.43E+03	1.18	[1]
4-Methylpentan-2-one	3.31	2.05E+03	0.00	0.51	0.97	3.089	0.65	3.46	2.91E+03	1.42	[1]
Cyclopentanone	4.05	1.12E+04	0.00	0.52	0.72	3.221	0.86	3.85	7.06E+03	0.63	[1,3]
Cyclohexanone	4.29	1.94E+04	0.00	0.56	0.86	3.792	0.86	4.37	2.36E+04	1.22	[1,3]
Acetophenone	5.22	1.65E+05	0.00	0.49	1.01	4.501	1.01	4.97	9.40E+04	0.57	[1]
Methyl acetate	2.50	3.17E+02	0.00	0.45	0.61	1.911	0.64	2.42	2.61E+02	0.82	[1]
Ethyl acetate	2.39	2.47E+02	0.00	0.45	0.75	2.314	0.62	2.71	5.11E+02	2.07	[1]
n-Propyl acetate	2.85	7.15E+02	0.00	0.45	0.89	2.819	0.60	3.08	1.21E+03	1.69	[1]
n-Butyl acetate	3.28	1.92E+03	0.00	0.45	1.03	3.353	0.60	3.50	3.18E+03	1.66	[1]
Isobutyl acetate	3.40	2.49E+03	0.00	0.47	1.03	3.161	0.57	3.35	2.24E+03	0.90	[1]
n-Pentyl acetate	3.72	5.27E+03	0.00	0.45	1.17	3.844	0.60	3.89	7.72E+03	1.47	[1]
Methyl benzoate	5.01	1.02E+05	0.00	0.48	1.07	4.704	0.85	4.93	8.54E+04	0.84	[1]
Benzyl acetate	5.32	2.10E+05	0.00	0.65	1.21	5.012	1.06	5.73	5.35E+05	2.55	[2,8]
Di-n-butyl ether	3.22	1.66E+03	0.00	0.45	1.29	3.924	0.25	3.54	3.49E+03	2.11	[1]
Di-n-pentylether	4.23	1.71E+04	0.00 ^{a)}	0.45 ^{a)}	1.58	4.800 ^{c)}	0.25 ^{a)}	4.23	1.69E+04	0.99	
Methyl tert-butyl ether	1.94	8.69E+01	0.00	0.45	0.87	2.270 ^{e)}	0.19	2.17	1.49E+02	1.71	[1]
Tetrahydrofuran	2.70	5.04E+02	0.00	0.48	0.62	2.636	0.52	2.92	8.34E+02	1.65	[1]
1,4-Dioxane	3.82	6.55E+03	0.00	0.64	0.68	2.892	0.75	3.69	4.86E+03	0.74	[1]
Benzofurane	4.09	1.24E+04	0.00	0.15	0.91	4.355	0.83	4.02	1.04E+04	0.84	[2,3]
Dibenzofuran	5.80	6.35E+05	0.00	0.17	1.27	6.716	1.02	6.15	1.40E+06	2.21	[2,3]
Methyl phenyl ether	3.72	5.22E+03	0.00	0.29	0.92	3.890	0.74	3.80	6.36E+03	1.22	[1]

Compound	$\log(K_{HA,air}/[L/kg_{HA}])$ 15°C <i>measured</i>	$K_{HA,air}/[L/kg_{HA}]$ 15°C <i>measured</i>	A_i	B_i	V_i [10 ⁻⁴ m ³ /mol]	L_i [m ³ /m ³]	S_i	$\log(K_{HA,air}/[L/kg_{HA}])$ 15°C <i>fitted</i> by pp-LFER	$K_{HA,air}/[L/kg_{HA}]$ 15°C <i>fitted</i> by pp-LFER	<i>fitted /</i> <i>measured</i>	Ref $A_i, B_i,$ $V_i,$ L_i, S_i
Benzene	2.18	1.51E+02	0.00	0.14	0.72	2.786	0.52	2.39	2.48E+02	1.65	[1]
Toluene	2.29	1.94E+02	0.00	0.14	0.86	3.325	0.52	2.82	6.58E+02	3.39	[1]
p-Xylene	2.88	7.58E+02	0.00	0.16	1.00	3.839	0.52	3.26	1.82E+03	2.40	[1]
Ethylbenzene	2.78	6.09E+02	0.00	0.15	1.00	3.778	0.51	3.18	1.52E+03	2.49	[1]
n-Propylbenzene	3.10	1.25E+03	0.00	0.15	1.14	4.230	0.50	3.52	3.33E+03	2.67	[1]
n-Butylbenzene	3.53	3.41E+03	0.00	0.15	1.28	4.730	0.51	3.93	8.45E+03	2.48	[1]
n-Pentylbenzene	4.03	1.08E+04	0.00	0.15	1.42	5.230	0.51	4.32	2.09E+04	1.94	[1]
n-Hexylbenzene	4.53	3.36E+04	0.00	0.15	1.56	5.720	0.50	4.69	4.92E+04	1.47	[1]
1,2,4-Trimethylbenzene	3.33	2.14E+03	0.00	0.19	1.14	4.441	0.56	3.84	6.87E+03	3.20	[1]
1,3,5-Trimethylbenzene	3.05	1.13E+03	0.00	0.19	1.14	4.344	0.52	3.71	5.16E+03	4.59	[1]
Styrene	3.34	2.18E+03	0.00	0.16	0.96	3.856	0.65	3.43	2.66E+03	1.22	[1]
Indane	3.49	3.07E+03	0.00	0.17	1.03	4.590	0.62	4.00	9.92E+03	3.23	[1]
Naphthalene	4.66	4.58E+04	0.00	0.20	1.09	5.161	0.92	4.85	7.11E+04	1.55	[1]
1-Methylnaphthalene	5.48	3.01E+05	0.00	0.20	1.23	5.789	0.90	5.32	2.11E+05	0.70	[1]
Acenaphthene	5.75	5.62E+05	0.00	0.20	1.26	6.469	1.04	6.03	1.07E+06	1.91	[1]
<i>Anthracene</i>	7.29	1.93E+07	0.00	0.28	1.45	7.568	1.34	7.40	2.49E+07	1.29	[2,8]
<i>Phenanthrene</i>	7.17	1.48E+07	0.00	0.29	1.45	7.632	1.29	7.41	2.56E+07	1.73	[2,8]
Biphenyl	5.58	3.76E+05	0.00	0.26	1.32	6.014	0.99	5.71	5.18E+05	1.38	[2,8]
<i>p-Terphenyl</i>	9.49	3.11E+09	0.00	0.30	1.93	9.689	1.48	9.27	1.86E+09	0.60	[2,3]
Chlorobenzene	3.05	1.13E+03	0.00	0.07	0.84	3.657	0.65	3.10	1.27E+03	1.12	[5]
1,2-Dichlorobenzene	4.01	1.02E+04	0.00	0.04	0.96	4.518	0.78	3.88	7.61E+03	0.75	[5]
1,3-Dichlorobenzene	3.81	6.46E+03	0.00	0.02	0.96	4.410	0.73	3.70	5.01E+03	0.78	[5]
1,4-Dichlorobenzene	3.87	7.37E+03	0.00	0.02	0.96	4.435	0.75	3.74	5.53E+03	0.75	[5]
1,4-Dibromobenzene	4.69	4.86E+04	0.00	0.04	1.07	5.324	0.86	4.62	4.13E+04	0.85	[2,3]
1,2,4-Trichlorobenzene	4.51	3.27E+04	0.00	0.00	1.08	5.248	0.81	4.42	2.63E+04	0.81	[5]
1,2,3,4-Tetrachlorobenz.	5.36	2.31E+05	0.00	0.00	1.21	6.171	0.92	5.28	1.91E+05	0.83	[5]

Compound	$\log(K_{HA,air}/[L/kg_{HA}])$ 15°C <i>measured</i>	$K_{HA,air}/[L/kg_{HA}]$ 15°C <i>measured</i>	A_i	B_i	V_i [10 ⁻⁴ m ³ /mol]	L_i [m ³ /m ³]	S_i	$\log(K_{HA,air}/[L/kg_{HA}])$ 15°C <i>fitted</i> by pp-LFER	$K_{HA,air}/[L/kg_{HA}]$ 15°C <i>fitted</i> by pp-LFER	<i>fitted /</i> <i>measured</i>	Ref $A_i, B_i,$ $V_i,$ L_i, S_i
1,2,3,5-Tetrachlorobenz.	5.14	1.39E+05	0.00	0.00	1.21	5.922	0.85	5.00	1.00E+05	0.72	[5]
1,2,4,5-Tetrachlorobenz.	5.79	6.14E+05	0.00	0.00	1.21	5.926	0.86	5.01	1.03E+05	0.17	[5]
Pentachlorobenzene	6.05	1.13E+06	0.00	0.00	1.33	6.716	0.96	5.76	5.71E+05	0.51	[5]
Hexachlorobenzene	6.50	3.19E+06	0.00	0.00	1.45	7.624	0.99	6.51	3.27E+06	1.03	[5]
Fluorobenzene	2.21	1.63E+02	0.00	0.10	0.73	2.788	0.57	2.38	2.38E+02	1.46	[1]
Bromobenzene	3.54	3.45E+03	0.00	0.09	0.89	4.041	0.73	3.54	3.46E+03	1.00	[5]
Iodobenzene	4.03	1.08E+04	0.00	0.12	0.97	4.502	0.82	4.06	1.16E+04	1.07	[5]
4-Fluorotoluene	2.60	3.96E+02	0.00	0.10 ^{e)}	0.88	3.366	0.55	2.81	6.44E+02	1.63	[2]
1,1,1,2-Tetrachloroeth.	3.01	1.02E+03	0.10	0.08	0.88	3.641	0.63	3.45	2.79E+03	2.75	[1]
1,1,2,2-Tetrachloroeth.	3.70	5.06E+03	0.16	0.12	0.88	3.803	0.76	4.02	1.04E+04	2.06	[1]
1-Chlorohexane	2.50	3.19E+02	0.00	0.10	1.08	3.777	0.40	2.95	8.99E+02	2.82	[1]
1-Chloroheptane	3.10	1.26E+03	0.00	0.10	1.22	4.282	0.40	3.35	2.24E+03	1.77	[1]
1-Chlorooctane	3.82	6.63E+03	0.00	0.10	1.36	4.772	0.40	3.73	5.43E+03	0.82	[2,3]
1-Chlorodecane	4.67	4.72E+04	0.00 ^{a)}	0.10 ^{a)}	1.64	5.827 ^{a)}	0.40 ^{a)}	4.56	3.67E+04	0.78	[3]
1-Bromopentane	2.32	2.09E+02	0.00	0.12	0.99	3.611	0.40	2.86	7.32E+02	3.49	[1]
Butanal/Butyraldehyde	2.41	2.57E+02	0.00	0.45	0.69	2.270	0.65	2.71	5.15E+02	2.01	[1]
Pentanal	2.59	3.92E+02	0.00	0.45	0.83	2.851	0.65	3.17	1.48E+03	3.77	[1]
Benzaldehyde	4.70	4.97E+04	0.00	0.39	0.87	4.008	1.00	4.39	2.44E+04	0.49	[1]
1-Cyanopropane	3.44	2.74E+03	0.00	0.36	0.69	2.548	0.90	3.05	1.13E+03	0.41	[1]
Aniline	5.81	6.49E+05	0.26	0.50	0.82	3.934	0.96	5.43	2.72E+05	0.42	[2,8]
2-Methylaniline	5.82	6.58E+05	0.23	0.59	0.96	4.442	0.92	5.85	7.05E+05	1.07	[2,8]
4-Methylaniline	6.63	4.28E+06	0.23	0.52	0.96	4.452	0.95	5.76	5.74E+05	0.13	[2,8]
2,6-Dimethylaniline	5.76	5.73E+05	0.20	0.46	1.10	5.028	0.89	5.92	8.37E+05	1.46	[1]
N,N-Dimethylaniline	5.12	1.31E+05	0.00	0.42	1.10	4.701	0.84	4.80	6.35E+04	0.48	[1]
4-Iodoaniline	7.10	1.26E+07	0.31	0.40	1.07	5.695	1.28	7.19	1.55E+07	1.23	[2,8]
Nitrobenzene	5.02	1.04E+05	0.00	0.28	0.89	4.557	1.11	4.75	5.58E+04	0.54	[1]

Compound	$\log(K_{\text{HA,air}}/[\text{L/kg}_{\text{HA}}])$ 15°C <i>measured</i>	$K_{\text{HA,air}}/[\text{L/kg}_{\text{HA}}]$ 15°C <i>measured</i>	A_i	B_i	V_i [10 ⁻⁴ m ³ /mol]	L_i [m ³ /m ³]	S_i	$\log(K_{\text{HA,air}}/[\text{L/kg}_{\text{HA}}])$ 15°C <i>fitted</i> by pp-LFER	$K_{\text{HA,air}}/[\text{L/kg}_{\text{HA}}]$ 15°C <i>fitted</i> by pp-LFER	<i>fitted /</i> <i>measured</i>	Ref $A_i, B_i,$ $V_i,$ L_i, S_i
2-Nitrotoluene	5.12	1.31E+05	0.00	0.28	1.03	4.878	1.11	4.99	9.88E+04	0.75	[1]
Benzonitrile	4.60	4.02E+04	0.00	0.33	0.87	4.039	1.11	4.42	2.66E+04	0.66	[1]
Acetonitrile	3.16	1.46E+03	0.04	0.33	0.40	1.739	0.90	2.51	3.23E+02	0.22	[1]
Nitromethane	3.28	1.88E+03	0.06	0.32	0.42	1.892	0.95	2.74	5.53E+02	0.29	[1]
Nitroethane	3.29	1.94E+03	0.02	0.33	0.56	2.414	0.95	3.03	1.06E+03	0.55	[1]
1-Nitropropane	3.32	2.07E+03	0.00	0.31	0.71	2.894	0.95	3.29	1.96E+03	0.95	[1]
2-Nitropropane	3.02	1.04E+03	0.00	0.32	0.71	2.550	0.92	3.00	1.00E+03	0.96	[1]
Pyridine	3.36	2.27E+03	0.00	0.52	0.68	3.022	0.84	3.67	4.66E+03	2.05	[1]
2-Methylpyrazine	4.99	9.72E+04	0.00	0.67	0.78	3.254	0.86	4.15	1.42E+04	0.15	[1]
N,N-Dimethylacetamide	6.31	2.04E+06	0.00	0.78	0.79	3.717	1.33	5.27	1.87E+05	0.09	[2,3]
<i>Indole (1H-Indole)</i>	6.48	3.00E+06	0.44	0.22	0.95	5.505	1.13	7.00	1.01E+07	3.37	[2,3]
Chinoline	6.25	1.76E+06	0.00	0.54	1.04	5.460	0.97	5.79	6.22E+05	0.35	[1]
Propanoic acid	5.51	3.25E+05	0.60	0.45	0.61	3.020 ^{c)}	0.65	5.50	3.13E+05	0.96	[1]
Butanoic acid	5.73	5.33E+05	0.60	0.45	0.75	3.473 ^{c)}	0.62	5.82	6.55E+05	1.23	[1]
Pentanoic acid	6.17	1.49E+06	0.60	0.45	0.89	3.969 ^{c)}	0.60	6.18	1.52E+06	1.02	[1]
3-Methylbutanoic acid	5.77	5.94E+05	0.60	0.50	0.89	3.140	0.57	5.57	3.74E+05	0.63	[1]
<i>1,3-Dinitrobenzene</i>	7.25	1.77E+07	0.00	0.47	1.06	5.848 ^{b)}	1.60	6.69	4.92E+06	0.28	[7]
<i>4-Nitroanisole</i>	6.55	3.54E+06	0.00	0.40	1.09	5.850 ^{c)}	1.21	6.11	1.30E+06	0.37	[2,7]
<i>Dimethylphthalate</i>	6.57	3.74E+06	0.00	0.84	1.43	6.051	1.41	7.30	2.01E+07	5.38	[2,8]
<i>Diethylphthalate</i>	7.68	4.78E+07	0.00	0.88	1.71	7.061 ^{d)}	1.40	8.16	1.46E+08	3.05	[3]
Triethylphosphate	6.15	1.42E+06	0.00	1.06	1.39	4.750	1.00	6.21	1.61E+06	1.13	[1]
Thiophene	2.55	3.58E+02	0.00	0.15	0.64	2.819	0.56	2.49	3.10E+02	0.87	[1]
Thiophenol	4.18	1.50E+04	0.09	0.16	0.88	4.110	0.80	4.13	1.36E+04	0.90	[1]
Dimethylsulfoxide	6.02	1.06E+06	0.00	0.88	0.61	3.437	1.74	5.71	5.16E+05	0.49	[1,9]
2,4-Pentanedione	4.14	1.39E+04	0.00	0.63	0.84	3.237 ^{c)}	0.78	3.97	9.28E+03	0.67	[10]
Dimethyl succinate	5.35	2.24E+05	0.003 ^{e)}	0.80 ^{e)}	1.10	4.133 ^{c)}	1.03 ^{e)}	5.28	1.90E+05	0.85	

Compound	$\log(K_{HA,air}/[L/kg_{HA}])$ 15°C <i>measured</i>	$K_{HA,air}/[L/kg_{HA}]$ 15°C <i>measured</i>	A_i	B_i	V_i [10 ⁻⁴ m ³ /mol]	L_i [m ³ /m ³]	S_i	$\log(K_{HA,air}/[L/kg_{HA}])$ 15°C <i>fitted</i> by pp-LFER	$K_{HA,air}/[L/kg_{HA}]$ 15°C <i>fitted</i> by pp-LFER	<i>fitted /</i> <i>measured</i>	Ref $A_i, B_i,$ $V_i,$ L_i, S_i
Lindane (gamma-HCH)	7.27	1.88E+07	0.00	0.68	1.58	7.467	0.91	7.57	3.69E+07	1.96	[6]
2-Methoxyethanol	5.00	1.00E+05	0.30	0.84	0.65	2.490	0.50	4.54	3.48E+04	0.35	[1]
2-Ethoxyethanol	4.94	8.77E+04	0.30	0.83	0.79	2.815	0.50	4.77	5.95E+04	0.68	[1]
2-Nitroaniline	7.03	1.08E+07	0.30	0.36	0.99	5.627	1.37	7.13	1.35E+07	1.25	[1]
1,4-Dimethoxybenzene	5.42	2.65E+05	0.00	0.50	1.12	5.044	1.00	5.41	2.48E+05	0.97	[3,4]
3-Hydroxybenzonitrile	8.30	2.01E+08	0.84	0.25	0.93	5.181	1.55	8.73	5.38E+08	2.68	[2,8]
Azobenzene	6.45	2.83E+06	0.00	0.44	1.48	7.195 ^{b)}	1.20	7.23	1.71E+07	6.05	[5]

A_i , B_i , V_i , L_i , and S_i and are referred to as $\Sigma\alpha^{H_2}$, $\Sigma\beta^{H_2}$, V_x , $\log L_{16}$ ($\log P_{16}$) and π^{H_2} in most references 1-8.

A_i : electron acceptor property of the molecule; B_i : electron donor property of the molecule; V_i : McGowan volume in units of (cm³/mol)/100;

L_i : logarithmic hexadecane/air partition coefficient (25°C, m³/m³); S_i : molecule's dipolarity/polarizability

Substances in **bold** have been extrapolated to 15 °C using the experimental sorption enthalpies $\Delta_{abs}H_i$ (for values see Niederer et al. 2006a *Environ. Sci. Technol.*)

^{a)} alpha and beta values assumed the same as homologue series, $\log K_{i\text{hexadecane,air}}$ extrapolated from homologue series, based on it's proportionality to the number of carbons

^{b)} $K_{i\text{hexadecane,air}}$ value calculated by the SPARC online calculator (<http://ibmlc2.chem.uga.edu/sparc/>) accessed September 25, 2005.

^{c)} value measured in our lab, experimental method to be given in an upcoming publication.

^{d)} estimated from dimethylphthalate with an increment of 0.505 log-units per one -CH₂- group.

^{e)} from in-house databases

References

- [1] Abraham, M.H.; Andonian-Haftvan, J.; Whiting, G.S.; Leo, A. and Taft, S. Hydrogen bonding. Part 34. The factors that influence the solubility of gases and vapours in water at 298 K, and a new method for its determination. *J. Chem. Soc. Perkin Trans. 2*. **1994**, 8: 1777-1791.
- [2] Abraham, M.H. Hydrogen bonding XXVII. Solvation parameters for functionally substituted aromatic compounds and heterocyclic compounds, from gas-liquid chromatographic data. *J. Chromatogr.* **1993**. 644: 95-139.
- [3] Abraham, M.H.; Chadha, H.S.; Whiting, G.S.; Mitchell, R.C. Hydrogen bonding. 32. An analysis of water-octanol and water-alkane partitioning and the $\Delta \log P$ parameter of Seiler. *J. Pharmaceut. Sci.* **1994**. 83(8): 1085-1100.
- [4] Abraham, M.H.; Grellier, P.L.; McGill, R.A.; Determination of olive oil-gas and hexadecane-gas partition coefficients, and calculation of the corresponding olive oil-water and hexadecane-water partition coefficients. *J. Chem. Soc. Perkin Trans. II*. **1987**. 797-803.
- [5] Poole, S.K.; Poole, C.F. Chromatographic models for the sorption of neutral organic compounds by soil from water and air. *J. Chromatogr. A*. **1999**. 845: 381-400.
- [6] Abraham, M.H.; Enomoto, K.; Clarke, E.D.; Sexton, G. Hydrogen bond basicity of the chlorogroup; hexachlorocyclohexanes as strong hydrogen bond bases. *J. Org. Chem.* **2002**. 67(14): 4782-4786.
- [7] Gunatilleka, A.D.; Poole, C.F. Models for estimating the nonspecific toxicity of organic compounds in short term bioassays. *Analyst*. **2000**. 125: 127-132.
- [8] Torres-Lapasio, J.R.; Garcia-Alvarez-Coque, M.C.; Roses, M.; Bosch, E.; Zissimos, A.M.; Abraham, M.H. Analysis of a solute polarity parameter in reversed-phase liquid chromatography on a linear solvation relationship basis. *Anal. Chim. Acta*. **2004**. 515: 209-227.
- [9] Abraham, MH; Andonian-Haftven, J.; Du, CM; Osei-Owusu, JP; Sakellariou, P; Shuely, WJ; Poole, CF; Poole, SK. Comparison of uncorrected retention data on a capillary and a packed hexadecane column with corrected retention data on a packed squalane column. *J. Chromatogr. A*. **1994**. 688: 125-134.
- [10] Abraham, MH; Acree, WE Jr. Correlation and prediction of partition coefficients between the gas phase and water, and the solvents dodecane and undecane.. *New J. Chem.*, **2004**. 12: 1538-1543.

SI-4 Sensitivity analysis: limited pp-LFER

Table SI-4 shows the compounds that are part of the limited pp-LFER (101 compounds) and the compounds that had been removed from the original pp-LFER shown in SI-3. **Bold** compounds have been extrapolated using the experimental $\Delta_{\text{abs}}H_i$.

Data set for the <i>limited</i> pp-LFER (n=101)				Evaluation set, not part of the <i>limited</i> pp-LFER (n=57)	
n-Nonane	2-Pentanone	n-Hexylbenzene	2-Methylaniline	n-Octane	1,3,5-Trimethylbenzene
n-Decane	2-Hexanone	1,2,4-Trimethylbenzene	4-Methylaniline	n-Undecane	Phenanthrene
n-Tridecane	2-Heptanone	Styrene	Nitrobenzene	n-Dodecane	Biphenyl
1-Octene	2-Decanone	Indane	2-Nitrotoluene	n-Tetradecane	1,2-Dichlorobenzene
1-Nonene	3-Methylbutan-2-one	Naphthalene	Nitromethane	1-Dodecene	1,2,3,4-Tetrachlorobenzene
1-Decene	Cyclopentanone	1-Methylnaphthalene	Nitroethane	Butan-1-ol	Pentachlorobenzene
1-Undecene	Cyclohexanone	Acenaphthene	2-Nitropropane	Heptan-1-ol	Fluorobenzene
1-Tridecene	Methyl acetate	Anthracene	2-Methylpyrazine	Octan-1-ol	Iodobenzene
Ethanol	Ethyl acetate	p-Terphenyl	Indole (1H-Indole)	Nonan-1-ol	1-Chlorohexane
Propan-1-ol	n-Propyl acetate	Chlorobenzene	Chinoline	2-Methylpropan-2-ol	1-Chloroheptane
Pentan-1-ol	n-Butyl acetate	1,3-Dichlorobenzene	Propanoic acid	3-Methylbutan-1-ol	1-Bromopentane
Hexan-1-ol	n-Pentyl acetate	1,4-Dichlorobenzene	Butanoic acid	1-Naphthol	Pentanal
Decan-1-ol	Methyl benzoate	1,4-Dibromobenzene	3-Methylbut. acid	Cyclopentanol	1-Cyanopropane
Undecan-1-ol	Benzyl acetate	1,2,4-Trichlorobenzene	1,3-Dinitrobenzene	2-Methylphenol)	Aniline
Propan-2-ol	Di-n-butyl ether	1,2,3,5-Tetrachlorobenz.	4-Nitroanisole	3-Methylphenol)	2,6-Dimethylaniline
2-Methylpropan-1-ol	Methyl tert-butyl ether	1,2,4,5-Tetrachlorobenz.	Diethylphthalate	2-Chlorophenol	N,N-Dimethylaniline
Benzyl alcohol	Tetrahydrofuran	Hexachlorobenzene	Triethylphosphate	4-Chlorophenol	4-Iodoaniline
Cyclohexanol	1,4-Dioxane	Bromobenzene	Thiophene	2,4,6-Trichlorophenol	Benzonitrile
2,2,2-Trifluoroethanol	Benzofuran	4-Fluorotoluene	Dimethylsulfoxide	2-Butanone	Acetonitrile
Hexafluoropropanol	Dibenzofuran	1,1,1,2-Tetrachloroeth.	2,4-Pentanedione	2-Octanone	1-Nitropropane

Data set for the <i>limited</i> pp-LFER (n=101)				Evaluation set, not part of the <i>limited</i> pp-LFER (n=57)	
Phenol	Benzene	1,1,2,2-Tetrachloroeth.	<i>Lindane</i>	2-Nonanone	Pyridine
4-Methylphenol	Toluene	1-Chlorooctane	2-Ethoxyethanol	2-Undecanone	N,N-Dimethylacetamide
2,3-Dichlorophenol	Ethylbenzene	1-Chlorodecane	<i>2-Nitroaniline</i>	4-Methylpentan-2-one	Pentanoic acid
2,6-Dichlorophenol	n-Butylbenzene	Butanal/Butyraldehyde	1,4-Dimethoxybenz.	Acetophenone	<i>Dimethylphthalate</i>
<i>2,4,5-Trichlorophenol</i>	n-Pentylbenzene	Benzaldehyde	<i>Azobenzene</i>	Isobutyl acetate	Thiophenol
2-Propanone				Di-n-pentylether	Dimethyl succinate
				Methyl phenyl ether	2-Methoxyethanol
				p-Xylene	<i>3-Hydroxybenzonitrile</i>
				n-Propylbenzene	

Table SI-5

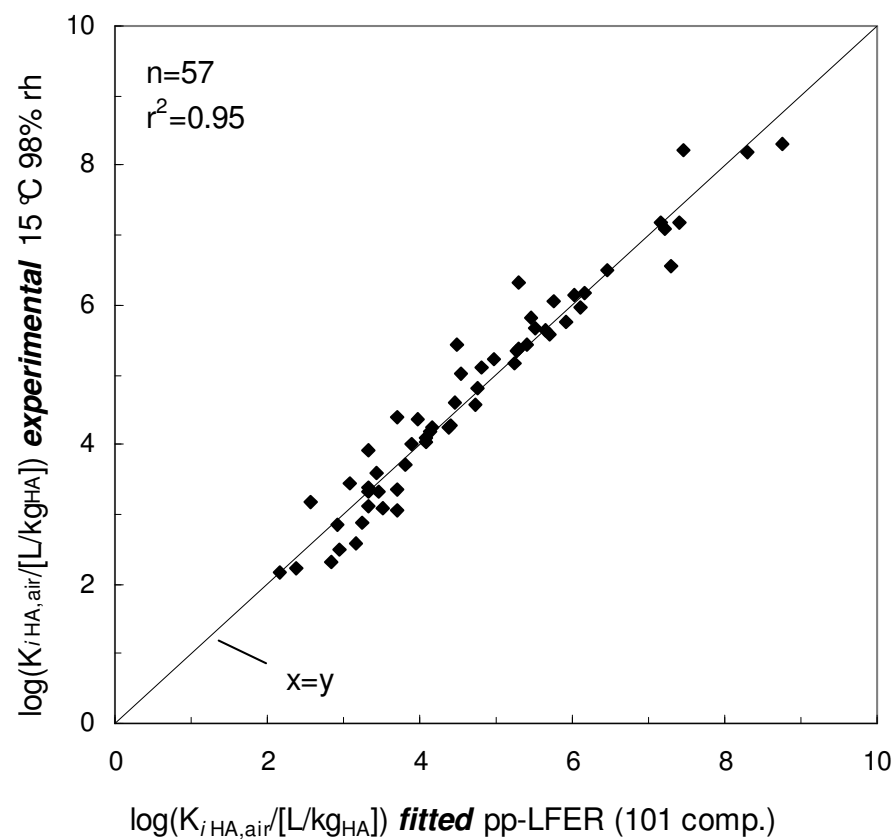
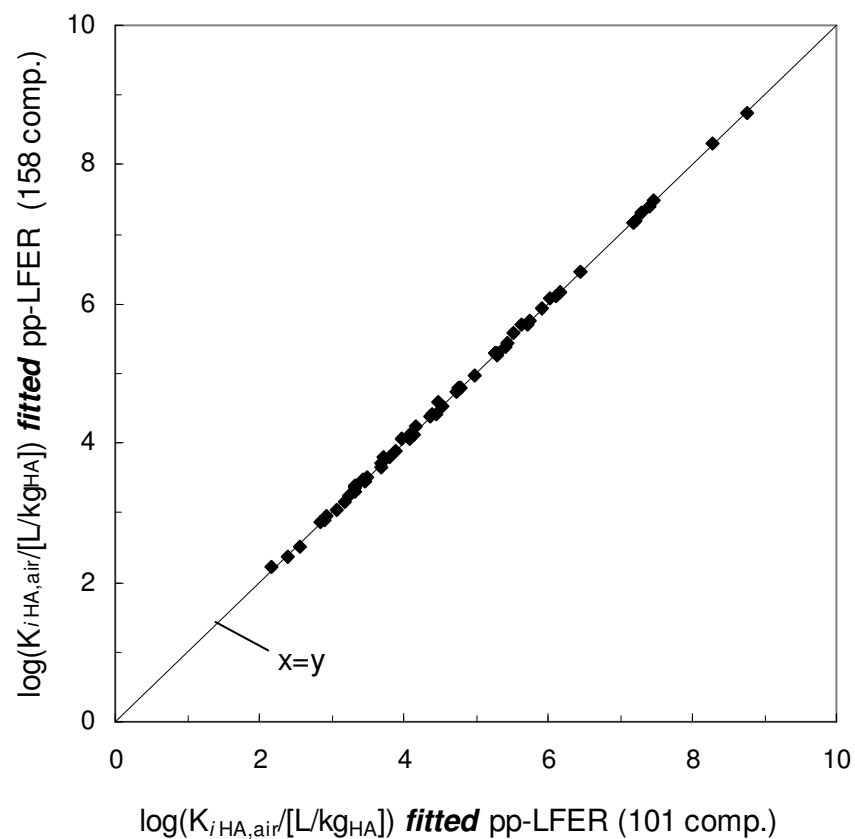
Table 5 shows the sorbent parameters of the pp-LFER calculated with 158 compounds and 101 compounds.

pp-LFER: 15 °C, 98% rh	s	l	v	b	a	c
pp-LFER 158 compounds	1.14	0.81	-0.08	1.88	3.62	-0.65
pp-LFER 101 compounds	1.20	0.81	-0.14	1.86	3.59	-0.62

Figure SI-1/SI-2

Figure SI-1 (left) compares $K_{iHA,air}$ partition coefficients (15 °C, 98% rh) *predicted* by the original pp-LFER (158 compounds) and *predicted* with the limited pp-LFER (101 compounds). The *predicted* values do not differ substantially. The $K_{iHA,air}$ partition coefficients of the compounds that are not part of the limited pp-LFER are

predicted by the limited pp-LFER and compared with the respective *experimental* partition coefficients in Figure SI-2 (right). As seen for the original pp-LFER (Figure 2 in the article), the limited pp-LFER describes the experimental data (of the removed compounds) very well ($r^2 = 0.95$; $\text{rmse} = 0.364$).



SI-5: Correlation of the experimental $\Delta_{\text{abs}}H_i$ with $\Delta_{\text{vap}}H_i$ and $\ln K_{i\text{HA},\text{air}}$

Table SI-6 contains vapor pressures [Pa], heats of vaporization $\Delta_{\text{vap}}H_i$ (estimated from vapor pressure using an equation from [3]) and experimental sorption enthalpies $\Delta_{\text{abs}}H_i$ (this study). Figure SI-3 shows a correlation between heats of vaporization $\Delta_{\text{vap}}H_i$ and the experimental determined sorption enthalpies $\Delta_{\text{abs}}H_i$. Figure SI-4 shows experimental sorption enthalpies plotted against the natural logarithm of the corresponding humic acid/air partition coefficients $\ln K_{i\text{HA},\text{air}}$.

Compound	p_{iL} [Pa]	Ref	$\Delta_{\text{abs}}H_i$ <i>exp.</i>	$\Delta_{\text{vap}}H_i$ <i>est. a)</i>	Compound	p_{iL} [Pa]	Ref	$\Delta_{\text{abs}}H_i$ <i>exp.</i>	$\Delta_{\text{vap}}H_i$ <i>est. a)</i>
n-Decane	1.70E+02	[1]	-46.4	-50.5	Indane	1.95E+02	[2]	-32.9	-49.9
n-Undecane	4.51E+01	[1]	-62.8	-55.6	Naphthalene	3.70E+01	[1]	-54.7	-56.4
n-Dodecane	1.60E+01	[1]	-64.1	-59.6	1-Methylnaphthalene	8.84E+00	[1]	-76.9	-61.9
Ethanol	7.87E+03	[1]	-42.3	-35.7	Acenaphthene	1.52E+00	[1]	-59.3	-68.7
Propan-1-ol	2.76E+03	[1]	-43.2	-39.7	Anthracene	8.91E-02	[1]	-79.6	-79.6
Butan-1-ol	8.60E+02	[1]	-58.4	-44.2	Phenanthrene	7.24E-02	[1]	-79.0	-80.4
Pentan-1-ol	2.59E+02	[1]	-61.2	-48.9	Biphenyl	3.70E+00	[1]	-68.9	-65.2
Hexan-1-ol	1.10E+02	[1]	-65.3	-52.2	Chlorobenzene	1.60E+03	[1]	-27.4	-41.8
Heptan-1-ol	3.00E+01	[1]	-68.6	-57.2	1,2-Dichlorobenzene	1.80E+02	[1]	-53.3	-50.3
Octan-1-ol	1.00E+01	[1]	-75.8	-61.4	1,3-Dichlorobenzene	2.52E+02	[1]	-51.8	-49.0
Nonan-1-ol	2.87E+00	[1]	-83.5	-66.2	1,4-Dichlorobenzene	2.35E+02	[1]	-53.5	-49.2
Decan-1-ol	9.00E+00	[1]	-79.2	-61.8	1,2,4-Trichlorobenzene	5.70E+01	[2]	-53.3	-54.7
Propan-2-ol	6.02E+03	[1]	-53.3	-36.7	1,2,3,4-Tetrachlorobenzene	8.67E+00	[1]	-58.6	-62.0
2-Methylpropan-1-ol	1.39E+03	[1]	-60.1	-42.4	1,2,3,5-Tetrachlorobenzene	1.92E+01	[1]	-45.6	-58.9
2-Methylpropan-2-ol	5.52E+03	[1]	-44.9	-37.0	1,2,4,5-Tetrachlorobenzene	9.60E+00	[1]	-66.3	-61.6
3-Methylbutan-1-ol	3.15E+02	[2]	-63.5	-48.1	Bromobenzene	5.56E+02	[1]	-45.0	-45.9

Compound	p _{iL} [Pa]	Ref	$\Delta_{\text{abs}}H_i$ <i>exp.</i>	$\Delta_{\text{vap}}H_i$ <i>est. a)</i>	Compound	p _{iL} [Pa]	Ref	$\Delta_{\text{abs}}H_i$ <i>exp.</i>	$\Delta_{\text{vap}}H_i$ <i>est. a)</i>
Benzyl alcohol	1.50E+01	[1]	-68.9	-59.8	Iodobenzene	1.33E+02	[1]	-61.9	-51.4
Cyclopentanol	2.94E+02	[1]	-57.4	-48.4	1,1,1,2-Tetrachloroethane	1.60E+03	[1]	-26.4	-41.8
Cyclohexanol	1.00E+02	[1]	-62.1	-52.5	1,1,2,2-Tetrachloroethane	6.22E+02	[1]	-55.3	-45.5
2,2,2-Trifluoroethanol	9.87E+03	[1]	-40.8	-34.8	Butanal/Butyraldehyde	1.57E+04	[1]	-35.5	-33.0
Hexafluoropropan-2-ol	2.12E+04	[1]	-61.2	-31.8	Benzaldehyde	1.69E+02	[1]	-49.9	-50.5
Phenol	5.50E+01	[1]	-65.1	-54.8	1-Cyanopropane	2.58E+03	[1]	-37.1	-40.0
o-Cresol (2-Methylphenol)	4.10E+01	[1]	-67.0	-56.0	Aniline	9.00E+01	[1]	-72.0	-52.9
m-Cresol (3-Methylphenol)	1.90E+01	[1]	-74.4	-58.9	o-Toluidine (2-Methylaniline)	4.30E+01	[1]	-65.0	-55.8
p-Cresol (4-Methylphenol)	1.70E+01	[1]	-75.1	-59.4	p-Toluidine (4-Methylaniline)	3.60E+01	[1]	-85.9	-56.5
2-Chlorophenol	3.08E+02	[1]	-60.9	-48.2	N,N-Dimethylaniline	1.07E+02	[1]	-65.0	-52.3
4-Chlorophenol	2.64E+01	[1]	-83.9	-57.7	Nitrobenzene	3.00E+01	[1]	-50.0	-57.2
2-Pentanone	4.97E+03	[1]	-43.3	-37.4	2-Nitrotoluene	1.80E+01	[1]	-52.1	-59.1
2-Hexanone	1.54E+03	[1]	-49.6	-42.0	Benzonitrile	1.10E+02	[1]	-46.3	-52.2
2-Heptanone	4.90E+02	[1]	-54.5	-46.4	Acetonitrile	1.19E+04	[1]	-34.9	-34.1
2-Octanone	1.85E+02	[1]	-56.1	-50.1	Nitromethane	4.79E+03	[1]	-37.7	-37.6
2-Nonanone	6.63E+01	[2]	-64.4	-54.1	Nitroethane	2.79E+03	[1]	-38.8	-39.7
3-Methylbutan-2-one	6.99E+03	[1]	-33.7	-36.1	1-Nitropropane	1.36E+03	[1]	-45.6	-42.4
4-Methylpentan-2-one	2.64E+03	[1]	-41.9	-39.9	2-Nitropropane	2.30E+03	[1]	-56.5	-40.4
Cyclopentanone	1.55E+03	[1]	-48.2	-41.9	2-Methylpyridine	1.50E+03	[1]	-51.9	-42.1
Cyclohexanone	5.71E+02	[1]	-50.5	-45.8	N,N-Dimethylformamide	5.37E+02	[2]	-44.9	-46.0
Acetophenone	5.23E+01	[1]	-59.2	-55.0	Chinoline	7.94E+00	[2]	-111.7	-62.3
n-Butyl acetate	1.66E+03	[1]	-49.3	-41.7	Propanoic acid	5.53E+02	[1]	-38.5	-45.9
Isobutyl acetate	2.39E+03	[2]	-40.8	-40.3	Butanoic acid	2.21E+02	[1]	-43.7	-49.5

Compound	p_{iL} [Pa]	Ref	$\Delta_{abs}H_i$ <i>exp.</i>	$\Delta_{vap}H_i$ <i>est.</i> ^{a)}	Compound	p_{iL} [Pa]	Ref	$\Delta_{abs}H_i$ <i>exp.</i>	$\Delta_{vap}H_i$ <i>est.</i> ^{a)}
n-Pentyl acetate	6.00E+02	[1]	-57.0	-45.6	Pentanoic acid	2.40E+01	[2]	-61.0	-58.0
Methyl benzoate	5.20E+01	[1]	-57.0	-55.0	3-Methylbutanoic acid	6.70E+01	[1]	-48.4	-54.1
Di-n-butyl ether	8.98E+02	[2]	-51.4	-44.1	1,3-Dinitrobenzene	1.20E-02	[3]	-108.6	-87.4
1,4-Dioxane	4.95E+03	[1]	-44.9	-37.5	2,4-Dinitrotoluene	2.88E-02	[3]	-97.0	-84.0
Methyl phenyl ether	4.72E+02	[1]	-46.7	-46.5	Dimethylphthalate	3.40E+00	[3]	-63.9	-65.6
n-Propylbenzene	3.91E+02	[1]	-51.3	-47.3	Triethylphosphate	5.44E+01	[1]	-65.4	-54.9
n-Butylbenzene	1.50E+02	[1]	-48.1	-51.0	Dimethylsulfoxide	8.73E+01	[1]	-85.7	-53.0
n-Pentylbenzene	5.78E+01	[1]	-56.7	-54.6	1,2-Ethanediol	1.00E+01	[1]	-79.0	-61.4
n-Hexylbenzene	1.36E+01	[2]	-66.1	-60.2	Dimethyl succinate	1.30E+02	[1]	-54.3	-51.5
1,2,4-Trimethylbenzene	3.00E+02	[1]	-47.1	-48.3	2-Methoxyethanol	8.46E+02	[2]	-55.7	-44.3
1,3,5-Trimethylbenzene	3.25E+02	[1]	-43.7	-48.0	2-Ethoxyethanol	7.10E+02	[1]	-58.9	-45.0
Styrene	8.10E+02	[2]	-30.2	-44.4	2-Nitroaniline	9.56E-02	[1]	-91.4	-79.4

^{a)} $\Delta_{vap}H_i$ (298K)/(kJ·mol⁻¹) = -8.80(±0.07)·log p_{iL} (298K)/Pa+70.0(±0.2); from reference [3], Equation (4-29)

References

- [1] Lide, D.R. CRC Handbook of Chemistry and Physics. CRC Press, Boca Raton. **1995**.
- [2] Daubert, T.E.; Danner, R.P. Physical and Thermodynamic Properties of Pure Chemicals. Taylor and Francis. **1997**.
- [3] Schwarzenbach, R.P.; Gschwend, P.M.; Imboden, D.M. Environmental Organic Chemistry. 2nd Edition. **2003**. Wiley Interscience, Hoboken, New Jersey.

Figure SI-3 shows $\Delta_{\text{vap}}H_i$ plotted against the experimental sorption enthalpy. Statistics: $n = 102$; $r^2 = 0.58$; $\text{rmse} = 12.2$; **Figure SI-4** shows: $\ln(K_{i\text{HA},\text{air}})$ plotted against the experimental sorption enthalpy. Statistics: $n = 167$; $r^2 = 0.67$; $\text{rmse} = 9.82$

Figure SI-3

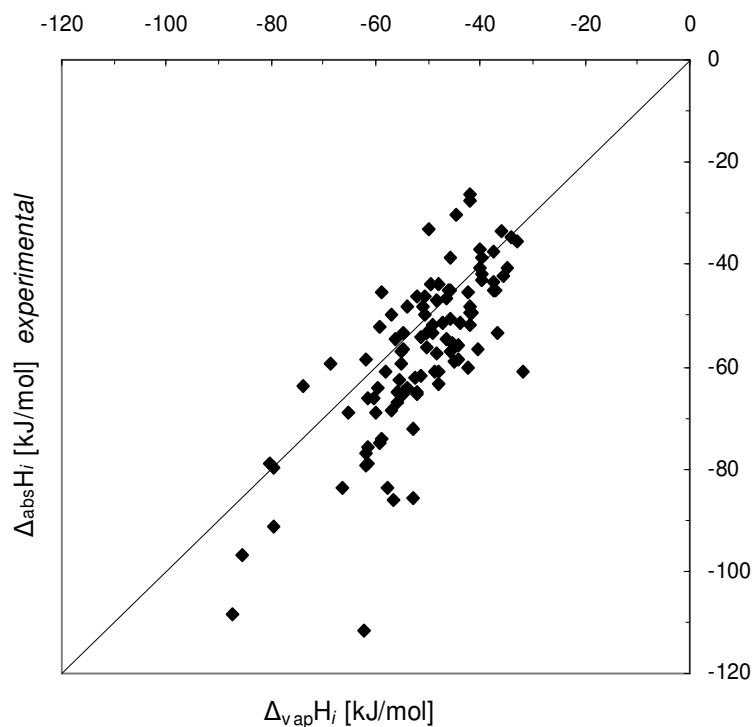
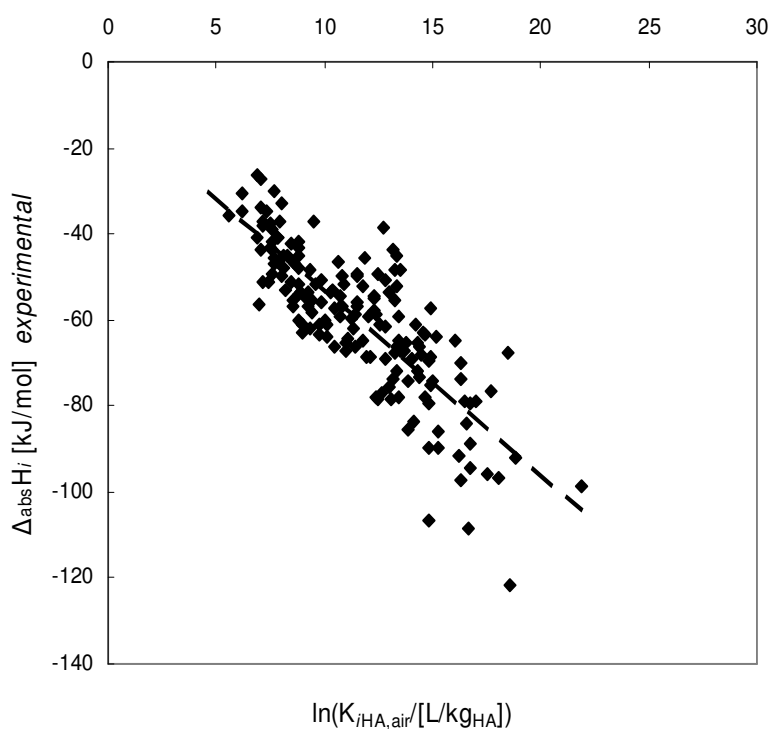


Figure SI-4



SI-6: pp-LFER parameters as a function of temperature

Figure SI-5 compares the experimental sorbent parameters of the humic acid phase at 5 °C (from the pp-LFER calculated with the experimental partition coefficients at 5 °C) with the sorbent parameters predicted for 5 °C by the sorbent-parameter-temperature relationship.

In Figure SI-6, two data sets are shown: 1) the experimental Leonardite humic acid/air partition coefficients (5 °C) plotted against the fitted values by the pp-LFER at 5 °C (shown in black) 2) the experimental Leonardite humic acid/air partition coefficients (5 °C) plotted against partition coefficients that are predicted by a pp-LFER whose sorbent parameters have been predicted with the sorbent-parameter-temperature relationship (shown in grey). The humic acid/air partition coefficients predicted by the pp-LFER and predicted by the predicted pp-LFER do not vary substantially.

Figure SI-5

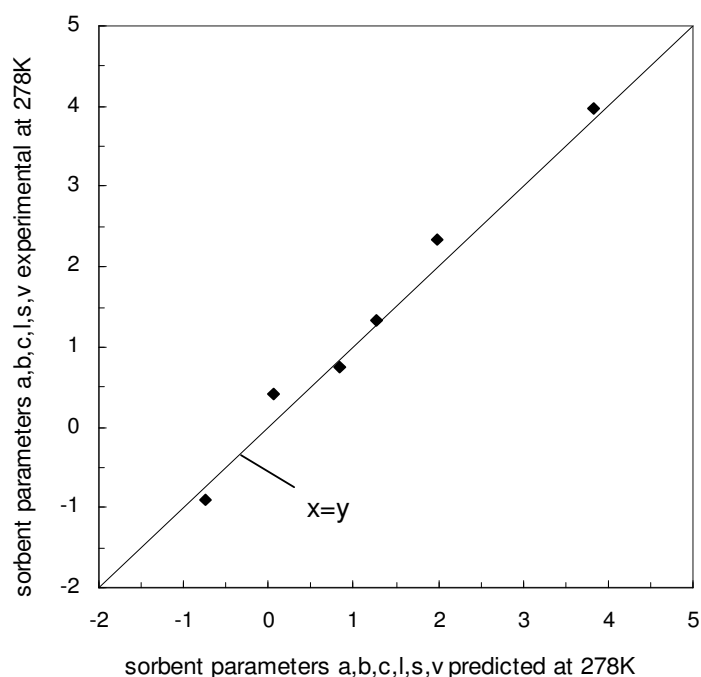
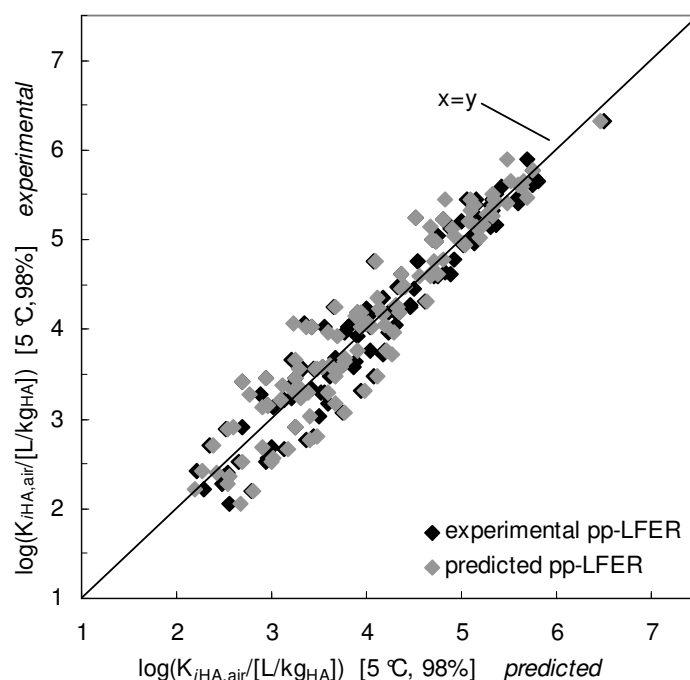


Figure SI-6



SI-7: Comparison with data from Nguyen et al. [8]

Column ^{a)} in Table SI-7 shows experimental organic-C/water partition coefficients (K_{ioc}) collected by Nguyen et al. [8]. Nguyen et al. calculated a pp-LFER using these K_{ioc} -values with the solvation parameters A_i , B_i , V_i , S_i and E_i (E_i : *excess molar refractivity*). In order to compare Nguyen's equation with our pp-LFER, the pp-LFER is recalculated with the solvation parameters A_i , B_i , V_i , L_i and S_i that are used in this study. The fitted $\log K_{ioc}$ values for the compounds from Nguyen et al. using this new pp-LFER are shown in Column ^{b)}.

Our pp-LFER for Leonardite humic acid/air partitioning (at 25 °C) is transferred into a humic acid/water partition pp-LFER using the water/air pp-LFER from [9]. The predicted humic acid/water partition coefficients are shown in Column ^{c)}. Column ^{d)} shows the $K_{iHA,water}$ partition coefficients transferred into humic acid organic-C/water partition coefficients ($C_{org} = 63.81\%$) that are directly comparable with the experimental K_{ioc} values in Column ^{a)} (Figure 4 in the article). All data and equations are at 25 °C. All relevant pp-LFER equations are shown in SI-11. For further evaluations see SI-8. $K_{iHA,water}$ are in [L/kg_{HA}] and $K_{iHA-oc,water}$ are in [L/kg_{oc}].

Compound	^{a)} averaged exp. $\log(K_{ioc}/[L/kg_{oc}])$ from [8]	S_i	A_i	B_i	V_i	L_i	Ref [S_i, A_i, B_i, V_i]	Ref [L_i]	^{b)} new pp-LFER for Nguyen et al. <i>fitted values</i>	^{c)} predicted $K_{iHA,water}$ with pp-LFER from this study	^{d)} predicted $K_{iHA-oc,water}$ with pp-LFER from this study
Benzene	1.60	0.52	0.00	0.14	0.72	2.79	[6]	[1]	1.51	1.63	1.83
Toluene	1.92	0.52	0.00	0.14	0.86	3.33	[6]	[1]	2.02	2.12	2.31
p-Xylene	2.51	0.52	0.00	0.16	1.00	3.84	[6]	[1]	2.48	2.53	2.72
o-Xylene	2.35	0.56	0.00	0.16	1.00	3.94	[6]	[1]	2.49	2.51	2.71
Ethylbenzene	2.19	0.51	0.00	0.15	1.00	3.78	[6]	[1]	2.49	2.55	2.75
1,3,5-Trimethylbenzene	2.82	0.52	0.00	0.19	1.14	4.34	[1,4]	[1]	2.93	2.91	3.10
1,2,3-Trimethylbenzene	2.80	0.61	0.00	0.19	1.14	4.57	[1,4]	[1]	2.94	2.88	3.07
n-Propylbenzene	2.87	0.50	0.00	0.15	1.14	4.23	[6]	[1]	2.97	3.02	3.22

Compound	^{a)} <i>averaged exp.</i> log($K_{ioc}/[L/kg_{oc}]$) from [8]	S_i	A_i	B_i	V_i	L_i	Ref [S_i, A_i, B_i, V_i]	Ref [L_i]	^{b)} new pp-LFER for Nguyen et al. <i>fitted values</i>	^{c)} <i>predicted</i> $K_{iHA, water}$ with pp-LFER from this study	^{d)} <i>predicted</i> $K_{iHA-oc, water}$ with pp-LFER from this study
n-Butylbenzene	3.39	0.51	0.00	0.15	1.28	4.73	[6]	[1]	3.46	3.48	3.68
Chlorobenzene	2.25	0.65	0.00	0.07	0.84	3.66	[1]	[4]	2.13	2.23	2.43
1,2-Dichlorobenzene	2.59	0.78	0.00	0.04	0.96	4.52	[1]	[4]	2.67	2.71	2.90
1,4-Dichlorobezene	2.65	0.75	0.00	0.02	0.96	4.44	[1]	[4]	2.70	2.78	2.98
1,3-Dichlorobenzene	2.47	0.73	0.00	0.02	0.96	4.41	[1]	[4]	2.70	2.79	2.99
1,2,3-Trichlorobenzene	3.22	0.86	0.00	0.00	1.08	5.42	[1]	[2]	3.28	3.28	3.48
1,2,4-Trichlorobenzene	3.25	0.81	0.00	0.00	1.08	5.25	[1]	[4]	3.26	3.29	3.48
1,2,3,4-Tetrachlorobenz.	3.84	0.92	0.00	0.00	1.21	6.17	[1]	[4]	3.78	3.71	3.91
1,2,4,5-Tetrachlorobenz.	3.93	0.86	0.00	0.00	1.21	5.93	[1]	[4]	3.74	3.71	3.91
Trichloromethane	1.52	0.49	0.15	0.02	0.62	2.48	[1]	[1]	1.39	1.63	1.83
Tetrachloromethane	1.90	0.38	0.00	0.00	0.74	2.82	[1]	[1]	1.92	2.27	2.46
1,2-Dichloroethane	1.52	0.64	0.10	0.11	0.64	2.57	[1]	[1]	1.20	1.29	1.49
1,2-Dibromoroethane	1.74	0.76	0.10	0.17	0.74	3.40	[1]	[3]	1.54	1.46	1.66
1,1,1-Trichloroethane	2.25	0.41	0.00	0.09	0.76	2.73	[1]	[1]	1.75	1.98	2.18
1,1,2-Trichloroethylene	1.53	0.40	0.08	0.03	0.71	3.00	[1]	[1]	1.85	2.11	2.30
1,1,2,2-Tetrachloroetha.	1.90	0.76	0.16	0.12	0.88	3.80	[1]	[1]	2.08	2.02	2.22
Tetrachloroethene	2.29	0.42	0.00	0.00	0.84	3.58	[1]	[1]	2.38	2.66	2.86
1,2-Dichloropropane	1.67	0.60	0.00	0.11	0.78	2.86	[1]	[1]	1.67	1.80	1.99
Naphthalene	2.87	0.92	0.00	0.20	1.09	5.16	[1]	[1]	2.79	2.55	2.74
Phenanthrene	4.34	1.29	0.00	0.26	1.45	7.63	[1]	[1]	4.13	3.52	3.72
Anthracene	4.31	1.34	0.00	0.26	1.45	7.57	[1]	[1]	4.07	3.45	3.65
Fluoranthene	4.75	1.53	0.00	0.20	1.59	8.83	[2,4]	[2]	4.79	4.08	4.28

Compound	^{a)} <i>averaged exp.</i> log($K_{ioc}/[L/kg_{oc}]$) from [8]	S_i	A_i	B_i	V_i	L_i	Ref [S_i, A_i, B_i, V_i]	Ref [L_i]	^{b)} new pp-LFER for Nguyen et al. <i>fitted values</i>	^{c)} <i>predicted</i> $K_{iHA, water}$ with pp-LFER from this study	^{d)} <i>predicted</i> $K_{iHA-oc, water}$ with pp-LFER from this study
1-Methylnaphthalene	3.36	0.90	0.00	0.20	1.23	5.79	[1]	[1]	3.35	3.08	3.27
2-Methylnaphthalene	3.66	0.92	0.00	0.20	1.23	5.77	[4,10]	[7]	3.33	3.05	3.24
1-Ethylnaphthalene	3.77	0.87	0.00	0.20	1.37	6.14	[1]	[2]	3.81	3.54	3.73
2-Ethylnaphthalene	3.76	0.87	0.00	0.20	1.37	6.14	[2,4]	[2]	3.81	3.54	3.73
9-methylanthracene	4.81	1.30	0.00	0.26	1.60	8.44	[4,10]	[2]	4.73	4.07	4.26
Pyrene	4.81	1.71	0.00	0.29	1.58	8.83	[1]	[2]	4.50	3.62	3.81
Tetracene	4.93	1.70	0.00	0.32	1.82	10.75	[4,10]	[2]	5.67	4.63	4.82
2,3-Dichlorophenol	2.60	0.94	0.48	0.20	1.02	4.99	[2,5]	[2,4]	2.50	2.09	2.28
2,4-Dichlorophenol	2.70	0.84	0.53	0.19	1.02	4.94	[5]	[2]	2.56	2.19	2.38
2,4,6-Trichlorophenol	3.02	1.01	0.82	0.08	1.14	5.66	[4]	[2,5]	3.13	2.68	2.88
Pentachlorophenol	4.51	0.88	0.97	0.00	1.39	6.82	[4]	[2]	4.31	3.89	4.09
3-Methylaniline	1.41	0.95	0.23	0.55	0.96	4.46	[4]	[2]	1.57	0.85	1.05
4-Bromoaniline	1.96	1.19	0.31	0.35	0.99	5.28	[2,4]	[2]	2.11	1.46	1.66
4-Methoxyaniline	1.93	1.19	0.23	0.61	1.02	4.95	[1]	[2]	1.60	0.69	0.88
Acetophenone	1.55	1.01	0.00	0.48	1.01	4.50	[1,4]	[1]	1.83	1.26	1.45
Benzamide	1.12	1.50	0.49	0.67	0.97	5.77	[4]	[2]	1.42	0.17	0.37
Acridine	4.14	1.32	0.00	0.58	1.41	7.64	[2,4]	[2]	3.45	2.43	2.63
Anisole	1.54	0.75	0.00	0.29	0.92	3.89	[1,4]	[1]	1.92	1.71	1.90
Nitrobenzene	1.94	1.11	0.00	0.28	0.89	4.56	[6]	[1]	1.86	1.48	1.67
m-Nitroaniline	1.73	1.71	0.40	0.35	0.99	5.88	[1]	[1]	1.94	1.03	1.22
p-Nitroaniline	1.88	1.91	0.42	0.38	0.99	6.34	[1]	[1]	1.91	0.84	1.03
Benzyl alcohol	1.43	0.87	0.33	0.56	0.92	4.22	[1]	[1]	1.42	0.70	0.89

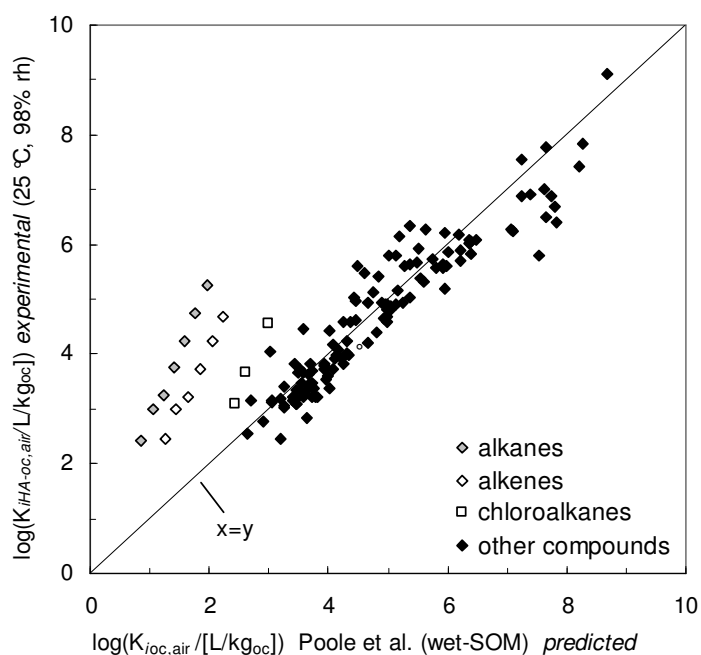
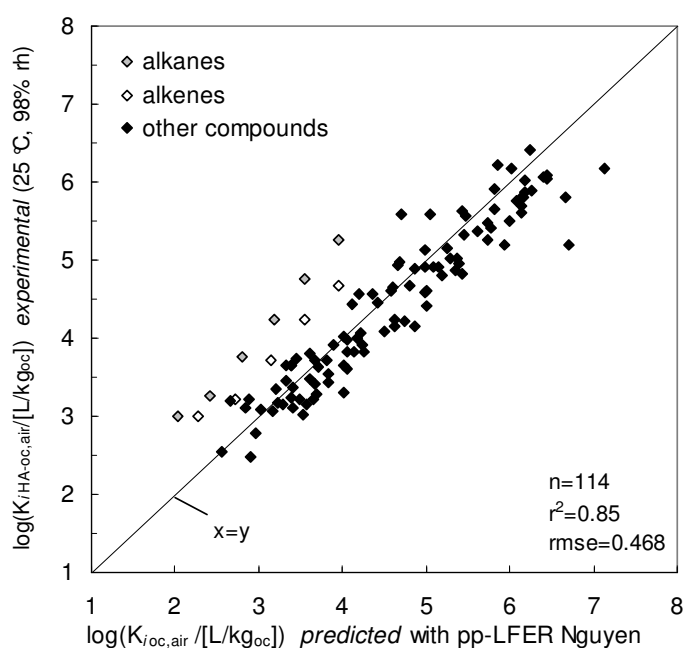
References

- [1] Abraham, M.H.; Andonian-Haftvan, J.; Whiting, G.S.; Leo, A.; Taft, S. Hydrogen bonding. Part 34. The factors that influence the solubility of gases and vapours in water at 298 K, and a new method for its determination. *J. Chem. Soc. Perkin Trans. 2*. **1994**, 8: 1777-1791.
- [2] Abraham, M.H. Hydrogen bonding XXVII. Solvation parameters for functionally substituted aromatic compounds and heterocyclic compounds, from gas-liquid chromatographic data. *J. Chromatogr.* **1993**, 644: 95-139.
- [3] Abraham, M.H.; Grellier, P.L.; McGill, R.A.; Determination of olive oil-gas and hexadecane-gas partition coefficients, and calculation of the corresponding olive oil-water and hexadecane-water partition coefficients. *J. Chem. Soc. Perkin Trans. II*. **1987**, 797-803.
- [4] Poole, S.K.; Poole, C.F. Chromatographic models for the sorption of neutral organic compounds by soil from water and air. *J. Chromatogr. A*. **1999**, 845: 381-400.
- [5] Torres-Lapasio, J.R.; Garcia-Alvarez-Coque, M.C.; Roses, M.; Bosch, E.; Zissimos, A.M.; Abraham, M.H. Analysis of a solute polarity parameter in reversed-phase liquid chromatography on a linear solvation relationship basis. *Anal. Chim. Acta*. **2004**, 515: 209-227.
- [6] Abraham, M.H.; Roses, M. Hydrogen bonding. 38. Effect of solute structure and mobile phase composition in reversed-phase high-performance liquid chromatographic capacity factors. *J. Phys. Org. Chem.* **1994**, 672-684.
- [7] Mutelet, F.; Rogalski, M. Experimental determination and prediction of the gas-liquid n-hexadecane partition coefficients. *J. Chromatogr. A*. **2001**, 923: 153-163.
- [8] Nguyen, T.; Goss, K.U.; Ball, W.P. Polyparameter linear free energy relationships for estimating the equilibrium partition of organic compounds between water and the natural organic matter in soils and sediments. *Env. Sci. Technol.* **2005**, 913-923.
- [9] Goss, K.U. Predicting the equilibrium partitioning of organic compounds using just one linear solvation energy relationship (LSER). *Fluid Phase Equilib.* **2005**, 233(1): 19-22.
- [10] Abraham, M.H.; Chadha, H.S.; Whiting, G.S.; Mitchell, R.C. Hydrogen bonding. 32. An analysis of water-octanol and water-alkane partitioning and the $\Delta\log P$ parameter of Seiler. *J. Pharm. Sci.* **1994**, 83: 1085-1100.

SI-8: Comparison of the exp. Leonardite HA partition coefficients with pp-LFER predictions from the literature

Figure SI-7 (left) compares the organic-C/air partition coefficients predicted by the pp-LFER from Nguyen et al. (Ref 2 article, Equation 3 SI-11) compared with the *experimental* Leonardite humic acid org-C/air partition coefficients from this study (org-C content: 63.8%). The alkanes deviate up to a factor of 20. Please note the difference between SI-8 Figure SI-7 and Figure 4 in the article: Figure 4 in the article compares the literature K_{ioc} partition coefficients with $K_{iHA-oc,water}$ partition coefficients predicted by the pp-LFER from this study; SI-8 Figure 7 compares experimental $K_{iHA-oc,air}$ partition coefficients from this study with $K_{ioc,air}$ partition coefficients predicted by the pp-LFER from Nguyen et al. Therefore, Figure 4 in the article tests the performance of the pp-LFER from this study.

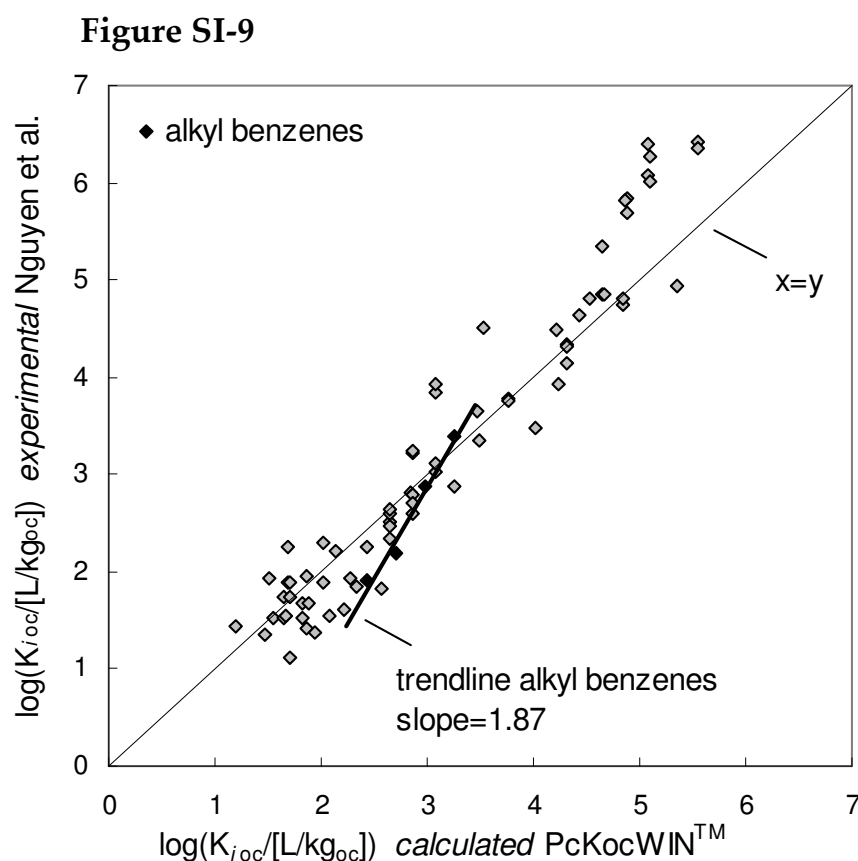
Figure SI-8 (right) shows the *experimental* humic acid organic-C/air partition coefficients from this study plotted against organic-C/air partition coefficients predicted with the equation from Poole et al. (Ref 30 article). The alkanes deviate up to a factor of 2000. All data are at 25 °C.



SI-9 Data of Nugyen et al. compared to calcuated K_{ioc} values from PcKocWIN

Figure SI-9 compares the experimental K_{ioc} partition coefficients from Nguyen et al. with predicted K_{ioc} partition coefficients by PcKocWIN.

About 75% of the compounds in Nguyen's data set are part of the calibration data set of PcKocWIN. This explains the relatively good accordance between the experimental and the predicted values. The homologous series of the alkylbenzenes (methylbenzene, (= toluene), ethylbenzene, propylbenzene, butylbenzene) is plotted separately in Figure SI-9. The trendline exhibits a slope of 1.87 ($r^2 = 0.97$) instead of unity. Hence, there is a systematic error in the prediction of K_{ioc} values by PcKocWIN that has already been discussed in the article (Figure 2).



SI-10 pp-LFERs for the prediction of $K_{i\text{HA-oc,water}}$ partition coefficients

Table SI-8 contains sorbent descriptors for HA org-C/water pp-LFERs at different temperatures. The pp-LFERs in Table 1 (Table 1 in the article) have been transformed to HA organic-C/water pp-LFERs with pp-LFERs for air/water partitioning [1] and an org-C content of 63.8% for Leonardite HA. The difference between HA and HA-org-C based pp-LFERs appears only as a shift in the constant c (0.2 units).

Sorbent descriptors $sd(T) = \text{slope} \cdot T/[K] + \text{intercept}$

sorbent descriptor	288K	298K	308K	318K	slope 1/[K]	intercept	r ²
$l_{\text{HA-oc,water}}$	0.29	0.23	0.21	0.2	-	1.056	0.88
$V_{\text{HA-oc,water}}$	2.50	2.52	2.41	2.45	-	3.173	0.37
$CH_{\text{A-oc,water}}$	0.00	0.27	0.58	0.59	0.0207	-5.909	0.90
$b_{\text{HA-oc,water}}$	-3.29	-3.08	-3.01	-2.89	0.0125	-6.863	0.96
$a_{\text{HA-oc,water}}$	-0.21	-0.49	-0.61	-0.63	-	3.714	0.85
$SH_{\text{A-oc,water}}$	-0.79	-0.93	-1.14	-1.19	-	3.299	0.95

Reference

1. Goss, K.-U. Prediction of the temperature dependency of Henry's law constant using poly-parameter linear free energy relationships. *Chemosphere* 2006, 64: 1369-1374.

SI-11 Relevant Equations

Table SI-9 provides all relevant equations for the comparison of Leonardite humic acid/air partitioning (this study) with the pp-LFER from Nguyen et al. [1] and Poole et al. [3].

equation	description	predicted parameter	l	v	b	a	s	c	e
0	Nguyen et al. [1]: pp-LFER with E_i without L_i	${}^b)\log K_{ioc}$	-	2.28	-2.05	0.15	-0.72	0.14	1.10
1	Nguyen et al. [1]: pp-LFER with L_i without E_i	${}^b)\log K_{ioc}$	0.35	2.28	-1.80	-0.15	-0.70	-0.49	-
2	pp-LFER for water/air partitioning at 25 °C [2]	$\log K_{iwater,air}$	0.48	-2.55	4.87	3.67	2.07	-0.59	-
3	Eq. 1 converted to org-C/air partitioning (with Eq. 2)	${}^b)\log K_{ioc,air}$	0.83	-0.26	3.07	3.52	1.37	-1.08	-
4	pp-LFER <i>experimental</i> (this study) at 25 °C	${}^c)\log K_{iHA,air}$	0.75	-0.17	1.86	3.18	1.01	-0.44	-
5	Eq. 4 converted from total HA content to HA-org-Ccontent ^{a)}	${}^b)\log K_{iHA-oc,air}$	0.75	-0.17	1.86	3.18	1.01	-0.24	-
6	Eq. 4 converted from HA/air to HA/water partitioning (with Eq. 2)	${}^c)\log K_{iHA,water}$	0.27	2.38	-3.01	-0.49	-1.07	0.15	-
7	Eq. 5 converted from HA-oc/air to HA-oc/water partitioning	${}^b),d)\log K_{iHA-oc,water}$	0.27	2.38	-3.01	-0.49	-1.07	0.34	-
8	Poole et al. [3]: organic carbon/air partitioning	${}^b)\log K_{ioc,air}$	0.36	-	2.57	3.39	2.40	-0.46	0.65

a) organic-carbon content of Leonardite humic acid: 63.8%

b) in [L/kg_{oc}]

c) in [L/kg_{HA}]

d) This equation differs slightly from the equation in the article at 25°C because in the article the equations for $K_{iwater,air}$ at different temperatures are from [4].

References

- [1] Nguyen, T.; Goss, K.-U.; Ball, W.P. Polyparameter linear free energy relationships for estimating the equilibrium partition of organic compounds between air and the neutral organic matter in soil and sediments. *Environ. Sci. Technol.* **2005**, 913-923.
- [2] Goss, K.-U. Predicting the equilibrium partitioning of organic compounds using just one linear solvation energy relationship (LSER). *Fluid Phase Equilib.* **2005**, 19-22.
- [3] Poole, S.K.; Poole, C.F. Chromatographic models for the sorption of neutral organic compounds by soil from water and air. *J. Chromatogr. A.* **1999**, 845: 381-400.
- [4] Goss, KU. Prediction of the temperature dependency of Henry's law constant using poly-parameter linear free energy relationships. 2006. *Chemosphere* **2006**, 64: 1369-1374.

3

Quantum-Chemical Modeling of Humic Acid/Air Equilibrium Partitioning of Organic Vapors

reproduced from
Environmental Science and Technology, 2007, 41, 3646-3652.
Copyright 2007 American Chemical Society

Abstract

Classical approaches for predicting soil organic matter partition coefficients of organic compounds require a calibration with experimental partition data and, for good accuracy, experimental compound descriptors. In this study we evaluate the quantum chemical model COSMO-RS in its COSMOtherm implementation for the prediction of about 200 experimental Leonardite humic acid/air partition coefficients without calibration or experimental compound descriptors, but simply based on molecular structures. For this purpose a Leonardite Humic Acid model monomer limited to 31 carbon atoms was derived from ^{13}C NMR analysis, elemental analysis, and acidic function analysis provided in the literature.

Altogether the COSMOtherm calculations showed a good performance and we conclude that it may become a very promising tool for the prediction of sorption in soil organic matter for compounds for which the molecular structure is the only reliable information available. COSMOtherm can be expected to be very robust with respect to new and complex compound structures because its calculations are based on a fundamental assessment of the underlying intermolecular forces. In contrast, other empirical models that are also based on the molecular structure of the sorbate have an application domain that is limited by their calibration data set that is often unknown to the user.

Introduction

Experimental determinations of soil/air or soil/water partition coefficients of organic compounds are often tedious and time-consuming. In view of a daily increasing number of new compounds, reliable predictive models for these sorption data are needed. In (1), several prediction models for soil organic matter (SOM) partitioning were evaluated using about 190 experimental Leonardite humic acid/air partition coefficients from (2). A polyparameter model (pp-LFER) turned out to be the most appropriate model for the prediction of Leonardite HA/air partition coefficients for both nonpolar and polar compounds. However, the polyparameter approach is limited in its applicability because for every sorbate of interest its van-der-Waals (vdW) and H-donor/acceptor (i.e., electron donor/acceptor) descriptors have to be known. These descriptors are tabulated for many compounds in the literature (3, 4) but for many other compounds they have yet to be determined experimentally. Hence, the screening of large and diverse compound sets or the estimation of the sorption behavior of new compounds that have not yet been synthesized will require approaches based on the molecular structures of the compound alone. To this end a combination of K_{ow} -based sorption models with octanol/water partition coefficients (K_{ow}) predicted from the molecular structure of the compounds would be a conceivable, but not a promising approach because K_{ow} -sorption models do not provide satisfying results for polar compounds even with experimental K_{ow} -input data (1). Other tools, such as PckocWIN (5) or the model published by Schüürmann et al. (6), calculate K_{ioc} (organic-C/water partition coefficients) from the molecular structure of the sorbate molecules based on group contribution or incremental methods. These methods have the disadvantage that their applicability domain is limited by the used training compound set (discussed in (1)). Problems arise if this training set is not very diverse and/or not documented so that the applicability domain is not known to the user. Many organic pollutants of environmental concern such as pharmaceuticals or pesticides exhibit several functional groups that

cannot be expected to interact independently from each other and that are likely outside the application domain of models whose training data set mainly contains mono-functional compounds. In fact, in a recent work we found that PcKocWIN even fails to predict partitioning for a diverse set of mainly mono-functional molecules into a humic acid (1). It must further be noted that all models – those based on molecular structure and those based on experimental compound descriptors – require a calibration with experimental sorption coefficients and they only work for the type of organic matter for which they have been calibrated. In order to account for any variability in the sorption behavior of various humic and fulvic acids (HA/FA) or humin, additional calibrations are required.

Approaches from molecular modeling that simulate sorbent-sorbate molecular interactions based on molecular structure of the interaction partner should not be susceptible to these limitations, namely, that new calibrations are required for new sorbent phases (e.g., HA or FA) and that the diversity of the training data limits the applicability domain. However, a difficulty for the simulation of partition coefficients in HA and FA is that the molecular structures of these materials have to be described. Several approaches have already been published: Kubicki and Apitz (7) modeled the sorption of PAHs to various SOM sorbents (Suwannee River FA, lignin, HA) using molecular mechanics that avoid the calculation of molecular electron densities. In a follow-up paper Kubicki and Trout considered HA/FA molecules together with water molecules as well as Al^{3+} ions that formed complexes with the HA/FA (8). They simulated the sorption of benzene and pyridine into this complex system. The simulation identified preferential sorption sites in the HA and FA for benzene. Similarly, Schulten et al. (9) simulated the sorption of diethyl phthalate into a HA model molecule (molecular weight 5547 g/mol) and identified possible sorption sites. However, the practical benefits of both studies are limited because no partition coefficients are provided. Diallo et al. (10) modeled the 3D structure of HA and combined this information with the empirical Flory-Huggins solution theory to derive partition coefficients for hydrophobic compounds. This

approach may help to elucidate the influence of the molecular structure of HA on their sorbent properties but it does not provide any information on how to derive sorption coefficients for various compounds from their molecular structure. In addition, the approach is limited to hydrophobic compounds. In summary, these examples show that molecular modeling approaches for the prediction of quantitative SOM partition constants are still missing.

Here, we evaluate the performance of the commercial software COSMOtherm for the prediction of Leonardite HA/air partition coefficients using experimental data of 184 non-ionic organic compounds that were reported in (2). COSMOtherm combines the calculation of intermolecular interactions with statistical thermodynamics and can thus provide partition coefficients of organic molecules in various partition systems if the molecular structures of the sorbates as well as the sorbent phase are known. This software has several attractive features as compared to other sorption models that are also based on the compound's molecular structure: (a) Due to the fundamental approach, we expect this software to be quite robust, i.e., the predictive quality should be similar for simple and complex molecules and neither the sorbate diversity nor the definition of an applicability domain should be an issue; (b) calibration to the considered type of SOM may not be necessary if essential structural information of the SOM is known; (c) with its ability to account for various conformers of a molecule and with its lack of any calibration this model may provide very fundamental mechanistic insights into the sorption mechanisms if the model predictions are found to be close to experimental results.

Calculations were done for infinite-dilution conditions. Under these conditions the calculated sorption isotherm will always be linear because COSMOtherm is not able to account for any – possibly existing – heterogeneities in the sorbent that might cause nonlinear sorption. This linearity is in agreement with our experimental results for Leonardite HA (2) but it may not necessarily apply to other types of SOM.

Method

COSMOtherm (COSMO-RS)

The calculations of the COSMOtherm software (Version C2.1 (11), COSMOlogic GmbH, Leverkusen, Germany) are based on a combination of quantum theory, dielectric continuum models, surface interaction concepts and statistical thermodynamics. In a first step, for each kind of molecule (solvent or solute) a density functional (DFT) calculation is performed with the dielectric continuum solvation model COSMO as implemented in the TURBOMOLE software (TURBOMOLE: Program Package for ab initio Electronic Structure Calculations, COSMOlogic, Leverkusen, Germany; Version 5.7). These calculations yield the total energy of the molecule and the screening charge density on its molecular surface. In the next step, solvent and solute molecules are considered as an ensemble of pairwise interacting surfaces. The specific parts of the intermolecular interactions (i.e., electrostatic interactions and hydrogen bonds) are expressed by the screening charge densities of the contacting surface pieces. In addition, vdW interactions are covered by element-specific empirical coefficients. The chemical potentials in each phase and thus the partition constants are eventually calculated by a statistical thermodynamics procedure within the COSMOtherm software. A flow diagram showing all relevant steps is provided in Supporting Information (SI)-1. More details can be found in (12-14). COSMOtherm depends only on a very small number of adjusted parameters (one adjusted parameter for electrostatic interactions, two parameters for H-bond interactions, and one vdW-parameter for each element to be modeled), some of which are physically predetermined (13). COSMOtherm parameters are not specific for functional groups or molecule types. Thus, the resulting parametrization is completely general and can be used to predict the partition properties of almost any compound or mixture.

Input Structures

As discussed above, TURBOMOLE requires three-dimensional structures of sorbate and sorbent molecules as input. 3D input structures

of the sorbent and the sorbate molecules were generated with CS ChemDraw Ultra® (15) and CS Chem3D Pro (16). While this procedure is straight forward for the sorbate molecules, the molecular structure of HA and FA is not known. Numerous studies have investigated the molecular structure of SOM (e.g., Steelink (17), Stevenson (18), Schulten and Schnitzer (19), Leenheer et al. (20), and Diallo et al. (21)). Different analytical methods such as ^{13}C NMR/ ^1H NMR, IR spectroscopy, pyrolysis GC/MS and pyrolysis-field ionization MS (19) etc. were applied. However, the postulated HA models are either too big to be handled in our computer system or not specific for Leonardite HA. We therefore set up a Leonardite HA model monomer limited to about 30 carbon atoms based on published elemental analysis data, ^{13}C NMR studies, and acid function analysis. It was not our intention to postulate a new structure that would realistically represent Leonardite HA in all its properties. Instead, we needed a model structure that reflects all those physical-chemical properties (i.e., the vdW interaction and H-donor/acceptor interaction properties) of Leonardite HA that are relevant for the sorption process. The monomers that were constructed for this purpose were based on the following considerations:

Based on *elemental analysis* (22) the composition of Leonardite HA is: 63.8% C, 3.7% H, 31.3% O, and 1.2% N. From these data an empirical formula – normalized to one nitrogen atom – can be calculated: $\text{C}_{61}\text{H}_{47}\text{O}_{24}\text{N}$. Considering the limited calculation capacity of COSMOtherm, this monomer is further reduced to $\text{C}_{31}\text{H}_{24}\text{O}_{12}$. The nitrogen atom is omitted in this step.

Acidic function analysis from Ritchie and Perdue (23) provide the concentration of carboxyl- and phenolic groups in Leonardite HA. The carboxylic carbon content was found to be 7.46 meq/gC and the phenolic carbon content 2.31 meq/gC. Considering these findings, about three COOH groups and one phenolic OH group in the monomer should be present. The COOH groups are likely to be aromatically bound because of the postulated high aromatic content. This is in agreement with the structure proposed by Stevenson (18). Milne and Kinniburgh (24) published a (*phenolic groups*)/(*carboxyl groups*) ratio of 1:2. However,

Ritchie and Perdue (23) found a ratio of 1:4. According to these findings, the ratio 1:3 for Leonardite HA seems to be reasonable.

Mao et al. (25) conducted ^{13}C NMR measurements with various HA and FA. For Leonardite HA they found a sp^2/sp^3 ratio of 3.44. This leads to 7 sp^3 -hybridized carbons and 24 sp^2 -hybridized carbons for our model monomer. Table 1 shows the chemical shifts in the ^{13}C NMR determined for Leonardite HA in the study of Mao et al. (25) that are in good agreement with the ^{13}C NMR data recorded by Thorn et al. (26) (not shown).

chemical shift description		0-50 ppm aliphatic	50-108 ppm carbohydrate	108-162 ppm aromatic	162-220 ppm carboxylic
Ref (25)		14.9%	7.7%	54.8%	22.3%
#C allocated to 31 carbons ¹		4	2	18	7
Monomer M1	carbons in M1	16,17, 18,19	15,30	2,3,4,5,6,7,8, 9,11,12,13,14,20, 21,23,24,26,27,29	1,10,22, 25,28,31
	(Figure 1)				
	# C in M1	4	2	19	6

¹rounded

Table 1 ^{13}C -NMR analysis data from Mao et al. (25) for Leonardite HA and ^{13}C -NMR shifts for the theoretical monomer M1 estimated with Chemdraw and with (27) showing the percentage distributions of the four carbon types.

Quinones (1,4-benzoquinone/hydroquinone redox system) have been found to be important constituents in humic substances (28, 29) and therefore such a structure was introduced in our Leonardite HA model. The carbons in the (oxidized) quinone structure are 6 sp^2 carbons. Two carbons belong to the carboxylic/carbonyl group. With 18 aromatic carbons 3 aromatic rings can be set up (18 sp^2 carbons). Furthermore, the three carboxylic groups (3 sp^2 carbons) are likely to be attached to aromatic structures. This leads to the following preliminary balance: $\text{C}_{27}\text{O}_9\text{H}_x$, 27 sp^2 -hybridized carbons; sp^2/sp^3 ratio = 6.75 (in the case of the remaining 4 carbons are sp^3 hybridized). For the expected sp^2/sp^3 -ratio of 3.4 a combination of 24:7 ($sp^2\text{-C}/sp^3\text{-C}$) is expected; 25:6 ($sp^2/sp^3 = 4.2$) seems acceptable. Therefore, the remaining four carbons have to be

aliphatic because, besides the aromatic skeleton, aliphatic C chains should be present in the core structure of HA. To gain the missing two sp^3 carbons the quinone structure is coupled with an aromatic ring, resulting in a naphthoquinone, which allows for the allocation of two sp^3 carbons in the monomer. Three oxygen atoms are remaining that induce substantial chemical shifts to their neighbors. The data of Mao et al. indicate that four carbons are aliphatic while two carbons are in the 50-108 (carbohydrate) region where aliphatic ether groups are found (60-74 ppm (27)). To fulfill these requirements, two methoxy groups are introduced. The resulting building blocks for a Leonardite HA model monomer are shown in SI-2. There are many possibilities to join these building blocks to a HA monomer. Here, we have worked out four constitutional isomers (M1-M4, for M2-M4 see SI-3); monomer M1 is shown in Figure 1.

The monomers M1-M4 exhibit the empirical formula $C_{31}H_{26}O_{12}$. The chemical shifts of the carbons in M1 are estimated by ChemDraw (15) and (27) and are shown in Table 1. Compared to the experimentally determined shifts in Table 1, there is an extra aromatic carbon and a missing carboxylic carbon. This deviation is acceptable because the group allocation is rounded and because carbon #20 exhibits a calculated chemical shift of 158.6, which is close to the expected range for carboxylic carbons. Hence, our Leonardite HA model monomer fulfills various expectations from the analytical data.

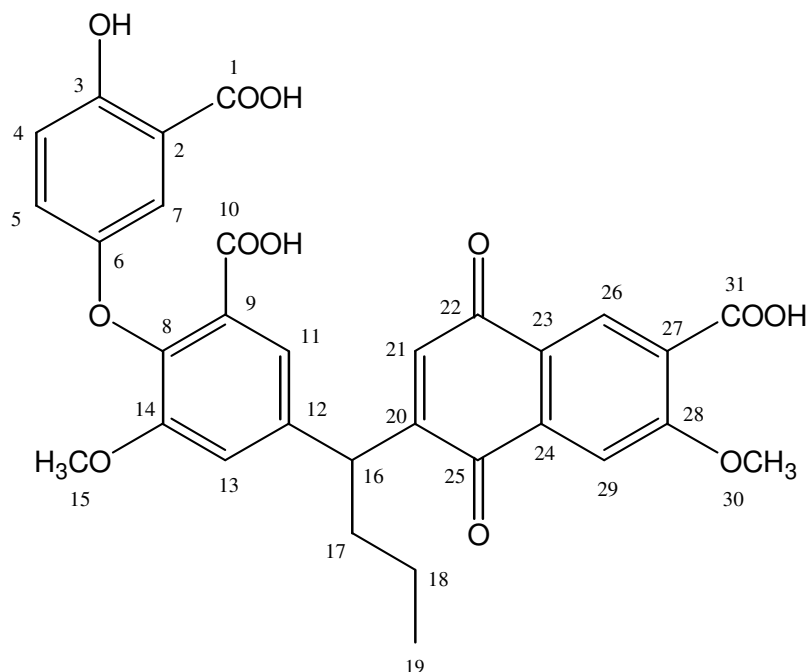


Figure 1 Leonardite HA model monomer M1. The calculated range of chemical shifts of the carbons is shown in Table 1.

Results and Discussion

Leonardite HA/air partition coefficients ($K_{i\text{HA,air}}$) at different relative humidities (rh; 0%, 45%, 70%, and 98%) and temperatures (15 – 55 °C) were calculated for 184 organic compounds for which experimental data have been measured (2). The HA was simulated as a polymer consisting of the monomers deduced above. The HA monomers M1 and M3 were simulated with three conformers each; M2 and M4 were simulated with two conformers (not shown; for a discussion of conformers see below). To model the influence of the rh in COSMOtherm, the HA was simulated as a mixed phase consisting of the monomers and water molecules. To estimate the amount of water that is sorbed in the HA model polymer in equilibrium with a given rh, COSMOtherm was used to calculate the relevant phase diagram (for details see SI-4). COSMOtherm calculations predicted a water content of 5.9 mass % in Leonardite HA when in equilibrium with 98% rh. Figure 2 compares the calculated M1/air partition coefficients at 15 °C and 98% rh with the experimental $K_{i\text{HA,air}}$ from (2) at 15 °C and 98% rh. There is moderate data scatter and a

systematic error toward too high calculated partition coefficient (root-mean-square error $\text{rmse} = 0.84$). Strong outliers (2-2.7 log units) include the following: pentanoic acid, dimethyl phthalate, triethyl phosphate, γ -hexachlorocyclohexane (lindane), 1,2-naphthoquinone, and 4-aminobenzonitrile (see SI-5 for all experimental and calculated data). Dimethyl sulfoxide is a very strong outlier (3.2 log units); however, this compound was identified as a problematic compound for quantum chemical calculation before by COSMOlogic (30).

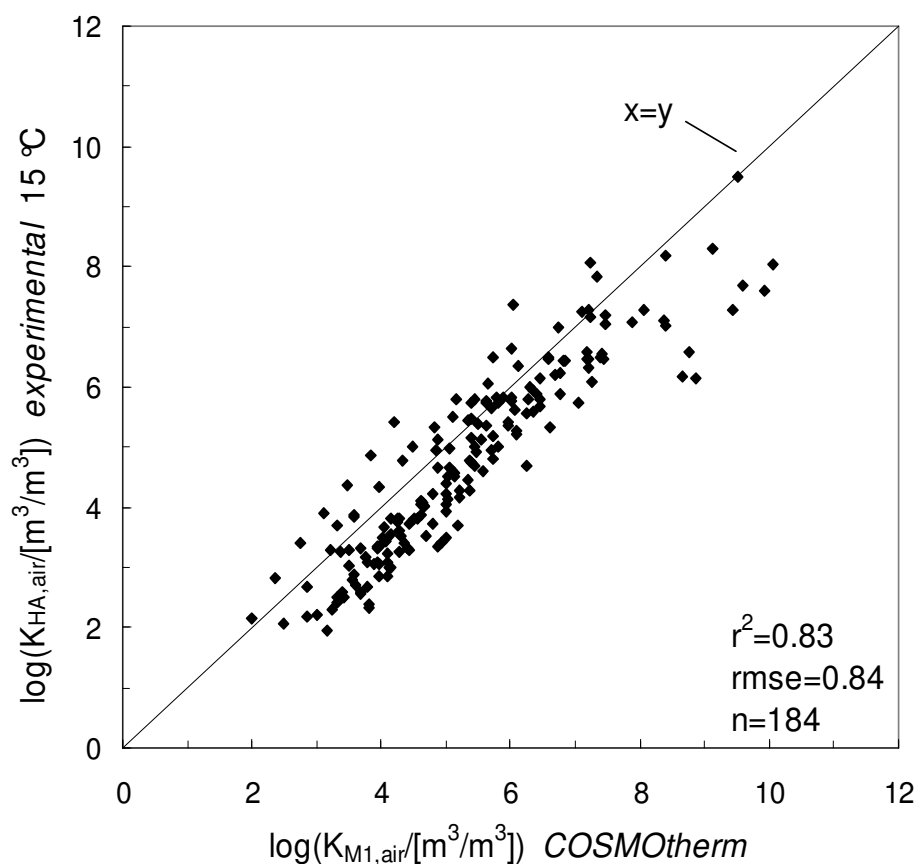


Figure 2 Calculated M1/air partition coefficients plotted against experimental Leonardite HA/air partition coefficients from (2) (15 °C, 98% rh).

This is a remarkably good performance considering that absolutely no calibration with experimental data has been used. But there is still room to improve these results. COSMOtherm's focus lies in the calculation of electrostatic interactions between sorbate and sorbent molecules. vdW interactions are only considered empirically. Partitioning between two

condensed phases depends only a little on vdW interactions because these are similar in strength in various condensed phases and therefore largely cancel in their effect on partitioning. Sorption from the gas phase into any condensed phase, however, is dominated by vdW interactions because these are strong in any condensed phase but almost nonexistent in the gas phase. To circumvent this problem, all further HA/air partition coefficients were generated by applying a thermodynamic cycle: COSMOtherm HA/hexadecane partition coefficients were calculated and then transformed into HA/air partition coefficients using experimental $K_{\text{ihexadecane,air}}$ -values from the literature (4, 31). Figure 3 shows a plot of M1/air partition coefficients at 98% rh that result from this approach (please note: an additional, empirical correction that is discussed below has also been implemented in Figure 3). Compared to Figure 2, the scatter of the data decreases substantially ($r^2 = 0.83$ to $r^2 = 0.90$); the root-mean-square errors decrease from 0.84 to 0.72 (without empirical correction) and the outliers mentioned above vanish. For example, the discrepancy between the experimental and the calculated value for triethyl phosphate decreases from 2.7 to 0.21 log units and for lindane from 2.2 to 0.62 log units. As expected, these findings indicate that COSMOtherm provides better results for the partitioning between two condensed phases than for gas/condensed phase partitioning. In Figure SI-2 a comparison of experimental and predicted hexadecane/air partition coefficients allows for direct evaluation of COSMOtherm's ability to predict vdW interactions.

Another problem of our COSMOtherm calculations comes from the unknown molecular volume of the polymeric HA structure. The selection of our HA monomers automatically implies a specific, very small value for molecular volume of the HA which is certainly not realistic. This results in a systematic shift of all calculated partition coefficients by a constant factor. At the moment there is no theoretically satisfying solution to this problem. A practical solution is the introduction of an empirical correction term which is derived by minimizing the difference between calculated and experimental values:

$$\log(K_{\text{experimental}}) = \log(K_{\text{calculated}}) + C_{\text{corr}} \quad (1)$$

For the calculated data presented in Figure 2 a fitted c_{corr} of -0.49 was calculated. This correction has been implemented in Figure 3. Future studies with different HA and FA will show whether c_{corr} has to be determined for each HA and FA separately or whether $c_{\text{corr}} = -0.49$ is universally valid for humic and fulvic acids.

Performance of Monomer M1

The M1/air partition coefficients calculated via hexadecane and corrected with c_{corr} agree well with the experimental partition coefficients (Figure 3; $\text{rmse} = 0.53$), 68% of the compounds are predicted within a factor of 3, 84% of the compounds are predicted within a factor of 5 (for data see SI-5). COSMOtherm performs somewhat better for polar compounds ($\text{rmse} = 0.49$) than for nonpolar compounds ($\text{rmse} = 0.61$). The inferior performance of the nonpolar compounds mainly comes from systematic deviation of the alkanes (nonpolar compounds without alkanes: $\text{rmse} = 0.52$). The alkenes also deviate systematically but not to the extent of the alkanes (see SI-7). As mentioned above, vdW interactions are only modeled empirically in COSMOtherm; thus, nonpolar compounds (which are capable of only vdW interactions) are most prone to prediction errors. None of the other compound class shows such systematic deviations. The biggest outliers compared to the experimental values are as follows: 2-methylpyridine (1.47 log units), 1,4-dibromobenzene (1.54 log units), tetradecane (1.58 log units), and 4-aminobenzonitrile (1.33 log units) (see SI-5). The performance of COSMOtherm with an empirically calibrated constant and the calculation via hexadecane clearly outcompetes the K_{ow} sorption model even if the latter is used in combination with experimentally determined K_{ow} values. In fact, the corrected COSMOtherm results come close to the best prediction model found in Niederer et al. (1), i.e., a polyparameter model based on experimentally derived sorbate descriptors as well as six empirically calibrated descriptors for the HA.

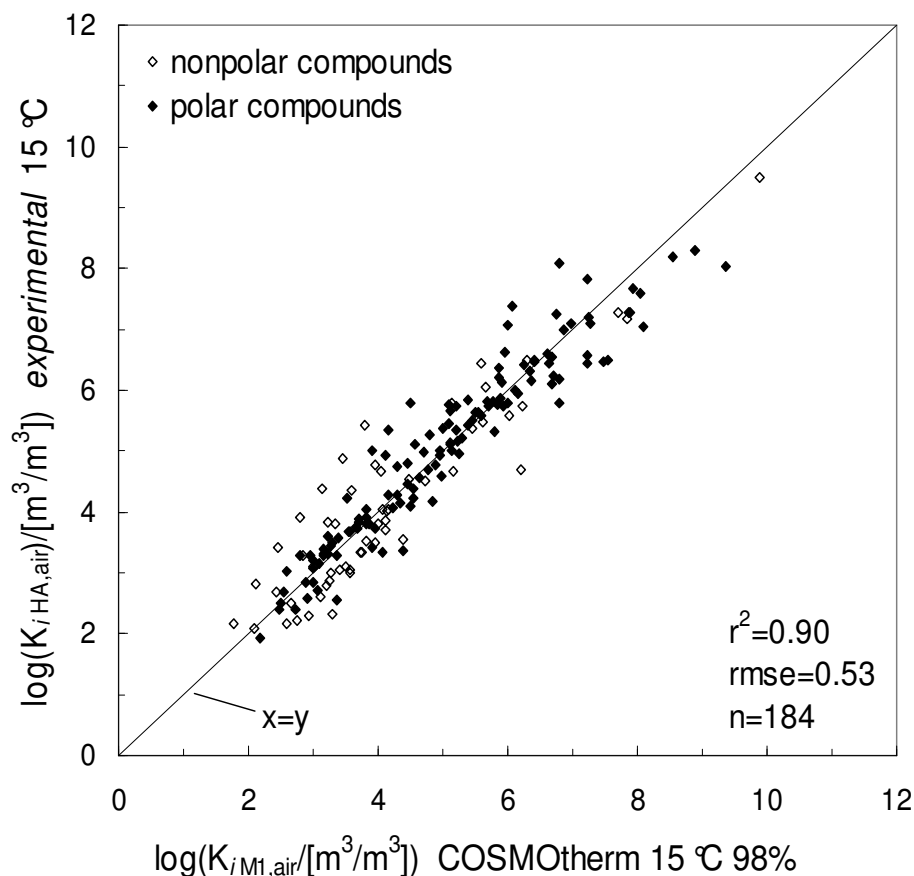


Figure 3 Compares the experimental partition coefficients (15 °C, 98% rh) with calculated partition coefficients (calculated via hexadecane and corrected with c_{corr}). Correlation coefficients of the virtual regression between the experimental and calculated partition coefficients: $r^2 = 0.90$.

Variations between the Monomers M1-M4

The models M1-M4 differ only in the locations of the functional groups (SI-3). Consequently, the calculated partition coefficients do not differ substantially (deviations up to 0.3-0.5 log units, for data see SI-8). The best performances compared to the experimental values were obtained with M1 and M4 (rmse: 0.53 (M1), 0.58 (M2), 0.58 (M3), 0.48 (M4)). The biggest differences in the predicted values occurred between M1 and M2. Almost all polar compounds exhibit higher partition coefficients in M2, and all nonpolar compounds exhibit higher partition coefficients in M1 (see Figure SI-5). This is likely due to the number of intramolecular H-bonds that can be formed in both monomers: M1 has three intramolecular H-bonds between two directly neighboring functional groups while M2 has only one (see SI-3). Intramolecular H-bonds cause a

decrease in the cavity energy because they lower the strength of intermolecular H-bonds. In addition, less H-donor/acceptor sites for H-bonds with sorbate molecules are available. Nonpolar compounds benefit from the lower cavity energy in M1 while the polar compounds benefit from the better availability of H-bonds in M2. However, not all polar compounds sorb more strongly in M2, because they have to compete with intermolecular H-bonds that are formed between M2-monomers.

M1 and M4 show very similar calculated partition coefficients. The aliphatic carboxy group in M4 obviously does not have a substantially different influence on the sorption properties compared to an aromatic carboxy group. Because aliphatic carboxy groups are less likely than aromatic carboxy groups in HA structures, M1 was considered to be the most appropriate monomer for further calculations. However, comparing the different monomers reveals that only small differences in the calculated partition coefficients result from the variation of the locations of functional groups in the core structure of the HA.

Conformers

Conformers are molecules in which atoms are linked together in the same way, but in different spatial arrangement. The conformer distribution of a molecule is a function of its chemical environment; e.g., different distributions are expected when the compound is sorbed in a solvent compared to the gas phase. In this respect, conformers containing an intramolecular H-bond are especially important because these can strongly influence their intermolecular interactions with neighboring molecules. With COSMOtherm it is possible to calculate partition coefficients for individual conformers of a compound and derive an overall partition constant based on the Boltzmann-weighted contributions from the individual conformers. According to COSMOtherm calculations, HA/air partition coefficients of different conformers of certain molecules (chloroacetone, hydroxyacetone, and 2-ethoxyethanol) may differ by up to 3 orders of magnitude (see extended discussion in SI-9). This demonstrates that sound mechanistic

understanding of partitioning cannot be achieved without considering the role of conformers. Arp et al. (32) have shown that a conformer-specific approach is also needed to understand the partitioning of various perfluorinated compounds. Empirical tools for the prediction of partitioning are not conformer-specific but work with averaged molecular values instead. These models work well if the conformer distribution does not change much between various phases but they may produce erroneous results otherwise. Our HA monomers M1-M4 also occur in various conformations due to the various possibilities of intramolecular H-bonds. However, the COSMOtherm calculations suggested that different conformers differed only little (less than a factor of 2) in their sorption properties for organic sorbates.

Simulation of the Influence of Relative Humidity

In previous work we found relative humidity (rh) to affect Leonardite HA/air partition coefficients up to a factor of 3 (0.5 log units) (2). While nonpolar compounds exhibited lower partition coefficients in the hydrated HA (98% rh) compared to the dry HA (<0.01% rh), most bipolar compounds (i.e., those with H-donor and H-acceptor properties) such as alcohols and carboxylic acids sorbed more strongly into the hydrated HA. Monopolar compounds (ethers, ketones, and acetates) revealed no systematic dependence on rh (see Figure SI-6; for details see (2)).

The COSMOtherm calculations showed a correct but smaller trend than in the experimental data: for the nonpolar compounds the calculated effect was up to 0.14 log units (tetradecane) while for polar compounds (propanoic acid) it was up to 0.4 log units. In the experiments, preference of n-alkanes, n-aliphatic ketones, n-aliphatic alcohols, and other compound classes for the dry rather than the wet humic acid increased with increasing n-chain lengths. This trend was also predicted by COSMOtherm although less pronounced (see Figures SI-6 to SI-9). The cause of this trend has been discussed and interpreted in details in (2): Briefly, as the rh increases, the cavity energy of the HA increases. The polar compounds can compensate the increased cavity energy by

additional H-bonds interactions with the sorbed water molecules in the HA.

Simulation of Temperature Dependence

The sorption enthalpies calculated by COSMOtherm do not compare especially well to the experimental sorption enthalpies from ref (2) (rmse = 13.0 kJ/mol; Figure SI-10); however, the agreement is sufficient to estimate partition coefficients at ambient temperatures (in the range of 0 to 40 °C). Substantial outliers in the sorption enthalpies are as follows: 2,4,5-trichlorophenol, 1,4-diiodobenzene, 4-aminobenzonitril, 3-hydroxybenzonitril, and 1,3-dinitrobenzene (for data see SI-11).

Figure SI-11 compares calculated partition coefficients with experimental partition coefficients at two different temperatures (15 °C and 35 °C). The calculated partition coefficients at 35 °C agree well with the experimental data (rmse = 0.49), similar to what we have seen at 15 °C.

SPARC

It is interesting to compare the performance of COSMOtherm with the one of SPARC. Although being a more empirical model, SPARC also predicts partitioning solely based on the molecular structures of the sorbate and the sorbent without further calibration. SPARC calculations can be performed free of charge on-line (<http://ibmlc2.chem.uga.edu/sparc/>) by entering the molecular structures of the sorbates as well as the sorbent as SMILES string (SMILES: Simplified Molecular Input Line Entry Specification). SPARC calculates vdW and H-bond interactions between sorbate and sorbent by using various empirical molecular descriptors that are determined by their molecular structure (33). Here we used the Leonardite HA model monomer M1 (for SMILES string see SI-12) to calculate partition coefficients between HA and air. Figure 4 compares the M1/air partition coefficients calculated by SPARC at 15 °C with the experimental Leonardite HA/air partition coefficients. The data sets compare quite well, although SPARC predicts slightly higher partition coefficients for most of the compounds (rmse = 0.71). About 65% of the partition coefficients are predicted within a factor of 3

in the nonlogarithmic partition coefficients, 79% within a factor of 5. The aliphatic alcohols are strong outliers (decan-1-ol: 1.5 log units; undecan-1-ol: 1.8 log units); the strongest deviation shows 1,1,1,3,3,3-hexafluoropropan-2-ol (2.8 log units). However, the alcohols are the only systematic outliers (see Figure SI-4). Further outliers (>1.3 log units) are as follows: acenaphthene, lindane, 1,4-naphthoquinone, triethyl phosphate, and 2-methylpyridine (see SI-5).

SPARC exhibits a slightly better performance than COSMOtherm when both are applied directly to HA/air partitioning. After an empirical correction of both models (accounting for the systematic deviations in the original predictions), COSMOtherm performs somewhat better provided that it is used within a thermodynamic cycle with hexadecane/air partition coefficients (rmse = 0.53 for COSMOtherm, see above, and rmse = 0.59 for SPARC, not shown).

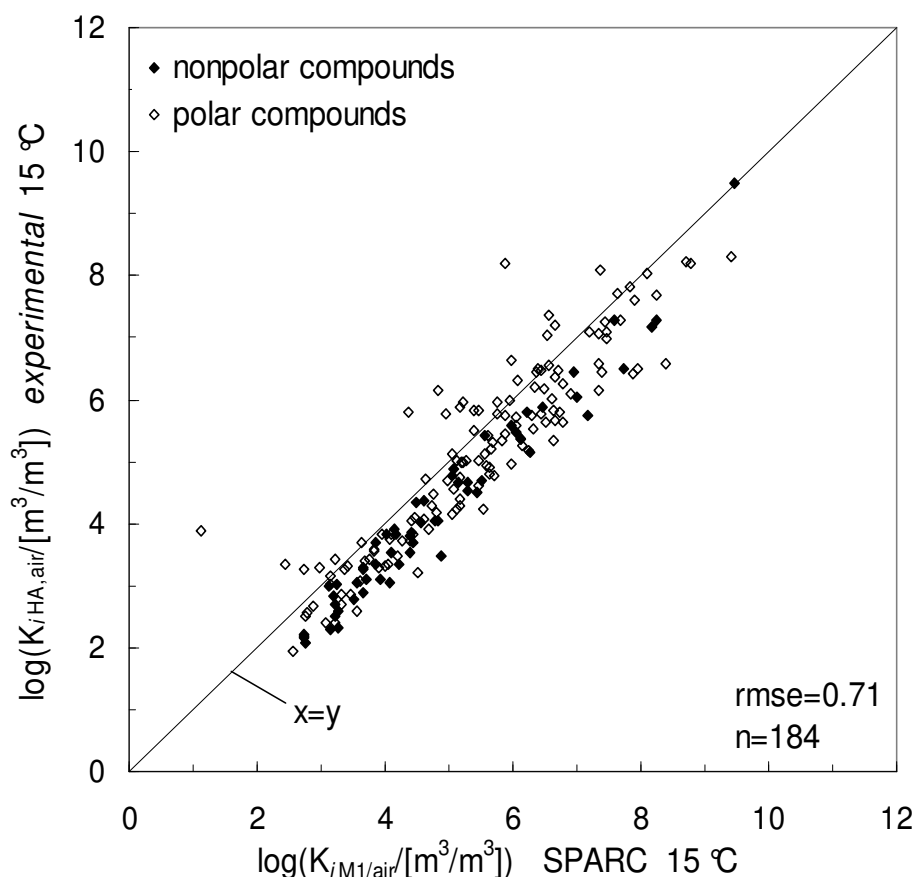


Figure 4 Compares the experimental Leonardite HA partition coefficients with partition coefficients calculated by SPARC at 15 °C.

Unfortunately, there is no documentation on how SPARC works in detail and no mechanistic insights can be gained from the model calculations. SPARC does not allow the input of different conformers of a molecule and it is unclear how the program deals with intramolecular H-bonds. SPARC depends on empirical calibrations but neither the calibration data sets nor any other hint on the applicability domain of SPARC is provided to the user. Thus, it remains unclear whether SPARC would also provide reliable predictions for molecules that are more complex than those used here.

In summary, COSMOtherm and SPARC gave both good results for Leonardite HA/air partitioning of a large and diverse set of compounds using a rather simple molecular structure as representative monomer for the HA. This indicates that all features of the HA that are important for its sorption properties were represented sufficiently well in the selected monomer. Furthermore, COSMOtherm calculations provided detailed insights into the various intermolecular interactions governing the sorption process including the role of conformational changes. SPARC and COSMOtherm might be suitable tools for the screening of large sets of compounds from molecular structure. Both models perform better than PckocWIN or any kind of K_{ow} model. Due to its empirical nature, SPARC's applicability domain is limited by its calibration data. Specific information on this applicability domain is not available. COSMOtherm has a much more fundamental basis and is not principally limited to specific molecular structures. Future work will have to show how both models perform for pesticides and pharmaceuticals that are more complex than the molecules studied in this first evaluation.

Acknowledgements

We thank Andreas Klamt (COSMOlogic), Hans Peter Arp, and René Schwarzenbach for critical comments on the manuscript and Gérard Mohler (EAWAG) for computer support. We also thank Baoshan Xing for his comments on the HA monomer structures. This research was financially supported by the Swiss National Science Foundation (project-No. 200020-111753/1).

References Chapter 3

- (1) Niederer, C., Goss, K.U., Schwarzenbach, R.P. Sorption equilibrium of a wide spectrum of organic vapors in Leonardite humic acid: Modeling of experimental data *Environ. Sci. Technol.* **2006**, *40*, 5374-5379.
- (2) Niederer, C., Goss, K.U., Schwarzenbach, R.P. Sorption equilibrium of a wide spectrum of organic vapors in Leonardite humic acid: Experimental setup and experimental data *Environ. Sci. Technol.* **2006**, *40*, 5368-5373.
- (3) Abraham, M. H., Chadha, H.S., Whiting, G.S., Mitchell, R.C. Hydrogen bonding. 32. An analysis of water-octanol and water-alkane partitioning and the Dlog P parameter of Seiler *J. Pharm. Sci.* **1994**, *83*, 1085-1100.
- (4) Abraham, M. H., Andonian-Haftvan, J., Whiting, G.S., Leo, A., Taft, R.S. Hydrogen bonding. Part 34. The factors that influence the solubility of gases and vapors in water at 298 K, and a new method for its determination *J. Chem. Soc., Perkin Trans. 2* **1994**, 1777-1791.
- (5) US-EPA EPI Suite V3.12;
<http://www.epa.gov/opptintr/exposure/pubs/episuite.htm> **2004**.
- (6) Schüürmann, G., Ebert, R.-U., Kühne, R. Prediction of the sorption of organic compounds into soil organic matter from molecular structure *Environ. Sci. Technol.* **2006**, *40*, 7005-7011.
- (7) Kubicki, J., Apitz, S.E. Models of natural organic matter and interactions with organic contaminants *Org. Geochem.* **1999**, *30*, 911-927.

- (8) Kubicki, J. D., Trout, C.C. Molecular modeling of fulvic and humic acids: charging effects and interactions with Al^{3+} , benzene, and pyridine. In *Geochemical and hydrological reactivity of heavy metals in soils*; Kingery, W. L., Selim, H.M., Ed.; CRC Press: Boca Raton, FL, 2003; pp 113-143.
- (9) Schulten, H.-R., Thomsen, M., Carlsen, L. Humic complexes of diethyl phthalate: molecular modelling of the sorption process *Chemosphere* **2001**, 45, 357-369.
- (10) Diallo, M. S., Faulon, J.L., Goddard, W.A., III., Johnson, J.H., Jr. Binding of hydrophobic organic compounds to dissolved humic substances: a predictive approach based on computer assisted structure elucidation, atomistic simulations and flory-huggins solution theory. In *Humic Substances: Structures, Models and Functions*; Ghabbour, E. A., Davies, G., Ed.; The Royal Chemical Society: Cambridge, UK, 2001; pp 221-237.
- (11) Eckert, F., Klamt, A.; COSMOtherm software, Version C2.1 ed.; COSMOlogic GmbH & Co.: Leverkusen, Germany, 2004.
- (12) Klamt, A., Eckert, F. COSMO-RS: a novel and efficient method for the a priori prediction of thermophysical data of liquids *Fluid Phase Equilib.* **2000**, 172, 43-72.
- (13) Klamt, A. Conductor-like screening model for real solvents: a new approach to the quantitative calculation of solvation phenomena *J. Phys. Chem.* **1995**, 99, 2224-2235.
- (14) Klamt, A. *COSMO-RS: from quantum chemistry to fluid phase thermodynamics and drug design*; Elsevier Science: Amsterdam, 2005.
- (15) CS Chem3Draw Ultra, V. C.; V 5.0 ed.: Cambridge, MA, 1999.
- (16) CS Chem3D Pro, V. C.; V 5.0 ed.: Cambridge, MA, 1999.
- (17) Steelink, C. Implication of elemental characteristics of humic substances. In *Humic substances in soil, sediment and water.*; Aiken, G. R., Ed.; John Wiley & Sons: New York, 1985; pp 457-476.
- (18) Stevenson, F. J. *Humus chemistry: Genesis, composition, reactions.*; 2nd edition ed.; John Wiley & Sons: New York, 1994.
- (19) Schulten, H.-R., Schnitzer, M. Chemical model structures for soil organic matter and soils *Soil Sci.* **1997**, 162, 115-130.
- (20) Leenheer, J. A., Wershaw, R.L., Reddy, M.M. Strong-acid, carboxyl-group structures in fulvic acid from the Suwannee River, Georgia. Major structures *Environ. Sci. Technol.* **1995**, 29, 399-405.

- (21) Diallo, M. S., Simpson, A., Gassman, P., Faulon, J.L., Johnson, J.H., Jr., Goddard W.A. III, Hatcher, P.G. 3-D Structure modeling of humic acids through experimental characterization, computer assisted structure elucidation and atomistic simulations. 1. Chelsea soil humic acid *Environ. Sci. Technol.* **2003**, 37, 1783-1793.
- (22) International Humic Substances Society,
<http://www.ihss.gatech.edu>; (accessed January 2006).
- (23) Ritchie, J. D., Perdue, E.M. Proton-binding study of standard and reference fulvic acids, humic acids, and natural organic matter *Geochim. Cosmochim. Acta* **2003**, 67, 85-96.
- (24) Milne, C. J., Kinniburgh, D.G., Tipping, E. Generic NICA-Donnan model parameters for proton binding by humic substances *Environ. Sci. Technol.* **2001**, 35, 2049-2059.
- (25) Mao, J. D., Hu, W.G., Schmidt-Rohr, K., Davies, G., Ghabbour, E.A., Xing, B. Quantitative characterization of humic substances by solid-state carbon-13 nuclear magnetic resonance *Soil Sci. Soc. Am. J.* **2000**, 64, 873-883.
- (26) Thorn, K. A., Folan, D.W., MacCarthy, P. "Characterization of the International Humic Substances Society standard and reference fulvic and humic acids by solution state carbon-13 (¹³C) and hydrogen-1 (¹H) nuclear magnetic resonance spectroscopy," U.S. Geological Survey, 1989.
- (27) Pretsch, E., Buehlmann, P., Affolter, C. *Structure determination of organic compounds: tables of spectral data*; 3rd ed.; Springer: Berlin, Germany, 2000.
- (28) Scott, D. T., McKnight, D.M., Blunt-Harris, E., Kolesar, S., Lovely, D. Quinone moieties act as electron acceptors in the reduction of humic substances by humics reducing microorganisms *Environ. Sci. Technol.* **1998**, 32, 2984-2989.
- (29) Cory, R. M., McKnight, D.M. Fluorescence spectroscopy reveals ubiquitous presence of oxidized and reduced quinones in dissolved organic matter *Environ. Sci. Technol.* **2005**, 39, 8142-8149.
- (30) Eckert, F. *COSMOtherm users manual* Leverkusen, Germany 2005.
- (31) Abraham, M. H. Hydrogen Bonding, XXVII. Solvation parameters for functionally substituted aromatic compounds and heterocyclic compounds, from gas-liquid chromatographic data *J. Chromatogr.* **1993**, 644, 95-139.

- (32) Arp, H. P. H., Niederer, C., Goss, K.-U. Predicting the partition behavior of various highly fluorinated compounds *Environ. Sci. Technol.* **2006**, *40*, 7298-7304.
- (33) Hilal, S. H., Karickhoff, S.W., Carreira, L.A. Prediction of the solubility, activity coefficient and liquid/liquid partition coefficient of organic compounds. *QSAR Comb. Sci.* **2004**, *23*, 709-720.

Appendix 3

Quantum-Chemical Modeling

Content

SI-1 flow diagram: COSMOtherm calculations

SI-2 building blocks for Leonardite HA monomer

SI-3 Leonardite HA model monomers M1-M4

SI-4 phase diagram: binary mixture M1/H₂O

SI-5 extensive table: experimental and calculated (SPARC, COSMOtherm) partition coefficients and sorption enthalpies, experimental hexadecane/air partition coefficients

SI-6 Experimental hexadecane/air partition coefficients vs. calculated partition coefficients

SI-7 substance-class specific comparison of experimental and calculated partition coefficients

SI-8 calculated partition coefficients for all model monomers M1-M4

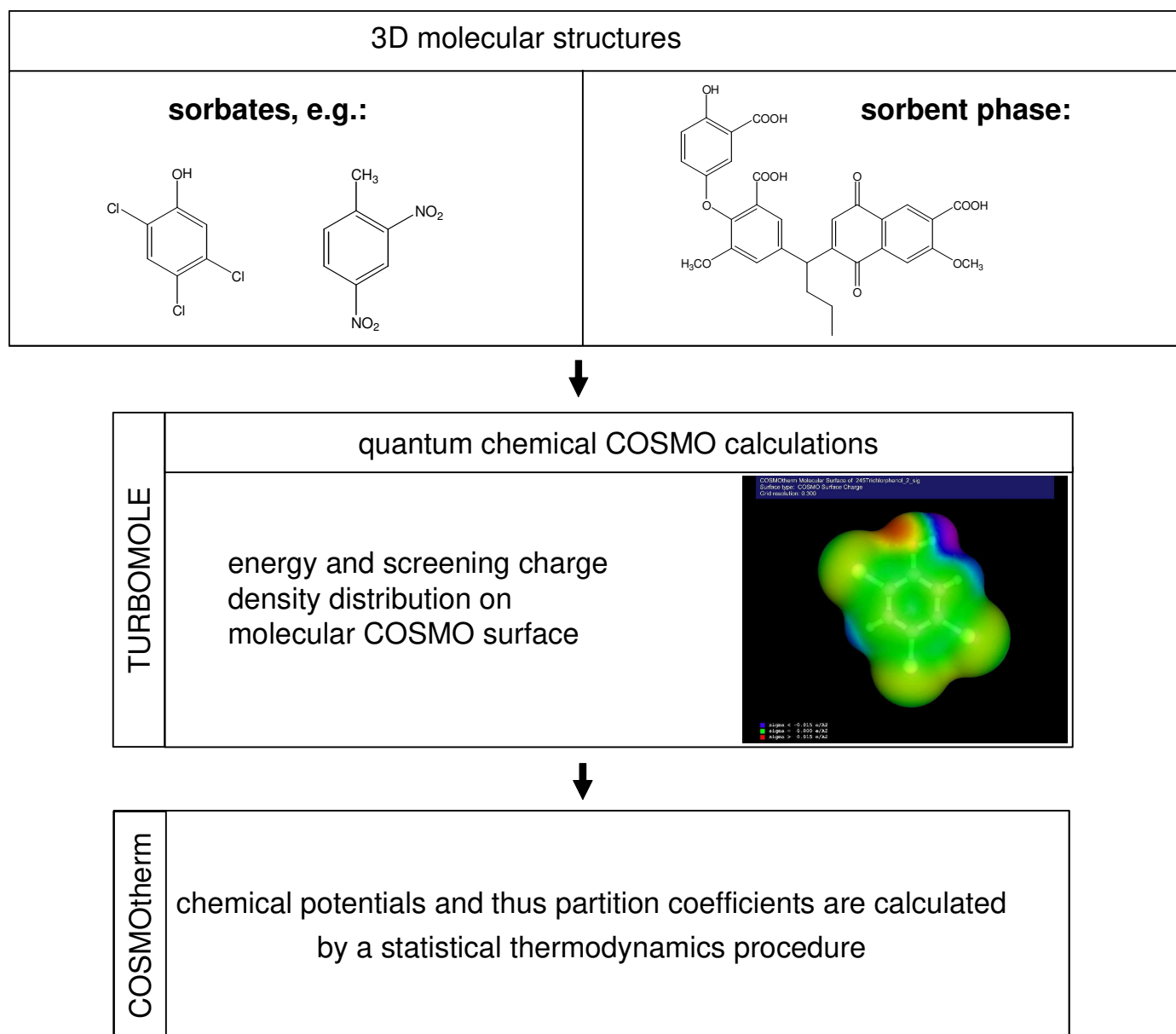
SI-9 sorbate conformers

SI-10 calculated M1/air partition coefficients at different relative humidities

SI-11 calculated partition coefficients at different temperatures

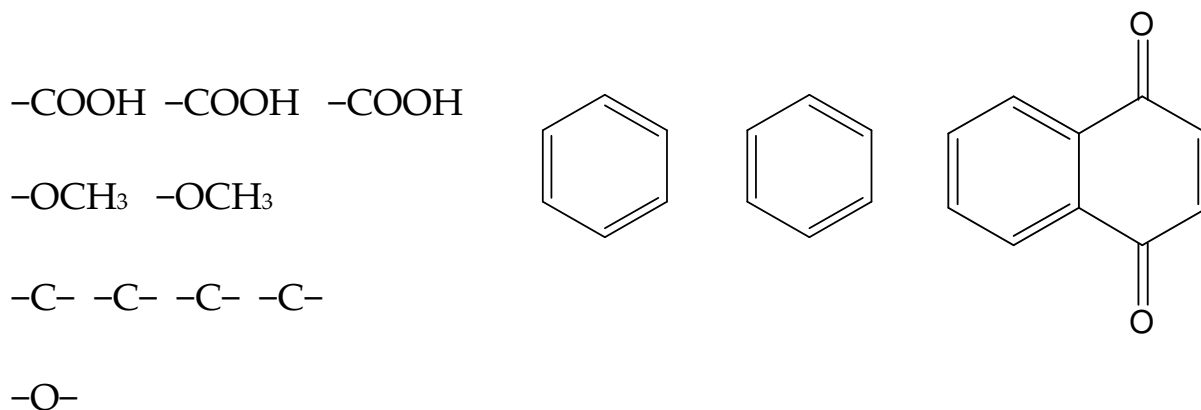
SI-12 SMILES structure of monomer M1

SI-1 Flow Diagram: COSMOtherm Calculations



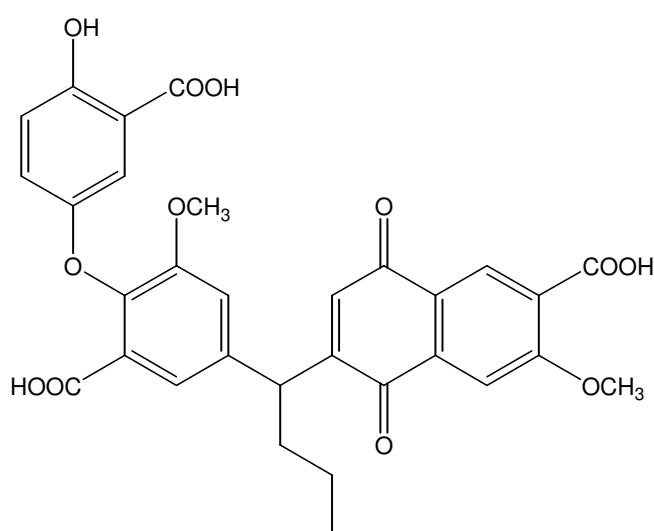
SI-2 Building blocks for the Leonardite HA monomer

According to the discussion in the article, the following building blocks are postulated for a Leonardite HA monomer with 31 carbon atoms

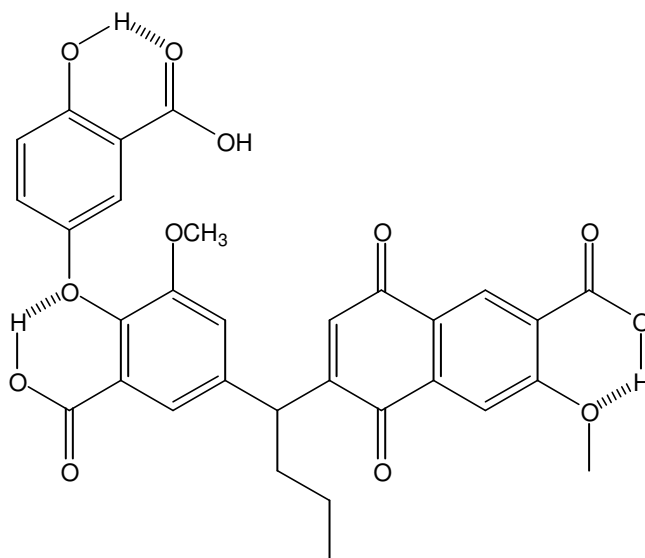


SI-3 Leonardite HA model monomers M1-M4

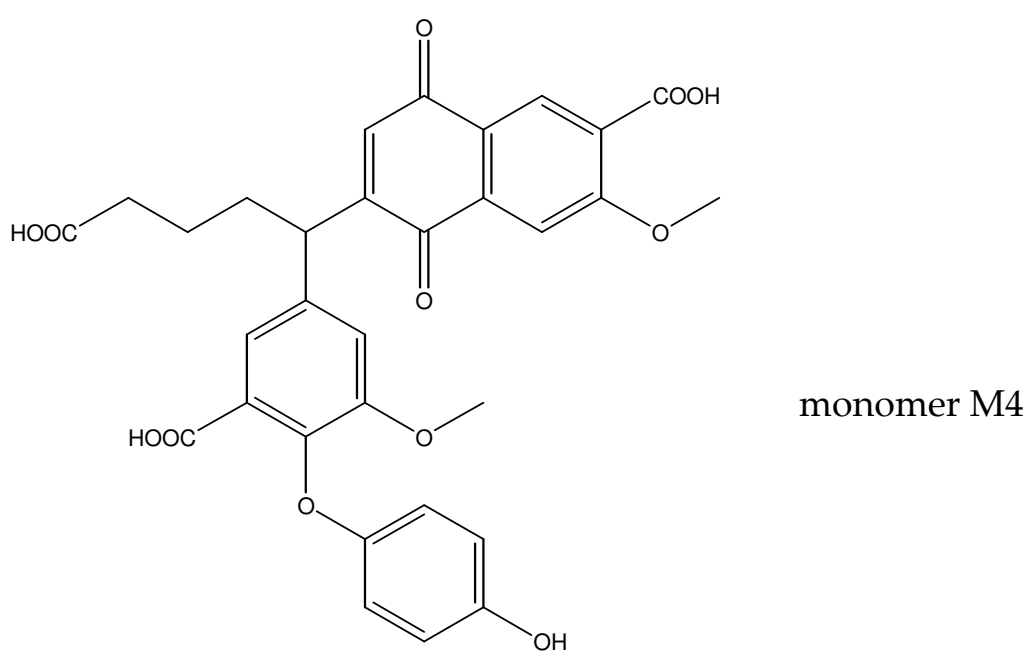
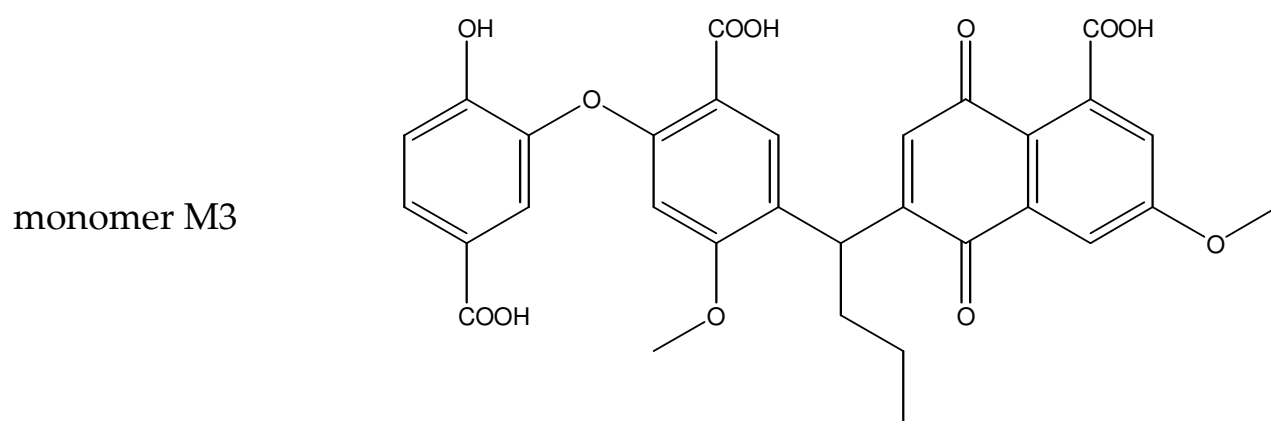
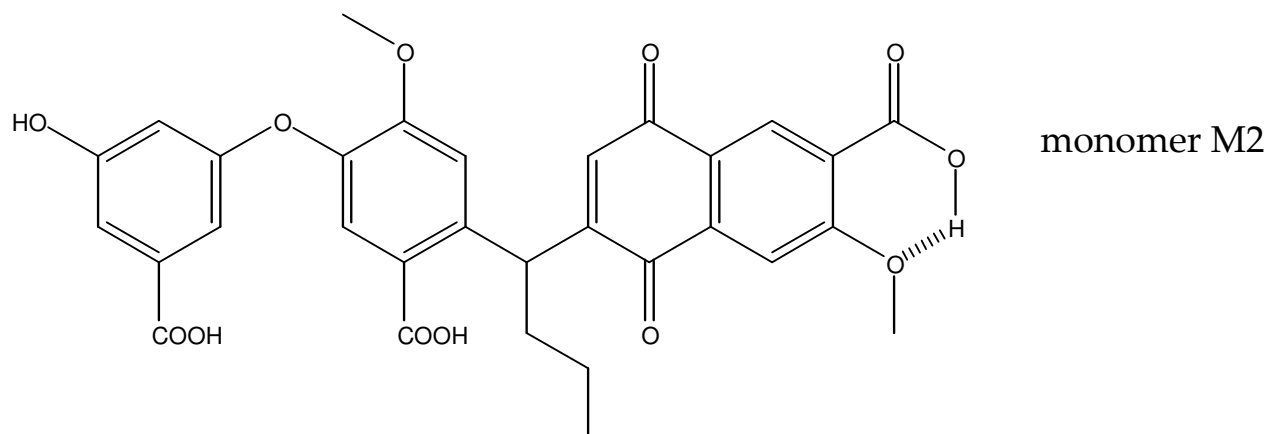
This section shows the Leonardite HA model monomers that were postulated and used for the COSMOtherm calculations. Possible intramolecular H-bonds between directly neighboured functional groups are accented in M1.



monomer M1



|||||| possible intramolecular H-bonds



SI-4 Binary mixture M1/H₂O

Soil organic matter in equilibrium with water-saturated air can take up a substantial amount of water. To model the partitioning of water molecules into the humic acid, the HA phase is simulated as a mixture of M1 and water. For that purpose the mole fraction of water in the M1/water mixture as a function of relative humidity has to be known. We calculated a phase diagram of the total pressure over the M1/water mixture as a function of the mole fraction of water in the mixture (see Figure SI-1). From this phase diagram, the mole fraction of water at every relative humidity can be obtained. The contribution of the Monomer M1 to the total pressure p_{tot} can be neglected. This partition system is temperature dependent and hence for other temperatures these calculations have been performed accordingly.

Saturation vapor pressure of pure H₂O: p_L (288 K) = 1705 Pa

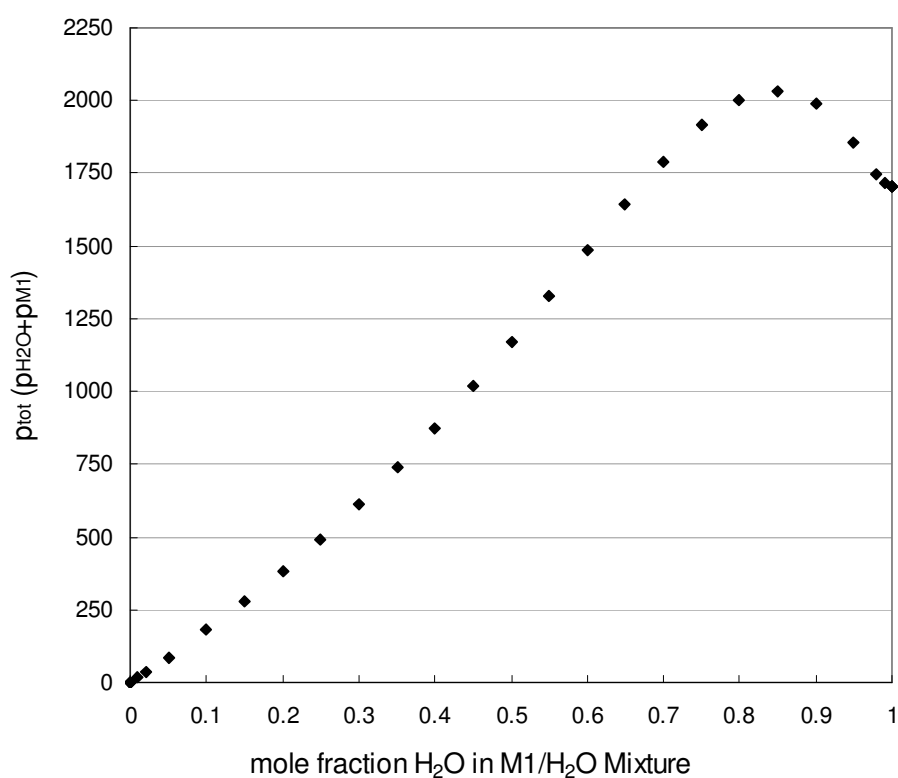
	$p_{\text{H}_2\text{O}}$ [Pa]	mole fraction H ₂ O	mole fraction M1
45% rh	767	0.36	0.64
70% rh	1194	0.51	0.49
98% rh	1671	0.66	0.34

Mole Fraction H ₂ O	Mole Fraction M1	p_{tot} [Pa]
0.00000001	0.99999999	1.695E-05
0.00001	0.99999	1.700E-02
0.001	0.999	1.696E+00
0.01	0.99	1.705E+01
0.02	0.98	3.428E+01
0.05	0.95	8.715E+01
0.1	0.9	1.793E+02
0.15	0.85	2.772E+02
0.2	0.8	3.814E+02
0.25	0.75	4.924E+02
0.3	0.7	6.109E+02
0.35	0.65	7.377E+02
0.4	0.6	8.731E+02
0.45	0.55	1.017E+03
0.5	0.5	1.169E+03
0.55	0.45	1.327E+03

Mole Fraction H ₂ O	Mole Fraction M1	p _{tot} [Pa]
0.6	0.4	1.487E+03
0.65	0.35	1.645E+03
0.7	0.3	1.792E+03
0.75	0.25	1.915E+03
0.8	0.2	2.001E+03
0.85	0.15	2.032E+03
0.9	0.1	1.989E+03
0.95	0.05	1.857E+03
0.98	0.02	1.745E+03
0.99	0.01	1.714E+03
0.999	0.001	1.704E+03
0.99999	0.00001	1.705E+03
0.9999999	0.00000001	1.705E+03

For 98% relative humidity, a mole fraction of 0.66/0.34 (H₂O/M1) has been calculated.

Figure SI-1



SI-5 Experimental and calculated partition coefficients (COSMOtherm, SPARC) and sorption enthalpies, exp. hexadecane/air values

Partition coefficients are in [m³/m³]

Compound	logK _{iHA,air} <i>experim.^{d)}</i> 15 °C, 98% rh	Δ _{abs} H _i <i>experim.</i> [kJ/mol]	Δ _{abs} H _i <i>COSMOt.</i> [kJ/mol]	logK _{iM1,air} <i>COSMOt.</i> 15 °C, 98% rh <i>via air</i>	log(K _{ihexadec.,air}) [m ³ /m ³] <i>experim.</i> 15 °C ^{e)}	Ref	logK _{iM1,air} <i>COSMOt.</i> 15 °C, 98% rh <i>via hexadec.</i>	logK _{iM1,air} <i>COSMOt.</i> 15 °C, 98% rh <i>linear corrected</i>	<i>predicted/ experim.</i> (lin.corr. hexadec.)	SPARC logK _{iM1,air} 15 °C
n-Octane	2.16		-33.4	2.00	3.93	[1]	2.27	1.77	0.41	2.72
n-Nonane	2.82		-36.9	2.37	4.47	[1]	2.61	2.11	0.20	3.20
n-Decane	3.41	-46.4	-40.4	2.74	5.00	[1]	2.94	2.45	0.11	3.67
n-Undecane	3.91	-62.8	-43.9	3.11	5.53	[3,4]	3.28	2.79	0.08	4.14
n-Dodecane	4.38	-64.1	-47.4	3.47	6.07	[3,4]	3.62	3.13	0.06	4.61
n-Tridecane	4.88	-59.6	-50.9	3.84	6.60	[3,4]	3.96	3.46	0.04	5.08
n-Tetradecane	5.43	-78.4	-54.4	4.21	7.14	[3,4]	4.30	3.80	0.02	5.55
Cyclodecane	3.69	-51.2	-49.5	3.33	5.69	[2]	4.06	3.56	0.75	4.45
1-Octene	2.08		-35.6	2.49	3.82	[1]	2.58	2.09	1.03	2.76
1-Nonene	2.69		-39.1	2.86	4.35	[1]	2.92	2.43	0.55	3.23
1-Decene	3.28	-43.5	-43.4	3.22	4.97	[1]	3.35	2.85	0.37	3.67
1-Undecene	3.83	-54.2	-47.1	3.59	5.54	[3]	3.71	3.22	0.25	4.03
1-Dodecene	4.35	-60.3	-50.9	3.96	6.10	[3]	4.08	3.59	0.17	4.49
1-Tridecene	4.77	-67.2	-54.7	4.32	6.67	[3]	4.45	3.96	0.15	5.06
Ethanol	3.68	-42.3	-56.7	4.04	1.61	[1]	4.04	3.54	0.72	3.64
Propan-1-ol	3.82	-43.2	-59.2	4.28	2.19	[1]	4.32	3.83	1.02	4.10
Butan-1-ol	4.08	-58.4	-63.2	4.65	2.79	[1]	4.72	4.22	1.39	4.62
Pentan-1-ol	4.39	-61.2	-66.6	4.99	3.33	[1]	5.05	4.55	1.46	5.16
Hexan-1-ol	4.76	-65.3	-70.1	5.37	3.86	[1]	5.39	4.89	1.35	5.71
Heptan-1-ol	5.18	-68.6	-73.6	5.72	4.40	[1]	5.72	5.23	1.13	6.25
Octan-1-ol	5.63	-75.8	-76.8	6.06	4.93	[1]	6.04	5.55	0.83	6.79
Nonan-1-ol	6.14	-83.5	-80.6	6.44	5.46	[1]	6.40	5.90	0.58	7.33
Decan-1-ol	6.42	-79.2	-84.0	6.81	6.00	[1]	6.73	6.24	0.65	7.87

Compound	$\log K_{i,HA,air}$ <i>experim.</i> ^{d)} 15 °C, 98% rh	$\Delta_{abs}H_i$ <i>experim.</i> [kJ/mol]	$\Delta_{abs}H_i$ <i>COSMOt.</i> [kJ/mol]	$\log K_{iM1,air}$ <i>COSMOt.</i> 15 °C, 98% rh <i>via air</i>	$\log(K_{i,hexadec.,air})$ [m ³ /m ³] <i>experim.</i> 15 °C ^{e)}	Ref	$\log K_{iM1,air}$ <i>COSMOt.</i> 15 °C, 98% rh <i>via hexadec.</i>	$\log K_{iM1,air}$ <i>COSMOt.</i> 15 °C, 98% rh <i>linear corrected</i>	<i>predicted/ experim.</i> (lin.corr. hexadec.)	SPARC $\log K_{iM1,air}$ 15 °C
Undecan-1-ol	6.59	-73.8	-88.0	7.17	6.58	[3]	7.12	6.62	1.09	8.40
Propan-2-ol	3.56	-53.3	-54.6	4.15	1.91	[1]	3.87	3.38	0.65	3.84
2-Methylpropan-1-ol	3.82	-60.1	-57.0	4.26	2.59	[1]	4.19	3.70	0.75	4.45
2-Methylpropan-2-ol	3.60	-44.9	-52.9	4.27	2.12	[1,3]	3.71	3.22	0.41	3.83
3-Methylbutan-1-ol	4.23	-63.5	-66.6	5.01	3.23	[1]	5.04	4.55	2.05	5.11
2-Ethyl-1-hexanol	5.37	-78.2	-69.9	5.48	4.68	c)	5.50	5.00	0.42	6.13
5-Hexen-1-ol	4.95	-66.1	-72.5	5.71	3.80	b)	5.75	5.25	2.01	5.97
Benzyl alcohol	6.10	-68.9	-84.0	7.26	4.51	[1]	7.17	6.68	3.78	6.90
1-Naphthol	8.20	-92.1	-100.1	8.39	6.53	[1]	9.04	8.54	2.22	8.79
Cyclopentanol	4.56	-57.4	-66.5	5.13	3.47	[1]	5.12	4.63	1.16	5.08
Cyclohexanol	4.92	-62.1	-69.0	5.47	4.02	[1]	5.45	4.96	1.10	5.63
2,2,2-Trifluoroethanol	3.42	-40.8	-56.5	4.92	1.34	[1]	4.41	3.92	3.12	3.21
Hexafluoropropanol	3.88	-61.2	-57.6	3.59	1.51	[1]	4.20	3.71	0.67	1.11
Phenol	6.00	-65.1	-77.0	6.30	4.03	[2,8]	6.61	6.12	1.32	5.95
o-Cresol	5.96	-67.0	-77.5	6.34	4.50	[2,8]	6.64	6.15	1.57	5.76
m-Cresol	6.50	-74.4	-79.9	6.58	4.60	[2,8]	6.91	6.41	0.81	6.39
p-Cresol	6.48	-75.1	-79.9	6.59	4.60	[2,8]	6.90	6.41	0.85	6.45
2-Chlorophenol	5.44	-60.9	-66.7	5.35	4.46	[2,5]	5.59	5.10	0.45	5.89
4-Chlorophenol	7.19	-83.9	-88.2	7.46	5.09	[2,8]	7.73	7.24	1.12	6.67
2-Chloro-4-methylphen.	5.65	-53.4	-70.5	5.70	5.14	c)	5.98	5.49	0.70	6.51
2,3-Dichlorophenol	6.36	-63.2	-75.0	6.11	5.32	[2,5]	6.35	5.86	0.31	6.65
2,6-Dichlorophenol	5.87	-48.2	-73.6	6.39	5.42	[2,8]	6.39	5.90	1.06	5.18
2,4,5-Trichlorophenol	8.08	-121.7	-87.1	7.23	6.10	[2,8]	7.29	6.79	0.05	7.37
2-Propanone	2.68		-38.4	3.78	1.84	[1]	3.04	2.54	0.74	2.88
2-Butanone	2.85		-42.2	3.97	2.46	[1]	3.38	2.89	1.09	3.31
2-Pentanone	3.28	-43.3	-45.0	4.27	2.96	[1]	3.64	3.15	0.75	3.37
2-Hexanone	3.49	-49.6	-47.2	5.01	3.49	[1]	3.79	3.30	0.64	4.19
2-Heptanone	3.92	-54.5	-52.0	5.01	4.02	[1]	4.32	3.82	0.80	4.68
2-Octanone	4.29	-56.1	-55.4	5.38	4.55	[1]	4.65	4.15	0.74	5.18

Compound	$\log K_{iHA,air}$ <i>experim.^{d)}</i> 15 °C, 98% rh	$\Delta_{abs}H_i$ <i>experim.</i> [kJ/mol]	$\Delta_{abs}H_i$ <i>COSMOt.</i> [kJ/mol]	$\log K_{iM1,air}$ <i>COSMOt.</i> 15 °C, 98% rh <i>via air</i>	$\log(K_{ihexadec.,air})$ [m ³ /m ³] <i>experim.</i> 15 °C ^{e)}	Ref	$\log K_{iM1,air}$ <i>COSMOt.</i> 15 °C, 98% rh <i>via hexadec.</i>	$\log K_{iM1,air}$ <i>COSMOt.</i> 15 °C, 98% rh <i>linear corrected</i>	<i>predicted/ experim.</i> (lin.corr. hexadec.)	SPARC $\log K_{iM1,air}$ 15 °C
2-Nonanone	4.81	-64.4	-58.6	5.73	5.05	[1]	4.96	4.46	0.45	5.64
2-Decanone	5.27	-68.5	-62.2	6.09	5.59	[1]	5.30	4.80	0.34	6.15
2-Undecanone	5.67	-78.6	-65.5	6.46	6.11	[1]	5.62	5.12	0.29	6.66
3-Methylbutan-2-one	3.08	-33.7	-43.1	4.11	2.89	[1]	3.48	2.99	0.81	3.61
4-Methylpentan-2-one	3.31	-41.9	-45.8	4.40	3.31	[1]	3.71	3.22	0.80	3.99
Cyclopentanone	4.05	-48.2	-50.3	4.60	3.45	[1,3]	4.32	3.83	0.60	4.42
Cyclohexanone	4.29	-50.5	-55.4	5.20	4.05	[1,3]	4.79	4.29	1.01	4.72
Cycloheptanone	4.75	-51.6	-55.8	5.39	4.65	a)	4.78	4.28	0.70	5.16
Acetophenone	5.22	-59.2	-63.3	6.08	4.80	[1]	5.78	5.29	1.17	5.65
Methyl acetate	2.50		-36.9	3.33	2.06	[1]	2.99	2.50	0.99	2.75
Ethyl acetate	2.39		-39.7	3.80	2.49	[1]	3.22	2.72	2.14	3.08
n-Propyl acetate	2.85		-42.8	4.10	3.02	[1]	3.50	3.01	1.43	3.46
n-Butyl acetate	3.28	-49.3	-46.4	4.44	3.59	[1]	3.86	3.36	1.20	3.91
Isobutyl acetate	3.40	-40.8	-44.7	4.35	3.39	[1]	3.65	3.16	0.58	3.68
n-Pentyl acetate	3.72	-57.0	-49.8	4.81	4.11	[1]	4.18	3.69	0.92	4.38
Methyl benzoate	5.01	-57.0	-61.5	5.79	5.02	[1]	5.63	5.14	1.36	5.11
Benzyl acetate	5.32	-57.7	-67.4	6.62	5.34	[2,8]	6.30	5.80	3.04	5.69
2-Phenylethylacetate	5.74	-73.6	-69.3	7.06	5.72	[2]	6.43	5.94	1.59	6.30
Di-n-butyl ether	3.22	-51.4	-47.2	4.08	4.19	[1]	3.49	2.99	0.59	4.52
Di-n-pentylether	4.23	-61.1	-52.8	4.79	5.12	c)	4.01	3.52	0.19	5.54
Methyl t-butyl ether	1.94		-39.6	3.15	2.44	[1]	2.67	2.18	1.73	2.55
Tetrahydrofuran	2.70		-46.9	3.59	2.83	[1]	3.56	3.07	2.33	3.31
1,4-Dioxane	3.82	-44.9	-52.6	4.51	3.10	[1]	4.36	3.86	1.11	3.95
Benzofuran	4.09	-55.5	-55.3	4.62	4.65	[2,3]	4.99	4.49	2.51	4.46
Dibenzofuran	5.80	-50.5	-76.8	6.45	7.15	[2,3]	7.28	6.79	9.68	6.74
Methyl phenyl ether	3.72	-46.7	-50.1	4.42	4.16	[1]	4.45	3.95	1.72	4.26
Benzene	2.18		-37.8	2.85	2.99	[1]	3.09	2.60	2.64	2.72
Toluene	2.29		-41.4	3.23	3.56	[1]	3.43	2.94	4.49	3.15
p-Xylene	2.88		-44.6	3.57	4.10	[1]	3.74	3.25	2.33	3.66

Compound	$\log K_{iHA,air}$ <i>experim.^{d)}</i> 15 °C, 98% rh	$\Delta_{abs}H_i$ <i>experim.</i> [kJ/mol]	$\Delta_{abs}H_i$ <i>COSMOt.</i> [kJ/mol]	$\log K_{iM1,air}$ <i>COSMOt.</i> 15 °C, 98% rh <i>via air</i>	$\log(K_{ihexadec.,air})$ [m ³ /m ³] <i>experim.</i> 15 °C ^{e)}	Ref	$\log K_{iM1,air}$ <i>COSMOt.</i> 15 °C, 98% rh <i>via hexadec.</i>	$\log K_{iM1,air}$ <i>COSMOt.</i> 15 °C, 98% rh <i>linear corrected</i>	<i>predicted/ experim.</i> (lin.corr. hexadec.)	SPARC $\log K_{iM1,air}$ 15 °C
Ethylbenzene	2.78		-44.3	3.55	4.04	[1]	3.71	3.22	2.70	3.52
n-Propylbenzene	3.10	-51.3	-47.3	3.93	4.52	[1]	3.99	3.49	2.51	3.93
n-Butylbenzene	3.53	-48.1	-50.7	4.30	5.05	[1]	4.32	3.83	1.98	4.38
n-Pentylbenzene	4.03	-56.7	-54.2	4.66	5.58	[1]	4.65	4.16	1.34	4.83
n-Hexylbenzene	4.53	-66.1	-57.5	5.03	6.09	[1]	4.97	4.48	0.90	5.29
1,2,4-Trimethylbenz.	3.33	-47.1	-49.3	3.93	4.74	[1]	4.22	3.73	2.48	4.21
1,3,5-Trimethylbenz.	3.05	-43.7	-48.0	3.97	4.64	[1]	4.06	3.57	3.29	4.07
Styrene	3.34	-30.2	-48.6	3.95	4.12	[1]	4.23	3.74	2.52	3.86
Indane	3.49	-32.9	-51.2	4.01	4.90	[1]	4.46	3.96	3.00	4.87
Naphthalene	4.66	-54.7	-61.5	5.06	5.50	[1]	5.64	5.15	3.07	5.30
1-Methylnaphthalene	5.48	-76.9	-66.1	5.40	6.17	[1]	6.10	5.61	1.35	6.05
Acenaphthene	5.75	-59.3	-71.6	5.81	6.89	[1]	6.71	6.22	2.93	7.16
Anthracene	7.29	-79.6	-85.3	7.20	8.05	[2,8]	8.20	7.71	2.65	8.25
Phenanthrene	7.17	-79.0	-86.5	7.23	8.12	[2,8]	8.34	7.85	4.77	8.16
Biphenyl	5.58	-68.9	-69.7	6.25	6.41	[2,8]	6.51	6.02	2.76	5.98
p-Terphenyl	9.49	-98.7	-105.7	9.51	10.29	[2,3]	10.38	9.88	2.45	9.46
Chlorobenzene	3.05	-27.4	-45.6	3.87	3.91	[5]	3.90	3.40	2.24	3.56
1,2-Dichlorobenzene	4.01	-53.3	-52.8	4.68	4.82	[5]	4.63	4.14	1.36	4.55
1,3-Dichlorobenzene	3.81	-51.8	-51.8	4.56	4.71	[5]	4.50	4.01	1.58	4.38
1,4-Dichlorobenzene	3.87	-53.5	-52.7	4.62	4.73	[5]	4.61	4.12	1.78	4.42
1,4-Dibromobenzene	4.69	-56.9	-71.4	6.25	5.67	[2,3]	6.70	6.21	33.02	5.52
1,4-Diiodobenzene	6.45	-106.7	-66.2	6.85	6.66	[2]	6.08	5.58	0.14	6.95
1,2,4-Trichlorobenzene	4.51	-53.3	-59.0	5.14	5.59	[5]	5.22	4.73	1.63	5.43
1,2,3,4-Tetrachlorobenz.	5.36	-58.6	-66.1	5.61	6.57	[5]	5.95	5.46	1.25	6.13
1,2,3,5-Tetrachlorobenz.	5.14	-45.6	-63.3	5.38	6.31	[5]	5.60	5.11	0.92	6.26
1,2,4,5-Tetrachlorobenz.	5.79	-66.3	-63.6	5.45	6.31	[5]	5.64	5.14	0.23	6.21
Pentachlorobenzene	6.05	-71.3	-68.7	5.66	7.15	[5]	6.16	5.66	0.41	7.01
Hexachlorobenzene	6.50	-89.9	-74.6	5.74	8.11	[5]	6.79	6.29	0.61	7.74
Fluorobenzene	2.21		-39.4	3.01	2.99	[1]	3.24	2.75	3.41	2.74

Compound	$\log K_{iHA,air}$ <i>experim.^{d)}</i> 15 °C, 98% rh	$\Delta_{abs}H_i$ <i>experim.</i> [kJ/mol]	$\Delta_{abs}H_i$ <i>COSMOt.</i> [kJ/mol]	$\log K_{iM1,air}$ <i>COSMOt.</i> 15 °C, 98% rh <i>via air</i>	$\log(K_{ihexadec.,air})$ [m ³ /m ³] <i>experim.</i> 15 °C ^{e)}	Ref	$\log K_{iM1,air}$ <i>COSMOt.</i> 15 °C, 98% rh <i>via hexadec.</i>	$\log K_{iM1,air}$ <i>COSMOt.</i> 15 °C, 98% rh <i>linear corrected</i>	<i>predicted/ experim.</i> (lin.corr. hexadec.)	SPARC $\log K_{iM1,air}$ 15 °C
Bromobenzene	3.54	-45.0	-54.5	4.70	4.32	[5]	4.89	4.39	7.18	4.10
Iodobenzene	4.03	-61.9	-51.8	5.01	4.81	[5]	4.57	4.08	1.10	4.79
4-Fluorotoluene	2.60		-43.2	3.41	3.60	[2]	3.61	3.11	3.28	3.27
4-Chlorobenzotrifluor.	3.00	-40.7	-48.2	4.11	3.90	c)	4.05	3.56	3.63	3.12
1,1,1,2-Tetrachloroetha.	3.01	-26.4	-45.6	4.14	3.89	[1]	3.78	3.28	1.89	3.25
1,1,2,2-Tetrachloroetha.	3.70	-55.3	-54.0	5.19	4.07	[1]	4.62	4.12	2.63	3.85
1-Chlorohexane	2.50		-39.7	3.41	4.04	[1]	3.16	2.67	1.46	3.22
1-Chloroheptane	3.10	-38.2	-43.2	3.77	4.57	[1]	3.50	3.01	0.80	3.71
1-Chlorooctane	3.82	-48.1	-46.6	4.14	5.09	[2,3]	3.82	3.33	0.32	4.16
1-Chlorodecane	4.67	-59.4	-54.0	4.87	6.21	[3]	4.55	4.05	0.24	5.14
1-Bromopentane	2.32		-44.9	3.82	3.86	[1]	3.78	3.29	9.26	3.26
Butanal	2.41	-35.5	-37.1	3.32	2.44	[1]	2.98	2.49	1.19	3.21
Pentanal	2.59		-41.3	3.68	3.06	[1]	3.40	2.90	2.03	3.57
Benzaldehyde	4.70	-49.9	-57.7	5.43	4.28	[1]	5.27	4.78	1.21	4.97
1-Cyanopropane	3.44	-37.1	-43.0	4.07	2.74	[1]	3.76	3.26	0.67	3.75
Aniline	5.81	-72.0	-69.5	5.77	4.20	[2,8]	6.18	5.68	0.74	5.47
2-Methylaniline	5.82	-65.0	-69.8	5.89	4.74	[2,8]	6.26	5.76	0.88	5.40
4-Methylaniline	6.63	-85.9	-72.6	6.02	4.75	[2,8]	6.45	5.95	0.21	5.97
2,6-Dimethylaniline	5.76	-67.9	-69.6	6.01	5.36	[1]	6.33	5.83	1.19	5.75
N,N-Dimethylaniline	5.12	-65.0	-55.7	4.88	5.02	[1]	5.05	4.56	0.28	5.06
2-Iodoaniline	6.45	-89.9	-78.5	7.18	5.94	[2]	7.14	6.65	1.56	6.36
4-Iodoaniline	7.10	-69.9	-84.5	8.37	6.07	[2,8]	7.77	7.27	1.49	7.47
Nitrobenzene	5.02	-50.0	-58.4	5.43	4.86	[1]	5.45	4.95	0.87	5.26
2-Nitrotoluene	5.12	-52.1	-60.2	5.54	5.20	[1]	5.61	5.11	0.99	5.55
2-Chlornitrobenzene	5.59	-61.7	-64.6	6.36	5.58	[2]	6.09	5.59	1.02	6.04
Benzonitrile	4.60	-46.3	-58.6	5.58	4.32	[1]	5.46	4.97	2.32	5.46
Acetonitrile	3.16	-34.9	-40.5	3.76	1.88	[1]	3.60	3.10	0.87	3.15
Nitromethane	3.28	-37.7	-37.2	3.36	2.04	[1]	3.29	2.80	0.33	2.73
Nitroethane	3.29	-38.8	-39.1	3.49	2.60	[1]	3.45	2.96	0.47	2.98

Compound	$\log K_{iHA,air}$ <i>experim.^{d)}</i> 15 °C, 98% rh	$\Delta_{abs}H_i$ <i>experim.</i> [kJ/mol]	$\Delta_{abs}H_i$ <i>COSMOt.</i> [kJ/mol]	$\log K_{iM1,air}$ <i>COSMOt.</i> 15 °C, 98% rh <i>via air</i>	$\log(K_{ihexadec.,air})$ [m ³ /m ³] <i>experim.</i> 15 °C ^{e)}	Ref	$\log K_{iM1,air}$ <i>COSMOt.</i> 15 °C, 98% rh <i>via hexadec.</i>	$\log K_{iM1,air}$ <i>COSMOt.</i> 15 °C, 98% rh <i>linear corrected</i>	<i>predicted/ experim.</i> (lin.corr. hexadec.)	SPARC $\log K_{iM1,air}$ 15 °C
1-Nitropropane	3.32	-45.6	-41.5	3.68	3.10	[1]	3.66	3.16	0.70	3.41
2-Nitropropane	3.02	-56.5	-36.3	3.50	2.74	[1]	3.08	2.58	0.37	3.15
Pyridine	3.36		-59.5	4.88	3.24	[1]	4.89	4.39	10.86	4.06
2-Methylpyridine	5.80	-51.9	-61.3	5.15	3.48	[1]	4.99	4.50	0.05	4.36
2-Acetylpyridine	5.83	-78.1	-64.6	6.02	4.78	[2]	5.89	5.40	0.37	6.64
2-Methylpyrazine	4.99	-49.4	-62.7	5.05	3.48	[2]	5.19	4.70	0.51	5.19
Methylamine	3.34		-64.6	3.93	1.42	[1]	4.56	4.07	5.35	2.45
N,N-Dimethylformam.	5.78	-44.9	-75.8	6.27	3.26	^{c)}	6.50	6.01	1.68	4.94
N,N-Dimethylacetam.	6.31	-63.1	-83.0	7.20	3.97	[2,3]	6.83	6.34	1.06	6.07
Indole (1H-Indole)	6.48	-68.6	-85.9	7.21	5.87	[2,3]	7.98	7.48	10.14	6.71
Chinoline	6.25	-111.7	-80.3	6.76	5.82	[1]	7.19	6.70	2.85	6.79
Propanoic acid	5.51	-38.5	-71.6	5.10	3.24	[1]	5.96	5.46	0.89	5.40
Butanoic acid	5.73	-43.7	-74.2	5.40	3.72	[1]	6.20	5.70	0.95	6.06
Pentanoic acid	6.17	-61.0	-78.9	8.66	4.24	[1]	7.29	6.80	4.23	6.48
2-Methylbutanoic acid	5.74	-55.4	-70.2	5.63	3.48	^{b)}	5.71	5.21	0.29	5.88
3-Methylbutanoic acid	5.77	-48.4	-69.1	5.61	3.36	[1]	5.59	5.10	0.21	6.43
1,2-Dinitrobenzene	7.08	-97.1	-76.6	7.87	6.39	^{b)}	7.48	6.99	0.80	7.20
1,3-Dinitrobenzene	7.25	-108.6	-74.2	7.10	6.23	[7]	7.25	6.76	0.32	7.45
1,4-Dinitrobenzene	7.00	-64.7	-75.2	6.73	6.28	^{b)}	7.35	6.86	0.73	7.46
2,4-Dinitrotoluene	7.83	-97.0	-78.6	7.34	6.91	^{b)}	7.72	7.23	0.25	7.84
α -Acetylbutyllactone	7.06	-50.3	-66.7	7.46	4.68	^{c)}	6.49	6.00	0.09	7.33
4-Nitroanisole	6.55	-78.1	-73.9	7.40	6.23	[2,7]	7.18	6.68	1.37	6.56
Dimethylphthalate	6.57	-63.9	-79.3	8.75	6.44	[2,8]	7.72	7.23	4.51	7.35
Diethylphthalate	7.68	-76.5	-87.1	9.58	7.51	[3]	8.44	7.94	1.83	8.24
Triethylphosphate	6.15	-65.4	-76.7	8.87	5.07	[1]	6.85	6.36	1.61	4.82
Thiophene	2.55		-44.1	3.69	3.02	[1]	3.85	3.36	6.39	2.77
Thiophenol	4.18	-51.5	-58.0	5.21	4.39	[1]	5.34	4.84	4.64	4.80
2,4-Pentanedione	4.14	-37.2	-52.9	5.03	3.47	[10]	4.84	4.35	1.60	5.06
1,2-Ethanediole	7.37	-79.0	-82.1	6.05	2.93	^{c)}	6.55	6.06	0.05	6.55

Compound	$\log K_{iHA,air}$ <i>experim.</i> ^{d)} 15 °C, 98% rh	$\Delta_{abs}H_i$ <i>experim.</i> [kJ/mol]	$\Delta_{abs}H_i$ <i>COSMOt.</i> [kJ/mol]	$\log K_{iM1,air}$ <i>COSMOt.</i> 15 °C, 98% rh <i>via air</i>	$\log(K_{ihexadec.,air})$ [m ³ /m ³] <i>experim.</i> 15 °C ^{e)}	Ref	$\log K_{iM1,air}$ <i>COSMOt.</i> 15 °C, 98% rh <i>via hexadec.</i>	$\log K_{iM1,air}$ <i>COSMOt.</i> 15 °C, 98% rh <i>linear corrected</i>	<i>predicted/ experim.</i> (lin.corr. hexadec.)	SPARC $\log K_{iM1,air}$ 15 °C
Chloroacetone	3.75	-46.9	-46.8	4.25	2.91	c)	4.15	3.66	0.82	4.08
Benzoylchloride	4.46	-53.6	-54.9	5.34	4.82	b)	4.95	4.46	0.99	4.75
Hydroxyacetone	5.34	-55.1	-54.8	4.82	2.81	b)	4.65	4.15	0.06	6.64
Dimethyl succinate	5.35	-54.3	-61.1	5.95	4.41	c)	5.71	5.21	0.73	5.84
Lindane (γ -HCH)	7.27	-89.0	-88.7	9.43	7.94	[6]	8.36	7.87	3.95	7.59
2-Methoxyethanol	5.00	-55.7	-56.6	4.47	2.68	[1]	4.40	3.90	0.08	5.21
2-Ethoxyethanol	4.94	-58.9	-61.7	4.83	3.02	[1]	4.60	4.11	0.15	5.58
1,2-Naphthoquinone	7.60	-95.8	-88.7	9.92	6.47	b)	8.54	8.05	2.84	7.91
1,4-Naphthoquinone	6.50	-57.2	-82.2	7.39	6.75	[2]	8.04	7.55	11.01	7.94
2-Nitroaniline	7.03	-91.4	-91.7	8.39	6.00	[1]	8.59	8.10	11.72	6.54
3-Methoxybenzaldehy.	6.20	-71.8	-67.4	6.68	5.28	b)	6.35	5.85	0.45	6.33
1,4-Dimethoxybenzene	5.42	-49.2	-63.1	5.95	5.38	[3,4]	5.88	5.39	0.93	5.60
3-Hydroxybenzonitrile	8.30	-62.8	-102.9	9.11	5.52	[2,8]	9.37	8.88	3.76	9.42
2-Aminobenzonitrile	7.28	-94.6	-90.5	8.07	5.35	[2]	8.39	7.89	4.06	7.68
4-Aminobenzonitrile	8.03	-67.7	-104.6	10.07	6.01	[2]	9.87	9.37	21.88	8.09
Azobenzene	6.45	-69.4	-81.6	7.45	7.65	[5]	7.73	7.24	6.10	7.38

a) $\log K_{ihexadecane,air}$ extrapolated from homologue series, based on it's proportionality to the number of carbons

b) $K_{ihexadecane,air}$ value calculated by the SPARC online calculator (<http://ibmcl2.chem.uga.edu/sparc/>) accessed September 25 2005.

c) value measured in our lab, experimental method to be given in an upcoming publication.

d) from Niederer, C., Goss, K.-U., Schwarzenbach, R.P. Sorption equilibrium of a wide spectrum of organic vapors in Leonardite humic acid: experimental setup and experimental data. *Environ. Sci. Technol.* **2006**, 5368-5373.

e) Hexadecane/air partition coefficients at 15 °C were calculated from tabulated experimental partition coefficients at 25 °C using the empirical equation: $\Delta_{12}H_i = 1.68 \cdot (-R \cdot T \cdot \ln(K_{ihexadecane,air})) - 6.75$ [kJ/mol] from: Abraham, M.H., Whiting, G.S., Fuchs, R., Chambers, E.J. Thermodynamics of solute transfer from water to hexadecane. *J. Chem. Soc. Perkin Trans. 2* **1990**, 291-300.

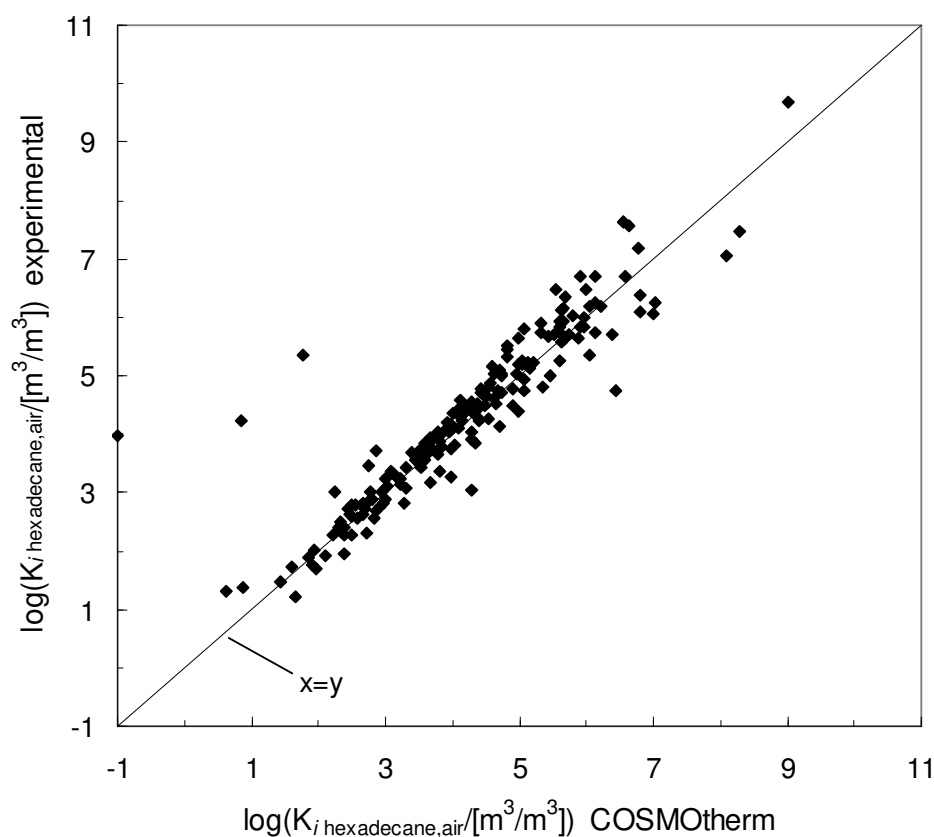
References

- [1] Abraham, M.H.; Andonian-Haftvan, J.; Whiting, G.S.; Leo, A. and Taft, S. Hydrogen bonding. Part 34. The factors that influence the solubility of gases and vapours in water at 298 K, and a new method for its determination. *J. Chem. Soc. Perkin Trans. 2*. **1994**, 8: 1777-1791.
- [2] Abraham, M.H. Hydrogen bonding XXVII. Solvation parameters for functionally substituted aromatic compounds and heterocyclic compounds, from gas-liquid chromatographic data. *J. Chromatogr.* **1993**. 644: 95-139.
- [3] Abraham, M.H.; Chadha, H.S.; Whiting, G.S.; Mitchell, R.C. Hydrogen bonding. 32. An analysis of water-octanol and water-alkane partitioning and the $\Delta \log P$ parameter of Seiler. *J. Pharmaceut. Sci.* **1994**. 83(8): 1085ff.
- [4] Abraham, M.H.; Grellier, P.L.; McGill, R.A.; Determination of olive oil-gas and hexadecane-gas partition coefficients, and calculation of the corresponding olive oil-water and hexadecane-water partition coefficients. *J. Chem. Soc. Perkin Trans. II*. **1987**. 797-803.
- [5] Poole, S.K.; Poole, C.F. Chromatographic models for the sorption of neutral organic compounds by soil from water and air. *J. Chromatogr. A*. **1999**. 845: 381-400.
- [6] Abraham, M.H.; Enomoto, K.; Clarke, E.D.; Sexton, G. Hydrogen bond basicity of the chlorogroup; hexachlorocyclohexanes as strong hydrogen bond bases. *J. Org. Chem.* **2002**. 67(14): 4782-4786.
- [7] Gunatilleka, A.D.; Poole, C.F. Models for estimating the nonspecific toxicity of organic compounds in short term bioassays. *Analyst*. **2000**. 125: 127-132.
- [8] Torres-Lapasio, J.R.; Garcia-Alvarez-Coque, M.C.; Roses, M.; Bosch, E.; Zissimos, A.M.; Abraham, M.H. Analysis of a solute polarity parameter in reversed-phase liquid chromatography on a linear solvation relationship basis. *Anal. Chim. Acta*. **2004**. 515: 209-227.
- [9] Abraham, MH; Andonian-Haftven, J.; Du, CM; Osei-Owusu, JP; Sakellariou, P; Shuely, WJ; Poole, CF; Poole, SK. Comparison of uncorrected retention data on a capillary and a packed hexadecane column with corrected retention data on a packed squalane column. *J. Chromatogr. A*. **1994**. 688: 125-134.
- [10] Abraham, MH; Acree, WE Jr. Correlation and prediction of partition coefficients between the gas phase and water, and the solvents dodecane and undecane. *New J. Chem.* **2004** 12: 1538-1543.

SI-6 Comparison of experimental and calculated hexadecane/air partition coefficients

In the main text we have presented two variants of the COSMOtherm calculations: a) a direct prediction of the measured HA/air partition coefficients and b) a prediction of the humic acid/hexadecane partition coefficients that were afterwards transformed into HA/air coefficients using experimental hexadecane/air partition coefficients. The latter results were significantly better because COSMOtherm is focused on the description of electrostatic interactions rather than vdW interactions. vdW interactions govern all types of gas phase/condensed phase partitioning but mostly cancel out in condensed phase/condensed phase partitioning. Hence predictions of HA/hexadecane were superior to HA/air. Figure SI-2 shows a direct comparison of experimental and predicted (with COMSOtherm) hexadecane/air partition coefficients. This gives direct account for the ability of COSMOtherm to predict vdW interactions.

Figure SI-2



The outliers are: pentanoic acid, cyclodecane, and o-cresol
 statistics (with outliers): $r^2 = 0.82$, $rmse = 0.65$ $n = 188$ with outliers
 statistics (without outliers): $r^2 = 0.93$, $rmse = 0.41$, $n = 185$)

Compound	$\log(K_{i\text{hexadecane,air}})$ [m ³ /m ³], 25 °C COSMOtherm	$\log(K_{i\text{hexadecane,air}})$ [m ³ /m ³] 25 °C <i>experimental</i>	Compound	$\log(K_{i\text{hexadecane,air}})$ [m ³ /m ³], 25 °C COSMOtherm	$\log(K_{i\text{hexadecane,air}})$ [m ³ /m ³] 25 °C <i>experimental</i>
n-Octane	3.38	3.68	Anthracene	6.63	7.57
n-Nonane	3.92	4.18	Phenanthrene	6.56	7.63
n-Decane	4.45	4.69	Biphenyl	5.78	6.01
n-Undecane	4.99	5.19	p-Terphenyl	9.01	9.69
n-Dodecane	5.52	5.70	Chlorobenzene	3.56	3.66
n-Tridecane	6.05	6.20	1,2-Dichlorobenzene	4.38	4.52
n-Tetradecane	6.59	6.71	1,3-Dichlorobenzene	4.36	4.41
Cyclodecane^{a)}	1.77	5.34	1,4-Dichlorobenzene	4.37	4.44
1-Octene	3.45	3.57	1,4-Dibromobenzene	4.83	5.32
1-Nonene	3.98	4.07	1,2-Diiodobenzene	6.82	6.40
1-Decene	4.52	4.66	1,4-Diiodobenzene	7.02	6.26
1-Undecene	5.05	5.19	1,2,4-Trichlorobenzene	5.05	5.25
1-Dodecene	5.59	5.73	1,2,3,4-Tetrachlorobenz.	5.65	6.17
1-Tridecene	6.12	6.26	1,2,3,5-Tetrachlorobenz.	5.61	5.92
Ethanol	1.42	1.49	1,2,4,5-Tetrachlorobenz.	5.65	5.93
Propan-1-ol	1.95	2.03	Pentachlorobenzene	6.13	6.72
Butan-1-ol	2.49	2.60	Hexachlorobenzene	6.56	7.62
Pentan-1-ol	3.02	3.11	Fluorobenzene	2.50	2.79
Hexan-1-ol	3.55	3.61	Bromobenzene	3.79	4.04
Heptan-1-ol	4.09	4.12	Iodobenzene	4.91	4.50
Octan-1-ol	4.62	4.62	4-Fluorotoluene	3.08	3.37
Nonan-1-ol	5.16	5.12	4-Chlorobenzotrifluoride	3.61	3.65
Decan-1-ol	5.69	5.63	1,1,1,2-Tetrachloroethane	3.79	3.64
Undecan-1-ol	6.23	6.18	1,1,2,2-Tetrachloroethane	4.05	3.80
Propan-2-ol	1.92	1.76	1-Chlorohexane	3.84	3.78
2-Methylpropan-1-ol	2.39	2.41	1-Chloroheptane	4.37	4.28
2-Methylpropan-2-ol	2.37	1.96	1-Chlorooctane	4.90	4.77
3-Methylbutan-1-ol	2.94	3.01	1-Chlorodecane	5.97	5.83
2-Ethyl-1-hexanol	4.29	4.38	1-Bromopentane	3.46	3.61
5-Hexen-1-ol	3.58	3.55	Butanal/Butyraldehyde	2.22	2.27
Benzyl alcohol	4.40	4.22	Pentanal	2.75	2.85
1-Napthol	5.63	6.13	Benzaldehyde	3.84	4.01
Cyclopentanol	3.19	3.24	1-Cyanopropane	2.58	2.55
Cyclohexanol	3.71	3.76	Aniline	3.68	3.93
2,2,2-Trifluoroethanol	1.66	1.22	2-Methylaniline	4.12	4.44
Hexafluoropropanol	0.87	1.39	4-Methylaniline	4.16	4.45
Phenol	3.60	3.77	2,6-Dimethylaniline	4.62	5.03

Compound	$\log(K_{\text{ihexadecane,air}})$ [m ³ /m ³], 25 °C COSMOtherm	$\log(K_{\text{ihexadecane,air}})$ [m ³ /m ³] 25 °C <i>experimental</i>	Compound	$\log(K_{\text{ihexadecane,air}})$ [m ³ /m ³], 25 °C COSMOtherm	$\log(K_{\text{ihexadecane,air}})$ [m ³ /m ³] 25 °C <i>experimental</i>
o-Cresol^{a)}	0.84	4.22	N,N-Dimethylaniline	4.44	4.70
m-Cresol	4.13	4.31	2-Iodoaniline	5.64	5.57
p-Cresol	4.12	4.31	4-Iodoaniline	6.37	5.70
2-Chlorophenol	3.98	4.18	Nitrobenzene	4.30	4.56
4-Chlorophenol	4.43	4.78	2-Nitrotoluene	4.56	4.88
2-Chloro-4-methylph.	4.55	4.82	2-Chlornitrobenzene	5.12	5.24
2,3-Dichlorophenol	4.74	4.99	Benzonitrile	3.96	4.04
2,6-Dichlorophenol	4.72	5.09	Acetonitrile	1.59	1.74
2,4,5-Trichlorophenol	5.31	5.73	Nitromethane	1.86	1.89
2,4,6-Trichlorophenol	5.43	5.66	Nitroethane	2.29	2.41
2-Propanone	1.98	1.70	1-Nitropropane	2.80	2.89
2-Butanone	2.38	2.29	2-Nitropropane	2.83	2.55
2-Pentanone	2.91	2.76	Pyridine	2.77	3.02
2-Hexanone	3.99	3.26	2-Methylpyridine	3.31	3.42
2-Heptanone	3.99	3.76	2-Acetylpyridine	4.40	4.48
2-Octanone	4.53	4.26	2-Methylpyrazine	3.03	3.25
2-Nonanone	5.06	4.74	Methylamine	0.61	1.30
2-Decanone	5.60	5.25	N,N-Dimethylformamide	2.87	3.72
2-Undecanone	6.13	5.73	N,N-Dimethylacetamide	3.49	3.72
3-Methylbutan-2-one	2.85	2.69	Indole (1H-Indole)	4.82	5.51
4-Methylpentan-2-one	3.31	3.09	Chinoline	4.81	5.46
Cyclopentanone	3.20	3.22	Propanoic acid	2.23	3.02
Cyclohexanone	3.83	3.79	Butanoic acid	2.76	3.47
Cycloheptanone	4.28	4.05	Pentanoic acid^{a)}	-1.01	3.97
Acetophenone	4.49	4.50	2-Methylbutanoic acid	3.23	3.25
Methyl acetate	2.11	1.91	3-Methylbutanoic acid	3.23	3.14
Ethyl acetate	2.73	2.31	1,2-Dinitrobenzene	5.96	6.00
n-Propyl acetate	3.27	2.82	1,3-Dinitrobenzene	5.60	5.85
n-Butyl acetate	3.81	3.35	1,4-Dinitrobenzene	5.33	5.90
Isobutyl acetate	3.67	3.16	2,4-Dinitrotoluene	6.01	6.49
n-Pentyl acetate	4.34	3.84	gamma-Butyrolactone	4.28	3.03
Methyl benzoate	4.73	4.70	alpha-Acetylbutyllactone	4.99	4.38
Benzyl acetate	5.46	5.01	4-Nitroanisole	5.90	5.85
2-Phenylethylacetate	6.06	5.36	Dimethylphthalate	7.01	6.05
Di-n-butyl ether	4.27	3.92	Diethylphthalate	8.08	7.06
Di-n-pentylether	5.34	4.80	Triethylphosphate	6.45	4.75
Methyl t-butyl ether	2.51	2.27	Thiophene	2.66	2.82
Tetrahydrofuran	2.46	2.64	Thiophenol	3.91	4.11
1,4-Dioxane	3.01	2.89	Dimethylsulfoxide	3.52	3.44
Benzofuran	4.00	4.36	2,4-Pentanedione	3.01	3.24
Dibenzofuran	5.91	6.72	1,2-Ethanediole	2.43	2.73
Methyl phenyl ether	3.80	3.89	Chloroacetone	2.70	2.71

Compound	$\log(K_{i\text{hexadecane,air}})$ [m ³ /m ³], 25 °C COSMOtherm	$\log(K_{i\text{hexadecane,air}})$ [m ³ /m ³] 25 °C <i>experimental</i>	Compound	$\log(K_{i\text{hexadecane,air}})$ [m ³ /m ³], 25 °C COSMOtherm	$\log(K_{i\text{hexadecane,air}})$ [m ³ /m ³] 25 °C <i>experimental</i>
Benzene	2.55	2.79	Benzoylchloride	4.65	4.52
Toluene	3.11	3.33	Hydroxyacetone	2.67	2.62
p-Xylene	3.63	3.84	Dimethyl succinate	4.70	4.13
Ethylbenzene	3.59	3.78	Lindane (gamma-HCH)	8.28	7.47
n-Propylbenzene	4.14	4.23	2-Methoxyethanol	2.32	2.49
n-Butylbenzene	4.68	4.73	2-Ethoxyethanol	2.96	2.82
n-Pentylbenzene	5.21	5.23	1,2-Naphthoquinone	6.82	6.08
n-Hexylbenzene	5.75	5.72	1,4-Naphthoquinone	5.69	6.34
1,2,4-Trimethylbenz.	4.11	4.44	2-Nitroaniline	4.97	5.63
1,3,5-Trimethylbenz.	4.18	4.34	3-Methoxybenzaldehyde	5.06	4.95
Styrene	3.59	3.86	1,4-Dimethoxybenzene	4.97	5.04
Indane	4.13	4.59	3-Hydroxybenzonitrile	5.11	5.18
Naphthalene	4.59	5.16	2-Aminobenzonitrile	4.74	5.02
1-Methylnaphthalene	5.07	5.79	4-Aminobenzonitrile	5.87	5.64
Acenaphthene	5.55	6.47	Azobenzene	6.77	7.20

^{a)} strong outliers

Note: the experimental hexadecane/air partition coefficients are referenced in SI-5

SI-7 Substance class-specific comparison of experimental Leonardite HA partition coefficients with calculated partition coefficients

Substance class-specific comparison of experimental Leonardite HA partition coefficients with calculated partition coefficients by COSMOtherm (Figure SI-3) and by SPARC (Figure SI-4). The systematic deviation of the alkanes and alkenes is discussed in the main text.

Figure SI-3 COSMOtherm

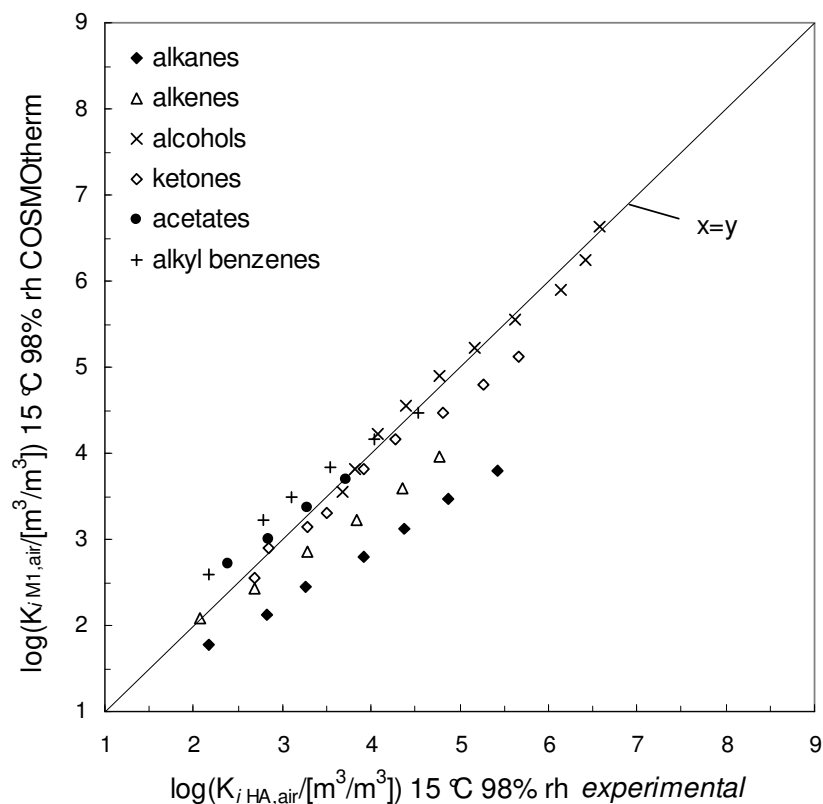
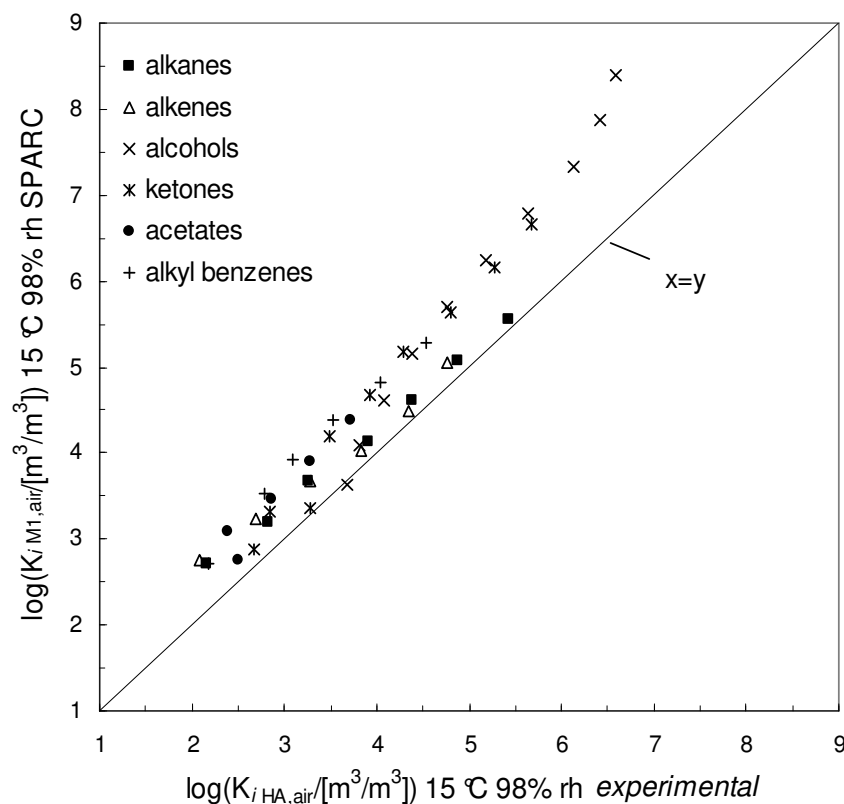


Figure SI-4 SPARC



SI-8 Calculated partition coefficients for all model monomers M1-M4

The partition coefficients have been calculated via hexadecane and corrected with c_{corr} . Partition coefficients are in (m^3/m^3).

Compound	$\log K_{\text{M1,air}}$ M1 15 °C 98% rh	$\log K_{\text{M2,air}}$ M2 15 °C 98% rh	$\log K_{\text{M3,air}}$ M3 15 °C 98% rh	$\log K_{\text{M4,air}}$ M4 15 °C 98% rh
n-Octane	1.77	1.78	1.97	1.59
n-Nonane	2.11	2.12	2.33	1.91
n-Decane	2.45	2.46	2.68	2.23
n-Undecane	2.79	2.80	3.04	2.55
n-Dodecane	3.13	3.14	3.40	2.88
n-Tridecane	3.46	3.48	3.76	3.20
n-Tetradecane	3.80	3.82	4.12	3.52
Cyclodecane	3.56	3.57	3.75	3.38
1-Octene	2.09	2.08	2.25	1.91
1-Nonene	2.43	2.42	2.61	2.23
1-Decene	2.85	2.84	3.05	2.64
1-Undecene	3.22	3.21	3.44	2.99
1-Dodecene	3.59	3.58	3.83	3.34
1-Tridecene	3.96	3.95	4.22	3.69
Ethanol	3.54	3.75	3.58	3.63
Propan-1-ol	3.83	4.03	3.89	3.89
Butan-1-ol	4.22	4.43	4.31	4.28
Pentan-1-ol	4.55	4.76	4.66	4.59
Hexan-1-ol	4.89	5.10	5.02	4.91
Heptan-1-ol	5.23	5.43	5.37	5.23
Octan-1-ol	5.55	5.75	5.71	5.53
Nonan-1-ol	5.90	6.11	6.09	5.87
Decan-1-ol	6.24	6.45	6.45	6.19
Undecan-1-ol	6.62	6.84	6.85	6.56
Propan-2-ol	3.38	3.62	3.44	3.47
2-Methylpropan-1-ol	3.70	3.83	3.77	3.71
2-Methylpropan-2-ol	3.22	3.47	3.30	3.30
3-Methylbutan-1-ol	4.55	4.75	4.64	4.58
2-Ethyl-1-hexanol	5.00	5.13	5.15	4.94
5-Hexen-1-ol	5.25	5.42	5.34	5.27
Benzyl alcohol	6.68	6.78	6.71	6.68
1-Napthol	8.54	8.16	8.52	8.20
Cyclopentanol	4.63	4.84	4.71	4.68
Cyclohexanol	4.96	5.20	5.07	5.02
2,2,2-Trifluoroethanol	3.92	3.65	3.87	3.72
Hexafluoropropanol	3.71	3.35	3.71	3.36

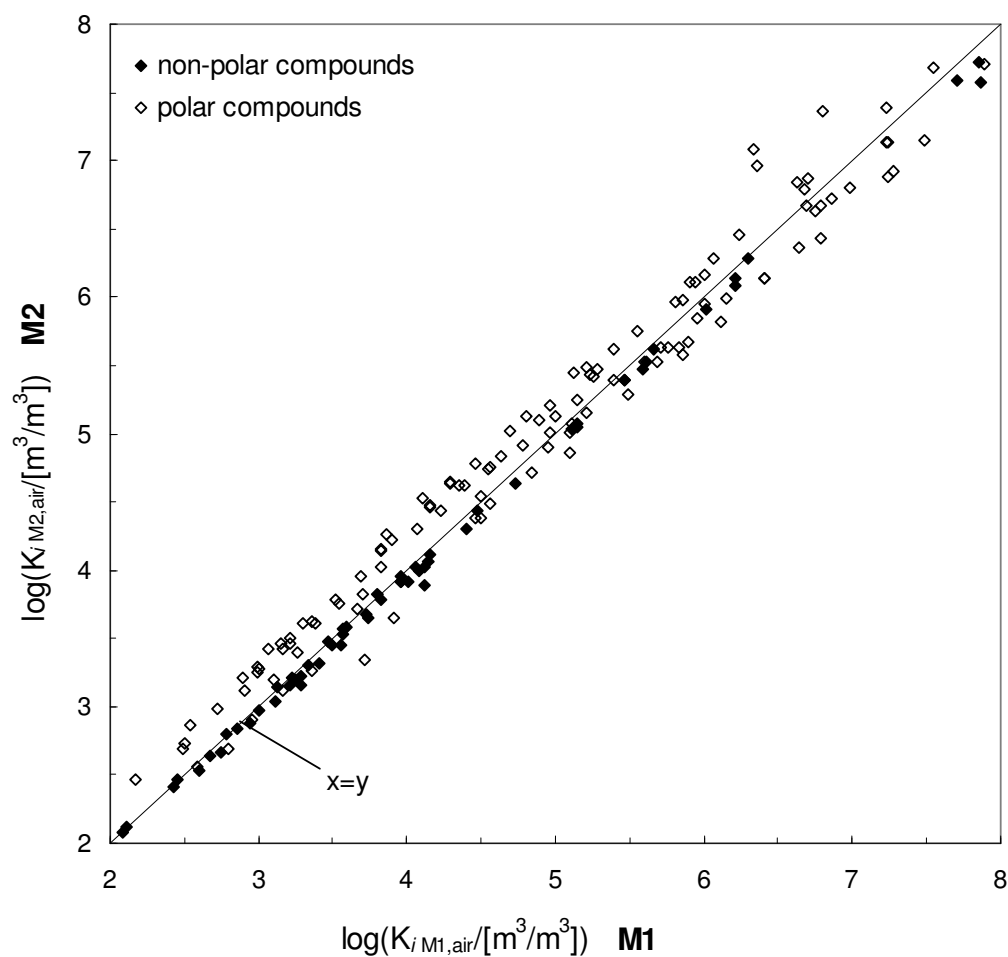
Compound	logK _{M1,air} M1 15 °C 98% rh	logK _{M2,air} M2 15 °C 98% rh	logK _{M3,air} M3 15 °C 98% rh	logK _{M4,air} M4 15 °C 98% rh
Phenol	6.12	5.82	6.09	5.87
o-Cresol	6.15	5.99	6.17	5.97
m-Cresol	6.41	6.14	6.41	6.16
p-Cresol	6.41	6.14	6.41	6.16
2-Chlorophenol	5.10	4.86	5.10	4.86
4-Chlorophenol	7.24	6.88	7.21	6.94
2-Chloro-4-methylph.	5.49	5.28	5.53	5.25
2,3-Dichlorophenol	5.86	5.58	5.88	5.58
2,6-Dichlorophenol	5.90	5.67	5.93	5.65
2,4,5-Trichlorophenol	6.79	6.43	6.83	6.44
2-Propanone	2.54	2.86	2.62	2.73
2-Butanone	2.89	3.21	2.99	3.05
2-Pentanone	3.15	3.47	3.28	3.29
2-Hexanone	3.30	3.61	3.46	3.40
2-Heptanone	3.82	4.14	3.99	3.93
2-Octanone	4.15	4.47	4.34	4.24
2-Nonanone	4.46	4.78	4.67	4.54
2-Decanone	4.80	5.12	5.03	4.86
2-Undecanone	5.12	5.45	5.37	5.16
3-Methylbutan-2-one	2.99	3.29	3.11	3.12
4-Methylpentan-2-one	3.22	3.50	3.36	3.32
Cyclopentanone	3.83	4.15	3.94	4.00
Cyclohexanone	4.29	4.65	4.43	4.46
Cycloheptanone	4.28	4.64	4.44	4.44
Acetophenone	5.29	5.47	5.37	5.33
Methyl acetate	2.50	2.73	2.56	2.63
Ethyl acetate	2.72	2.99	2.82	2.85
n-Propyl acetate	3.01	3.28	3.13	3.11
n-Butyl acetate	3.36	3.63	3.50	3.45
Isobutyl acetate	3.16	3.43	3.30	3.24
n-Pentyl acetate	3.69	3.96	3.85	3.76
Methyl benzoate	5.14	5.25	5.21	5.12
Benzyl acetate	5.80	5.96	5.88	5.83
2-Phenylethylacetate	5.94	6.11	6.04	5.96
Di-n-butyl ether	2.99	3.25	3.21	2.99
Di-n-pentylether	3.52	3.78	3.78	3.48
Methyl t-butyl ether	2.18	2.47	2.32	2.26
Tetrahydrofuran	3.07	3.42	3.19	3.22
1,4-Dioxane	3.86	4.26	3.96	4.09
Benzofuran	4.49	4.38	4.51	4.33

Compound	logK _{M1,air} M1 15 °C 98% rh	logK _{M2,air} M2 15 °C 98% rh	logK _{M3,air} M3 15 °C 98% rh	logK _{M4,air} M4 15 °C 98% rh
Dibenzofuran	6.79	6.67	6.84	6.57
Methyl phenyl ether	3.95	3.91	3.99	3.85
Benzene	2.60	2.54	2.64	2.47
Toluene	2.94	2.88	3.00	2.80
p-Xylene	3.25	3.20	3.33	3.09
Ethylbenzene	3.22	3.16	3.30	3.06
n-Propylbenzene	3.49	3.44	3.60	3.32
n-Butylbenzene	3.83	3.78	3.95	3.63
n-Pentylbenzene	4.16	4.11	4.30	3.95
n-Hexylbenzene	4.48	4.43	4.64	4.25
1,2,4-Trimethylbenz.	3.73	3.68	3.83	3.55
1,3,5-Trimethylbenz.	3.57	3.53	3.68	3.39
Styrene	3.74	3.65	3.78	3.57
Indane	3.96	3.92	4.05	3.80
Naphthalene	5.15	5.05	5.19	4.97
1-Methylnaphthalene	5.61	5.52	5.68	5.41
Acenaphthene	6.22	6.14	6.30	6.02
Anthracene	7.71	7.58	7.77	7.47
Phenanthrene	7.85	7.72	7.90	7.61
Biphenyl	6.02	5.91	6.07	5.80
p-Terphenyl	9.88	9.73	9.96	9.58
Chlorobenzene	3.40	3.32	3.45	3.26
1,2-Dichlorobenzene	4.14	4.06	4.20	3.98
1,3-Dichlorobenzene	4.01	3.92	4.07	3.84
1,4-Dichlorobenzene	4.12	4.02	4.17	3.95
1,4-Dibromobenzene	6.21	6.08	6.24	5.92
1,4-Diiodobenzene	5.58	5.48	5.65	5.42
1,2,4-Trichlorobenzene	4.73	4.63	4.80	4.54
1,2,3,4-Tetrachlorobenz.	5.46	5.39	5.57	5.27
1,2,3,5-Tetrachlorobenz.	5.11	5.04	5.22	4.90
1,2,4,5-Tetrachlorobenz.	5.14	5.07	5.25	4.94
Pentachlorobenzene	5.66	5.62	5.81	5.46
Hexachlorobenzene	6.29	6.28	6.47	6.09
Fluorobenzene	2.75	2.66	2.77	2.60
Bromobenzene	4.39	4.30	4.43	4.18
Iodobenzene	4.08	3.99	4.13	3.93
4-Fluorotoluene	3.11	3.04	3.17	2.95
4-Chlorobenzotrifluor.	3.56	3.45	3.62	3.35
1,1,1,2-Tetrachloroetha.	3.28	3.15	3.32	3.12
1,1,2,2-Tetrachloroetha.	4.12	3.89	4.11	3.91

Compound	logK _{M1,air} M1 15 °C 98% rh	logK _{M2,air} M2 15 °C 98% rh	logK _{M3,air} M3 15 °C 98% rh	logK _{M4,air} M4 15 °C 98% rh
1-Chlorohexane	2.67	2.64	2.78	2.53
1-Chloroheptane	3.01	2.98	3.14	2.85
1-Chlorooctane	3.33	3.30	3.49	3.16
1-Chlorodecane	4.05	4.03	4.25	3.85
1-Bromopentane	3.29	3.23	3.37	3.09
Butanal	2.49	2.70	2.58	2.58
Pentanal	2.90	3.12	3.01	2.98
Benzaldehyde	4.78	4.91	4.83	4.81
1-Cyanopropane	3.26	3.40	3.30	3.31
Aniline	5.68	5.53	5.62	5.54
2-Methylaniline	5.76	5.63	5.74	5.61
4-Methylaniline	5.95	5.84	5.93	5.81
2,6-Dimethylaniline	5.83	5.63	5.82	5.61
N,N-Dimethylaniline	4.56	4.49	4.61	4.41
2-Iodoaniline	6.65	6.36	6.61	6.39
4-Iodoaniline	7.27	6.92	7.20	6.99
Nitrobenzene	4.95	4.91	4.97	4.88
2-Nitrotoluene	5.11	5.07	5.14	5.02
2-Chlornitrobenzene	5.59	5.52	5.61	5.50
Benzonitrile	4.97	5.00	4.98	4.93
Acetonitrile	3.10	3.20	3.07	3.18
Nitromethane	2.80	2.69	2.72	2.78
Nitroethane	2.96	2.90	2.93	2.94
1-Nitropropane	3.16	3.11	3.16	3.12
2-Nitropropane	2.58	2.57	2.60	2.56
Pyridine	4.39	4.62	4.42	4.46
2-Methylpyridine	4.50	4.55	4.37	4.36
2-Acetylpyridine	5.40	5.61	5.47	5.47
2-Methylpyrazine	4.70	5.02	4.75	4.83
Methylamine	4.07	4.30	3.95	4.09
N,N-Dimethylformam.	6.01	5.96	5.42	5.69
N,N-Dimethylacetamid	6.34	7.09	6.48	6.74
Indole (1H-Indole)	7.48	7.15	7.43	7.20
Chinoline	6.70	6.87	6.75	6.69
Propanoic acid	5.46	5.40	5.48	5.40
Butanoic acid	5.70	5.64	5.75	5.62
Pentanoic acid	6.80	7.36	6.87	7.18
2-Methylbutanoic acid	5.21	5.16	5.28	5.11
3-Methylbutanoic acid	5.10	5.01	5.15	4.98
1,2-Dinitrobenzene	6.99	6.80	6.93	6.87

Compound	logK _{M1,air} M1 15 °C 98% rh	logK _{M2,air} M2 15 °C 98% rh	logK _{M3,air} M3 15 °C 98% rh	logK _{M4,air} M4 15 °C 98% rh
1,3-Dinitrobenzene	6.76	6.63	6.71	6.68
1,4-Dinitrobenzene	6.86	6.72	6.81	6.77
2,4-Dinitrotoluene	7.23	7.13	7.21	7.15
α -Acetylbutyllactone	6.00	6.17	6.00	6.14
4-Nitroanisole	6.68	6.67	6.69	6.64
Dimethylphthalate	7.23	7.38	7.28	7.27
Diethylphthalate	7.94	8.18	8.07	8.00
Triethylphosphate	6.36	6.97	6.54	6.69
Thiophene	3.36	3.26	3.37	3.19
Thiophenol	4.84	4.72	4.85	4.62
2,4-Pentanedione	4.35	4.62	4.40	4.52
1,2-Ethanediol	6.06	6.28	6.07	6.20
Chloroacetone	3.66	3.71	3.64	3.71
Benzoylchloride	4.46	4.38	4.50	4.32
Hydroxyacetone	4.15	4.47	4.18	4.37
Dimethyl succinate	5.21	5.49	5.27	5.37
Lindane (γ -HCH)	7.87	7.57	7.84	7.59
2-Methoxyethanol	3.90	4.23	3.98	4.07
2-Ethoxyethanol	4.11	4.53	4.21	4.31
1,2-Naphthoquinone	8.05	8.33	8.10	8.19
1,4-Naphthoquinone	7.55	7.68	7.59	7.58
2-Nitroaniline	8.10	7.94	8.06	7.96
3-Methoxybenzaldehy.	5.85	5.98	5.90	5.88
1,4-Dimethoxybenzene	5.39	5.39	5.43	5.32
3-Hydroxybenzonitrile	8.88	8.59	8.83	8.64
2-Aminobenzonitrile	7.89	7.70	7.83	7.71
4-Aminobenzonitrile	9.37	9.20	9.29	9.23
Azobenzene	7.24	7.13	7.31	7.00

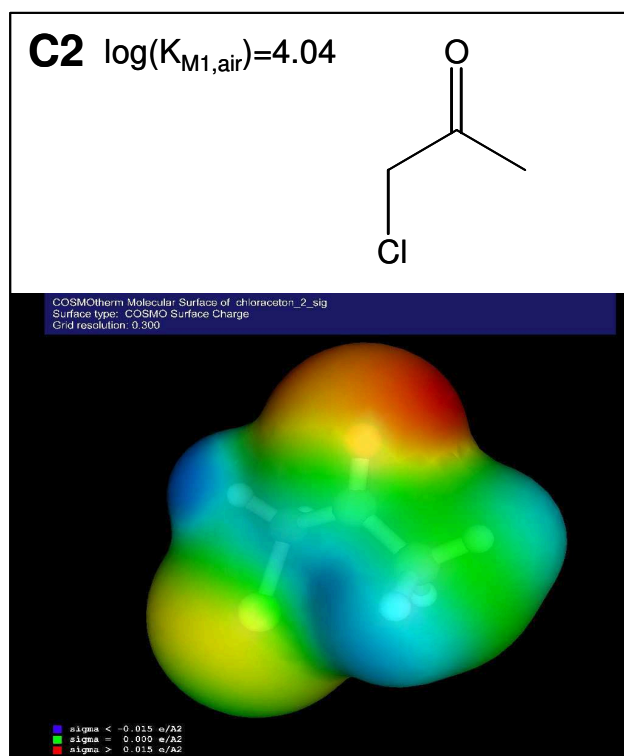
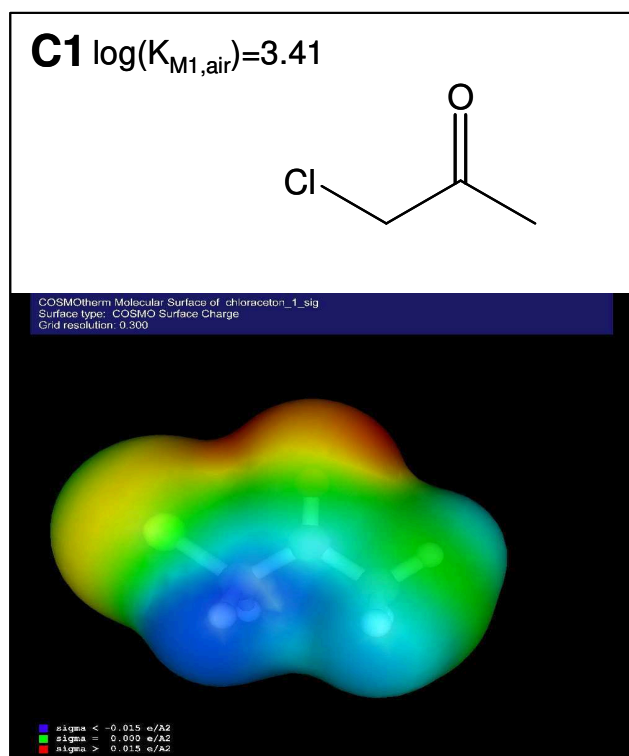
Figure SI-5 Compares calculated partition coefficients in M1 and M2. Almost all nonpolar compounds sorb more strongly into monomer M1. Polar compounds do not show a uniform pattern. An interpretation of the data is provided in the main text.



SI-9 Sorbate conformers

As discussed in the main text, COSMOtherm is able to calculate partition coefficients for individual conformers of a compound and also to calculate partition coefficients that are based on automatically Boltzmann-weighted contributions from the individual conformers. In this section differences in the calculated partition coefficients of different conformers are discussed using chloroacetone, hydroxyacetone and 2-ethoxyethanol as examples. VRML images (Virtual Reality Modeling Language) visualize COSMO surface charges of molecules by representing electron-rich (red) and electron-deficient (purple) areas in different colors.

Chloroacetone

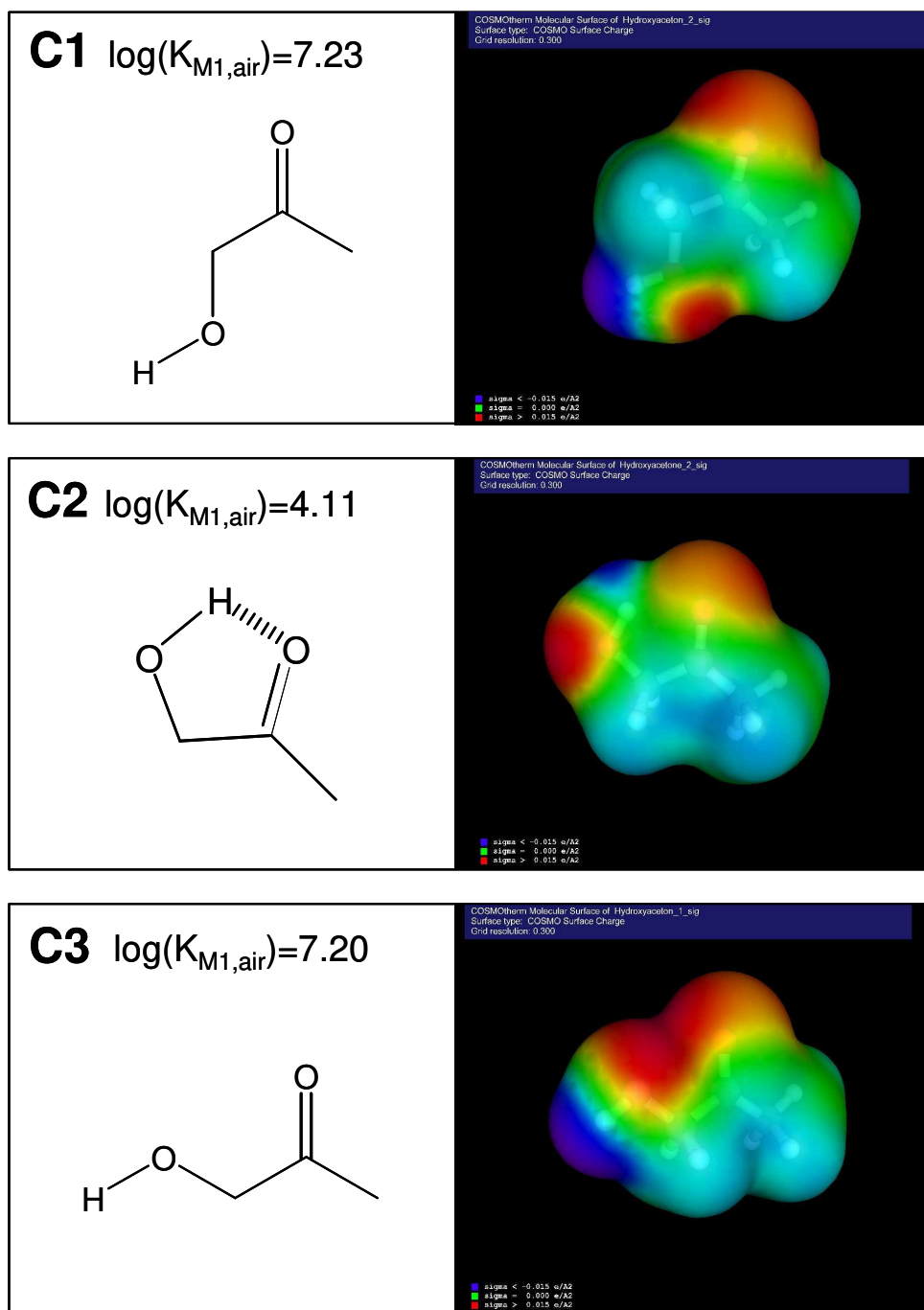


The chlorine atom has the possibility to point towards the oxygen of the keto-group (conformer C1) or into opposite direction (conformer C2). The calculated partition coefficients of C1 ($\log K_{M1,air} = 3.41$) and C2 ($\log K_{M1,air} = 4.04$) differ about 0.6 log units. VRML images that represent the COSMO surface charges of the molecules in different colors show that the H-acceptor (electron donor) domain of the keto-oxygen in C1 is

only slightly reduced by the proximity of the chlorine atoms. However, the differences in the calculated values can be due to steric effects. The *weighted* partition coefficient ($\log K_{M1,air} = 3.65$) lies in the middle of C1 and C2. This indicates that both conformers are important for the partition process. The weighted value agrees very well with the experimental partition coefficient ($\log K_{HA,air} = 3.75$).

Hydroxyacetone

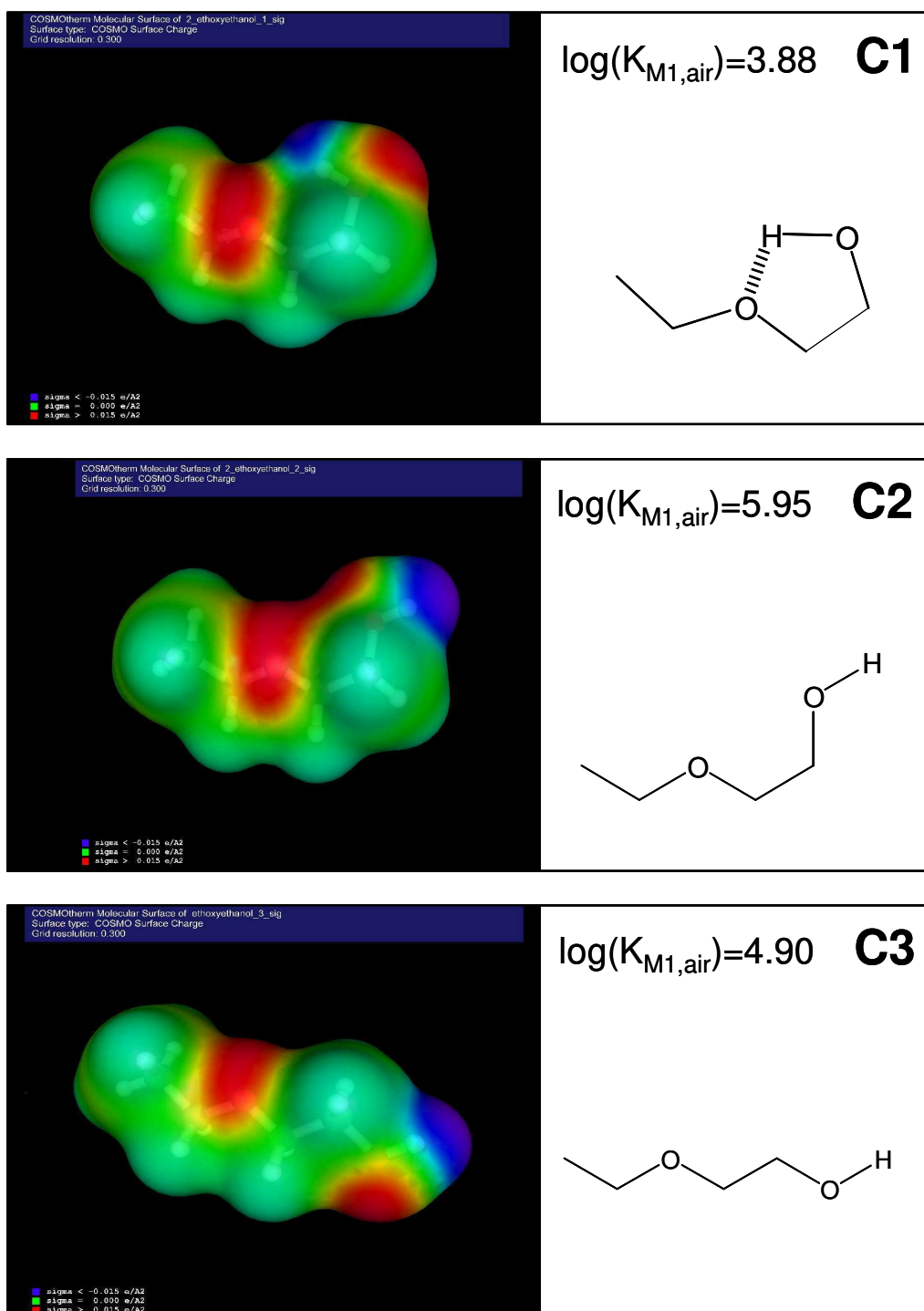
In hydroxyacetone an intramolecular H-bond between the oxygen of the keto-group and the hydroxy group can be formed (conformer C2), or the hydroxyl group can be in an opposite position to the keto-group (conformer C1). Conformer C3 represents a very unstable conformation because the lonepairs of the oxygen-atoms are very close. COSMOtherm calculations show that C3 ($\log K_{M1,air} = 7.20$) does not contribute to the weighted partition coefficient. According to the VRML image of C2, the H-donor (electron deficient) domain is substantially reduced by the presence of the intramolecular H-bond (although a 6-ring type H-bond would be more favorable compared to the 5-ring type of C2). This is reflected by the difference of more than 3 log units in the partition coefficients calculated for C1 and C2 (C1: $\log K_{M1,air} = 7.23$; C2: $\log K_{M1,air} = 4.11$). However, the weighted value ($\log K_{M1,air} = 4.14$) lies very close to C2 and underestimates the experimental value ($\log K_{HA,air} = 5.34$) by about 1.2 log units.



2-Ethoxyethanol

For 2-ethoxyethanol two stretched conformations (conformers C2/C3) and a conformation with an intramolecular H-bond between the ether and the hydroxy-group (C1) were considered. As already shown for hydroxyacetone, the electron acceptor property of C1 is substantially reduced compared to C2/C3 by the internal H-bond. This is reflected by the calculated partition coefficients: the coefficient of C1 ($\log K_{M1,air} = 3.88$)

lies about 2 log units below the partition coefficients calculated for C2 ($\log K_{M1,air} = 5.95$). The partition coefficient calculated for C3 ($\log K_{M1,air} = 4.90$) corresponds exactly to the experimental value ($\log K_{HA,air}=4.94$). The weighted value ($\log K_{M1,air} = 4.12$) lies about 0.2 log units above the partition coefficient of C1, but 0.8 log units below the experimental value.

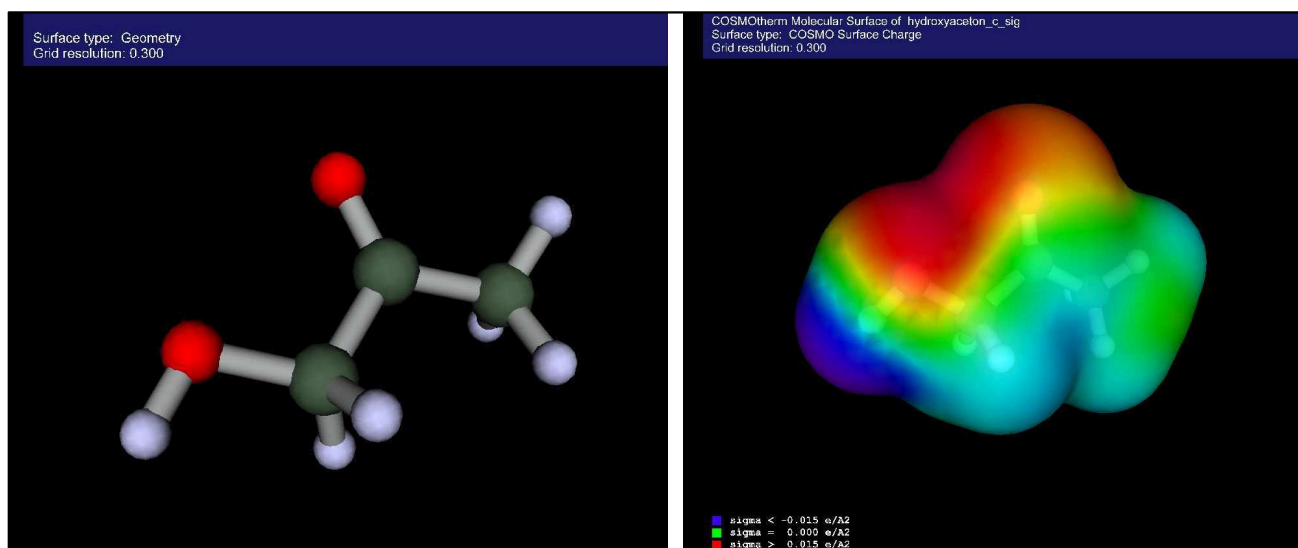


Conformers: concluding remarks

The three examples discussed above show that the sorption properties of different conformers of one compound can differ substantially. The prediction of the partition coefficients of chloroacetone and hydroxyacetone can be improved by considering different conformers compared to calculations that are based on only one conformer. However, for ethoxyethanol and hydroxyacetone which both exhibit conformers with intramolecular H-bonds, the weighted partition coefficients are nevertheless too low compared to the experimental values. A possible explanation is that COSMOtherm overpredicts the probability of the formation of intramolecular H-bonds in the polar environment provided by the humic acid.

The discussion above points at a specific problem: If only one single conformer is given as input, severe prediction errors may occur. As an example we refer to conformer C3 of hydroxyacetone: The image on the left side below shows a 3D image of hydroxyacetone as it is given as output from the 3D structure generation tool CORINA (V3.4, Molecular Networks GmbH, <http://www.mol-net.de>). As discussed above, the structure is a very unlikely conformation and the calculated partition coefficient lies two orders of magnitude above the experimental value. Consequently, without an accurate review of the input structures, e.g., when a list of chemicals is processed batch-wise and/or only one conformer is used as input, erroneous partition coefficients may be predicted.

¹because the lonepairs of the oxygen atoms are very close (also shown in the VRML image on the right side).



SI-10 Calculated M1/air partition coefficients at different relative humidities

The humic acid phase in equilibrium with a given relative humidity has been simulated as M1/H₂O mixture and corrected with c_{corr} . See SI-4 for phase diagrams and further information. Partition coefficients are in [m³/m³].

Compound	logK _{M1,air}	logK _{M1,air}	logK _{M1,air}	logK _{M1,air}
	15 °C 0% rh	15 °C 45% rh	15 °C 70% rh	15 °C 98% rh
n-Octane	1.78	1.81	1.81	1.77
n-Nonane	2.14	2.17	2.16	2.11
n-Decane	2.51	2.53	2.51	2.45
n-Undecane	2.88	2.89	2.86	2.79
n-Dodecane	3.24	3.24	3.22	3.13
n-Tridecane	3.61	3.60	3.57	3.46
n-Tetradecane	3.98	3.96	3.92	3.80
Cyclodecane	3.54	3.58	3.59	3.56
1-Octene	2.08	2.12	2.12	2.09
1-Nonene	2.45	2.48	2.48	2.43
1-Decene	2.91	2.93	2.91	2.85
1-Undecene	3.30	3.31	3.29	3.22
1-Dodecene	3.70	3.70	3.68	3.59
1-Tridecene	4.10	4.09	4.06	3.96
Ethanol	3.37	3.43	3.47	3.54
Propan-1-ol	3.67	3.72	3.76	3.83
Butan-1-ol	4.09	4.14	4.17	4.22
Pentan-1-ol	4.45	4.49	4.51	4.55
Hexan-1-ol	4.82	4.85	4.87	4.89
Heptan-1-ol	5.18	5.20	5.21	5.23
Octan-1-ol	5.53	5.54	5.55	5.55
Nonan-1-ol	5.92	5.92	5.92	5.90
Decan-1-ol	6.28	6.28	6.26	6.24
Undecan-1-ol	6.69	6.68	6.66	6.62
Propan-2-ol	3.25	3.29	3.32	3.38
2-Methylpropan-1-ol	3.52	3.59	3.63	3.70
2-Methylpropan-2-ol	3.12	3.15	3.18	3.22
3-Methylbutan-1-ol	4.45	4.48	4.51	4.55
2-Ethyl-1-hexanol	4.93	4.97	4.99	5.00
5-Hexen-1-ol	5.17	5.20	5.22	5.25
Benzyl alcohol	6.57	6.61	6.64	6.68
1-Napthol	8.30	8.41	8.47	8.54

Compound	logK _{M1,air}	logK _{M1,air}	logK _{M1,air}	logK _{M1,air}
	15 °C 0% rh	15 °C 45% rh	15 °C 70% rh	15 °C 98% rh
Cyclopentanol	4.52	4.56	4.59	4.63
Cyclohexanol	4.85	4.89	4.92	4.96
2,2,2-Trifluoroethanol	3.55	3.70	3.79	3.92
Hexafluoropropan-2-ol	3.40	3.54	3.62	3.71
Phenol	5.79	5.93	6.01	6.12
o-Cresol	5.89	6.00	6.07	6.15
m-Cresol	6.12	6.25	6.32	6.41
p-Cresol	6.11	6.24	6.32	6.41
2-Chlorophenol	4.88	4.98	5.04	5.10
4-Chlorophenol	6.92	7.06	7.14	7.24
2-Chloro-4-methylphenol	5.31	5.40	5.45	5.49
2,3-Dichlorophenol	5.64	5.75	5.80	5.86
2,6-Dichlorophenol	5.74	5.83	5.86	5.90
2,4,5-Trichlorophenol	6.52	6.64	6.71	6.79
2-Propanone	2.31	2.41	2.46	2.54
2-Butanone	2.69	2.78	2.82	2.89
2-Pentanone	2.98	3.06	3.10	3.15
2-Hexanone	3.19	3.24	3.27	3.30
2-Heptanone	3.71	3.77	3.80	3.82
2-Octanone	4.07	4.12	4.14	4.15
2-Nonanone	4.41	4.45	4.46	4.46
2-Decanone	4.78	4.81	4.82	4.80
2-Undecanone	5.13	5.15	5.15	5.12
3-Methylbutan-2-one	2.81	2.89	2.93	2.99
4-Methylpentan-2-one	3.07	3.14	3.17	3.22
Cyclopentanone	3.62	3.70	3.75	3.83
Cyclohexanone	4.11	4.19	4.23	4.29
Cycloheptanone	4.13	4.20	4.23	4.28
Acetophenone	5.16	5.23	5.26	5.29
Methyl acetate	2.27	2.37	2.42	2.50
Ethyl acetate	2.52	2.61	2.66	2.72
n-Propyl acetate	2.83	2.92	2.96	3.01
n-Butyl acetate	3.22	3.29	3.33	3.36
Isobutyl acetate	3.01	3.09	3.12	3.16
n-Pentyl acetate	3.57	3.64	3.66	3.69
Methyl benzoate	5.03	5.10	5.13	5.14
Benzyl acetate	5.71	5.77	5.79	5.80
2-Phenylethylacetate	5.87	5.93	5.94	5.94
Di-n-butyl ether	3.00	3.02	3.02	2.99
Di-n-pentylether	3.58	3.58	3.57	3.52

Compound	logK _{M1,air}	logK _{M1,air}	logK _{M1,air}	logK _{M1,air}
	15 °C 0% rh	15 °C 45% rh	15 °C 70% rh	15 °C 98% rh
Methyl tert-butyl ether	2.12	2.15	2.16	2.18
Tetrahydrofuran	2.97	3.01	3.03	3.07
1,4-Dioxane	3.68	3.75	3.79	3.86
Benzofuran	4.44	4.49	4.51	4.49
Dibenzofuran	6.82	6.84	6.84	6.79
Methyl phenyl ether	3.87	3.93	3.95	3.95
Benzene	2.50	2.57	2.59	2.60
Toluene	2.87	2.93	2.94	2.94
p-Xylene	3.20	3.25	3.26	3.25
Ethylbenzene	3.17	3.22	3.23	3.22
n-Propylbenzene	3.48	3.52	3.52	3.49
n-Butylbenzene	3.84	3.87	3.87	3.83
n-Pentylbenzene	4.20	4.22	4.21	4.16
n-Hexylbenzene	4.55	4.56	4.55	4.48
1,2,4-Trimethylbenzene	3.70	3.75	3.75	3.73
1,3,5-Trimethylbenzene	3.55	3.59	3.60	3.57
Styrene	3.69	3.75	3.76	3.74
Indane	3.92	3.97	3.98	3.96
Naphthalene	5.12	5.17	5.17	5.15
1-Methylnaphthalene	5.61	5.64	5.64	5.61
Acenaphthene	6.22	6.26	6.25	6.22
Anthracene	7.76	7.78	7.77	7.71
Phenanthrene	7.90	7.92	7.91	7.85
Biphenyl	6.04	6.07	6.06	6.02
p-Terphenyl	10.03	10.02	9.99	9.88
Chlorobenzene	3.33	3.39	3.41	3.40
1,2-Dichlorobenzene	4.09	4.14	4.16	4.14
1,3-Dichlorobenzene	3.97	4.02	4.03	4.01
1,4-Dichlorobenzene	4.08	4.12	4.13	4.12
1,4-Dibromobenzene	6.24	6.26	6.26	6.21
1,4-Diiodobenzene	5.58	5.62	5.62	5.58
1,2,4-Trichlorobenzene	4.70	4.75	4.75	4.73
1,2,3,4-Tetrachlorobenz.	5.46	5.49	5.50	5.46
1,2,3,5-Tetrachlorobenz.	5.11	5.14	5.14	5.11
1,2,4,5-Tetrachlorobenz.	5.14	5.18	5.18	5.14
Pentachlorobenzene	5.68	5.71	5.71	5.66
Hexachlorobenzene	6.32	6.35	6.34	6.29
Fluorobenzene	2.66	2.72	2.74	2.75
Bromobenzene	4.36	4.41	4.42	4.39
Iodobenzene	4.02	4.08	4.09	4.08

Compound	logK _{M1,air}	logK _{M1,air}	logK _{M1,air}	logK _{M1,air}
	15 °C 0% rh	15 °C 45% rh	15 °C 70% rh	15 °C 98% rh
4-Fluorotoluene	3.06	3.11	3.12	3.11
4-Chlorobenzotrifluoride	3.54	3.59	3.59	3.56
1,1,1,2-Tetrachloroethane	3.21	3.27	3.28	3.28
1,1,2,2-Tetrachloroethane	4.04	4.10	4.12	4.12
1-Chlorohexane	2.63	2.68	2.69	2.67
1-Chloroheptane	3.00	3.04	3.04	3.01
1-Chlorooctane	3.35	3.38	3.38	3.33
1-Chlorodecane	4.13	4.14	4.13	4.05
1-Bromopentane	3.26	3.31	3.31	3.29
Butanal/Butyraldehyde	2.28	2.37	2.42	2.49
Pentanal	2.72	2.81	2.85	2.90
Benzaldehyde	4.62	4.70	4.74	4.78
1-Cyanopropane	3.06	3.15	3.20	3.26
Aniline	5.56	5.63	5.66	5.68
2-Methylaniline	5.66	5.72	5.75	5.76
4-Methylaniline	5.87	5.92	5.94	5.95
2,6-Dimethylaniline	5.76	5.82	5.84	5.83
N,N-Dimethylaniline	4.52	4.57	4.58	4.56
2-Iodoaniline	6.56	6.62	6.64	6.65
4-Iodoaniline	7.18	7.24	7.27	7.27
Nitrobenzene	4.86	4.92	4.95	4.95
2-Nitrotoluene	5.03	5.09	5.11	5.11
2-Chlornitrobenzene	5.52	5.58	5.60	5.59
Benzonitrile	4.83	4.91	4.94	4.97
Acetonitrile	2.84	2.95	3.02	3.10
Nitromethane	2.60	2.70	2.74	2.80
Nitroethane	2.78	2.87	2.92	2.96
1-Nitropropane	3.01	3.10	3.13	3.16
2-Nitropropane	2.43	2.52	2.55	2.58
Pyridine	4.38	4.39	4.39	4.39
2-Methylpyridine	4.34	4.35	4.34	4.50
2-Acetylpyridine	5.25	5.32	5.36	5.40
2-Methylpyrazine	4.65	4.67	4.68	4.70
Methylamine	4.18	4.14	4.11	4.07
N,N-Dimethylformamide	5.22	5.23	5.24	6.01
N,N-Dimethylacetamide	6.42	6.37	6.34	6.34
Indole (1H-Indole)	7.34	7.42	7.45	7.48
Chinoline	6.73	6.74	6.73	6.70
Propanoic acid	5.02	5.19	5.30	5.46
Butanoic acid	5.29	5.46	5.56	5.70

Compound	logK _{M1,air}	logK _{M1,air}	logK _{M1,air}	logK _{M1,air}
	15 °C 0% rh	15 °C 45% rh	15 °C 70% rh	15 °C 98% rh
Pentanoic acid	6.62	6.68	6.72	6.80
2-Methylbutanoic acid	4.83	4.98	5.08	5.21
3-Methylbutanoic acid	4.72	4.87	4.97	5.10
1,2-Dinitrobenzene	6.95	7.00	7.01	6.99
1,3-Dinitrobenzene	6.70	6.75	6.77	6.76
1,4-Dinitrobenzene	6.80	6.85	6.87	6.86
2,4-Dinitrotoluene	7.18	7.23	7.24	7.23
alpha-Acetylbutyllactone	5.77	5.88	5.93	6.00
4-Nitroanisole	6.59	6.66	6.68	6.68
Dimethylphthalate	7.12	7.19	7.21	7.23
Diethylphthalate	7.86	7.92	7.94	7.94
Triethylphosphate	6.29	6.31	6.33	6.36
Thiophene	3.27	3.33	3.35	3.36
Thiophenol	4.80	4.85	4.86	4.84
2,4-Pentanedione	4.10	4.21	4.27	4.35
1,2-Ethanediol	5.81	5.88	5.94	6.06
Chloroacetone	3.46	3.55	3.60	3.66
Benzoylchloride	4.41	4.46	4.47	4.46
Hydroxyacetone	3.95	4.03	4.08	4.15
Dimethyl succinate	5.01	5.11	5.15	5.21
Lindane (gamma-HCH)	7.89	7.92	7.92	7.87
2-Methoxyethanol	3.75	3.80	3.84	3.90
2-Ethoxyethanol	4.02	4.05	4.07	4.11
1,2-Naphthoquinone	7.94	8.00	8.02	8.05
1,4-Naphthoquinone	7.40	7.48	7.51	7.55
2-Nitroaniline	7.89	7.99	8.04	8.10
3-Methoxybenzaldehyde	5.72	5.80	5.83	5.85
1,4-Dimethoxybenzene	5.31	5.37	5.39	5.39
3-Hydroxybenzonitrile	8.46	8.63	8.74	8.88
2-Aminobenzonitrile	7.68	7.78	7.83	7.89
4-Aminobenzonitrile	9.13	9.24	9.30	9.37
Azobenzene	7.30	7.32	7.30	7.24

Figure SI-6 to SI-9

Figure SI-6 compares experimental HA/air partition coefficients measured at <0.01% and 98% rh (ref mentioned below). Figure SI-7 compares calculated HA/air partition coefficients at 0% and 98% rh. The sorption behavior of polar and nonpolar substances is discussed in the main text. Figure SI-8 and SI-9 show the same plots as Figure SI-7 and SI-8 but only for the compounds classes alkanes, ketones, and alcohols. The slopes of the trendlines are <1 indicating that with increasing chainlength the substances of nonpolar as well as polar compounds prefer more and more the dry phase. This effect can be predicted by COSMOtherm, but the extent of the effect is higher in the experimental data. A detailed interpretation of the effect is provided in:

Niederer, C., Goss, K.-U., Schwarzenbach, R.P. Sorption Equilibrium of a Wide Spectrum of Organic Vapors in Leonardite Humic Acid: Experimental Setup and Experimental Data. *Environ. Sci. Technol.* **2006**, pp. 5368-5373.

Figure SI-6 Experimental

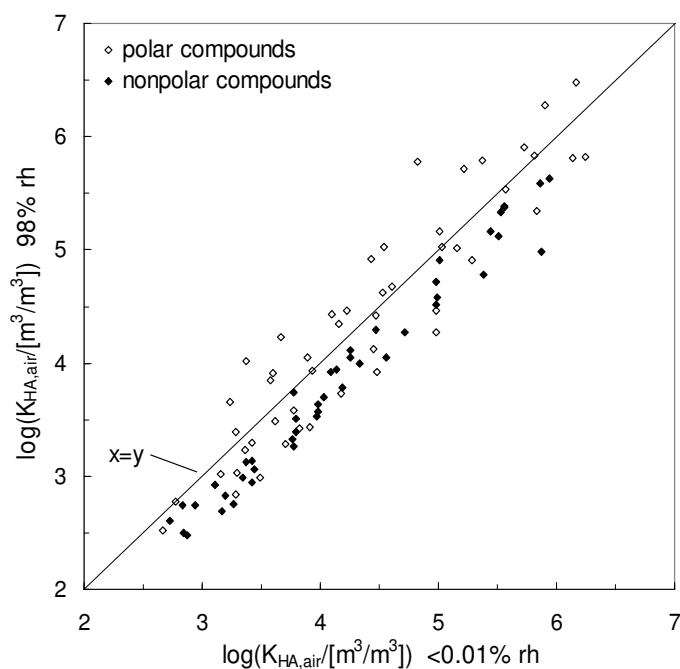


Figure SI-7 COSMOtherm

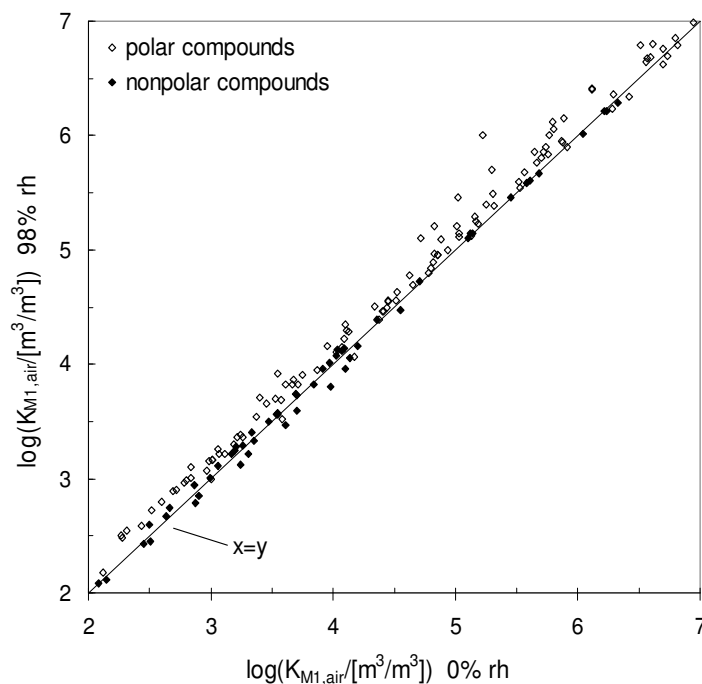


Figure SI-8

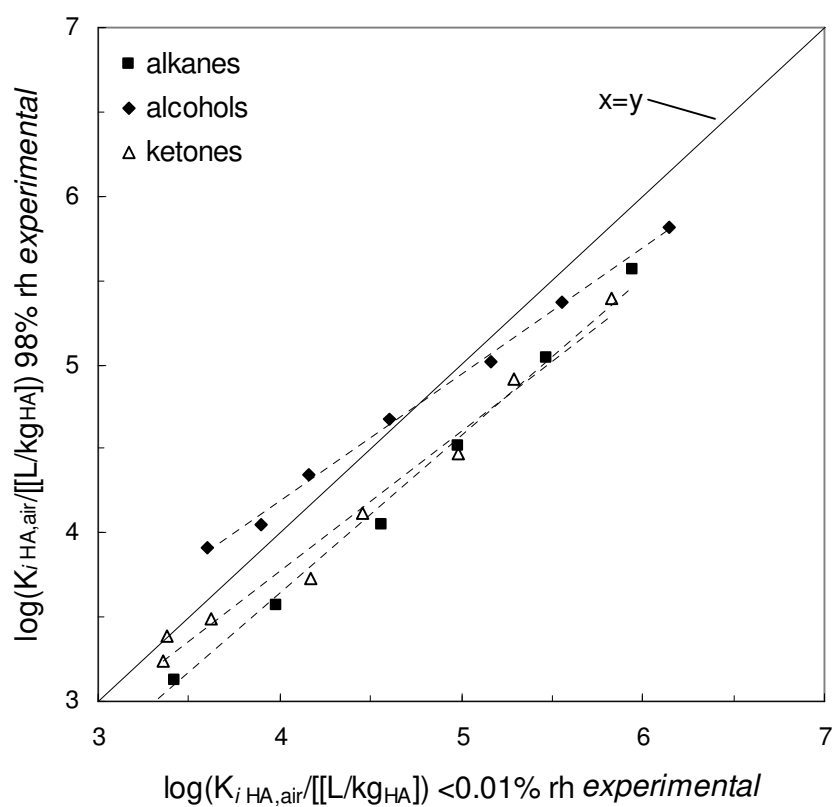
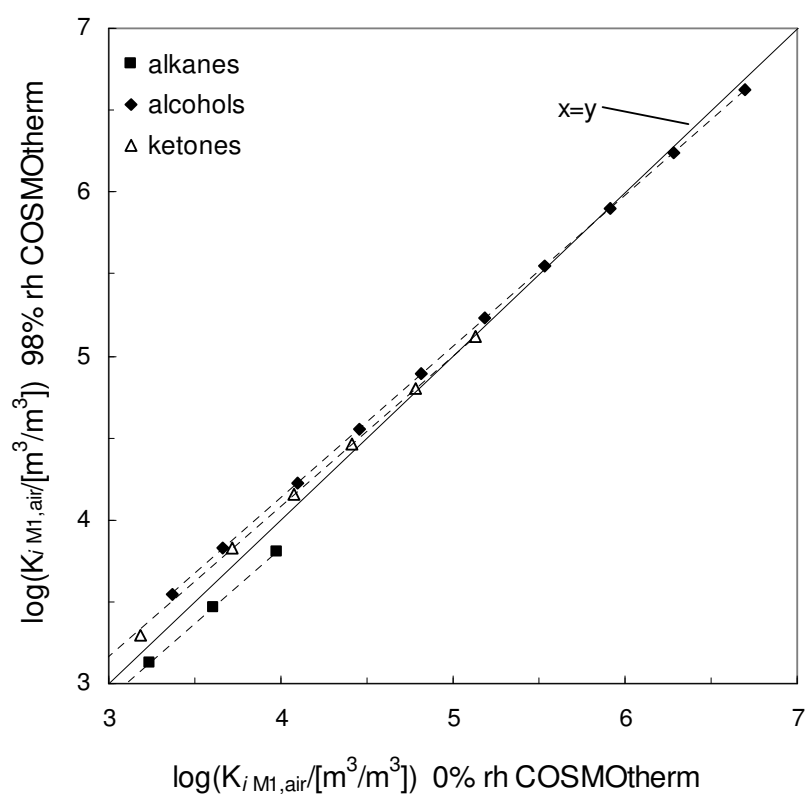


Figure SI-9



SI-11 Calculated partition coefficients at 15 °C - 55 °C

Simulations have been conducted with M1 at 98% rh, via hexadecane and linear correction. Partition coefficients are in (m³/m³).

Compound	logK _{M1,air} 15 °C 98% rh COSMOt.	logK _{M1,air} 25 °C 98% rh COSMOt.	logK _{M1,air} 35 °C 98% rh COSMOt.	logK _{M1,air} 45 °C 98% rh COSMOt.	logK _{M1,air} 55 °C 98% rh COSMOt.	logK _{M1,air} $\Delta_{\text{abs}}H_i$ COSMOt.	logK _{M1,air} $\Delta_{\text{abs}}H_i$ <i>experiment.</i>
n-Octane	1.77	1.59	1.42	1.25	1.09	-33.4	
n-Nonane	2.11	1.91	1.72	1.53	1.36	-36.9	
n-Decane	2.45	2.23	2.02	1.81	1.62	-40.4	-46.4
n-Undecane	2.79	2.55	2.32	2.09	1.88	-43.9	-62.8
n-Dodecane	3.13	2.87	2.62	2.37	2.14	-47.4	-64.1
n-Tridecane	3.46	3.19	2.92	2.65	2.40	-50.9	-59.6
n-Tetradecane	3.80	3.51	3.22	2.93	2.66	-54.4	-78.4
Cyclodecane	3.56	3.28	3.02	2.76	2.53	-49.5	-51.2
1-Octene	2.09	1.90	1.71	1.53	1.36	-35.6	
1-Nonene	2.43	2.22	2.01	1.81	1.63	-39.1	
1-Decene	2.85	2.62	2.38	2.16	1.95	-43.4	-43.5
1-Undecene	3.22	2.97	2.71	2.46	2.24	-47.1	-54.2
1-Dodecene	3.59	3.31	3.04	2.77	2.53	-50.9	-60.3
1-Tridecene	3.96	3.66	3.37	3.08	2.81	-54.7	-67.2
Ethanol	3.54	3.19	2.87	2.60	2.34	-56.7	-42.3
Propan-1-ol	3.83	3.46	3.13	2.84	2.57	-59.2	-43.2
Butan-1-ol	4.22	3.83	3.48	3.17	2.88	-63.2	-58.4
Pentan-1-ol	4.55	4.14	3.78	3.44	3.14	-66.6	-61.2
Hexan-1-ol	4.89	4.47	4.08	3.73	3.40	-70.1	-65.3
Heptan-1-ol	5.23	4.78	4.37	4.00	3.66	-73.6	-68.6

Compound	logK _{M1,air} 15 °C 98% rh COSMOt.	logK _{M1,air} 25 °C 98% rh COSMOt.	logK _{M1,air} 35 °C 98% rh COSMOt.	logK _{M1,air} 45 °C 98% rh COSMOt.	logK _{M1,air} 55 °C 98% rh COSMOt.	logK _{M1,air} $\Delta_{\text{abs}}H_i$ COSMOt.	logK _{M1,air} $\Delta_{\text{abs}}H_i$ <i>experiment.</i>
Octan-1-ol	5.55	5.08	4.66	4.27	3.91	-76.8	-75.8
Nonan-1-ol	5.90	5.42	4.97	4.56	4.18	-80.6	-83.5
Decan-1-ol	6.24	5.74	5.27	4.84	4.44	-84.0	-79.2
Undecan-1-ol	6.62	6.10	5.61	5.16	4.74	-88.0	-73.8
Propan-2-ol	3.38	3.04	2.74	2.47	2.23	-54.6	-53.3
2-Methylpropan-1-ol	3.70	3.34	3.03	2.75	2.49	-57.0	-60.1
2-Methylpropan-2-ol	3.22	2.89	2.60	2.34	2.10	-52.9	-44.9
3-Methylbutan-1-ol	4.55	4.14	3.77	3.44	3.13	-66.6	-63.5
2-Ethyl-1-hexanol	5.00	4.58	4.19	3.84	3.51	-69.9	-78.2
5-Hexen-1-ol	5.25	4.81	4.41	4.04	3.71	-72.5	-66.1
Benzyl alcohol	6.68	6.16	5.69	5.27	4.88	-84.0	-68.9
1-Naphthol	8.54	7.93	7.37	6.86	6.39	-100.1	-92.1
Cyclopentanol	4.63	4.22	3.85	3.52	3.21	-66.5	-57.4
Cyclohexanol	4.96	4.54	4.15	3.81	3.49	-69.0	-62.1
2,2,2-Trifluoroethanol	3.92	3.56	3.25	2.98	2.72	-56.5	-40.8
Hexafluoropropan-2-ol	3.71	3.35	3.03	2.75	2.49	-57.6	-61.2
Phenol	6.12	5.64	5.21	4.83	4.47	-77.0	-65.1
o-Cresol (2-Methylphenol)	6.15	5.67	5.24	4.86	4.49	-77.5	-67.0
m-Cresol (3-Methylphenol)	6.41	5.92	5.48	5.08	4.70	-79.9	-74.4
p-Cresol (4-Methylphenol)	6.41	5.91	5.47	5.07	4.69	-79.9	-75.1
2-Chlorophenol	5.10	4.69	4.32	3.99	3.68	-66.7	-60.9
4-Chlorophenol	7.24	6.69	6.20	5.76	5.34	-88.2	-83.9
2-Chloro-4-methylphenol	5.49	5.06	4.68	4.32	3.99	-70.5	-53.4
2,3-Dichlorophenol	5.86	5.40	4.98	4.61	4.25	-75.0	-63.2

Compound	logK _{M1,air} 15 °C 98% rh COSMOt.	logK _{M1,air} 25 °C 98% rh COSMOt.	logK _{M1,air} 35 °C 98% rh COSMOt.	logK _{M1,air} 45 °C 98% rh COSMOt.	logK _{M1,air} 55 °C 98% rh COSMOt.	logK _{M1,air} $\Delta_{\text{abs}}H_i$ COSMOt.	logK _{M1,air} $\Delta_{\text{abs}}H_i$ <i>experiment.</i>
2,6-Dichlorophenol	5.90	5.45	5.05	4.67	4.33	-73.6	-48.2
2,4,5-Trichlorophenol	6.79	6.25	5.77	5.33	4.92	-87.1	-121.7
2-Propanone	2.54	2.31	2.10	1.92	1.75	-38.4	
2-Butanone	2.89	2.63	2.40	2.20	2.01	-42.2	
2-Pentanone	3.15	2.88	2.63	2.42	2.21	-45.0	-43.3
2-Hexanone	3.30	3.02	2.76	2.53	2.31	-47.2	-49.6
2-Heptanone	3.82	3.51	3.23	2.97	2.73	-52.0	-54.5
2-Octanone	4.15	3.82	3.52	3.24	2.99	-55.4	-56.1
2-Nonanone	4.46	4.12	3.80	3.50	3.22	-58.6	-64.4
2-Decanone	4.80	4.44	4.10	3.78	3.49	-62.2	-68.5
2-Undecanone	5.12	4.74	4.38	4.05	3.73	-65.5	-78.6
3-Methylbutan-2-one	2.99	2.73	2.49	2.29	2.09	-43.1	-33.7
4-Methylpentan-2-one	3.22	2.94	2.69	2.47	2.26	-45.8	-41.9
Cyclopentanone	3.83	3.52	3.24	3.00	2.77	-50.3	-48.2
Cyclohexanone	4.29	3.95	3.65	3.38	3.12	-55.4	-50.5
Cycloheptanone	4.28	3.95	3.64	3.36	3.11	-55.8	-51.6
Acetophenone	5.29	4.91	4.56	4.24	3.94	-63.3	-59.2
Methyl acetate	2.50	2.27	2.07	1.90	1.74	-36.9	
Ethyl acetate	2.72	2.48	2.27	2.08	1.90	-39.7	
n-Propyl acetate	3.01	2.75	2.52	2.31	2.12	-42.8	
n-Butyl acetate	3.36	3.09	2.84	2.61	2.39	-46.4	-49.3
Isobutyl acetate	3.16	2.89	2.65	2.43	2.23	-44.7	-40.8
n-Pentyl acetate	3.69	3.39	3.12	2.87	2.64	-49.8	-57.0
Methyl benzoate	5.14	4.78	4.44	4.13	3.84	-61.5	-57.0

Compound	logK _{M1,air} 15 °C 98% rh COSMOt.	logK _{M1,air} 25 °C 98% rh COSMOt.	logK _{M1,air} 35 °C 98% rh COSMOt.	logK _{M1,air} 45 °C 98% rh COSMOt.	logK _{M1,air} 55 °C 98% rh COSMOt.	logK _{M1,air} $\Delta_{\text{abs}}H_i$ COSMOt.	logK _{M1,air} $\Delta_{\text{abs}}H_i$ <i>experiment.</i>
Benzyl acetate	5.80	5.40	5.03	4.69	4.37	-67.4	-57.7
2-Phenylethylacetate	5.94	5.53	5.15	4.79	4.46	-69.3	-73.6
Di-n-butyl ether	2.99	2.72	2.47	2.23	2.01	-47.2	-51.4
Di-n-pentylether	3.52	3.22	2.93	2.66	2.41	-52.8	-61.1
Methyl tert-butyl ether /	2.18	1.94	1.73	1.54	1.36	-39.6	
Tetrahydrofuran	3.07	2.79	2.53	2.30	2.09	-46.9	
1,4-Dioxane	3.86	3.54	3.25	2.99	2.75	-52.6	-44.9
Benzofuran	4.49	4.17	3.87	3.59	3.33	-55.3	-55.5
Dibenzofuran	6.79	6.35	5.92	5.52	5.15	-76.8	-50.5
Methyl phenyl ether	3.95	3.66	3.39	3.14	2.90	-50.1	-46.7
Benzene	2.60	2.38	2.18	1.99	1.82	-37.8	
Toluene	2.94	2.71	2.48	2.28	2.08	-41.4	
p-Xylene	3.25	2.99	2.75	2.53	2.32	-44.6	
Ethylbenzene	3.22	2.96	2.73	2.50	2.29	-44.3	
n-Propylbenzene	3.49	3.23	2.97	2.73	2.51	-47.3	-51.3
n-Butylbenzene	3.83	3.54	3.27	3.01	2.77	-50.7	-48.1
n-Pentylbenzene	4.16	3.86	3.56	3.28	3.02	-54.2	-56.7
n-Hexylbenzene	4.48	4.16	3.85	3.54	3.27	-57.5	-66.1
1,2,4-Trimethylbenzene	3.73	3.45	3.18	2.93	2.69	-49.3	-47.1
1,3,5-Trimethylbenzene	3.57	3.30	3.04	2.79	2.57	-48.0	-43.7
Styrene	3.74	3.46	3.20	2.95	2.72	-48.6	-30.2
Indane	3.96	3.67	3.39	3.13	2.89	-51.2	-32.9
Naphthalene	5.15	4.79	4.46	4.14	3.85	-61.5	-54.7
1-Methylnaphthalene	5.61	5.23	4.87	4.52	4.21	-66.1	-76.9

Compound	logK _{M1,air} 15 °C 98% rh COSMOt.	logK _{M1,air} 25 °C 98% rh COSMOt.	logK _{M1,air} 35 °C 98% rh COSMOt.	logK _{M1,air} 45 °C 98% rh COSMOt.	logK _{M1,air} 55 °C 98% rh COSMOt.	logK _{M1,air} $\Delta_{\text{abs}}H_i$ COSMOt.	logK _{M1,air} $\Delta_{\text{abs}}H_i$ <i>experiment.</i>
Acenaphthene	6.22	5.80	5.41	5.04	4.69	-71.6	-59.3
Anthracene	7.71	7.22	6.75	6.30	5.88	-85.3	-79.6
Phenanthrene	7.85	7.35	6.87	6.42	6.00	-86.5	-79.0
Biphenyl	6.02	5.62	5.23	4.87	4.53	-69.7	-68.9
p-Terphenyl	9.88	9.27	8.69	8.13	7.61	-105.7	-98.7
Chlorobenzene	3.40	3.14	2.90	2.67	2.45	-45.6	-27.4
1,2-Dichlorobenzene	4.14	3.84	3.55	3.28	3.03	-52.8	-53.3
1,3-Dichlorobenzene	4.01	3.71	3.43	3.17	2.92	-51.8	-51.8
1,4-Dichlorobenzene	4.12	3.82	3.53	3.26	3.01	-52.7	-53.5
1,4-Dibromobenzene	6.21	5.80	5.41	5.03	4.69	-71.4	-56.9
1,4-Diiodobenzene	5.58	5.20	4.84	4.50	4.18	-66.2	-106.7
1,2,4-Trichlorobenzene	4.73	4.39	4.07	3.76	3.48	-59.0	-53.3
1,2,3,4-Tetrachlorobenzene	5.46	5.08	4.72	4.38	4.06	-66.1	-58.6
1,2,3,5-Tetrachlorobenzene	5.11	4.74	4.40	4.07	3.77	-63.3	-45.6
1,2,4,5-Tetrachlorobenzene	5.14	4.78	4.43	4.10	3.80	-63.6	-66.3
Pentachlorobenzene	5.66	5.27	4.90	4.54	4.21	-68.7	-71.3
Hexachlorobenzene	6.29	5.86	5.46	5.06	4.70	-74.6	-89.9
Fluorobenzene	2.75	2.52	2.31	2.11	1.93	-39.4	
Bromobenzene	4.39	4.08	3.79	3.51	3.25	-54.5	-45.0
Iodobenzene	4.08	3.78	3.50	3.23	2.99	-51.8	-61.9
4-Fluorotoluene	3.11	2.87	2.64	2.42	2.22	-43.2	
4-Chlorobenzotrifluoride	3.56	3.29	3.03	2.78	2.55	-48.2	-40.7
1,1,1,2-Tetrachloroethane	3.28	3.02	2.77	2.55	2.33	-45.6	-26.4
1,1,2,2-Tetrachloroethane	4.12	3.81	3.52	3.24	2.99	-54.0	-55.3

Compound	logK _{M1,air} 15 °C 98% rh COSMOt.	logK _{M1,air} 25 °C 98% rh COSMOt.	logK _{M1,air} 35 °C 98% rh COSMOt.	logK _{M1,air} 45 °C 98% rh COSMOt.	logK _{M1,air} 55 °C 98% rh COSMOt.	logK _{M1,air} $\Delta_{\text{abs}}H_i$ COSMOt.	logK _{M1,air} $\Delta_{\text{abs}}H_i$ <i>experiment.</i>
1-Chlorohexane	2.67	2.45	2.24	2.03	1.85	-39.7	
1-Chloroheptane	3.01	2.77	2.53	2.31	2.11	-43.2	-38.2
1-Chlorooctane	3.33	3.07	2.82	2.58	2.36	-46.6	-48.1
1-Chlorodecane	4.05	3.76	3.46	3.18	2.92	-54.0	-59.4
1-Bromopentane	3.29	3.03	2.79	2.56	2.35	-44.9	
Butanal/Butyraldehyde	2.49	2.26	2.06	1.89	1.72	-37.1	-35.5
Pentanal	2.90	2.65	2.43	2.23	2.04	-41.3	
Benzaldehyde	4.78	4.43	4.12	3.83	3.56	-57.7	-49.9
1-Cyanopropane	3.26	3.00	2.77	2.56	2.37	-43.0	-37.1
Aniline	5.68	5.26	4.88	4.53	4.20	-69.5	-72.0
2-Methylaniline	5.76	5.34	4.96	4.61	4.28	-69.8	-65.0
4-Methylaniline	5.95	5.52	5.12	4.75	4.40	-72.6	-85.9
2,6-Dimethylaniline	5.83	5.42	5.04	4.68	4.35	-69.6	-67.9
N,N-Dimethylaniline	4.56	4.24	3.94	3.65	3.39	-55.7	-65.0
2-Iodoaniline	6.65	6.18	5.75	5.34	4.97	-78.5	-89.9
4-Iodoaniline	7.27	6.77	6.30	5.87	5.46	-84.5	-69.9
Nitrobenzene	4.95	4.61	4.29	4.00	3.72	-58.4	-50.0
2-Nitrotoluene	5.11	4.76	4.43	4.13	3.84	-60.2	-52.1
2-Chlornitrobenzene	5.59	5.22	4.86	4.53	4.23	-64.6	-61.7
Benzonitrile	4.97	4.62	4.30	4.01	3.73	-58.6	-46.3
Acetonitrile	3.10	2.85	2.63	2.44	2.26	-40.5	-34.9
Nitromethane	2.80	2.58	2.38	2.20	2.03	-37.2	-37.7
Nitroethane	2.96	2.73	2.52	2.33	2.15	-39.1	-38.8
1-Nitropropane	3.16	2.92	2.69	2.49	2.30	-41.5	-45.6

Compound	logK _{M1,air} 15 °C 98% rh COSMOt.	logK _{M1,air} 25 °C 98% rh COSMOt.	logK _{M1,air} 35 °C 98% rh COSMOt.	logK _{M1,air} 45 °C 98% rh COSMOt.	logK _{M1,air} 55 °C 98% rh COSMOt.	logK _{M1,air} $\Delta_{\text{abs}}H_i$ COSMOt.	logK _{M1,air} $\Delta_{\text{abs}}H_i$ experiment.
2-Nitropropane	2.58	2.37	2.18	2.00	1.84	-36.3	-56.5
Pyridine	4.39	4.04	3.71	3.41	3.14	-59.5	
2-Methylpyridine	4.50	4.14	3.80	3.49	3.20	-61.3	-51.9
2-Acetylpyridine	5.40	5.01	4.65	4.33	4.02	-64.6	-78.1
2-Methylpyrazine	4.70	4.32	3.97	3.66	3.37	-62.7	-49.4
Methylamine	4.07	3.69	3.33	3.00	2.70	-64.6	
N,N-Dimethylformamide	6.01	5.54	5.11	4.74	4.39	-75.8	-44.9
N,N-Dimethylacetamide	6.34	5.83	5.37	4.95	4.56	-83.0	-63.1
Indole (1H-Indole)	7.48	6.97	6.49	6.05	5.64	-85.9	-68.6
Chinoline	6.70	6.23	5.78	5.37	4.98	-80.3	-111.7
Propanoic acid	5.46	5.01	4.61	4.26	3.93	-71.6	-38.5
Butanoic acid	5.70	5.24	4.82	4.46	4.12	-74.2	-43.7
Pentanoic acid	6.80	6.31	5.87	5.48	5.11	-78.9	-61.0
2-Methylbutanoic acid	5.21	4.77	4.38	4.04	3.71	-70.2	-55.4
3-Methylbutanoic acid	5.10	4.66	4.28	3.95	3.63	-69.1	-48.4
1,2-Dinitrobenzene	6.99	6.54	6.12	5.72	5.35	-76.6	-97.1
1,3-Dinitrobenzene	6.76	6.32	5.91	5.53	5.17	-74.2	-108.6
1,4-Dinitrobenzene	6.86	6.41	6.00	5.61	5.25	-75.2	-64.7
2,4-Dinitrotoluene	7.23	6.77	6.33	5.92	5.55	-78.6	-97.0
alpha-Acetylbutyllactone	6.00	5.59	5.23	4.90	4.58	-66.7	-50.3
4-Nitroanisole	6.68	6.25	5.84	5.46	5.11	-73.9	-78.1
Dimethylphthalate	7.23	6.75	6.31	5.91	5.53	-79.3	-63.9
Diethylphthalate	7.94	7.42	6.94	6.49	6.07	-87.1	-76.5
Triethylphosphate	6.36	5.89	5.47	5.08	4.72	-76.7	-65.4

Compound	logK _{M1,air} 15 °C 98% rh COSMOt.	logK _{M1,air} 25 °C 98% rh COSMOt.	logK _{M1,air} 35 °C 98% rh COSMOt.	logK _{M1,air} 45 °C 98% rh COSMOt.	logK _{M1,air} 55 °C 98% rh COSMOt.	logK _{M1,air} $\Delta_{\text{abs}}H_i$ COSMOt.	logK _{M1,air} $\Delta_{\text{abs}}H_i$ <i>experiment.</i>
Thiophene	3.36	3.11	2.87	2.65	2.44	-44.1	
Thiophenol	4.84	4.51	4.19	3.89	3.62	-58.0	-51.5
2,4-Pentanedione	4.35	4.02	3.73	3.48	3.23	-52.9	-37.2
1,2-Ethanediol	6.06	5.54	5.08	4.67	4.30	-82.1	-79.0
Chloroacetone	3.66	3.38	3.12	2.90	2.68	-46.8	-46.9
Benzoylchloride	4.46	4.14	3.84	3.56	3.30	-54.9	-53.6
Hydroxyacetone	4.15	3.81	3.51	3.25	3.00	-54.8	-55.1
Dimethyl succinate	5.21	4.84	4.51	4.20	3.92	-61.1	-54.3
Lindane (gamma-HCH)	7.87	7.35	6.86	6.40	5.97	-88.7	-89.0
2-Methoxyethanol	3.90	3.55	3.24	2.96	2.71	-56.6	-55.7
2-Ethoxyethanol	4.11	3.72	3.38	3.08	2.80	-61.7	-58.9
1,2-Naphthoquinone	8.05	7.51	7.02	6.57	6.14	-88.7	-95.8
1,4-Naphthoquinone	7.55	7.05	6.60	6.18	5.78	-82.2	-57.2
2-Nitroaniline	8.10	7.54	7.03	6.57	6.13	-91.7	-91.4
3-Methoxybenzaldehyde	5.85	5.45	5.08	4.74	4.42	-67.4	-71.8
1,4-Dimethoxybenzene	5.39	5.02	4.67	4.35	4.05	-63.1	-49.2
3-Hydroxybenzonitrile	8.88	8.23	7.66	7.14	6.66	-102.9	-62.8
2-Aminobenzonitrile	7.89	7.34	6.83	6.38	5.95	-90.5	-94.6
4-Aminobenzonitrile	9.37	8.73	8.14	7.61	7.11	-104.6	-67.7
Azobenzene	7.24	6.77	6.32	5.89	5.50	-81.6	-69.4

Figure SI-10: Calculated sorption enthalpies plotted against experimental sorption enthalpies for 161 compounds.

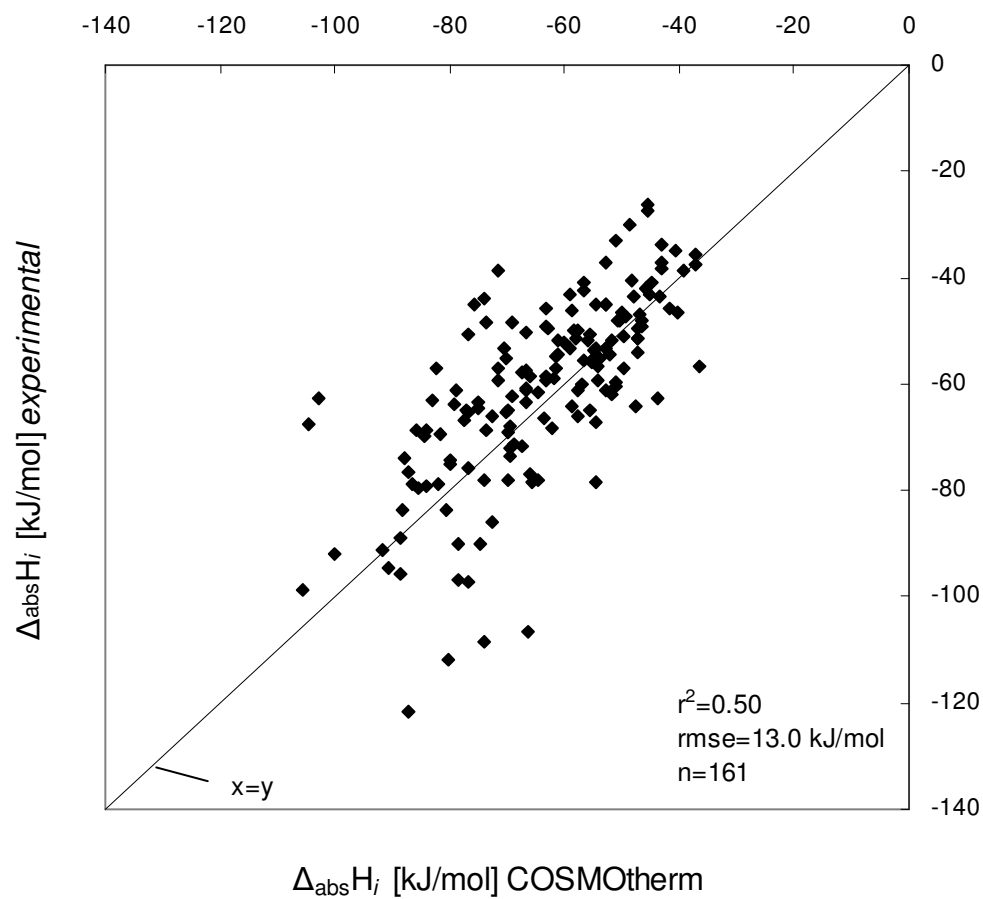
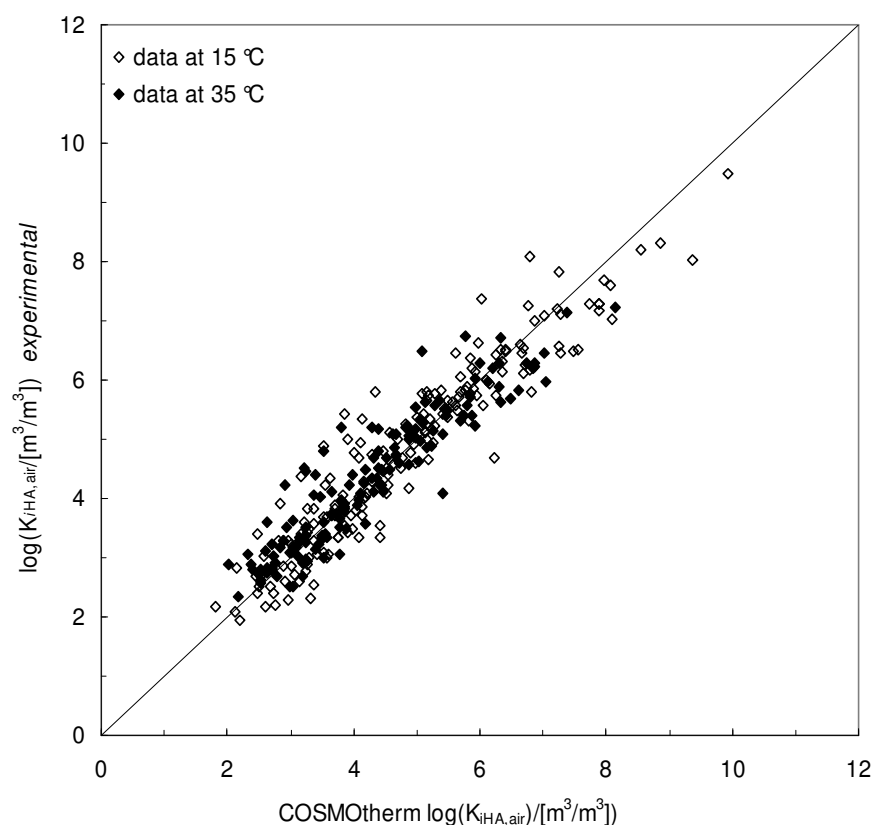


Figure SI-11 shows a comparison of experimental and calculated partition coefficients at 15 °C and 35 °C. The prediction at 35 °C shows the similar performance compared to 15 °C (see discussion in the main text). Thus, COSMOtherm is able to predict the temperature dependence of the sorption process satisfactorily although the correlation between the experimental and predicted sorption enthalpies is only moderate (see Figure SI-10).



SI-12 SMILES structure of M1

SMILES: Simplified Molecular Input Line Entry Specification

The following SMILES-structure of the M1 monomer was used as input for SPARC (Sparc Performs Automated Reasoning in Chemistry)

```
[O=C(C=C(C(CCC)C3=CC(C(O)=O)=C(OC4=CC(C(O)=O)=C(O)C=C4)C(OC)=C3)C2=O)C1=C2C=C(OC)C(C(O)=O)=C1]
```


Variations in the Sorption Properties of Nine Humic and Fulvic Acids from Different Origins

submitted to Environmental Science and Technology,
May 2007, unpublished work copyright 2007 American Chemical Society

Abstract

This work presents a dataset that consists of more than 1000 natural organic matter (NOM)/air partition coefficients covering polar and nonpolar organic compounds measured in 10 different humic and fulvic acids (HA/FA) from terrestrial and aquatic origins. Differences of more than one order of magnitude in the sorption coefficients of a given compound measured in HA and FA from different origins were found. The terrestrial HA exhibited substantially higher sorption coefficients compared to aquatic HA and FA. The difference between any two types of NOM is mainly reflected by a constant shift in the partition coefficients that applies to all compounds in the same way. This indicates that it is the number of available sorption sites per mass of sorbents rather than the types of intermolecular interactions between the sorbate and the sorbent that governs the major differences between the sorption properties of various types of NOM.

The experimental partition coefficients measured in all HA and FA were successfully described by Polyparameter Linear Free Energy Relationships (pp-LFERs) that explicitly account for van der Waals as well as H-donor/acceptor interactions between the sorbate and the sorbent. These pp-LFER equations provide for the first time a tool that allows including the variability in the sorption properties of NOM in environmental fate models.

Introduction

The transport and bioavailability of organic contaminants in soils, sediments, and aqueous systems is strongly affected by their sorption to dissolved and non-dissolved natural organic matter (NOM). NOM is a complex phase operationally divided into humic acids (HA), fulvic acids (FA), and humin (1). In soil organic matter (SOM), the relative contribution of each of the three NOM fractions varies substantially between different soil types (2); however, some generalizations can be made: The humin fraction represents generally the smallest fraction, except in Vertisols. The HA/FA ratios are generally >1 , with some exceptions: Stevenson reported a higher FA content in Alfisols and Spodosols, i.e., soils that are covered by forest vegetation. According to Malcolm (3), soils exhibit generally a HA to FA ratio of approximately 3:1, while in surface waters FA dominate (approximately 90%). Aquatic DOC is even more complex to handle because this fraction can exhibit enormous variations in time and space, as a function of season, stream discharge, vegetation of stream basins, etc. (3-5).

The chemical structures of NOM, e.g., acid/base properties, elemental compositions, functional group distribution, or aromaticity vary depending on their phase of origin, i.e., aquatic (freshwater or marine) or terrestrial origin, age, and environmental parameters such as vegetation or temperature. Table 1 clearly indicates this for ten HA and FA standards. These differences in the chemical structures of NOM should result in different molecular interactions within the NOM phase as well as with potential sorbate molecules and thus result in differing sorption characteristics of these materials. Indeed, several sorption studies reported differences in partition coefficients of up to one order of magnitude or even more for a given compound in HA and FA from different origins (6-9). Chin et al. as well as Chiou et al. reported differences in partition coefficients of about one order of magnitude between aquatic HA/FA compared to terrestrial HA (10, 11). Burkhard (12) collected DOC (dissolved organic carbon) partition coefficients from the literature, predominantly from aquatic systems. His empirical

equation ($K_{iDOC} = 0.08 \cdot K_{iow}$) reveals about a factor of five lower partition coefficients compared to the model published by Karickhoff ($K_{ioc} = 0.41 \cdot K_{iow}$ (13); K_{ioc} : NOM/water partition coefficient normalized to organic-C content) that is based on soil and sediment partition coefficients. The few works that have investigated the variability of sorption in whole soils (that represents a complex mixture of HA, FA, and humin) indicate that this variability is comparable to the variability found in isolated HA and FA. Krahe et al. (14) for example published experimental K_{ioc} values for nonylphenol measured in 135 different soils that scattered over almost 1.5 log units.

Most of the studies discussed above, however, were limited to a few nonpolar compounds, namely polycyclic aromatic hydrocarbons (PAHs) and polychlorinated biphenyls (PCBs). In addition, for HA and FA the literature data are dominated by partition coefficients measured in commercial HA such as Aldrich HA or Roth HA. In Supporting Information (SI-1) we provide an overview of experimental partition coefficients measured in various NOM (mostly HA and FA) materials collected from the literature. In a review Malcolm (15) concluded that commercial products should not be considered appropriate for use as analogues of true terrestrial and aquatic humic substances: Malcolm found that the ^{13}C -NMR spectra of commercial HA are distinctly different from those of stream and soil HA and FA. Other authors also advise against using commercial HA as a surrogate for NOM (16, 17).

Despite the considerable variance that has already been reported for sorption to different types of NOM it is still common practice in environmental fate modeling to use a single K_{ioc} -value for a given compound in different types of NOM. One explanation for this is that none of the studies conducted so far allow for generalizable conclusions about all types of chemicals and for all types of NOM.

A comprehensive understanding of the variability in the sorption properties of NOM necessarily includes the evaluation of sorption data of a wide range of organic compounds (i.e., polar and nonpolar compounds exhibiting various functional groups) in different types of representative HA and FA samples. It is likely that the variability in the

sorption properties of SOM from different origins is due to the differing sorption properties of the HA, FA, and humin fractions of the respective SOM. Understanding the variability in the sorption properties from a set of representative and well-defined HA and FA standards would allow for a better understanding of the sorption properties of SOM in general. In this work we studied the sorption of a diverse set of 80-100 polar and nonpolar compounds to nine different aquatic and terrestrial HA and FA that cover a wide range of chemical properties (Table 1). Note that this work focuses on HA and FA while the humin fraction will be included in future studies. This investigation builds on previous work (18) in which we evaluated how the sorption behavior of about 200 organic compounds to Leonardite HA varied depending on the structural properties of the sorbates. In two related studies (19, 20) we presented predictive tools that are able to qualitatively describe this variability. In the present study we focus on the variability in the sorption properties of different types of sorbents, i.e., HA and FA, based on a dataset of about 1000 experimental NOM/air partition coefficients. The partition coefficients are measured at 98% relative humidity where the NOM is almost completely hydrated. The thermodynamic cycle should therefore be valid in the NOM/air/water system (detailed discussion in (18, 20)), i.e., NOM/water partition coefficients can be calculated from experimental or predicted NOM/air partition coefficients and the air/water partitioning. This expands the practical applicability of this study. From the big experimental NOM/air partition dataset it is possible to a) assess the variability in the sorption properties of NOM from different origins; and b) to provide a set of predictive equations for NOM partitioning that allows considering this variability in chemical fate modeling.

Material and Methods

Experimental

NOM/air partition coefficients $K_{i\text{NOM},\text{air}}$ ($C_{i\text{NOM}}/C_{i\text{air}}$, [L/kg_{NOM}]) were determined via the retention in an Inverse Gas Chromatography System

(IGC) using coatings of HA and FA on silanized glassbeads (DMCS-treated) as the stationary phase. All experimental procedures were identical to those in a previous study (18) with the exception that the NOM were dissolved in a 1:1 mixture (volume-based) of 1-pentanol and *N,N*-dimethylformamide instead of a 3:2 mixture as before.

For each HA and FA replicates were measured on two separately prepared coatings. The reproducibility was very good for all 9 materials with an average standard deviation of $\pm 36\%$ in the measured sorption coefficients (for details see SI-2). As already observed for Leonardite HA (18), the relative precision of the partition coefficients determined on a single NOM coating was even higher (SI-2).

Natural Organic Matter

From the International Humic Substance Society IHSS (<http://www.ihss.gatech.edu>) the following standard and reference organic materials were obtained: Suwannee River FA (Cat. No. 1R101F-1), Suwannee River HA (Cat. No. 2S101H), Suwannee River NOM (Cat. No. 1R101N), Elliott Soil FA (Cat. No. 2S102F), Waskish Peat FA (Cat. No. 1R107F), Waskish Peat HA (Cat. No. 1R107H), and Nordic Lake HA (Cat. No. 1R105H). For more details on the origins of the IHSS samples see <http://www.ihss.gatech.edu>. A peat HA from Amherst (extracted from a Histosol) was obtained from the University of Massachusetts in Amherst. A detailed characterization of the Amherst HA is published in (21). A commercial HA was purchased from Aldrich (Buchs, Switzerland; Cat. No. H1,675-2). The analytical data of the ten NOM in Table 1 point out that these materials show substantial differences in elemental composition as well as functional group distribution.

Aldrich HA was delivered as sodium salt and was therefore insoluble in *N,N*-dimethylformamide. To convert the anionic HA into its protonated form the following steps were carried out: First, 200 mg Aldrich HA was dissolved in 200 ml nanopure water. Then, the solution was filtered (membrane filter, 0.45 μm , Schleicher and Schuell, Germany) and adjusted to pH = 1 in order to precipitate the protonated HA. The solution was centrifuged and the supernatant was decanted. The

precipitated and protonated HA was resuspended in 50 ml nanopure water (pH = 1) to remove remaining sodium ions. After a second centrifugation step the HA was dried and used as described in (18). The resulting Aldrich HA was completely soluble in *N,N*-dimethylformamide.

Table 1 Analytical data of the NOM investigated in this work: elemental composition, ^{13}C -NMR data, and acid/base properties.

NOM	elemental composition [%]					$^{\circ}\text{carboxylic}$ content [meq·gC ⁻¹]	$^{\circ}\text{phenolic}$ content [meq·gC ⁻¹]	carbonyl. [%]	carbox. [%]	aromat. [%]	aliphat. [%]
	C	H	O	N	C/O						
^{a)} Leonardite HA	63.8	3.7	31.3	1.2	2.04	7.46	2.31	8	15	58	14
^{b)} Amherst HA	52.9	4.5	40.0	2.6	1.32	<i>n.d.</i>	<i>n.d.</i>	<i>n.d.</i>	17	45	17
^{a)} Waskish Peat HA	54.7	4.0	38.5	1.5	1.42	<i>n.d.</i>	<i>n.d.</i>	8	18	42	18
^{a)} Nordic Lake HA	53.3	4.0	43.1	1.2	1.24	9.06	3.23	10	19	38	15
^{a)} Suw. Riv. HA	52.6	4.3	42.0	1.2	1.25	9.59	4.24	6	15	31	29
^{a)} Suw. Riv. NOM	52.5	4.2	42.7	1.1	1.23	9.85	3.94	8	20	23	27
^{a)} Waskish Peat FA	53.6	4.2	41.8	1.1	1.28	<i>n.d.</i>	<i>n.d.</i>	7	19	36	20
^{a)} Elliott Soil FA	50.1	4.3	42.6	3.8	1.18	13.24	2.27	12	25	30	22
^{a)} Suw. Riv. FA	53.0	4.4	43.9	0.8	1.21	12.23	3.11	7	20	24	33
^{b)} Aldrich HA	60.0	4.5	34.5	1.0	1.74	<i>n.d.</i>	<i>n.d.</i>	<i>n.d.</i>	16	45	33

^{a)} ^{13}C -NMR and elemental analysis data for the IHSS standards are from:

<http://www.ihss.gatech.edu>; aliphatic: 0-60 ppm, aromatic: 110-165 ppm, carboxyl: 165-190 ppm, carbonyl: 190-220 ppm

^{b)} ^{13}C -NMR and elemental analysis data for Amherst HA and Aldrich HA are from (21); aliphatic: 0-50 ppm, aromatic: 108-162 ppm, carboxylic: 162-220 ppm

^{c)} investigated using potentiometric titration (22)

Results and Discussion

Experimental Partition Coefficients: Scatter and Sorption Variability

For each of the nine NOM partition coefficients for 77 to 102 nonpolar and polar compounds from various compound classes at 15 °C and 98% relative humidity (rh) were measured. All experimental data are listed in SI-3. A comparison with experimental literature values shows that the data measured in our experimental system agree well with experimental literature data measured predominantly in batch systems (see SI-4). The

NOM/air partition coefficients determined for Leonardite HA (18) together with the experimental NOM/air partition coefficients from this study provide a dataset of more than 1000 experimental partition coefficients. Figure 1 shows a plot of the experimental partition coefficients for nine NOM (y-axes) plotted against those measured in Leonardite HA (x-axes). Leonardite HA was chosen as reference because it exhibited on average the highest partition coefficients. The compounds indicated by open symbols are small highly polar compounds and are discussed below. As can be seen from Figure 1, the terrestrial HA (i.e., Amherst HA, Aldrich HA, and Waskish Peat HA) exhibit the highest sorption coefficients while the aquatic FA exhibit the lowest partition coefficients. The differences between the sorption properties of FA and HA from aquatic systems are rather small; whereas, terrestrial FA and HA show much bigger differences of up to one order of magnitude in their sorption properties. The variability found in this study is similar compared to the variability found in various literature studies as discussed in the introduction (more details are shown in SI-5). However, the present study shows this variability for a big and diverse dataset containing polar and nonpolar compounds while the literature is mostly limited to nonpolar compounds.

Data from both this study and the literature clearly show that there is not a single K_{ioc} (or $K_{ioc,air}$) partition coefficient for a given compound, as is generally assumed in environmental fate modeling; the K_{ioc} (or $K_{ioc,air}$) values scatter over more than one order of magnitude depending on the NOM considered.

Different functional group contents of different HA and FA (see Table 1) result in different H-bond donor/acceptor properties of these NOM. This would affect the sorption of various organic compounds to a different extent depending on whether these compounds exhibit H-donor and/or H-acceptor properties or none of them (i.e., nonpolar compounds). Therefore, one would expect larger scatter when comparing the sorption data of a diverse compound set for HA and FA exhibiting different H-donor/H-acceptor interaction properties. However, as is evident from Figure 1, this is not what we observe here.

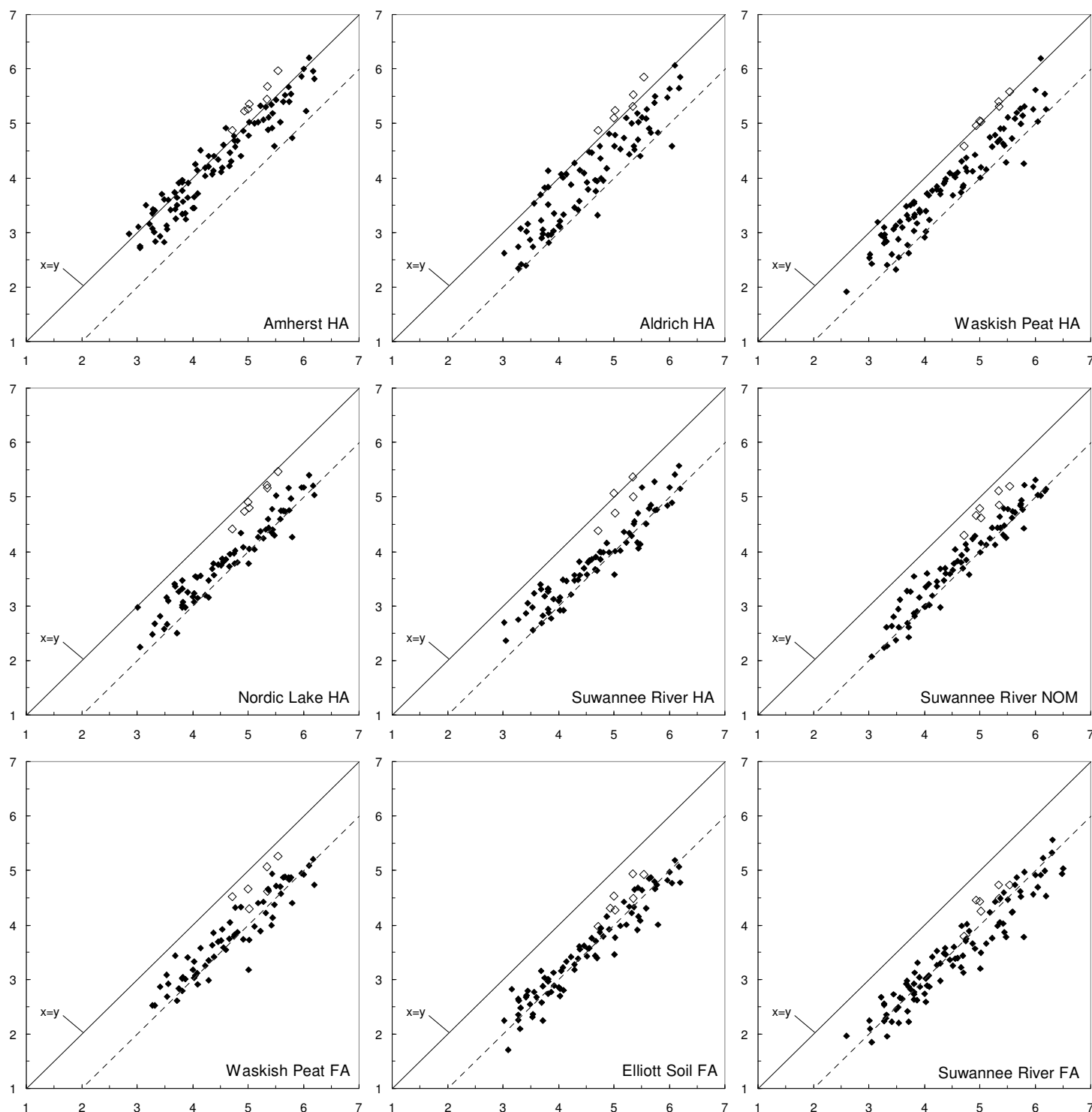


Figure 1 Experimental NOM/air partition coefficients measured for nine NOM (y-axes, see Table 1) plotted against Leonardite HA/air partition coefficients (x-axes) published in Ref (18). The dashed line indicates a factor of 10 lower partition coefficients compared to Leonardite HA. The compounds indicated by open symbols are small highly polar compounds (see discussion in the text).

Although the data show some scatter, it becomes clear that the difference between any two types of NOM is mainly reflected by a constant shift that applies to all compounds in the same way. This indicates that the differences in the partition coefficients are dominated by differences in the global sorption capacities of the NOM (i.e., the number of available sorption sites per mass of sorbent) rather than by differences in certain types of intermolecular interactions between the sorbate and the sorbent. In order to obtain a quantitative measure for this shift, the mean absolute deviation of the partition coefficients in a given type of NOM from the corresponding partition coefficients measured in Leonardite HA (the NOM exhibiting the highest sorption capacity) was calculated:

$$\text{mean absolute deviation} = -\frac{1}{n} \cdot \sum_n (\log(K_{\text{Leonardite,air}}) - \log(K_{\text{NOM,air}})) \quad (1)$$

These numbers allow a ranking of the different NOM according to their overall sorption capacities. The nine NOM in Table 1 and Table 2 are arranged according to these overall sorption capacities relative to Leonardite HA (except for Aldrich HA, see below). The standard deviations of these mean absolute deviations (roughly 0.25-0.3 log units, see Table 2) are significantly smaller than the range of absolute deviations that cover one order of magnitude between Leonardite HA and for example Suwannee River FA. This ranking according to the overall sorption capacities shows a clear trend, i.e., a decrease in the order: terrestrial HA > aquatic HA > terrestrial FA > aquatic FA.

The commercial Aldrich HA was not included in the above ranking because its scatter in Figure 1 is by far the highest compared to the other NOM and its H-donor/acceptor descriptors (see paragraph below) vary substantially from those measured in the other NOM materials indicating that its sorption properties are unique. This is supportive of conclusions by other authors that the commercial Aldrich HA is not an adequate representative of NOM.

Modeling Sorption Coefficients With a Polyparameter Linear Free Energy Relationship

In a previous work (20) we have demonstrated that a polyparameter linear free energy relationship (pp-LFER, Equation 2) can be used to quantitatively describe 158 Leonardite HA/air partition coefficients. This pp-LFER includes cavity formation in the NOM as well as nonspecific interactions (van der Waals forces) and specific interactions (electron donor/acceptor interactions including H-bonds) between sorbate and sorbent described by separate descriptors (Equation 2).

$$\log(K_{i\text{NOM,air}}/[L/\text{kg}_{\text{NOM}}]) = l_{\text{NOM,air}} \cdot L_i + v_{\text{NOM,air}} \cdot V_i + b_{\text{NOM,air}} \cdot B_i + a_{\text{NOM,air}} \cdot A_i + S_{\text{NOM,air}} \cdot S_i + c_{\text{NOM,air}} \quad (2)$$

Here, L_i , V_i , B_i , A_i and S_i are sorbate-specific descriptors (see SI-7). The McGowan volume of the compound i V_i [(cm³·mol⁻¹)/100] describes cavity formation in the NOM, the logarithm of the compound's hexadecane/air partition coefficient (L_i) describe nonspecific interactions of the compound i (i.e., van der Waals interactions) while the other descriptors stand for specific H-bond interactions (A_i : H-donor property; B_i : H-acceptor property) and polarizability (S_i : dipolarity/polarizability). The coefficients $a_{\text{NOM,air}}$, $b_{\text{NOM,air}}$, $l_{\text{NOM,air}}$, $S_{\text{NOM,air}}$, and $v_{\text{NOM,air}}$ in Equation 2 are the complementary interaction descriptors of the specific NOM. Equation 2 was fitted to the experimental NOM/air sorption coefficients for all types of NOM. The resulting equations are shown in Table 2. The correlation coefficients (r^2) for these fits are between $0.85 < r^2 < 0.92$ and the root mean square errors (rmse) of the sorption coefficients lie in the range of 0.24-0.32 log units (for details see SI-8). Hence, the pp-LFER models fit the experimental $K_{i\text{NOM,air}}$ partition coefficients generally within a factor of two for sorption coefficients that cover seven orders of magnitude (plot shown in SI-8). All equations in Table 2 are based on diverse compound sets. Therefore, they should be well suited to predict the sorption of compounds that were not included in the calibration data set, provided that reliable sorbate descriptors are available (descriptors can be found in the literature, such as in ref (23)). Here, we also provide

pp-LFER equations that predict NOM org-C/water partition coefficients at 15 °C (see SI-8).

Table 2 pp-LFER descriptors for nine NOM for $\log(K_{i\text{NOM,air}}/[L/kg_{\text{NOM}}])$ partition coefficients at 15 °C and 98% rh; mean absolute deviations from Leonardite HA partition coefficients (see text and Eq 1); for pp-LFER equations that predict NOM org-C/water partition coefficients see SI-8.

natural organic matter	origin	⁴ $l_{\text{NOM,air}}$	⁴ $v_{\text{NOM,air}}$	⁴ $b_{\text{NOM,air}}$	⁴ $a_{\text{NOM,air}}$	⁴ $s_{\text{NOM,air}}$	⁴ $c_{\text{NOM,air}}$	aromatic. [%]	mean absolute deviation ³	⁶ std. dev.
range of standard errors of pp-LFER descriptors		0.07-0.14	0.28-0.61	0.16-0.33	0.13-0.31	0.18-0.40	0.15-0.33			
Leonardite HA ⁵	terrestrial	0.81	-0.08	1.88	3.62	1.14	-0.65	58 ¹	0	-
Amherst HA	terrestrial	0.55	0.39	1.81	3.39	1.26	-0.20	45 ²	-0.16	0.31
Waskish Peat HA	terrestrial	0.60	0.51	1.78	3.68	0.95	-0.82	42 ¹	-0.56	0.33
Nordic Lake HA	aquatic	0.64	0.08	1.34	3.27	0.71	-0.35	38 ¹	-0.74	0.31
Suwannee River HA	aquatic	0.54	0.35	1.41	3.40	0.85	-0.35	31 ¹	-0.77	0.31
Suwannee Riv. NOM	aquatic	0.78	-0.53	1.62	3.04	0.64	-0.35	23 ¹	-0.82	0.26
Waskish Peat FA	terrestrial	0.55	0.81	1.01	3.52	0.97	-0.97	36 ¹	-0.86	0.30
Elliot Soil FA	terrestrial	0.72	0.22	1.67	3.40	0.65	-1.15	30 ¹	-0.97	0.25
Suwannee River FA	aquatic	0.60	0.68	1.58	3.52	0.76	-1.30	24 ¹	-1.06	0.31
Aldrich HA		0.95	-1.09	2.67	3.13	0.48	-0.38	45 ²	-0.49	0.39

¹from (24); aromaticity: 110-165 ppm

²from (21); aromaticity: 108-162 ppm

³mean absolute deviation from the experimental Leonardite HA/air partition coefficients, in log units (see Equation 1)

⁴sorbent descriptors: $l_{\text{NOM,air}}$ and $v_{\text{NOM,air}}$ account for nonspecific interactions and cavity formation; $s_{\text{NOM,air}}$: dipolarity/polarizability; $a_{\text{NOM,air}}$: electron-donor property (i.e., H-acceptor); $b_{\text{NOM,air}}$: electron-acceptor property (i.e., H-donor property); $c_{\text{NOM,air}}$: regression constant

⁵the pp-LFER equation for Leonardite HA has been published in a recent study (20)

⁶standard deviation: indicates the scatter of the experimental partition coefficient of a specific NOM around the mean absolute deviation from Leonardite HA in Figure 1.

These equations were fitted to NOM org-C/water partition coefficients that have been calculated from experimental NOM/air partition coefficients from this study, experimental water/air partition coefficients, and the org-C contents of the NOM (see Table 1). Note that these equations do not account for any – possibly existing – influence of pH, ionic strength or ionic composition. Therefore, sorption from the aqueous phase requires further investigations. The pp-LFER equations for the different NOM show only moderate differences in the sorbent

descriptors $a_{\text{NOM,air}}$ and $b_{\text{NOM,air}}$ (i.e., H-bond acceptor and donor property, respectively, of the NOM) or $s_{\text{NOM,air}}$ with the exception of $b_{\text{NOM,air}}$ for Waskish Peat HA which is quite low compared to the other materials. This is surprising because the chemical differences between the HA and FA are substantial, e.g., Suwannee River FA shows a 60% higher carboxylic group content compared to Leonardite HA (see Table 1 and an extended discussion in SI-9). These differences are for example reflected in the different water solubilities of HA and FA indicating that FA are more polar compared to HA. However, none of the sorbent descriptors $a_{\text{NOM,air}}$, $b_{\text{NOM,air}}$, or $s_{\text{NOM,air}}$ that should express the polarity of the sorbents show any such trend. The observed shift in the global sorption capacity of the various NOM types that is quantified by the mean absolute deviation in Table 2 can thus not be explained by the observed minor differences in the interaction descriptors; nor, as one might have expected, by differences in the constants $c_{\text{NOM,air}}$ of the pp-LFER equations. The $c_{\text{NOM,air}}$ values represent the hypothetical sorption of a compound without any interactions. These values involve a huge extrapolation from real compounds with substantial interactions to a virtual compound with zero interactions. Even small experimental errors will cause large errors in such extrapolated values so that their interpretation becomes meaningless (see example in SI-10 and (25) for a similar discussion). It must be noted that the standard errors in the sorbent descriptors of the pp-LFERs are relatively high (see Table 2) compared to typical fits for organic solvents or artificial polymers. This is due to the heterogeneity of the NOM phases compared to homogeneous systems such as organic solvents; the H-donor/H-acceptor sorbent descriptors therefore only represent averaged H-donor/H-acceptor properties of the NOM.

Influence of the Relative Humidity

In a previous study (18) we found that the relative humidity (rh) had only a minor effect (less than a factor of 3) on the partitioning of organic compounds in Leonardite HA from the gas phase. Here, we extended this work by measuring the partition coefficients of 64 polar and

nonpolar compounds in the weakest sorbent Suwannee River FA at 45% rh and 98% rh (Figure 2). A corresponding plot with the data measured in Leonardite HA in our previous study is shown in SI-11. The nonpolar compounds show similar pattern in both NOM: almost all compounds sorb up to a factor of 3 stronger at 45% rh compared to 98% rh. The polar compounds do not show such a uniform behavior in both HA and FA; only the short-chained alcohols sorb more strongly at 98% rh compared to 45% rh in Suwannee River FA while most polar compounds sorb slightly more strongly in Leonardite HA at 98% rh compared to 45% rh. Surprisingly, small highly polar compounds such as dicarboxylic acid methyl esters, 2-methoxyethanol, 2-ethoxyethanol, phenol, and propanoic acid sorbed much more strongly at 98% rh compared to 45% in Suwannee River FA (up to 1 log unit, marked by specific symbols in Figure 2).

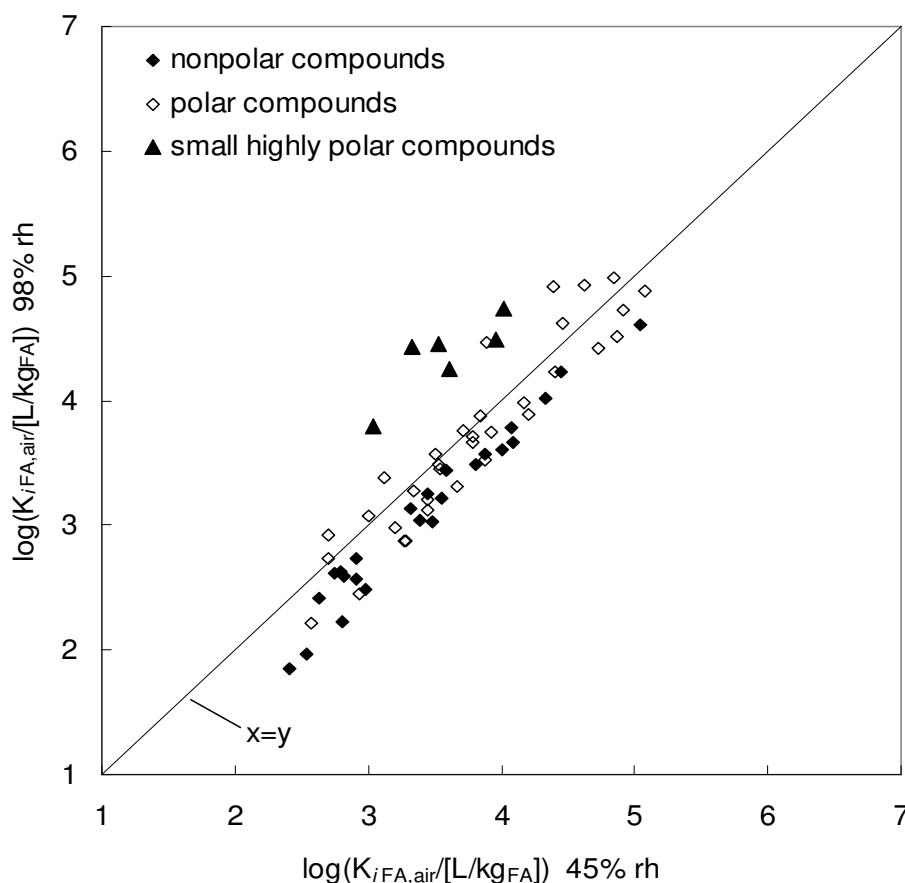


Figure 2 compares experimental partition coefficients measured at 45% and 98% relative humidity in Suwannee River FA.

This effect was not observed in Leonardite HA where these compounds showed similar partition coefficients at 45% rh and 98% rh (measured for phenol, propanoic acid, and dimethyl succinate, see SI-11).

Mechanistical Interpretation

The results discussed above suggest that the tested HA and FA mainly differ in the number of available sorption sites per mass of NOM rather than in the chemical characteristics of these sites. This explains why the sorbent descriptors $a_{\text{NOM,air}}$, $b_{\text{NOM,air}}$, and $s_{\text{NOM,air}}$ show no correlation with the different functional group contents of the tested NOM. This apparent similarity of the available sorption sites lets us further conclude that the chemical differences that obviously exist between HA and FA must reside in those parts of the material that are not available for the sorption process. It seems plausible to assume that these regions contain a high degree of cross-linking within the NOM due to a large number of internal H-bonds. This is consistent with the observation that the FA show the smallest accessibilities of all tested NOM (see Table 2) while at the same time they exhibit the highest density of carboxylic and phenolic groups (see Table 1). The following observation further supports this concept: small highly polar molecules, e.g, 2-methoxyethanol, 2-ethoxyethanol, dicarboxylic acid methyl esters, 2,5-hexanedione, and hydroxyacetone (shown by open symbols in Figure 1) did not follow the general trend, i.e., they sorbed more strongly in all HA and FA than expected from the respective pp-LFER fits and almost reached the level measured in Leonardite HA (see Figure 1 and SI-12). Hence, only these compounds appear to be able to sorb into these highly cross-linked regions by interacting via favorable H-bondings within this rigid environment.

The observed phenomena are to some extent comparable with observations of various researchers that suggest that NOM contains glassy regions (26-29) where diffusion is much slower compared to the rubbery regions that are also present. However, temperature-dependent sorption studies that we conducted with Leonardite HA (18) and with Suwannee River FA in this study (for data see SI-13) did not reveal any

distinct glass transition from 20 °C to 90 °C. Interestingly, we observed about two times higher sorption coefficients for a subset of polar and nonpolar compounds in Suwannee River FA after it had been cooled from 90 °C back to 20 °C again (see SI-13). Only the small highly polar molecules that had been less affected by the sorption restriction in the original Suwannee River FA did not show any sorption increase after the heating procedure. This indicates that the temperature treatment did indeed loosen some of the cross-linking in the NOM which could then not be recovered upon cooling (because of unfavorable orientation). If this change in the proposed cross-linking of the Suwannee River FA with increasing temperature occurred gradually (as can be expected for heterogeneous material) then this would explain why a clear and distinct glass transition effect was not observed during heating as is expected for homogeneous synthetic polymers. While the temperature treatment up to 90 °C made Suwannee River FA somewhat more accessible for organic sorbents, the number of available sorption sites per mass still remained much lower than in Leonardite HA. It is unclear whether these sites would become readily available at even higher temperatures or whether all these sites would become available if enough time was provided for diffusion into these rigid domains. Xing and coworkers have shown that sorption sites in rigid domains of NOM might become accessible if months or even years are provided for the equilibrium process (e.g., (29, 30)).

It should be noted that very recent studies indicate that humic substances are collections of diverse, relatively low molecular mass (200-2500 Da) components forming dynamic associations stabilized by nonspecific interactions and H-bond interactions (31, 32). This at least questions the traditional view that HA and FA are a distinct chemical category exhibiting a polymer-like structure. We are therefore somewhat reluctant to apply the classical polymer terminology (glassy/rubbery) to the NOM that we have investigated.

Predicting the Different Sorption Capacities of Various HA and FA

The discussion above provides a plausible mechanistic interpretation of our results but it does not offer a practical tool to predict the observed differences in the sorption capacities of HA and FA. However, there is a – purely empirical – correlation that describes much of this variability: the aromaticity of the HA and FA (Table 2) correlates reasonably well with the mean absolute deviations that quantify the differences in the sorption capacities ($r^2 = 0.81$, see SI-14). The following equation can be applied for a rough estimation of the sorption differences between Leonardite HA (as reference) and any other terrestrial or aquatic HA/FA:

$$\log(K_{NOM}) = \log(K_{Leonardite}) - 3 \cdot (f_{Leonardite}^{aromaticity} - f_{NOM}^{aromaticity}) \quad (3)$$

Such a correlation (with a similar slope) has been reported by others before (6, 7, 11, 33), however, only for a small number of nonpolar compounds (e.g., pyrene, fluoranthene, or anthracene). In addition to the aromaticity, Kopinke et al. (7) included the oxygen-content (wt %O) or alternatively the oxygen/hydrogen ratio (O/H) into such a correlation. However, including such additional predictors brought only a small improvement of the correlation in Equation 3 for our data (SI-14).

As mentioned in the introduction, the natural variability of NOM has so far been ignored when sorption coefficients were predicted, e.g., in environmental fate modeling. With the data presented here it becomes for the first time possible to quantify this variability and thus integrate it into predictions: (a) if the aromaticity of the considered NOM is known then predictions should be conducted with the pp-LFER of that NOM from Table 2 that comes closest in aromaticity; alternatively, sorption data can be estimated in a NOM of interest using Equation 3 and experimental partition coefficients measured in Leonardite HA or predicted partition coefficients with the pp-LFER fitted for Leonardite HA; (b) if a distinction between HA and FA can be made then Table 2 also allows to choose a predictive equation for a similar material; (c) if no further characterization of the considered NOM is possible then the use of all equations in Table 2 can at least serve to predict a range of values

that can be represented by a mean value with a realistic standard deviation. It is important to note that this standard deviation (which will lie in the range of 0.3-0.6 log units) is not due to uncertainties in the prediction but it reflects the natural variability in NOM. For the prediction of the temperature dependence which also is relevant for NOM/air partitioning we refer to our previous paper (20). The temperature dependence that we observed here for Suwannee River FA seems to be in the same range compared to the sorption enthalpies measured for Leonardite HA in (18). However, the dataset is not big enough for a precise comparison.

NOM/water partition coefficients can be calculated from experimental or predicted NOM/air partition coefficients and Henry's Law constants thus expanding the practical applicability of this study. An investigation of the influence of ionic strength, pH, or ionic composition on the partitioning from the aqueous phase is subject of our ongoing research.

Acknowledgements

We thank Hans Peter Arp for critical comments on the manuscript and Baoshan Xing from the University of Massachusetts in Amherst for providing NOM material. This research was financially supported by the Swiss National Science Foundation (project-no. 200020-111753/1) and partly by the European Union (European Commission, FP6 Contract No. 003956).

References Chapter 4

- (1) Sparks, D. L. *Environmental Soil Chemistry*; Academic Press: San Diego, 1995.
- (2) Stevenson, F. J. *Humus chemistry: Genesis, composition, reactions.*; 2nd edition ed.; John Wiley & Sons: New York, 1994.
- (3) Malcolm, R. L. Geochemistry of stream fulvic acids and humic acids. In *Humic substances in soils, sediments, and water. Geochemistry, isolation, and characterization*; Aiken, G. R., McKnight, D.M., Wershaw, R.L., MacCarthy, P., Ed.; Wiley-Interscience: NY, 1985.
- (4) Ozretich, R. J., Smith, L.M., Roberts, F.A. Reversed-phase separation of estuarine interstitial water fractions and the consequences of C18 retention of organic matter *Environ. Sci. Technol.* **1995**, *14*, 1261-1272.
- (5) Vannote, R. L., Minshall, G.W., Cummins, K.W., Sedell, J.R, Cushing, C.E. River continuum concept *Canadian Journal of Fisheries and Aquatic Sciences* **1980**, *37*, 130-137.
- (6) Gauthier, T. D., Seitz, W.R., Grant, C.L. Effects of structural and compositional variations of dissolved humic materials on pyrene Koc values *Environ. Sci. Technol.* **1987**, *21*, 243-248.
- (7) Kopinke, F. D., Georgi, A., Mackenzie, K. Sorption of pyrene to dissolved humic substances and related model polymers. 1. Structure-property correlation *Environ. Sci. Technol.* **2001**, *35*, 2536-2542.
- (8) Grathwohl, P. Influence of organic matter from soils and sediments from various origins on the sorption of some chlorinated aliphatic hydrocarbons: Implications on K_{oc} correlations *Environ. Sci. Technol.* **1990**, *24*, 1687-1693.
- (9) Brannon, J. M., Pennington, J.C., Davis, W.M., Hayes, C. Fluoranthene KDOC in sediment pore waters *Chemosphere* **1995**, *30*, 419-428.
- (10) Chiou, C. T., Malcolm, R., Brinton, T.I., Kile, D.E. Water solubility enhancement of some organic pollutants and pesticides by dissolved humic and fulvic acids *Environ. Sci. Technol.* **1986**, *20*, 502-508.
- (11) Chin, Y. P., Aiken, G.R., Danielsen, K.M. Binding of pyrene to aquatic and commercial humic substances: the role of molecular weight and aromaticity *Environ. Sci. Technol.* **1997**, *31*, 1630-1635.

- (12) Burkhard, L. P. Estimating dissolved organic carbon partition coefficients for nonionic organic chemicals *Environ. Sci. Technol.* **2000**, *34*, 4663-4667.
- (13) Karickhoff, S. W. Semi-empirical estimation of sorption of hydrophobic pollutants on natural sediments and soils *Chemosphere* **1981**, *10*, 833-846.
- (14) Krahe, S., Duering, R.-A., Huisman, J.A., Horn, A., Gaeth, S. Statistical modeling of the partitioning of nonylphenol in soil *Water, Air, Soil Pollut.* **2006**, 221-237.
- (15) Malcolm, R. L., MacCarthy, P. Limitations in the use of commercial humic acids in water and soil research *Environ. Sci. Technol.* **1986**, *20*, 904-911.
- (16) Perdue, E. M., Wolfe, N.L. Modification of pollutant hydrolysis kinetics in the presence of humic substances *Environ. Sci. Technol.* **1982**, 847-852.
- (17) Raber, B., Kögel-Knabner, I., Stein, C., Klem, D. Partitioning of polycyclic aromatic hydrocarbons to dissolved organic matter from different soils *Chemosphere* **1998**, *36*, 79-97.
- (18) Niederer, C., Goss, K.U., Schwarzenbach, R.P. Sorption equilibrium of a wide spectrum of organic vapors in Leonardite humic acid: Experimental setup and experimental data *Environ. Sci. Technol.* **2006**, *40*, 5368-5373.
- (19) Niederer, C., Goss, K.-U. Quantum chemical modeling of humic acid/air equilibrium partitioning of organic vapors *Environ. Sci. Technol.* **2007**, *accepted March 6*.
- (20) Niederer, C., Goss, K.U., Schwarzenbach, R.P. Sorption equilibrium of a wide spectrum of organic vapors in Leonardite humic acid: Modeling of experimental data *Environ. Sci. Technol.* **2006**, *40*, 5374-5379.
- (21) Mao, J. D., Hu, W.G., Schmidt-Rohr, K., Davies, G., Ghabbour, E.A., Xing, B. Quantitative characterization of humic substances by solid-state carbon-13 nuclear magnetic resonance *Soil Sci. Soc. Am. J.* **2000**, *64*, 873-883.
- (22) Ritchie, J. D., Perdue, E.M. Proton-binding study of standard and reference fulvic acids, humic acids, and natural organic matter *Geochim. Cosmochim. Acta* **2003**, *67*, 85-96.
- (23) Abraham, M. H. Hydrogen Bonding, XXVII. Solvation parameters for functionally substituted aromatic compounds and heterocyclic

compounds, from gas-liquid chromatographic data *J. Chromatogr.* **1993**, 644, 95-139.

(24) Thorn, K. A., Folan, D.W., MacCarthy, P. "Characterization of the International Humic Substances Society standard and reference fulvic and humic acids by solution state carbon-13 (^{13}C) and hydrogen-1 (^1H) nuclear magnetic resonance spectroscopy," U.S. Geological Survey, 1989.

(25) Pankow, J. F. Common gamma-intercept and single compound regressions of gas-particle partitioning data vs. $1/T$. *Atmos. Environ.* **1991**, 25, 2229-2239.

(26) Young, K. D., LeBoeuf, E.J. Glass transition behavior in a peat humic acid and an aquatic humic acid *Environ. Sci. Technol.* **2000**, 34, 4549-4553.

(27) Schaumann, G. E., LeBoeuf, E.J. Glass transitions in peat: their relevance and the impact of water *Environ. Sci. Technol.* **2005**, 39, 800-806.

(28) Xing, B., Pignatello, J.J. Dual-mode sorption of low polarity compounds in glassy poly(vinyl chloride) and soil organic matter *Environ. Sci. Technol.* **1997**, 31, 792-799.

(29) Xing, B., Pignatello, J.J. Time-dependent isotherm shape of organic compounds in soil organic matter: implications for sorption mechanism *Environ. Toxicol. Chem.* **1996**, 15, 1282-1288.

(30) Pignatello, J. J., Xing, B. Mechanisms of slow sorption of organic chemicals to natural particles *Environ. Sci. Technol.* **1996**, 30, 1-11.

(31) Sutton, R., Sposito, G. Molecular structure in soil humic substances: The new view *Environ. Sci. Technol.* **2005**, 39, 9009-9015.

(32) Kelleher, B. P., Simpson, A.J. Humic substances in soils: are they really chemically distinct? *Environ. Sci. Technol.* **2006**, 40, 4605-4611.

(33) Perminova, I. V., Grechishcheva, N.Y., Petrosyan, V.S. Relationships between structure and binding affinity of humic substances for polycyclic aromatic hydrocarbons: relevance of molecular descriptors *Environ. Sci. Technol.* **1999**, 33, 3781-3787.

Appendix 4

Variations in the Sorption Properties of NOM

Content

- SI-1** Experimental partition coefficients in various NOM from literature sources for comparison with our own data in SI-4.
- SI-2** Reproducibility of the experimental data on different columns
- SI-3** Experimental partition coefficients for 10 natural organic materials
- SI-4** Validation of experimental partition coefficients
- SI-5** Comparison of the natural variability with literature data
- SI-6** Comparison of polar and nonpolar compounds measured in Aldrich HA
- SI-7** Sorbate-specific descriptors used for the pp-LFER models
- SI-8** pp-LFER fits for 10 natural organic materials: prediction of $K_{i\text{NOM,air}}$ and $K_{i\text{NOM-oc,water}}$ partition coefficients
- SI-9** Elemental analysis and ^{13}C -NMR data of the tested NOM
- SI-10** Polyparameter model: regression constant $c_{\text{NOM,air}}$
- SI-11** Influence of relative humidity on the partition behavior of organic compounds
- SI-12** Experimental partition coefficients of small highly polar compounds
- SI-13** Temperature dependence study of partition coefficients in Suwannee River FA
- SI-14** Mean absolute deviations compared to aromaticity

SI-1 Experimental partition coefficients in various NOM from literature sources for comparison with our own data in SI-4

compound	exp. partition coeff.	$\log(K_{ioc})$ or $\log(K_{iDOC})$	description of sorbent phase	Ref
Toluene	$\log K_{oc}$	1.91	Sapsucker Woods humic acid	[1]
Toluene	$\log K_{oc}$	1.13	Sapsucker Woods fulvic acid	[1]
Toluene	$\log K_{DOC}$	2.39	DOM from heavily polluted coal wastewaters	[2]
Toluene	$\log K_{oc}$	1.94	Aldrich humic acid	[1]
Toluene	$\log K_{oc}$	1.94	Aldrich humic acid	[1]
Toluene	$\log K_{oc}$	2.12	Roth humic acid	[3]
Toluene	$\log K_{oc}$	2.27	Aldrich/ Fluka humic acid	[4]
Trichloroethene	$\log K_{oc}$	1.76	Sapsucker Woods humic acid	[1]
Trichloroethene	$\log K_{oc}$	0.62	Sapsucker Woods fulvic acid	[1]
Trichloroethene	$\log K_{oc}$	1.83	Aldrich humic acid	[1]
Trichloroethene	$\log K_{oc}$	1.83	Aldrich humic acid	[1]
Trichloroethene	$\log K_{oc}$	2.20	Aldrich/ Fluka humic acid	[4]
1,2,3-Trichlorobenz.	$\log K_{DOC}$	3.00	Sanhedron Soil humic acid	[5]
1,2,3-Trichlorobenz.	$\log K_{DOC}$	2.30	Sanhedron Soil fulvic acid	[5]
1,2,3-Trichlorobenz.	$\log K_{DOC}$	2.00	Suwannee River humic acid	[5]
1,2,3-Trichlorobenz.	$\log K_{DOC}$	2.00	Suwannee River fulvic acid	[5]
γ -HCH	$\log K_{DOC}$	2.70	Sanhedron Soil humic acid	[5]
γ -HCH	$\log K_{DOC}$	1.80	Sanhedron Soil fulvic acid	[5]
γ -HCH	$\log K_{DOC}$	1.50	Suwannee River humic acid	[5]
γ -HCH	$\log K_{DOC}$	1.50	Suwannee River fulvic acid	[5]
Phenanthrene	$\log K_{DOC}$	4.21	Forchheim: DOC from org. surface layers of org. acid soils	[6]
Phenanthrene	$\log K_{DOC}$	4.09	Tegernsee: DOC from org. surface layers of org. acid soils	[6]
Phenanthrene	$\log K_{DOC}$	4.76	Soxhlet: DOC: sandy soil, river sediment, pond sediment	[7]
Phenanthrene	$\log K_{DOC}$	4.91	Soxhlet: DOC: sandy soil, river sediment, pond sediment	[7]
Phenanthrene	$\log K_{oc}$	4.64	DOM from an organic muck	[8]
Phenanthrene	$\log K_{oc}$	4.69	one humic acid	[8]

compound	exp. partition coeff.	$\log(K_{ioc})$ or $\log(K_{iDOC})$	description of sorbent phase	Ref
Phenanthrene	$\log K_{DOC}$	4.56	Leonardite humic acid	[9]
Phenanthrene	$\log K_{oc}$	4.15	continuous extraction of HA from Oxhill soil (F1)	[10]
Phenanthrene	$\log K_{oc}$	4.29	continuous extraction of HA from Oxhill soil (F4)	[10]
Phenanthrene	$\log K_{oc}$	4.30	continuous extraction of HA from Oxhill soil (F7)	[10]
Phenanthrene	$\log K_{oc}$	4.38	continuous extraction of HA from Oxhill soil (F9)	[10]
Phenanthrene	$\log K_{DOC}$	4.07	humic acid from heavily polluted coal wastewaters	[2]
Phenanthrene	$\log K_{DOC}$	3.48	fulvic acid from heavily polluted coal wastewaters	[2]
Phenanthrene	$\log K_{DOC}$	4.63	Aldrich humic acid	[6]
Phenanthrene	$\log K_{oc}$	4.00	Aldrich or Fluka humic acid	[4]
Phenanthrene	$^1\log K_{DOM}$	3.93	Roth humic acid	[11]
Phenanthrene	$\log K_{oc}$	5.13	Aldrich humic acid	[12]
Phenanthrene	$\log K_{DOC}$	3.92	Aldrich humic acid	[13]
Phenanthrene	$\log K_{oc}$	4.65	Aldrich humic acid	[14]
Phenanthrene	$^1\log K_{DOM}$	4.56	Aldrich humic acid	[15]
Fluoranthene	$\log K_{DOC}$	4.14	Forchheim: DOC from org. surface layers of org. acid soils	[6]
Fluoranthene	$\log K_{DOC}$	4.28	Tegernsee: DOC from org. surface layers of org. acid soils	[6]
Fluoranthene	$\log K_{DOC}$	4.57	humic acid from heavily polluted coal wastewaters	[2]
Fluoranthene	$\log K_{DOC}$	4.95	Aldrich humic acid	[6]
Pyrene	$\log K_{DOC}$	4.62	Forchheim: DOC from org. surface layers of org. acid soils	[6]
Pyrene	$\log K_{DOC}$	4.94	Tegernsee: DOC from org. surface layers of org. acid soils	[6]
Pyrene	$\log K_{oc}$	4.46	marine humic acids	[16]
Pyrene	$\log K_{oc}$	4.81	marine humic acids	[16]
Pyrene	$\log K_{oc}$	4.94	soil humic acids	[16]
Pyrene	$\log K_{oc}$	5.51	soil humic acids	[16]
Pyrene	$\log K_{oc}$	4.73	soil fulvic acids	[16]
Pyrene	$\log K_{oc}$	5.02	soil fulvic acids	[16]
Pyrene	$\log K_{DOC}$	4.92	Leonardite humic acids	[9]

compound	exp. partition coeff.	$\log(K_{ioc})$ or $\log(K_{iDOC})$	description of sorbent phase	Ref
Pyrene	$\log K_{oc}$	3.64	Lake Fryxell fulvic acid	[17]
Pyrene	$\log K_{oc}$	3.96	Ohio River fulvic acid	[17]
Pyrene	$\log K_{oc}$	4.15	Coal Creek fulvic acid	[17]
Pyrene	$\log K_{oc}$	4.01	Suwannee River fulvic acid	[17]
Pyrene	$\log K_{oc}$	4.33	Suwannee River fulvic acid	[17]
Pyrene	$\log K_{oc}$	3.85	estuarine interstitial water: DOC sampled in spring	[18]
Pyrene	$\log K_{oc}$	3.78	estuarine interstitial water: DOC sampled in fall	[18]
Pyrene	$\log K_{oc}$	3.88	Suwannee River fulvic acid	[19]
Pyrene	$\log K_{oc}$	5.23	humic acid extracted from podzolic soil (Lee, NH)	[20]
Pyrene	$\log K_{oc}$	5.08	fulvic acid extracted from podzolic soil (Lee, NH)	[20]
Pyrene	$\log K_{oc}$	4.74	fulvic acid extracted from podzolic soil (North Conway, NH)	[20]
Pyrene	$\log K_{oc}$	5.00	Suwannee River fulvic acid	[20]
Pyrene	$\log K_{DOC}$	4.68	humic acid from heavily polluted coal wastewaters	[2]
Pyrene	$\log K_{oc}$	4.37	Suwannee River humic acid	[19]
Pyrene	$\log K_{DOC}$	4.03	fulvic acid from heavily polluted coal wastewaters	[2]
Pyrene	$\log K_{DOC}$	4.85	aquatic humic substance: River Moscow	[21]
Pyrene	$\log K_{DOC}$	4.60	aquatic humic substance: River North Dvina	[21]
Pyrene	$\log K_{DOC}$	5.08	aquatic humic substance: swamp water	[21]
Pyrene	$\log K_{DOC}$	5.08	peat humic substance: Sphagnum-Fuscum	[21]
Pyrene	$\log K_{DOC}$	5.08	peat humic subst.: Sphagnum peat	[21]
Pyrene	$\log K_{DOC}$	4.90	peat humic subst.: Sphagnum peat	[21]
Pyrene	$\log K_{DOC}$	4.85	peat humic subst.: sedge peat	[21]
Pyrene	$\log K_{DOC}$	5.23	peat humic substance: woody peat	[21]
Pyrene	$\log K_{DOC}$	5.15	peat humic substance: woody herbaceous peat	[21]
Pyrene	$\log K_{DOC}$	5.00	peat humic substance: woody herbaceous peat	[21]
Pyrene	$\log K_{DOC}$	5.00	soil HA: sod-podzolic soil, forest	[21]
Pyrene	$\log K_{DOC}$	5.11	soil HA: sod-podzolic soil, forest	[21]

compound	exp. partition coeff.	$\log(K_{ioc})$ or $\log(K_{iDOC})$	description of sorbent phase	Ref
Pyrene	$\log K_{DOC}$	5.08	soil HA: sod-podzolic soil, plough	[21]
Pyrene	$\log K_{DOC}$	4.85	soil HA: sod-podzolic soil, garden	[21]
Pyrene	$\log K_{DOC}$	5.15	soil HA: gray wooded soil, forest	[21]
Pyrene	$\log K_{DOC}$	5.26	soil HA: gray wooded soil, plough	[21]
Pyrene	$\log K_{DOC}$	5.34	soil HA: meadow chernozem	[21]
Pyrene	$\log K_{DOC}$	5.38	soil HA: typical chernozem	[21]
Pyrene	$\log K_{DOC}$	4.11	soil FA: sod-podzolic-soil, forest	[21]
Pyrene	$\log K_{DOC}$	4.70	soil FA: grey wooded soil, forest	[21]
Pyrene	$\log K_{DOC}$	5.04	soil FA: typical chernozem	[21]
Pyrene	$\log K_{DOC}$	5.00	soil humic subst.: typical chernozem	[21]
Pyrene	$\log K_{DOC}$	5.36	Aldrich humic acid	[21]
Pyrene	$\log K_{DOC}$	5.02	anthropogenic humic acid (coal wastewater pond)	[22]
Pyrene	$\log K_{DOC}$	4.95	Roth humic acid (coal-derived commercial humic acid)	[22]
Pyrene	$\log K_{DOC}$	4.80	anthropogenic sediment humic acid (coal wastewater pond)	[22]
Pyrene	$\log K_{DOC}$	4.77	soil humic acid, acidic moor	[22]
Pyrene	$\log K_{DOC}$	4.70	soil HA, forest soil (A-horizon)	[22]
Pyrene	$\log K_{DOC}$	4.47	soil HA, forest soil (B-horizon)	[22]
Pyrene	$\log K_{DOC}$	4.41	anthropogenic surface water HA (coal wastewater pond)	[22]
Pyrene	$\log K_{DOC}$	4.35	anthropogenic fulvic acid (coal wastewater pond)	[22]
Pyrene	$\log K_{DOC}$	4.23	anthropogenic surface water FA (coal wastewater pond)	[22]
Pyrene	$\log K_{DOC}$	4.21	brown water humic acid	[22]
Pyrene	$\log K_{DOC}$	4.01	brown water fulvic acid	[22]
Pyrene	$\log K_{DOC}$	5.23	Aldrich humic acid	[6]
Pyrene	$\log K_{OC}$	5.02	Aldrich humic acid	[16]
Pyrene	$^1\log K_{DOM}$	4.70	Roth humic acid	[11]
Pyrene	$\log K_{OC}$	5.18	Aldrich humic acid	[17]
Pyrene	$\log K_{OC}$	4.64	Aldrich humic acid	[18]
Naphthalene	$\log K_{DOC}$	3.27	Soxhlet: DOC: sandy soil, river sediment, pond sediment	[7]
Naphthalene	$\log K_{DOC}$	3.37	Soxhlet: DOC: sandy soil, river sediment, pond sediment	[7]
Naphthalene	$\log K_{DOC}$	2.69	well humidified but rel. young peat	[23]
Naphthalene	$\log K_{DOC}$	3.27	HA from heavily polluted coal wastewater	[2]

compound	exp. partition coeff.	$\log(K_{ioc})$ or $\log(K_{iDOC})$	description of sorbent phase	Ref
Naphthalene	$\log K_{DOC}$	2.84	fulvic acid from heavily polluted coal wastewaters	[2]
Naphthalene	$\log K_{OC}$	3.04	Aldrich or Fluka Humic acid	[4]
Naphthalene	$^1\log K_{DOM}$	2.93	Roth humic acid	[11]
Naphthalene	$\log K_{OC}$	3.74	Aldrich humic acid	[14]
Naphthalene	$^1\log K_{OM}$	3.02	Aldrich humic acid	[15]
Anthracene	$\log K_{DOC}$	3.95	DOC from Lake Erie	[13]
Anthracene	$\log K_{DOC}$	4.73	DOC from Lake Erie	[13]
Anthracene	$\log K_{DOC}$	4.87	DOC from Huron River	[13]
Anthracene	$\log K_{DOC}$	5.70	DOC from Huron River	[13]
Anthracene	$\log K_{DOC}$	3.81	DOC from natural waters	[13]
Anthracene	$\log K_{DOC}$	4.87	DOC from natural waters	[13]
Anthracene	$\log K_{OC}$	4.20	fulvic acid extracted from podzolic soil (North Conway, NH)	[20]
Anthracene	$\log K_{OC}$	4.51	fulvic acid extracted from podzolic soil (Lee, NH)	[20]
Anthracene	$\log K_{OC}$	<i>n.d.</i>	Suwannee River fulvic acid	[20]
Anthracene	$\log K_{OC}$	4.57	humic acid extracted from podzolic soil (Lee, NH)	[20]
Anthracene	$\log K_{OC}$	4.81	humic acid isolated from a dark lignite soil	[20]
Anthracene	$\log K_{OC}$	4.42	Suwannee River humic acid	[19]
Anthracene	$\log K_{DOC}$	4.19	humic acid from heavily polluted coal wastewaters	[2]
Anthracene	$\log K_{DOC}$	3.53	fulvic acid from heavily polluted coal wastewaters	[2]
Anthracene	$\log K_{OC}$	4.18	Suwannee River fulvic acid	[19]
Anthracene	$\log K_{OC}$	4.08	peat humic substances: Sphagnum Fuscum peat	[21]
Anthracene	$\log K_{OC}$	4.34	peat humic substances: Sphagnum peat	[21]
Anthracene	$\log K_{OC}$	4.20	peat humic substances: Sphagnum peat	[21]
Anthracene	$\log K_{OC}$	4.40	peat humic substances: sedge peat	[21]
Anthracene	$\log K_{OC}$	4.78	peat humic substances: woody peat	[21]
Anthracene	$\log K_{OC}$	4.70	peat humic substances: woody herbaceous peat	[21]
Anthracene	$\log K_{OC}$	4.70	soil HA: sod-podzolic soil, forest	[21]
Anthracene	$\log K_{OC}$	4.70	soil HA: sod-podzolic soil, plough	[21]
Anthracene	$\log K_{OC}$	4.70	soil HA: gray wooded soil, forest	[21]
Anthracene	$\log K_{OC}$	4.85	soil HA: gray wooded soil, plough	[21]

compound	exp. partition coeff.	$\log(K_{ioc})$ or $\log(K_{iDOC})$	description of sorbent phase	Ref
Anthracene	$\log K_{oc}$	5.00	soil HA: meadow chernozem	[21]
Anthracene	$\log K_{oc}$	5.00	soil humic acid: typical chernozem	[21]
Anthracene	$\log K_{oc}$	4.70	soil humic subst.: typical chernozem	[21]
Anthracene	$\log K_{oc}$	5.00	Aldrich humic acid	[21]
Anthracene	$\log K_{DOC}$	3.95-4.46	Aldrich humic acid	[13]
Anthracene	$\log K_{oc}$	4.21	Aldrich or Fluka Humic acid	[4]
Anthracene	$\log K_{oc}$	4.65	Aldrich humic acid	[14]
Anthracene	$\log K_{oc}$	4.72	Aldrich humic acid	[20]
Anthracene	$^1\log K_{OM}$	4.56	Aldrich humic acid	[15]
Biphenyl	$\log K_{DOC}$	3.57	DOC from Lake Erie	[13]
Biphenyl	$\log K_{DOC}$	3.72	DOC from Lake Erie	[13]
Biphenyl	$\log K_{DOC}$	4.04	DOC from Huron River	[13]
Biphenyl	$\log K_{DOC}$	5.58	DOC from Huron River	[13]
Biphenyl	$\log K_{DOC}$	3.0	Aldrich humic acid	[13]
Biphenyl	$\log K_{oc}$	3.27	Aldrich or Fluka Humic acid	[4]
Acenaphthene	$\log K_{oc}$	2.55	High DOC (spring)	[18]
Acenaphthene	$\log K_{DOC}$	3.60	humic acids from heavily polluted coal wastewaters	[2]
Acenaphthene	$\log K_{DOC}$	3.17	fulvic acids from heavily polluted coal wastewaters	[2]
Acenaphthene	$\log K_{oc}$	3.0	Aldrich humic acid	[18]
Benzo[a]pyrene	$\log K_{DOC}$	5.36	surface waters: pond (Walker Branch Watershed (WB))	[24]
Benzo[a]pyrene	$\log K_{DOC}$	5.66	surface waters: pond adjacent to the Oak Ridge (P1)	[24]
Benzo[a]pyrene	$\log K_{DOC}$	5.16	surface waters: pond adjacent to the Oak Ridge (P2)	[24]
Benzo[a]pyrene	$\log K_{DOC}$	5.26	surface waters: pond adjacent to the Oak Ridge (P3)	[24]
Benzo[a]pyrene	$\log K_{DOC}$	5.46	surface waters: stream located near a peat deposit	[24]
Benzo[a]pyrene	$\log K_{DOC}$	5.36	ground water sampled within the peat deposit (H-0)	[24]
Benzo[a]pyrene	$\log K_{DOC}$	5.26	ground water sampled from clay formation (H-15)	[24]
Benzo[a]pyrene	$\log K_{DOC}$	5.06	ground water sampled from clay formation (H-30)	[24]

compound	exp. partition coeff.	$\log(K_{ioc})$ or $\log(K_{iDOC})$	description of sorbent phase	Ref
Benzo[a]pyrene	$\log K_{DOC}$	4.86	ground water sampled from clay formation (H-100)	[24]
Benzo[a]pyrene	$\log K_{DOC}$	6.26	ground water: peat-filled depression in a sand aquifer (B-0)	[24]
Benzo[a]pyrene	$\log K_{DOC}$	5.36	ground water: peat-filled depression in a sand aquifer (B-50)	[24]
Benzo[a]pyrene	$^1\log K_{DOM}$	6.30	Aldrich humic acid	[24]
Benzo[a]pyrene	$\log K_{oc}$	6.31	Aldrich humic acid	[25]
Benzene	$\log K_{oc}$	1.68	Roth humic acid	[3]
Benzene	$\log K_{DOC}$	2.00	DOM from heavily polluted coal wastewaters	[2]
Benzene	$\log K_{oc}$	1.68	Roth humic acid	[3]
Benzene	$\log K_{DOC}$	2.0	DOM from heavily polluted coal wastewaters	[2]
Fluorene	$\log K_{DOC}$	3.77	humic acid from heavily polluted coal wastewaters	[2]
Fluorene	$\log K_{DOC}$	3.30	fulvic acid from heavily polluted coal wastewaters	[2]
Fluorene	$^1\log K_{DOM}$	3.55	humic acid from heavily polluted coal wastewaters	[2]
Fluorene	$^1\log K_{DOM}$	3.08	fulvic acid from heavily polluted coal wastewaters	[2]
Chrysene	$\log K_{DOC}$	4.97	humic acid from heavily polluted coal wastewaters	[2]
Chrysene	$\log K_{DOC}$	4.28	fulvic acid from heavily polluted coal wastewaters	[2]
Chrysene	$^1\log K_{DOM}$	4.75	humic acid from heavily polluted coal wastewaters	[2]
Chrysene	$^1\log K_{DOM}$	4.06	fulvic acid from heavily polluted coal wastewaters	[2]
p,p'-DDT	$\log K_{DOC}$	5.44	Aldrich humic acid	[13]
Decane	$^1\log K_{DOM}$	4.57	Roth humic acid	[11]
Undecane	$^1\log K_{DOM}$	5.20	Roth humic acid	[11]
Dodecane	$^1\log K_{DOM}$	5.48	Roth humic acid	[11]
Tridecane	$^1\log K_{DOM}$	6.00	Roth humic acid	[11]

compound	exp. partition coeff.	$\log(K_{ioc})$ or $\log(K_{iDOC})$	description of sorbent phase	Ref
Dibenzofurane	$\log K_{oc}$	4.15	Aldrich humic acid	[14]
Quinoline	$\log K_{oc}$	2.89	Aldrich humic acid	[14]
Fluoranthene	$^1\log K_{DOM}$	3.66	fulvic acid from heavily polluted coal wastewaters	[2]
1,4-Dichlorobenz.	$\log K_{oc}$	2.19	Aldrich humic acid	[26]
1,4-Dichlorobenz.	$\log K_{oc}$	2.92	Aldrich or Fluka humic acid	[4]
1,2,4-Trichlorobenz.	$\log K_{oc}$	2.77	Aldrich humic acid	[26]
1,2,4-Trichlorobenz.	$\log K_{oc}$	3.11	Aldrich/ Fluka humic acid	[4]

¹For the transformation from DOM to DOC an average org-C content of 60% in coal-derived materials was assumed

[1] Garbarini, D.R., Lion, L.W. Influence of the nature of soil organics on the sorption of toluene and trichloroethylene. *Environ. Sci. Technol.* **1986**, 20, 1263-1269.

[2] Poerschmann, J., Kopinke, F.-D., Plugge, J., Georgi, A. Interaction of organic chemicals (PAH, PCB, Triazines, Nitroaromatics and organotin compounds) with dissolved humic organic matter. In: Davies, G., Ghabbour, E.A. **1999**. Understanding Humic Substances: Advanced methods, properties, applications. The Royal Society of Chemistry.

[3] Kopinke, F.-D., Georgi, A., Voskamp, M., Richnow, H.H. Carbon isotope fractionation of organic contaminants due to retardation on humic substances: implications for natural attenuation studies in aquifers. *Environ. Sci. Technol.* **2005**, 39, 6052-6062.

[4] Chin, Y.-P. Estimating the effects of dispersed organic polymers on the sorption of contaminants by natural solids. 1. A predictive thermodynamic humic substance-organic solute interaction model. *Environ. Sci. Technol.* **1989**, 23, 978-984.

[5] Chiou, C.T., Malcolm, R.L., Brinton, T.I., Kile, D.E. Water solubility enhancement of some organic pollutants and pesticides by dissolved humic and fulvic acids. *Environ. Sci. Technol.* **1986**, 20, 502-508.

[6] Raber, B., Kögel-Knabner, I., Stein, C., Klem, D. Partitioning of polycyclic aromatic hydrocarbons to dissolved organic matter from different soils. *Chemosphere*, **1998**, 36, 79-97.

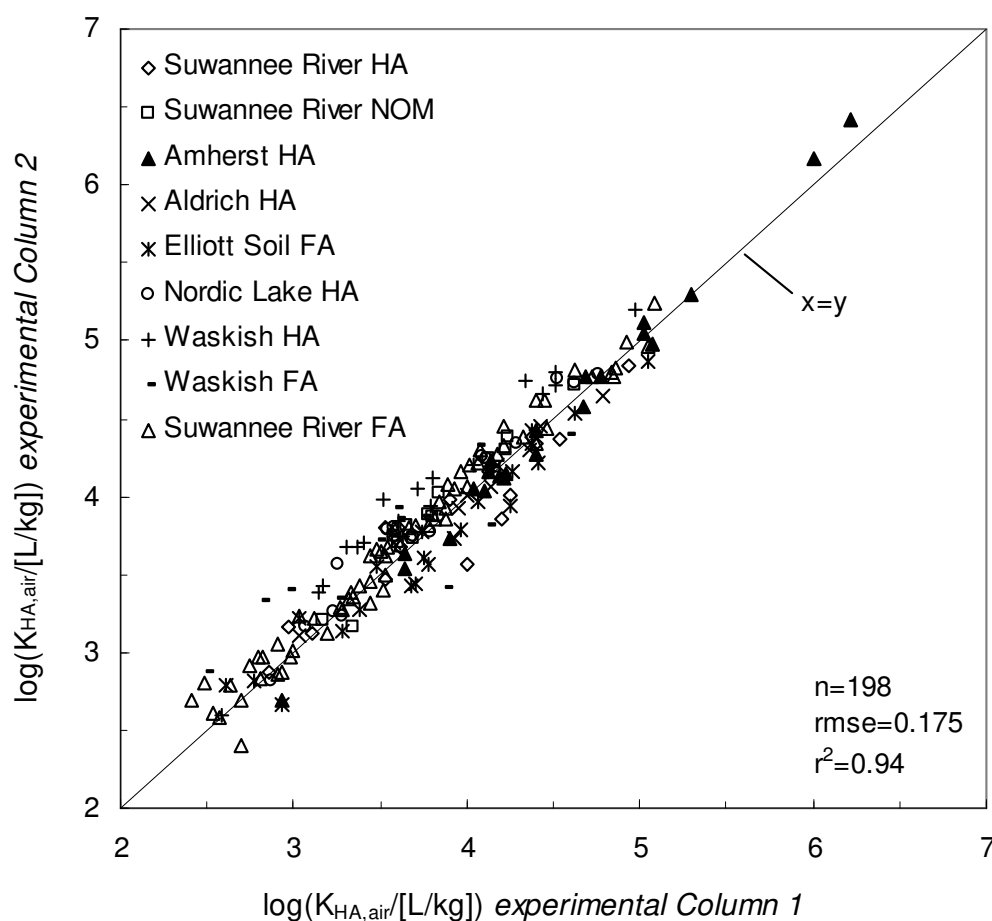
- [7] Xiao, B., Yu, Z., Huang, W., Song, J., Peng, P. Black carbon and kerogen in soils and sediments. 2. Their roles in equilibrium sorption of less-polar organic pollutants. *Environ. Sci. Technol.* **2004**, 38, 5842-5852.
- [8] Magee, B.R., Lion, L.W., Lemley, A.T. Transport of dissolved organic macromolecules and their effect on the transport of phenanthrene in porous media. *Environ. Sci. Technol.* **1991**, 25, 323-331.
- [9] Lee, C.-L., Kuo, L.-J., Wang, H.-L., Hsieh, P.-C. Effects of ionic strength on the binding of phenanthrene and pyrene to humic substances: three-stage variation model. *Wat. Res.*, **2003**, 37, 4250-4258.
- [10] Kang, S., Xing, B. Phenanthrene sorption to sequentially extracted soil humic acids and humins. *Environ. Sci. Technol.* **2005**, 39, 134-140.
- [11] Poerschmann, J., Kopinke, F.-D. Sorption of very hydrophobic organic compounds (VHOCs) on dissolved humic organic matter (DOM). 2. Measurement of sorption and application of a Flory-Huggins concept to interpret the data. *Environ. Sci. Technol.* **2001**, 35, 1142-1148.
- [12] Laor, Y., Farmer, W.J., Aochi, Y., Strom, P.F. Phenanthrene binding and sorption to dissolved and to mineral-associated humic acid. *Wat. Res.*, **1998**, 32, 1923-1931.
- [13] Landrum, P.F., Nihart, S.R., Eadle, B.J., Gardner, W.S. Reverse-phase separation method for determining pollutant binding to Aldrich humic acid and dissolved organic carbon of natural waters. *Environ. Sci. Technol.* **1984**, 18, 187-192.
- [14] Nielsen, T., Siigur, K., Helweg, C., Jørgensen, O., Hansen, P.E., Kirso, U. Sorption of polycyclic aromatic compounds to humic acid as studied by high-performance liquid chromatography. *Environ. Sci. Technol.* **1997**, 31, 1102-1108.
- [15] Rebhun, M., de Smedt, F., Rwetabula, J. Dissolved humic substances for remediation of sites contaminated by organic pollutants. Binding-desorption model predictions. *Wat. Res.*, **1996**, 30, 2027-2038.
- [16] Gauthier, T.D., Seitz, W.R., Grant, C.L. Effects of structural and compositional variations of dissolved humic materials on pyrene K_{oc} values. *Environ. Sci. Technol.* **1987**, 21, 243-248.
- [17] Chin, Y.-P., Aiken, G.R., Danielsén, K.M. Binding of pyrene to aquatic and commercial humic substances: the role of molecular weight and aromaticity. *Environ. Sci. Technol.* **1997**, 31, 1630-1635.

- [18] Ozretich, R.J., Smith, L.M., Roberts, F.A. Reversed-phase separation of estuarine interstitial water fractions and the consequences of C18 retention of organic matter. *Environ. Toxicol. Chem.* **1995**, 14, 1261-1272.
- [19] Schlautman, M.A., Morgan, J. Effects of aqueous chemistry on the binding of polycyclic aromatic hydrocarbons by dissolved humic materials. *Environ. Sci. Technol.* **1993**, 27, 961-969.
- [20] Gauthier, T.D., Shane, E.C., Guerin, W.F., Seitz, W.R., Grant, C.L. Fluorescence quenching method for determining equilibrium constants for polycyclic aromatic hydrocarbons binding to dissolved humic materials. *Environ. Sci. Technol.* **1986**, 20, 1162-1166.
- [21] Perminova, I.V., Grechishcheva, N.Y., Petrosyan, V.S. Relationships between structure and binding affinity of humic substances for polycyclic aromatic hydrocarbons: relevance of molecular descriptors. *Environ. Sci. Technol.* **1999**, 33, 3781-3787.
- [22] Kopinke, F.-D., Georgi, A., MacKenzie, K. Sorption of pyrene to dissolved humic substances and related model polymers. 1. Structure-property correlation. *Environ. Sci. Technol.* **2001**, 35, 2536-2542.
- [23] Xing, B. The effect of the quality of soil organic matter on sorption of naphthalene. *Chemosphere*, **1997**, 35, 633-642.
- [24] McCarthy, F.J., Roberson, L.E., Burrus, L.W. Association of Benzo(a)pyrene with dissolved organic matter: prediction of K_{DOM} from structural and chemical properties of the organic matter. *Chemosphere*, **1989**, 19, 1911-1920.
- [25] McCarthy, J.F., Jimenez, B.D. Interactions between polycyclic aromatic hydrocarbons and dissolved humic material: binding and dissociation. *Environ. Sci. Technol.* **1985**, 19, 1072-1076.
- [26] Chin, Y.-P. Weber, W.J.Jr., Eadie, B.J. Estimating the effects of dispersed organic polymers on the sorption of contaminants by natural solids. 2. Sorption in the presence of humic and other natural macromolecules. *Environ. Sci. Technol.* **1990**, 24, 837-842.

SI-2 Reproducibility of the experimental data on different columns

Figure SI-1 shows the partition coefficients measured in two replicate columns (separately prepared coatings) for each natural organic matter. The reproducibility is very good for all 9 materials with an average standard deviation of $\pm 36\%$ in the measured sorption coefficients. Only marginal systematic errors can be observed.

Figure SI-1



SI-3 Experimental NOM/air partition coefficients for 10 natural organic matters measured at 15 °C and 98% rh

All partition coefficients are in [L/kg_{NOM}] and were measured at 15 °C and 98% rh.; Suw. River = Suwannee River; Was. Peat = Waskish Peat

Compound	Leonardite ¹ humic acid	Suw. River fulvic acid	Wask.Peat humic acid	Amherst humic acid	Elliot Soil fulvic acid	Suw. River humic acid	Nordic Lake humic acid	Was. Peat fulvic acid	Aldrich humic acid	Suw. River NOM
n-Decane	3.41	2.22	2.60	2.93	2.67	2.87	2.81	2.87	2.40	2.63
n-Undecane	3.91	3.04	3.42	3.64	3.13	3.12	3.25	3.40	3.03	3.16
n-Dodecane	4.38	3.58	3.94	4.13	3.61	3.81	3.78	3.86	3.58	3.69
n-Tridecane	4.87	3.66	4.12	4.40	4.16	4.16	4.34	4.33	4.18	4.23
n-Tetradecane	5.43	4.60	4.91	4.92	4.68	4.70	4.78	4.94	4.70	4.79
1-Decene	3.28	2.56	2.80	3.07	2.26	2.75	2.48	2.52	2.34	2.23
1-Undecene	3.83	3.13	3.33	3.56	n.d.	2.88	3.07	3.04	2.81	2.81
1-Dodecene	4.35	3.48	3.90	4.07	3.38	3.48	3.68	3.63	3.41	3.47
1-Tridecene	4.77	4.02	4.12	4.57	3.94	3.98	4.02	4.32	3.99	4.04
Ethanol	3.68	2.92	3.48	3.74	n.d.	3.39	3.40	n.d.	3.69	n.d.
Propan-1-ol	3.82	2.92	3.57	3.92	3.01	3.31	3.32	n.d.	3.83	n.d.
Butan-1-ol	4.08	3.07	3.68	4.14	3.22	3.48	3.52	3.11	4.01	3.40
Pentan-1-ol	4.39	3.46	3.98	4.40	3.55	3.57	3.57	3.42	4.14	3.60
Hexan-1-ol	4.76	3.75	4.37	4.68	3.94	3.86	3.78	3.82	4.36	3.84
Heptan-1-ol	5.18	4.23	4.75	5.02	4.42	4.36	4.26	4.40	4.74	4.24
Octan-1-ol	5.63	4.73	5.09	5.40	4.85	4.79	4.75	4.87	4.91	4.71
Nonan-1-ol	6.14	5.23	n.d.	n.d.	n.d.	n.d.	n.d.	n.d.	n.d.	n.d.
Propan-2-ol	3.56	2.66	3.20	3.60	2.77	3.23	3.09	2.92	3.53	3.11
2-Methylpropan-1-ol	3.82	2.73	3.29	3.77	2.96	3.32	2.98	2.79	3.51	n.d.
2-Methylpropan-2-ol	3.60	2.64	3.09	3.42	2.67	n.d.	n.d.	n.d.	n.d.	n.d.
3-Methylbutan-1-ol	4.23	3.27	3.79	4.19	3.42	3.21	3.20	3.25	3.88	3.36
Benzyl alcohol	6.10	4.92	6.20	6.21	5.19	5.41	5.40	5.09	6.07	5.02
Cyclopentanol	4.56	3.38	4.02	4.61	3.58	3.83	3.81	3.59	4.48	4.04

Compound	Leonardite ¹ humic acid	Suw. River fulvic acid	Wask.Peat humic acid	Amherst humic acid	Elliot Soil fulvic acid	Suw. River humic acid	Nordic Lake humic acid	Was. Peat fulvic acid	Aldrich humic acid	Suw. River NOM
Cyclohexanol	4.92	3.57	4.42	4.86	3.92	3.98	4.08	3.74	4.81	4.28
2,2,2-Trifluoroethanol	3.42	n.d.	n.d.	n.d.	2.71	n.d.	n.d.	n.d.	3.02	n.d.
Hexafluoropropanol	3.88	3.31	n.d.	3.24	n.d.	n.d.	n.d.	n.d.	n.d.	n.d.
Phenol	6.00	4.92	5.62	6.00	4.97	5.17	5.18	4.93	5.64	5.31
o-Cresol	5.96	4.56	5.26	5.86	4.82	4.84	5.17	4.95	5.48	5.19
m-Cresol	6.50	5.04	n.d.	n.d.	n.d.	n.d.	n.d.	n.d.	n.d.	n.d.
p-Cresol	6.48	4.94	n.d.	n.d.	n.d.	n.d.	n.d.	n.d.	n.d.	n.d.
2-Chlorophenol	5.44	3.87	4.60	5.19	4.16	4.06	4.40	4.13	5.03	4.48
2-Pentanone	3.28	2.23	n.d.	n.d.	n.d.	n.d.	n.d.	n.d.	n.d.	n.d.
2-Hexanone	3.49	2.45	3.13	3.61	2.55	n.d.	n.d.	n.d.	n.d.	n.d.
2-Heptanone	3.92	2.87	3.37	3.91	2.89	n.d.	n.d.	n.d.	3.35	n.d.
2-Octanone	4.29	3.30	3.70	4.21	3.28	3.47	3.16	3.35	3.46	2.98
2-Nonanone	4.81	3.89	n.d.	4.68	3.79	3.98	3.80	3.87	3.95	3.58
2-Decanone	5.27	4.42	4.79	5.07	4.34	4.34	4.24	4.42	4.43	4.12
2-Undecanone	5.67	4.88	5.20	5.52	4.87	4.85	4.73	4.89	4.83	n.d.
4-Methylpentan-2-one	3.31	2.29	2.85	3.01	2.10	n.d.	n.d.	n.d.	n.d.	n.d.
Cyclopentanone	4.05	2.89	3.72	4.25	3.16	n.d.	3.54	3.07	4.07	3.60
Cyclohexanone	4.29	2.98	3.77	4.40	3.18	3.56	3.47	2.99	4.27	3.68
Acetophenone	5.22	3.76	4.57	5.33	4.01	4.17	4.37	3.89	5.10	4.43
n-Propyl acetate	2.85	n.d.	n.d.	2.97	n.d.	n.d.	n.d.	n.d.	n.d.	n.d.
n-Butyl acetate	3.28	2.54	2.91	3.35	2.35	n.d.	n.d.	n.d.	2.74	n.d.
n-Pentyl acetate	3.72	2.87	3.24	3.64	2.88	2.83	2.50	2.61	2.98	2.43
Methyl benzoate	5.01	3.20	4.01	4.78	3.46	3.58	3.78	3.18	4.58	3.98
Benzyl acetate	5.32	3.98	4.66	5.30	4.22	4.28	4.40	4.22	5.00	4.44
Di-n-butyl ether	3.22	2.67	2.95	3.16	n.d.	n.d.	n.d.	n.d.	n.d.	n.d.
Di-n-pentylether	4.23	3.52	3.84	4.04	n.d.	n.d.	n.d.	n.d.	n.d.	3.45
1,4-Dioxane	3.82	2.77	3.53	3.96	n.d.	3.27	3.47	3.03	4.13	3.54
Benzofurane	4.09	2.87	3.23	3.72	2.80	2.92	3.15	2.91	3.33	3.02

Compound	Leonardite ¹ humic acid	Suw. River fulvic acid	Wask.Peat humic acid	Amherst humic acid	Elliot Soil fulvic acid	Suw. River humic acid	Nordic Lake humic acid	Was. Peat fulvic acid	Aldrich humic acid	Suw. River NOM
Dibenzofuran	5.80	4.97	5.31	n.d.	n.d.	n.d.	n.d.	n.d.	n.d.	5.22
Methyl phenyl ether	3.72	2.22	2.62	3.50	2.24	n.d.	n.d.	n.d.	3.05	2.61
n-Propylbenzene	3.10	n.d.	n.d.	n.d.	1.71	n.d.	n.d.	n.d.	n.d.	n.d.
n-Butylbenzene	3.53	2.49	2.88	3.13	2.31	2.98	3.16	3.08	n.d.	2.94
n-Pentylbenzene	4.03	3.02	3.39	3.65	2.84	3.16	3.23	3.33	3.21	3.35
n-Hexylbenzene	4.53	3.60	4.05	4.19	3.57	3.80	3.87	3.92	3.79	3.78
1,2,4-Trimethylbenz.	3.33	1.96	2.41	2.84	n.d.	n.d.	n.d.	n.d.	2.42	2.27
1,3,5-Trimethylbenz.	3.05	1.85	2.43	2.75	n.d.	2.36	2.25	n.d.	n.d.	2.07
Indane	3.49	n.d.	2.32	2.83	n.d.	n.d.	2.58	n.d.	2.87	2.37
Naphthalene	4.66	3.22	3.74	4.22	3.44	3.67	3.73	3.75	3.96	3.80
1-Methylnaphthalene	5.48	3.78	4.28	4.59	4.08	4.13	4.30	4.37	4.40	4.25
Acenaphthene	5.75	n.d.	n.d.	n.d.	n.d.	n.d.	n.d.	n.d.	n.d.	4.94
Biphenyl	5.58	4.23	4.72	5.02	4.31	4.51	4.60	4.70	5.09	4.62
Chlorobenzene	3.05	n.d.	n.d.	2.72	n.d.	n.d.	n.d.	n.d.	n.d.	n.d.
1,2-Dichlorobenzene	4.01	2.74	2.91	3.45	2.86	3.09	3.17	3.18	3.13	2.99
1,3-Dichlorobenzene	3.81	2.63	3.03	3.34	2.74	2.94	3.02	3.02	2.95	2.87
1,4-Dichlorobenzene	3.87	2.62	3.17	3.35	2.77	2.77	2.97	3.01	2.96	2.90
1,4-Dibromobenzene	4.69	3.44	3.83	4.31	3.39	3.65	n.d.	n.d.	3.94	3.69
1,2,4-Trichlorobenzene	4.51	3.25	3.68	4.11	3.43	3.58	3.75	3.72	3.92	3.66
1,2,3,4-Tetrachlorobenz.	5.36	4.05	4.70	4.89	4.33	4.51	4.60	4.66	4.59	4.64
1,2,4,5-Tetrachlorobenz.	5.79	3.78	4.26	4.73	4.01	n.d.	4.26	4.40	4.83	4.42
Pentachlorobenzene	6.05	4.69	5.04	5.23	4.77	4.90	n.d.	n.d.	4.59	5.04
Bromobenzene	3.54	2.20	2.55	3.06	2.36	2.56	2.66	2.68	2.74	2.61
Iodobenzene	4.03	2.59	3.02	3.45	2.70	2.92	3.07	3.03	3.10	3.00
4-Fluorotoluene	2.60	1.97	1.91	n.d.	n.d.	n.d.	n.d.	n.d.	n.d.	n.d.
1,1,1,2-Tetrachloroetha.	3.01	2.25	2.53	n.d.	n.d.	n.d.	2.97	n.d.	n.d.	n.d.
1,1,2,2-Tetrachloroetha.	3.70	2.42	2.77	3.25	2.58	2.69	n.d.	n.d.	2.90	2.68
1-Chlorodecane	4.67	3.98	4.31	4.47	3.71	3.90	3.95	4.05	3.76	3.93

Compound	Leonardite ¹ humic acid	Suw. River fulvic acid	Wask.Peat humic acid	Amherst humic acid	Elliot Soil fulvic acid	Suw. River humic acid	Nordic Lake humic acid	Was. Peat fulvic acid	Aldrich humic acid	Suw. River NOM
Benzaldehyde	4.70	3.13	3.87	n.d.	n.d.	n.d.	n.d.	n.d.	3.32	n.d.
1-Cyanopropane	3.44	2.73	3.06	3.70	2.79	3.05	n.d.	n.d.	3.16	2.80
Aniline	5.81	5.56	5.72	n.d.	n.d.	5.77	n.d.	n.d.	n.d.	n.d.
Nitrobenzene	5.02	3.49	4.20	5.03	3.77	4.01	4.05	3.73	4.79	4.16
2-Nitrotoluene	5.12	3.66	4.16	5.00	3.98	4.02	4.04	3.97	4.53	4.12
Benzonitrile	4.60	3.39	4.10	4.92	3.76	3.85	3.86	3.54	4.47	3.82
Acetonitrile	3.16	n.d.	3.19	3.50	2.82	n.d.	n.d.	n.d.	n.d.	n.d.
Nitromethane	3.28	n.d.	3.09	n.d.	2.64	n.d.	n.d.	n.d.	n.d.	n.d.
Nitroethane	3.29	n.d.	2.96	3.43	2.61	n.d.	n.d.	n.d.	n.d.	n.d.
1-Nitropropane	3.32	2.35	2.84	3.40	2.48	n.d.	2.67	2.52	3.07	2.61
2-Nitropropane	3.02	2.10	2.60	3.10	2.24	2.70	n.d.	n.d.	2.62	n.d.
<i>N,N</i> -Dimethylacetam.	6.31	5.56	n.d.	n.d.	n.d.	n.d.	n.d.	n.d.	n.d.	n.d.
Chinoline	6.25	n.d.	4.55	n.d.	n.d.	n.d.	n.d.	n.d.	n.d.	n.d.
Propanoic acid	5.51	4.47	5.11	5.43	4.64	5.17	5.02	4.71	5.11	4.78
Butanoic acid	5.73	4.62	5.27	5.67	4.80	5.28	5.16	4.87	5.38	4.84
Pentanoic acid	6.17	4.99	5.54	5.96	5.07	5.57	5.21	5.21	5.65	5.11
3-Methylbut. acid	5.77	n.d.	5.14	5.54	4.74	4.77	4.97	4.87	n.d.	4.77
2,4-Pentandion	4.14	3.41	3.77	4.51	3.33	3.46	3.55	3.58	4.07	3.19
Dimethyl succinate	5.35	4.49	5.32	5.68	4.49	5.00	5.16	4.62	5.53	4.85
2-Methoxyethanol	5.00	4.43	5.05	5.26	4.53	5.07	4.91	4.66	5.10	4.79
2-Ethoxyethanol	4.94	4.46	4.96	5.23	4.31	n.d.	4.74	n.d.	n.d.	4.66
1,4-Dimethoxybenz.	5.42	4.03	4.63	5.35	3.91	4.17	4.35	3.99	5.19	4.31
2,5 Hexanedione	5.54	4.73	5.58	5.97	4.93	n.d.	5.47	5.26	5.85	5.20
dimethyl oxalate	4.71	3.79	4.59	4.87	3.97	4.38	4.41	4.52	4.87	4.30
dimethyl malonate	5.02	4.25	5.04	5.36	4.27	4.70	4.80	4.29	5.24	4.62
Cyclodecane	3.69	2.97	3.32	3.43	3.16	3.31	3.36	3.44	3.22	3.28
chloraceton	3.75	2.83	3.50	3.91	3.03	3.18	3.27	2.84	3.82	3.27
Benzoylchloride	4.46	3.36	4.09	4.34	3.62	3.69	3.76	3.69	4.09	3.59

Compound	Leonardite ¹ humic acid	Suw. River fulvic acid	Wask.Peat humic acid	Amherst humic acid	Elliot Soil fulvic acid	Suw. River humic acid	Nordic Lake humic acid	Was. Peat fulvic acid	Aldrich humic acid	Suw. River NOM
Hydroxyacetone	5.34	4.74	5.40	5.44	4.94	5.37	5.22	5.07	5.32	5.11
2-Ethylhexanol	5.37	4.49	4.91	5.11	4.65	4.55	4.43	4.64	4.52	4.43
Cycloheptanone	4.75	3.71	4.19	4.77	3.87	3.99	3.96	3.79	4.59	4.13
2-Phenylethylacetate	5.74	4.52	4.99	5.40	4.66	4.76	4.76	4.83	5.50	4.88
2-Chloronitrobenz.	5.59	4.24	n.d.	n.d.	n.d.	n.d.	4.75	4.57	5.26	4.74
3-Methoxybenzald.	6.20	4.53	5.26	5.82	4.78	5.15	5.04	4.74	5.85	5.14
2-Nitroanisoie	6.30	5.33	n.d.	n.d.	n.d.	n.d.	n.d.	n.d.	n.d.	n.d.
Propoxyethanol	n.d.	n.d.	4.91	5.30	4.12	4.58	4.63	4.06	5.19	4.49
Butoxyethanol	n.d.	n.d.	5.01	5.39	4.24	4.89	4.69	4.09	n.d.	4.53

¹Leonardite humic acid data are from: Niederer, C., Goss, K.-U., Schwarzenbach, R.P. Sorption equilibrium of a wide spectrum of organic vapors in Leonardite humic acid: Experimental setup and experimental data. *Environ. Sci. Technol.* **2006**, 40, 5368-5373.

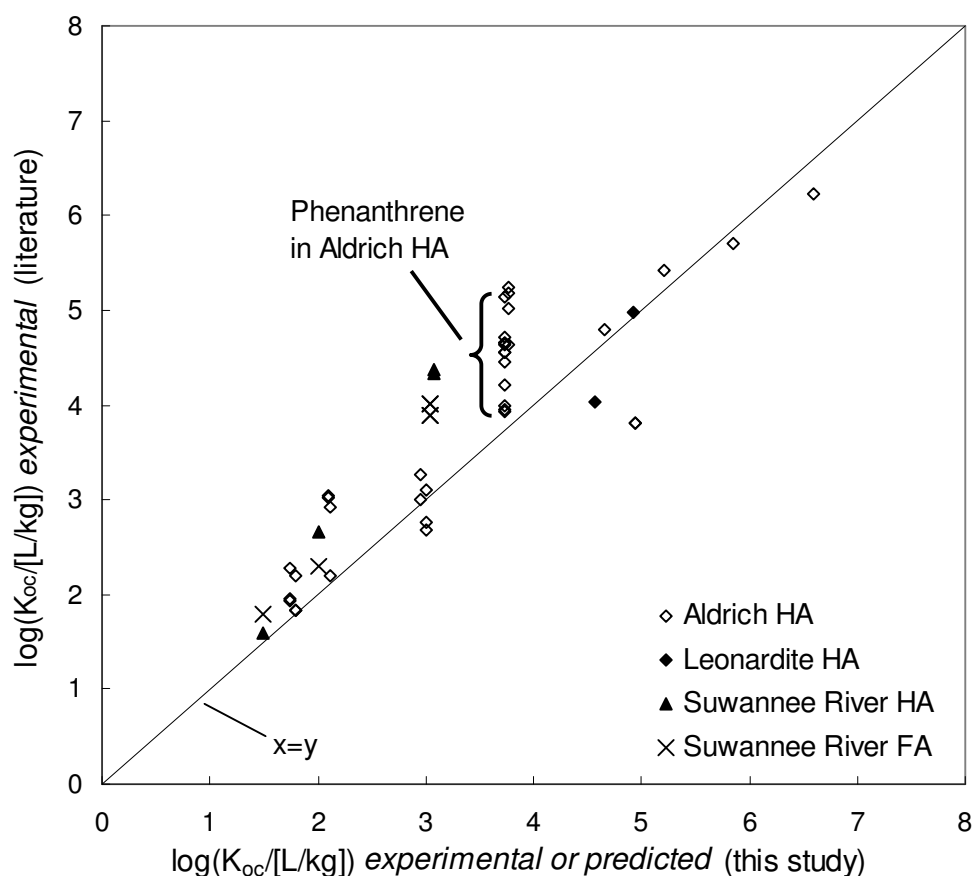
n.d.: no data

SI-4 Validation of experimental partition coefficients

NOM partition coefficients from the literature are mostly limited to nonpolar compounds measured in commercial HA such as Aldrich HA or in self-extracted materials. Apart from Suwannee River HA and FA, IHSS standards have seldom been used for such studies (see SI-1 for a detailed list of published partition data for various NOM). Therefore, only a few experimental values – for identical sorbates and NOM – are available for direct comparison. Some studies used the same NOM but different sorbates. In these cases it was possible to compare the experimental literature data with predicted partition coefficients from the present study (from equations shown in Table 2 in the article) in order to evaluate our experimental procedure. The partition data here have been measured from the gas phase at 15 °C while literature data are typically valid for sorption from the aqueous phase at 25 °C. Therefore, the experimental and the predicted data from our study had to be transformed before a comparison could be made. The air/water partition coefficients and the sorption enthalpies that have been used for the transformation are tabulated in SI-8.

Figure SI-2 compares the transformed NOM partition coefficients from the present study with K_{ioc} (i.e., organic-C/water partition coefficients) values from the literature for different natural organic materials (Aldrich HA, Suwannee River HA, Suwannee River FA, and Leonardite HA). Data points in vertical lines are related to one compound (indicated exemplarily for phenanthrene) and individual NOM are marked with unique symbols. As can be seen from Figure SI-2, the literature data for phenanthrene in Aldrich HA scatter over more than 1.2 log units. This indicates the overall experimental uncertainties in data from different labs using different methods. In general, Figure SI-2 shows good agreement between the literature data and the partition coefficients determined in this study taking into account the scatter in the literature data as well as the prediction errors of the pp-LFER models (about 0.3 log units, see SI-8).

Figure SI-2



SI-5 Comparison of the natural variability with literature data

In addition to the studies that used IHSS standards or commercial HA, numerous studies have been conducted with self-extracted NOM. SI-1 gives an overview of all experimental data including a short description of the used materials. For each compound between 2 and 22 experimental partition coefficients for 14 compounds measured in various HA, FA, and DOC (dissolved organic carbon) materials are provided. These experimental K_{ioc} values are presented by solid symbols in Figure SI-3. Partitioning data determined in Aldrich HA are not shown because of the concerns mentioned in the article. This data compilation shows that the K_{ioc} -values in organic materials from different origins scatter up to two log units. Part of this observed variability is likely caused by the use of different experimental procedures in different labs. Using the pp-LFER equations from Table 2 (see article), we predicted the respective sorption coefficients for the nine NOM tested here. This range of values is presented with open symbols

in Figure SI-3 (for data see SI-8). There is good agreement between the variability found in the literature data and the variability observed in this study. The data presented here, however, likely represent the natural variability in the sorption properties of NOM more realistically than the cited literature data, as this study is the only one that systematically investigated the variance of nine different types of NOM covering a wide spectrum of aquatic and terrestrial materials. In contrast, the literature data used different experimental procedures with more or less randomly chosen NOM. In conclusion, both the literature data and the data from this study clearly show that there is not only a single K_{ioc} value for a given compound, as is generally assumed in environmental fate modeling; instead, the K_{ioc} values scatter over more than one order of magnitude depending on the NOM considered.

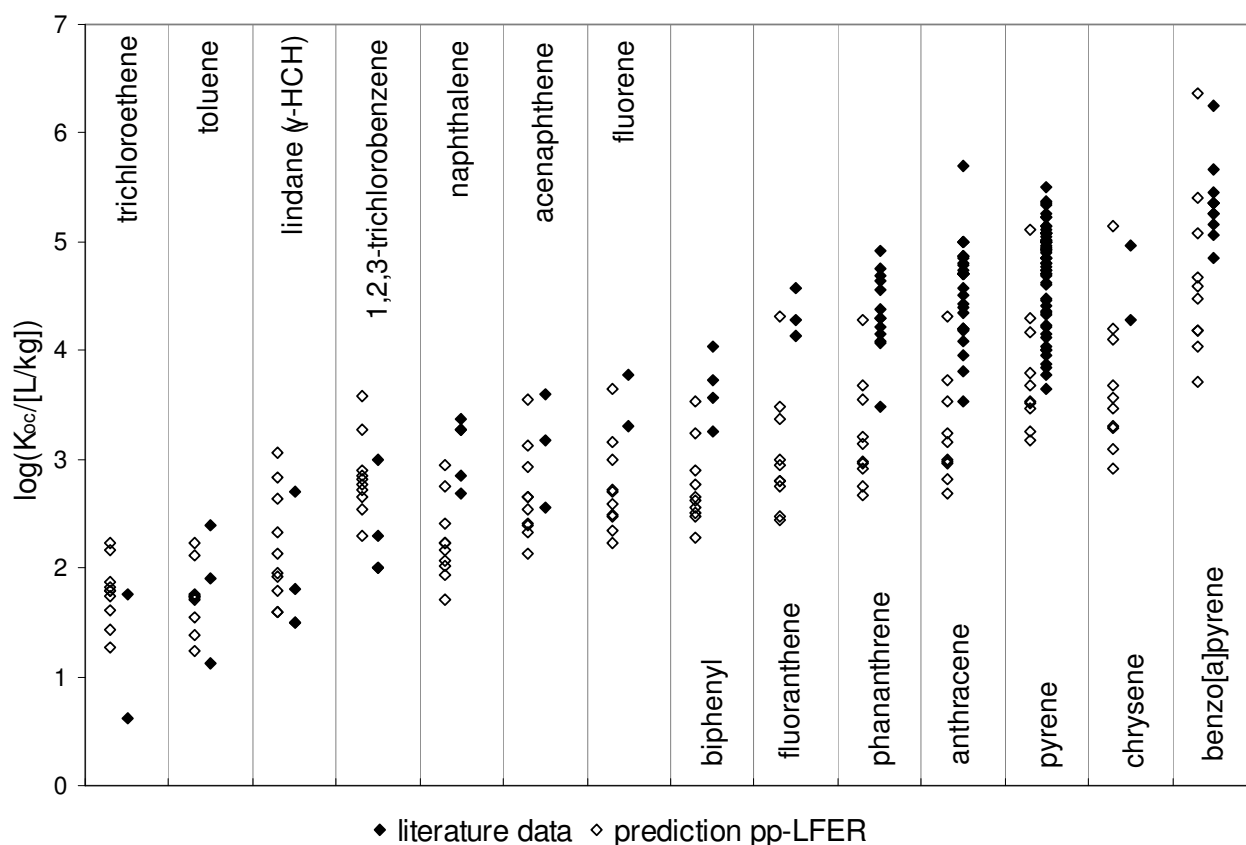
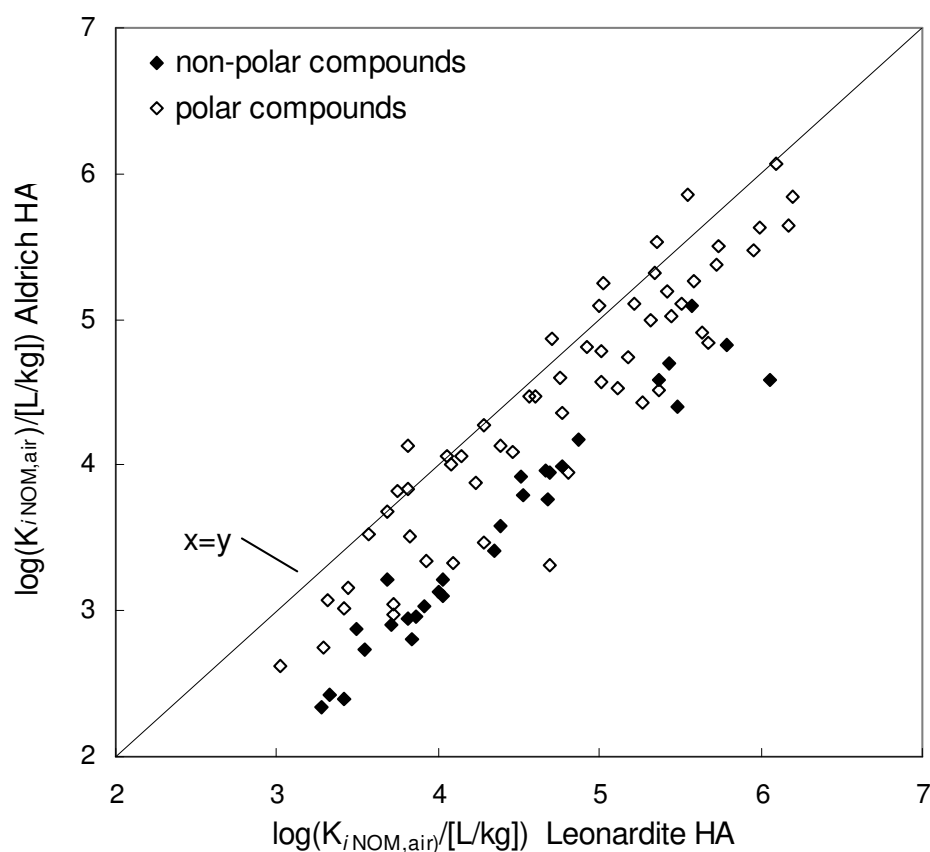


Figure SI-3 Natural variability in the sorption properties of NOM from different origins. The variability found in the literature (solid symbols) is compared with the variability found for 10 NOM in this study and in Niederer 2006a (open symbols).

SI-6 Comparison of polar and nonpolar compounds measured in Aldrich HA

Figure SI-4 shows experimental partition coefficients measured in Aldrich HA plotted against experimental partition coefficients measured in Leonardite HA. Polar and nonpolar compounds are discriminated and show different sorption behaviors.

Figure SI-4 Partition coefficients measured in Aldrich HA compared to partition coefficients measured in Leonardite HA



SI-7 Sorbate-specific descriptors used for the pp-LFER models

Compound	L_i [m ³ /m ³]	V_i [10 ⁻⁴ m ³ /mol]	B_i	A_i	S_i	References <i>A_i, B_i, V_i, L_i, S_i</i>
n-Decane	4.686	1.52	0.00	0.00	0.00	[1]
n-Undecane	5.191	1.66	0.00	0.00	0.00	[3,4]
n-Dodecane	5.696	1.80	0.00	0.00	0.00	[3,4]
n-Tridecane	6.200	1.96	0.00	0.00	0.00	[3,4]
n-Tetradecane	6.705 ^{a)}	2.08	0.00	0.00	0.00	[3,4]
1-Decene	4.658 ^{a)}	1.47	0.07 ^{a)}	0.00 ^{a)}	0.08 ^{a)}	[1]
1-Undecene	5.192 ^{a)}	1.62	0.07 ^{a)}	0.00 ^{a)}	0.08 ^{a)}	[3]
1-Dodecene	5.726 ^{a)}	1.76	0.07 ^{a)}	0.00 ^{a)}	0.08 ^{a)}	[3]
1-Tridecene	6.260 ^{a)}	1.90	0.07 ^{a)}	0.00 ^{a)}	0.08 ^{a)}	[3]
Cyclodecane	5.340	1.41	0.00 ^{a)}	0.00 ^{a)}	0.00 ^{a)}	[2]
Ethanol	1.485	0.45	0.48	0.37	0.42	[1]
Propan-1-ol	2.031	0.59	0.48	0.37	0.42	[1]
Butan-1-ol	2.601	0.73	0.48	0.37	0.42	[1]
Pentan-1-ol	3.106	0.87	0.48	0.37	0.42	[1]
Hexan-1-ol	3.610	1.01	0.48	0.37	0.42	[1]
Heptan-1-ol	4.115	1.15	0.48	0.37	0.42	[1]
Octan-1-ol	4.619	1.30	0.48	0.37	0.42	[1]
Nonan-1-ol	5.124	1.44	0.48	0.37	0.42	[1]
2-Ethylhexanol	4.380 ^{c)}	1.29	0.48 ^{a)}	0.37	0.39	[7]
Propan-2-ol	1.764	0.59	0.56	0.33	0.36	[1]
2-Methylpropan-1-ol	2.413	0.73	0.48	0.37	0.39	[1]
2-Methylpropan-2-ol	1.963	0.73	0.60	0.31	0.30	[1,3]
3-Methylbutan-1-ol	3.011	0.87	0.48	0.37	0.39	[1]
Benzyl alcohol	4.221	0.92	0.56	0.33	0.87	[1]
Cyclopentanol	3.241	0.76	0.56	0.32	0.54	[1]
Cyclohexanol	3.758	0.90	0.57	0.32	0.54	[1]
Hexafluoropropan-2-ol	1.390	0.70	0.10	0.77	0.55	[1]
2,2,2-Trifluoroethanol	1.224	0.50	0.25	0.57	0.60	[1]
Phenol	3.766	0.78	0.30	0.60	0.89	[2,8]
o-Cresol (2-Methylphenol)	4.218	0.92	0.30	0.52	0.86	[2,8]
m-Cresol (3-Methylphenol)	4.310	0.92	0.34	0.57	0.88	[2,8]
p-Cresol (4-Methylphenol)	4.312	0.92	0.31	0.57	0.87	[2,8]
4n-Nonylphenol	7.849	2.04	0.50	0.55	0.90	[11]
2-Chlorophenol	4.178	0.90	0.31	0.32	0.88	[2,5]
2-Pentanone	2.755	0.83	0.51	0.00	0.68	[1]
2-Hexanone	3.262	0.97	0.51	0.00	0.68	[1]
2-Heptanone	3.760	1.11	0.51	0.00	0.68	[1]
2-Octanone	4.257	1.25	0.51	0.00	0.68	[1]

Compound	L_i [m ³ /m ³]	V_i [10 ⁻⁴ m ³ /mol]	B_i	A_i	S_i	References A_i, B_i, V_i, L_i, S_i
2-Nonanone	4.735	1.39	0.51	0.00	0.68	[1]
2-Decanone	5.245	1.53	0.51	0.00	0.68	[1]
2-Undecanone	5.732	1.67	0.51	0.00	0.68	[1]
4-Methylpentan-2-one	3.089	0.97	0.51	0.00	0.65	[1]
Cyclopentanone	3.221	0.72	0.52	0.00	0.86	[1,3]
Cyclohexanone	3.792	0.86	0.56	0.00	0.86	[1,3]
Acetophenone	4.501	1.01	0.49	0.00	1.01	[1]
n-Butyl acetate	3.353	1.03	0.45	0.00	0.60	[1]
n-Pentyl acetate	3.844	1.17	0.45	0.00	0.60	[1]
Methyl benzoate	4.704	1.07	0.48	0.00	0.85	[1]
Benzyl acetate	5.012	1.21	0.65	0.00	1.06	[2,8]
2-Phenylethylacetate	5.36	1.35	0.65	0.00	1.10	[2,8]
Di-n-butyl ether	3.924	1.29	0.45	0.00	0.25	[1]
Di-n-pentylether	4.800 ^{c)}	1.58	0.45 ^{a)}	0.00 ^{a)}	0.25 ^{a)}	
1,4-Dioxane	2.892	0.68	0.64	0.00	0.75	[1]
Benzofurane	4.355	0.91	0.15	0.00	0.83	[2,3]
Dibenzofuran	6.716	1.27	0.17	0.00	1.02	[2,3]
Methyl phenyl ether	3.890	0.92	0.29	0.00	0.74	[1]
Benzene	2.786	0.72	0.14	0.00	0.52	[1,8]
Toluene	3.33	0.86	0.14	0.00	0.52	[1,8]
o-Xylene	3.939	1.00	0.16	0.00	0.56	[1,8]
n-Butylbenzene	4.730	1.28	0.15	0.00	0.51	[1]
n-Pentylbenzene	5.230	1.42	0.15	0.00	0.51	[1]
n-Hexylbenzene	5.720	1.56	0.15	0.00	0.50	[1]
Naphthalene	5.161	1.09	0.20	0.00	0.92	[1]
1-Methylnaphthalene	5.789	1.23	0.20	0.00	0.90	[1]
Biphenyl	6.014	1.32	0.26	0.00	0.99	[2,8]
Acenaphthene	6.469	1.26	0.20	0.00	1.04	[1]
Anthracene	7.568	1.45	0.28	0.00	1.34	[2,8]
Phenanthrene	7.632	1.45	0.29	0.00	1.29	[2,8]
Fluoranthene	8.827	1.58	0.20	0.00	1.55	[2,3]
Fluorene	6.922	1.36	0.20	0.00	1.03	[1,2]
Chrysene	10.334	1.82	0.36	0.00	1.73	[2,8]
Fluoranthene	8.827	1.58	0.20	0.00	1.55	[2,3]
Pyrene	8.833	1.71	0.29	0.00	1.59	[1,2]
Benz[a]pyrene	11.715	1.95	0.44	0.00	1.98	[2,3]
Tetrachlormethane	2.823	0.74	0.00	0.00	0.38	[1]
Trichloroethen	3.00	0.71	0.03	0.08	0.40	[1]
Lindane (γ -HCH)	7.467	1.58	0.68	0.00	0.91	[6]
1,2-Dichlorobenzene	4.518	0.96	0.04	0.00	0.78	[5]

Compound	L_i [m ³ /m ³]	V_i [10 ⁻⁴ m ³ /mol]	B_i	A_i	S_i	References A_i, B_i, V_i, L_i, S_i
1,3-Dichlorobenzene	4.410	0.96	0.02	0.00	0.73	[5]
1,4-Dichlorobenzene	4.435	0.96	0.02	0.00	0.75	[5]
1,4-Dibromobenzene	5.324	1.07	0.04	0.00	0.86	[2,3]
1,2,3-trichlorobenzene	5.419	1.08	0.00	0.00	0.86	[1,2]
1,2,4-Trichlorobenzene	5.248	1.08	0.00	0.00	0.81	[5]
1,2,3,4-Tetrachlorobenzene	6.171	1.21	0.00	0.00	0.92	[5]
1,2,4,5-Tetrachlorobenzene	5.926	1.21	0.00	0.00	0.86	[5]
Pentachlorobenzene	6.716	1.33	0.00	0.00	0.96	[5]
Bromobenzene	4.041	0.89	0.09	0.00	0.73	[5]
Iodobenzene	4.502	0.97	0.12	0.00	0.82	[5]
4-Fluorotoluene	3.366	0.88	0.10 ^{d)}	0.00	0.55	[2]
1,1,1,2-Tetrachloroethane	3.641	0.88	0.08	0.10	0.63	[1]
1,1,2,2-Tetrachloroethane	3.803	0.88	0.12	0.16	0.76	[1]
1-Chlorodecane	5.827 ^{a)}	1.64	0.10 ^{a)}	0.00 ^{a)}	0.40 ^{a)}	[3]
Benzaldehyde	4.008	0.87	0.39	0.00	1.00	[1]
1-Cyanopropane	2.548	0.69	0.36	0.00	0.90	[1]
Nitrobenzene	4.557	0.89	0.28	0.00	1.11	[1]
2-Nitrotoluene	4.878	1.03	0.28	0.00	1.11	[1]
Benzonitrile	4.039	0.87	0.33	0.00	1.11	[1]
Nitroethane	2.414	0.56	0.33	0.02	0.95	[1]
1-Nitropropane	2.894	0.71	0.31	0.00	0.95	[1]
2-Nitropropane	2.550	0.71	0.32	0.00	0.92	[1]
Chinoline	5.460	1.04	0.54	0.00	0.97	[1]
Propanoic acid	3.020 ^{c)}	0.61	0.45	0.60	0.65	[1]
Butanoic acid	3.473 ^{c)}	0.75	0.45	0.60	0.62	[1]
Pentanoic acid	3.969 ^{c)}	0.89	0.45	0.60	0.60	[1]
Hexanoic acid	4.430 ^{a)}	1.03	0.45	0.60	0.60	[1]
3-Methylbutanoic acid	3.140	0.89	0.50	0.60	0.57	[1]
2,4-Pentanedione	3.237 ^{c)}	0.84	0.63	0.00	0.78	[10]
Dimethyloxalat	3.202 ^{c)}	0.82	0.80 ^{d)}	0.00 ^{d)}	1.03 ^{d)}	
Dimethylmalonat	3.584 ^{c)}	0.96	0.80 ^{d)}	0.00 ^{d)}	1.03 ^{d)}	
Dimethyl succinate	4.133 ^{c)}	1.10	0.80 ^{d)}	0.003 ^{d)}	1.03 ^{d)}	
1,4-Dimethoxybenzene	5.044	1.12	0.50	0.00	1.00	[3,4]
2-Methoxyethanol	2.490	0.65	0.84	0.30	0.50	[1]
2-Ethoxyethanol	2.815	0.79	0.83	0.30	0.50	[1]
Propoxyethanol	3.34 ^{a)}	0.93	0.83	0.30	0.50	[1,10]
Butoxyethanol	3.81	1.07	0.83	0.30	0.50	[1]

A_i , B_i , V_i , L_i , and S_i and are referred to as $\Sigma\alpha^{H_2}$, $\Sigma\beta^{H_2}$, V_x , $\log L^{16}$ ($\log P_{16}$) and π^{H_2} in most references 1-8.

A_i : electron acceptor property of the molecule; B_i : electron donor property of the molecule; V_i : McGowan volume in units of (cm³/mol)/100; L_i : logarithmic hexadecane/air partition coefficient (25 °C, m³/m³); S_i : molecule's dipolarity/polarizability

^{a)}alpha and beta values assumed the same as homologue series, $\log(K_{i\text{hexadecane,air}})$ extrapolated from homologue series, based on it's proportionality to the number of carbons

^{b)} $K_{i\text{hexadecane,air}}$ value calculated by the SPARC online calculator (<http://ibmlc2.chem.uga.edu/sparc/>) September 25 2005.

^{c)}value measured in our lab, experimental method to be given in an upcoming publication.

^{d)}from in-house databases

References

1. Abraham, M.H.; Andonian-Haftvan, J.; Whiting, G.S.; Leo, A. and Taft, S. Hydrogen bonding. Part 34. The factors that influence the solubility of gases and vapours in water at 298 K, and a new method for its determination. *J. Chem. Soc. Perkin Trans. 2*. **1994**, 8: 1777-1791.
2. Abraham, M.H. Hydrogen bonding XXVII. Solvation parameters for functionally substituted aromatic compounds and heterocyclic compounds, from gas-liquid chromatographic data. *J. Chromatogr.* **1993**. 644: 95-139.
3. Abraham, M.H.; Chadha, H.S.; Whiting, G.S.; Mitchell, R.C. Hydrogen bonding. 32. An analysis of water-octanol and water-alkane partitioning and the $\Delta\log P$ parameter of Seiler. *J. Pharmaceut. Sci.* **1994**. 83(8): 1085-1100.
4. Abraham, M.H.; Grellier, P.L.; McGill, R.A.; Determination of olive oil-gas and hexadecane-gas partition coefficients, and calculation of the corresponding olive oil-water and hexadecane-water partition coefficients. *J. Chem. Soc. Perkin Trans. II*. **1987**. 797-803.
5. Poole, S.K.; Poole, C.F. Chromatographic models for the sorption of neutral organic compounds by soil from water and air. *J. Chromatogr. A*. **1999**. 845: 381-400.

6. Abraham, M.H.; Enomoto, K.; Clarke, E.D.; Sexton, G. Hydrogen bond basicity of the chlorogroup; hexachlorocyclohexanes as strong hydrogen bond bases. *J. Org. Chem.* **2002**. 67(14): 4782-4786.
7. Gunatilleka, A.D.; Poole, C.F. Models for estimating the nonspecific toxicity of organic compounds in short term bioassays. *Analyst.* **2000**. 125: 127-132.
8. Torres-Lapasio, J.R.; Garcia-Alvarez-Coque, M.C.; Roses, M.; Bosch, E.; Zissimos, A.M.; Abraham, M.H. Analysis of a solute polarity parameter in reversed-phase liquid chromatography on a linear solvation relationship basis. *Anal. Chim. Acta.* **2004**. 515: 209-227.
9. Abraham, MH; Andonian-Haftven, J.; Du, CM; Osei-Owusu, JP; Sakellariou, P; Shuely, WJ; Poole, CF; Poole, SK. Comparison of uncorrected retention data on a capillary and a packed hexadecane column with corrected retention data on a packed squalane column. *J. Chromatogr. A.* **1994**. 688: 125-134.
10. Abraham, MH; Acree, WE Jr. Correlation and prediction of partition coefficients between the gas phase and water, and the solvents dodecane and undecane. *New J. Chem.* **2004**. 12: 1538-1543.
11. Nguyen, T., Goss, K.-U., Ball, W.P. Polyparameter linear free energy relationships for estimating the equilibrium partition of organic compounds between water and the natural organic matter in soils and sediments. *Environ. Sci. Technol.* **2005**, 39: 913-923.

SI-8 pp-LFER fits for 10 natural organic materials: prediction of $K_{iNOM,air}$ and $K_{iNOM-oc,water}$ partition coefficients

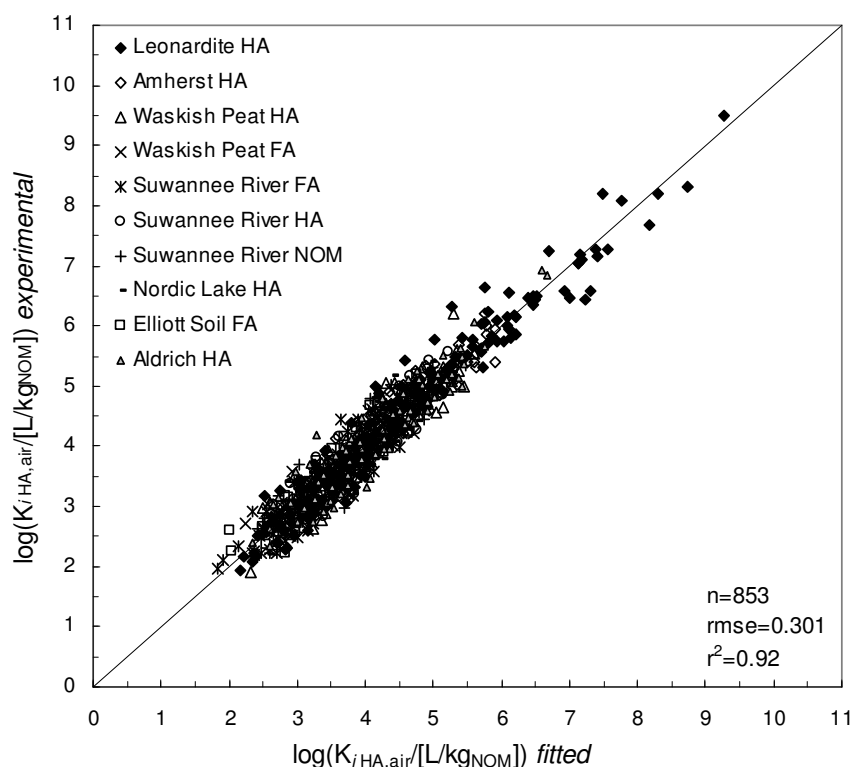


Figure SI-5 shows experimental NOM/air partition coefficients plotted against fitted NOM/air partition coefficients in ten tested natural organic materials. Data for Leonardite HA are from [1].

This table provides additional statistical information about the pp-LFER models presented in Table 2 in the article. Standard errors of sorbent descriptors are in parenthesis.

natural organic matter	$\ln_{NOM,air}$	$V_{NOM,air}$	$b_{NOM,air}$	$a_{NOM,air}$	$S_{NOM,air}$	$C_{NOM,air}$	r^2	1rmse	n
Leonardite HA ²	0.81 (0.07)	-0.08 (0.27)	1.88 (0.15)	3.62 (0.13)	1.14 (0.17)	-0.65 (0.15)	0.96	0.32	158
Amherst HA	0.55 (0.11)	0.39 (0.41)	1.81 (0.24)	3.39 (0.25)	1.26 (0.26)	-0.20 (0.24)	0.90	0.27	77
Waskish Peat HA	0.60 (0.10)	0.51 (0.40)	1.78 (0.23)	3.68 (0.25)	0.95 (0.26)	-0.82 (0.25)	0.89	0.29	84
Nordic Lake HA	0.64 (0.16)	0.08 (0.57)	1.34 (0.33)	3.27 (0.28)	0.71 (0.38)	-0.35 (0.29)	0.85	0.29	61
Suwannee River HA	0.54 (0.13)	0.35 (0.48)	1.41 (0.26)	3.40 (0.28)	0.85 (0.32)	-0.35 (0.29)	0.86	0.28	65
Suwannee River NOM	0.78 (0.11)	-0.53 (0.42)	1.62 (0.22)	3.04 (0.22)	0.64 (0.28)	-0.35 (0.28)	0.91	0.24	64
Waskish Peat FA	0.55 (0.14)	0.81 (0.50)	1.01 (0.30)	3.52 (0.27)	0.97 (0.34)	-0.97 (0.30)	0.86	0.28	65
Elliott Soil FA	0.72 (0.08)	0.22 (0.34)	1.67 (0.18)	3.40 (0.21)	0.65 (0.23)	-1.15 (0.27)	0.89	0.26	73
Suwannee River FA	0.60 (0.07)	0.68 (0.28)	1.58 (0.17)	3.52 (0.16)	0.76 (0.19)	-1.30 (0.21)	0.92	0.24	84
Aldrich HA	0.94 (0.12)	-1.09 (0.48)	2.67 (0.27)	3.13 (0.29)	0.48 (0.33)	-0.38 (0.31)	0.89	0.32	74

¹rmse: root mean square error in log units

This table provides pp-LFER equations for the prediction of NOM-oc/water partition coefficients at 15 °C (standard errors of regression are in parenthesis). The equations were fitted to NOM-oc/water partition coefficients calculated from experimental NOM/air partition coefficients (15 °C, 98% rh), the organic-C content of the corresponding natural organic materials (see Table 1 in the article) and water/air partition coefficients (see Supporting Information section in Niederer et al. 2006). These water/air partition coefficients were measured at 25 °C; air/water partition coefficients at 15 °C were calculated using standard enthalpies of transfer from water to air $\Delta_{aw}H_i$ that were estimated by pp-LFER equations published in Mintz et al. 2007.

$\log(K_{i\text{NOM-oc,water}}/[\text{L/kg}_{\text{oc}}])$	$\ln_{\text{NOM-oc,water}}$	$\mathbf{v}_{\text{NOM-oc,water}}$	$\mathbf{b}_{\text{NOM-oc,water}}$	$\mathbf{a}_{\text{NOM-oc,water}}$	$\mathbf{S}_{\text{NOM-oc,water}}$	$\mathbf{C}_{\text{NOM-oc,water}}$
Leonardite HA	0.30 (0.09)	2.78 (0.35)	-3.09 (0.20)	-0.17 (0.16)	-0.74 (0.23)	-0.43 (0.18)
Amherst HA	0.00 (0.13)	3.50 (0.52)	-3.17 (0.28)	-0.09 (0.30)	-0.37 (0.34)	-0.19 (0.31)
Waskish Peat HA	0.01 (0.12)	3.75 (0.50)	-3.29 (0.26)	0.24 (0.30)	-0.62 (0.34)	-0.80 (0.32)
Nordic Lake HA	0.20 (0.20)	2.75 (0.70)	-3.63 (0.40)	-0.41 (0.34)	-1.20 (0.46)	-0.12 (0.35)
Suwannee River HA	0.06 (0.16)	3.12 (0.58)	-3.53 (0.32)	-0.26 (0.34)	-1.04 (0.39)	-0.14 (0.36)
Suwannee River NOM	0.29 (0.13)	2.19 (0.50)	-3.39 (0.26)	-0.74 (0.26)	-1.25 (0.34)	0.03 (0.33)
Waskish Peat FA	0.08 (0.17)	3.58 (0.60)	-3.91 (0.36)	-0.14 (0.33)	-0.92 (0.41)	-0.80 (0.37)
Elliot Soil FA	0.19 (0.10)	3.13 (0.40)	-3.37 (0.22)	-0.22 (0.24)	-1.11 (0.28)	-0.92 (0.32)
Suwannee River FA	0.05 (0.08)	3.68 (0.32)	-3.51 (0.19)	-0.11 (0.18)	-0.96 (0.22)	-1.07 (0.23)
Aldrich HA	0.45 (0.14)	1.81 (0.57)	-2.31 (0.32)	-0.40 (0.35)	-1.25 (0.39)	-0.38 (0.37)

Standard errors of sorbent descriptors are in parenthesis

References:

- Niederer, C., Goss, K.-U., Schwarzenbach, R.P. Sorption equilibrium of a wide spectrum of organic vapors in Leonardite humic acid: Modeling of experimental data. *Environ. Sci. Technol.* **2006**, 40, 5374-5379.
- Mintz, C., Clark, M., Acree, W.E. Jr., Abraham, M.H. Enthalpy of salvation correlations for gaseous solutes dissolved in water and in 1-octanol based on the Abraham model. *J. Chem. Inf. Model.* **2007**, 47, 115-121.

Predicted partition NOM org-C/water partition coefficients for 10 natural organic materials

All partition coefficients are in [L/kg_{oc}] at 25 °C. Sorption enthalpies are in [kJ·mol⁻¹]

Compound	Sorpt. enthalpy experim. ^{a)} predicted ^{b)}	log(K _{air,water}) (mol/l)/ (mol/l)	Aldrich HA log(K _{oc,water}) ^{f)} f _{oc} = 0.60	Suw Riv HA log(K _{oc,water}) ^{g)} f _{oc} = 0.53	Leonar. HA ⁱ⁾ log(K _{oc,water}) ^{g)} f _{oc} = 0.64	Suw Riv FA log(K _{oc,water}) ^{g)} f _{oc} = 0.53	Suw Riv NOM log(K _{oc,water}) ^{g)} f _{oc} = 0.53	Elliott Soil FA log(K _{oc,water}) ^{g)} f _{oc} = 0.50	W. Peat HA log(K _{oc,water}) ^{g)} f _{oc} = 0.55	W. Peat FA log(K _{oc,water}) ^{g)} f _{oc} = 0.54	Nord Lake HA log(K _{oc,water}) ^{g)} f _{oc} = 0.53	Amherst HA log(K _{oc,water}) ^{h)} f _{oc} = 0.53
Tetrachlorometh.	-30.3	-0.06 ^{h)}	<i>n.d.</i>	1.90	2.07	1.33	1.85	1.46	1.75	1.69	1.94	2.26
Trichloroethene	-37.2	0.32 ^{h)}	1.87	1.90	2.15	1.33	1.88	1.50	1.79	1.67	1.95	2.27
1,2-Dichlorobenz.	-53.3	1.00 ^{h)}	<i>n.d.</i>	2.09	2.76	1.66	2.18	1.86	2.13	2.03	2.19	2.65
1,4-Dichlorobenz.	-53.5	0.74 ^{h)}	2.33	2.25	2.88	1.81	2.32	2.00	2.28	2.19	2.35	2.79
1,2,3-Trichloroben.	-53.3	0.91 ^{h)}	2.95	2.71	3.59	2.36	2.89	2.61	2.83	2.75	2.87	3.31
1,2,4-Trichloroben.	-53.3	0.82 ^{h)}	2.86	2.67	3.48	2.31	2.81	2.54	2.77	2.70	2.82	3.24
Lindane (γ-HCH)	-89.0	4.16 ^{h)}	2.72	1.52	3.02	1.57	1.89	1.88	2.11	1.54	1.71	2.45
Decane	-46.4	-2.32 ^{h)}	4.65	5.01	5.25	4.84	4.81	4.88	5.07	5.13	5.09	5.26
Undecane	-62.8	-2.33 ^{d)}	4.88	5.24	5.55	5.15	5.04	5.18	5.35	5.43	5.34	5.50
Dodecane	-64.1	-2.44 ^{d)}	5.31	5.67	6.06	5.65	5.46	5.68	5.84	5.93	5.78	5.94
Tridecane	-59.6	-2.56 ^{d)}	5.78	6.13	6.60	6.19	5.93	6.22	6.36	6.47	6.26	6.42
Benzene	-36.1	0.63 ^{h)}	1.46	1.47	1.74	0.89	1.43	1.03	1.38	1.20	1.48	1.93
Toluene	-40.3	0.65 ^{h)}	1.77	1.76	2.12	1.26	1.73	1.40	1.73	1.57	1.79	2.24
o-Xylene	-45.9	0.66 ^{h)}	2.23	2.16	2.64	1.74	2.14	1.89	2.20	2.03	2.21	2.67
Naphthalene	-54.7	1.76 ^{h)}	2.41	2.05	2.96	1.71	2.19	1.93	2.23	2.01	2.16	2.74
Biphenyl	-68.9	1.95 ^{h)}	2.87	2.46	3.55	2.26	2.59	2.47	2.76	2.52	2.58	3.22
Anthracene	-79.6	2.80 ^{e)}	3.50	2.75	4.32	2.66	3.08	2.96	3.22	2.93	2.95	3.69
Acenaphthene	-59.3	2.31 ^{h)}	2.94	2.34	3.56	2.13	2.62	2.41	2.64	2.41	2.52	3.10
Phenanthrene	-79.0	2.85 ^{h)}	3.52	2.71	4.28	2.63	3.06	2.94	3.18	2.88	2.92	3.63
Pyrene	-98.3	3.32 ^{h)}	3.79	3.07	5.02	3.12	3.53	3.48	3.63	3.54	3.39	4.03
Fluorene	-75.3	2.46 ^{h)}	3.01	2.36	3.65	2.21	2.66	2.50	2.71	2.48	2.56	3.13
Chrysene	-112.9	4.56 ^{e)}	4.15	2.84	5.15	3.02	3.45	3.45	3.61	3.24	3.18	4.01
Fluoranthene	-96.2	3.35 ^{e)}	3.79	2.89	4.77	2.88	3.34	3.24	3.44	3.19	3.16	3.89
Benzo[a]pyrene	-128.1	4.79 ^{e)}	5.32	3.63	6.36	3.93	4.43	4.44	4.57	4.10	4.04	4.96
Dibenzofuran	-50.5	2.37 ^{e)}	3.10	2.46	3.71	2.26	2.78	2.57	2.77	2.54	2.66	3.20
Quinoline	-69.6	4.20 ^{h)}	1.14	0.19	1.33	-0.09	0.50	0.21	0.51	0.01	0.31	1.04
p-Cresol	-75.1	4.50 ^{h)}	0.99	0.72	1.63	0.37	0.64	0.51	1.02	0.61	0.71	1.42
4n-Nonylphenol	-104.9	4.28 ^{e)}	<i>n.d.</i>	3.28	4.77	3.54	3.10	3.60	4.05	3.66	3.32	4.15

- a) comparable sorption enthalpies in different NOM are assumed; experimental sorption enthalpies were measured for Leonardite HA published in: Niederer, C., Goss, K.-U., Schwarzenbach, R.P. Sorption equilibrium of a wide spectrum of organic vapors in Leonardite humic acid: experimental setup and experimental data. *Environ. Sci. Technol.* **2006**, 40: 5368-5373.
- b) sorption enthalpies are predicted using the empirical equation $\Delta H_{\text{sorb}}[\text{kJ/mol}] = -4.28 \cdot \ln K_{i\text{HA,air}}/[\text{L/kg}] - 10.57$ determined in the study referenced in a).
- c) predicted with an pp-LFER for water/air partitioning from ref: Goss, K.-U. Predicting the equilibrium partitioning of organic compounds using just one linear solvation energy relationship (LSER). *Fluid Phase Equilib.* **2005**. 19-22.
- d) extrapolated from homologue series, based on it's proportionality to the number of carbons
- e) Schwarzenbach, R.P., Gschwend, P.M, Imboden, D.M. Environmental Organic Chemistry, 2nd Edition, **2003**, Wiley-Interscience, Hoboken, New Jersey.
- f) Mao, J.-D., Hu, W.-G., Schmidt-Rohr, K., Davies, G., Ghabbour, E.A., Xing, B. Quantitative characterization of humic substances by solid-state carbon-13 nuclear magnetic resonance. *Soil Sci. Soc. Am. J.* **2000**. 64: 873-883.
- g) Int. Humic Substance Society IHSS, <http://www.ihss.gatech.edu> (Elemental analyses by Huffman Laboratories, Wheat Ridge, CO, USA)
- h) Abraham, M.H.; Andonian-Haftvan, J.; Whiting, G.S.; Leo, A.; Taft, R.S. Hydrogen Bonding. Part 34. The factors that influence the solubility of gases and vapours in water at 298K, and a new method for its determination. *J. Chem. Soc. Perkin Trans. 2.* **1994**. 8: 1777-1791.
- i) for equation see: Niederer, C., Goss, K.-U., Schwarzenbach, R.P. Sorption equilibrium of a wide spectrum of organic vapors in Leonardite humic acid: Modeling of experimental data. *Environ. Sci. Technol.* **2006**, 40, 5374-5379.

SI-9 Elemental analysis and ^{13}C -NMR data of the tested NOM

Figure SI-6

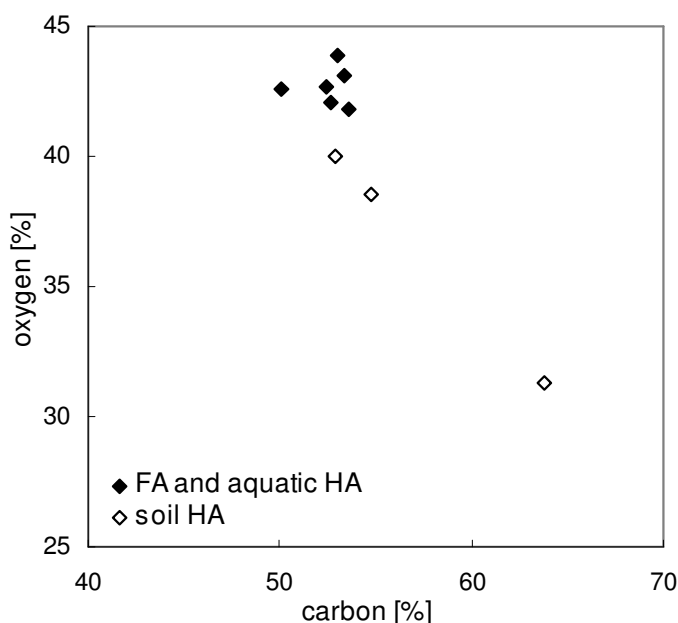


Figure SI-7

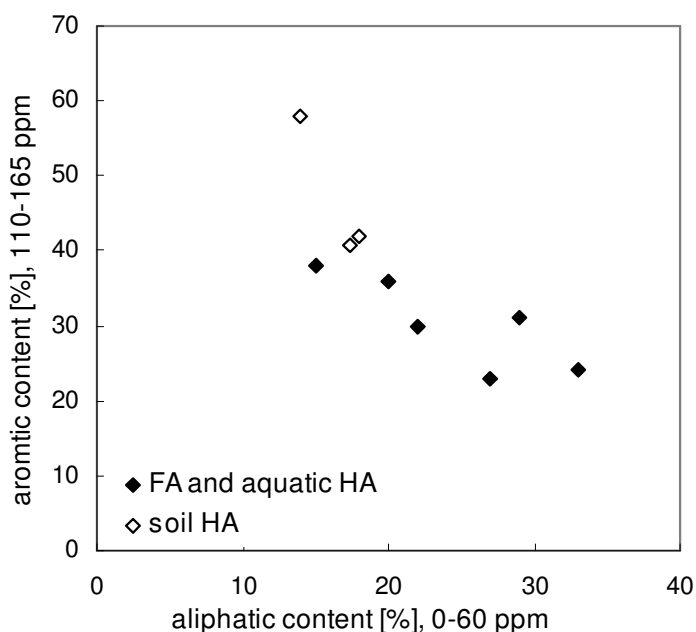


Table 1 in the article shows elemental analysis data, ^{13}C -NMR data and acid/base properties of the tested NOM. Figure SI-6 shows that the aquatic HA and all FA exhibit higher oxygen to carbon ratios compared to the terrestrial HA. In addition, the terrestrial HA show increased aromatic carbon contents and decreased aliphatic contents compared to the FA and the aquatic HA which exhibit a scatter in their aliphatic content between 15 and 33% at aromatic contents <38% (Figure SI-7). Based on potentiometric titrations, Ritchie et al. reported carboxylic contents for IHSS materials in the following order: terrestrial FA > aquatic FA > aquatic HA > terrestrial HA. The average contents of carboxylic groups were $12.8 \pm 1.5 \text{ meq} \cdot \text{gC}^{-1}$ for fulvic acids and $8.5 \pm 0.9 \text{ meq} \cdot \text{gC}^{-1}$ for humic acids respectively. Table 1 (article) shows that the fulvic acids used in this study exhibit also substantially higher carboxylic contents compared to the humic acid, e.g., Suwannee River FA shows a 60% higher content of carboxylic groups compared to Leonardite HA.

Ref: Internat. Humic Substances Society, IHSS. <http://www.ihss.gatech.edu>

Ritchie, J.D., Perdue, E.M. Proton-binding study of standard and reference fulvic acids, humic acids, and natural organic matter. *Geochim. Cosmochim. Acta*. 2003, 67, 85-96.

SI-10 Polyparameter model: regression constant $c_{\text{NOM,air}}$

As discussed in the article, we found that the observed shift in the global sorption capacity of the various NOM types cannot be explained by the observed minor differences in the interaction descriptors of the pp-LFER; in contrast to what one might expect this overall shift of the sorption constants is not reproduced in the constants, $c_{\text{NOM,air}}$, of the pp-LFER equations. The $c_{\text{NOM,air}}$ value represents the hypothetical sorption of a compound without any interactions. These values involve a huge extrapolation from real compounds with substantial interactions to zero interactions. Even small experimental errors will cause large errors in such extrapolated values so that their interpretation becomes meaningless. This is illustrated in Figure SI-8 with simple regression models [$y(x) = a \cdot x + c$]: three datasets and the corresponding linear regression models are shown. These regressions exhibit only small differences in their slopes (0.96; 1.06; 1.10); Nevertheless, high errors can be observed when extrapolating over a wide range (i.e., to $x = 0$ where $y(x=0) = c$). Consequently, the interpretation of the regression constant becomes meaningless. For more details see Pankow (1991).

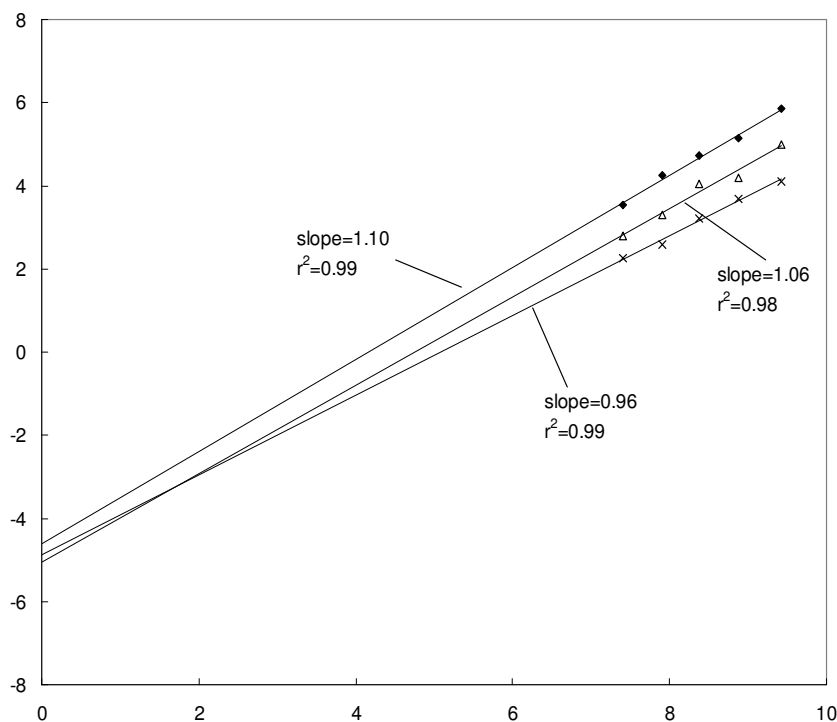


Figure SI-8: Arbitrary example illustrating the impact of small experimental errors in the slope on the difference between the y-values when extrapolated over a large range.

Reference: Pankow, J.F. Common gamma-intercept and single compound regressions of gas particle partitioning data vs. $1/T$. *Atmos. Environ.* **1991**, 2229-2239.

SI-11 Influence of relative humidity on the partition behavior of organic compounds

Experimental Suwannee River FA/air partition coefficients at 45% rh and 98% rh (15 °C). Compounds whose partition coefficients deviate more than 0.5 log units at 45% and 98% rh are in **bold**.

polar compounds			nonpolar compounds		
	log($K_{iFA,air}/[L/kg_{FA}]$)			log($K_{iFA,air}/[L/kg_{FA}]$)	
	45% rh	98% rh		45% rh	98% rh
Propan-1-ol	2.70	2.92	n-Decane	2.81	2.22
Butan-1-ol	3.00	3.07	n-Undecane	3.38	3.04
Pentan-1-ol	3.54	3.46	n-Dodecane	3.87	3.58
Hexan-1-ol	3.92	3.75	Tridecane	4.08	3.66
Heptan-1-ol	4.40	4.23	Tetradecane	5.04	4.60
Octan-1-ol	4.92	4.73	1-Decene	2.91	2.56
3-Methylbutan-1-ol	3.35	3.27	1-Undecene	3.32	3.13
Cyclopentanol	3.12	3.38	1-Dodecene	3.81	3.48
Cyclohexanol	3.50	3.57	1-Tridecene	4.33	4.02
Phenol	4.39	4.92	n-Butylbenzene	2.98	2.49
2-Chlorophenol	3.84	3.87	n-Pentylbenzene	3.48	3.02
Benzyl alcohol	4.62	4.92	n-Hexylbenzene	4.00	3.60
Hexan-2-one	2.93	2.45	1,3,5-Trimethylbenzene	2.41	1.85
Heptan-2-one	3.27	2.87	1,2,4-Trimethylbenzene	2.54	1.96
Octan-2-one	3.67	3.30	Naphthalene	3.55	3.22
Non-2-anone	4.21	3.89	1-Methylnaphthalene	4.07	3.78
Decan-2-one	4.72	4.42	Biphenyl	4.45	4.23
Undecan-2-one	5.08	4.88	1,2-Dichlorobenzene	2.91	2.74
Cyclohexanone	3.20	2.98	1,3-Dichlorobenzene	2.80	2.63
Cycloheptanone	3.78	3.71	1,4-Dichlorobenzene	2.75	2.62
Acetophenone	3.71	3.76	Iodobenzene	2.82	2.59
n-Pentyl acetate	3.28	2.87	1,2,4-Trichlorobenzene	3.45	3.25
Methyl benzoate	3.45	3.20	1,1,2,2-Tetrachloroetha.	2.64	2.42
Dipentylether	3.88	3.52	1,4-Dibromobenzene	3.58	3.44
Methyl phenyl ether	2.58	2.22			
Benzaldehyde	3.45	3.13			
1-Cyanopropane	2.70	2.73			
Nitrobenzene	3.52	3.49			
2-Nitrotoluene	3.79	3.66			
Propanoic acid	3.89	4.47			
Butanoic acid	4.46	4.62			
Pentanoic acid	4.85	4.99			
Dimethyl oxalate	3.03	3.79			
Dimethyl malonate	3.61	4.25			
Dimethyl succinate	3.96	4.49			
2,5 Hexandione	4.02	4.73			

polar compounds			nonpolar compounds		
	$\log(K_{iFA,air}/[L/kg_{FA}])$			$\log(K_{iFA,air}/[L/kg_{FA}])$	
	45% rh	98% rh		45% rh	98% rh
2-Methoxyethanol	3.33	4.43			
2-Ethoxyethanol	3.52	4.46			
Benzylacetate	4.17	3.98			
2-Phenylethylacet.	4.87	4.52			

Figure SI-9 compares partition coefficients measured in Suwannee River FA at 45% and 98% rh. The small highly polar compounds are marked in the table above. **Figure SI-10** compares partition coefficients in Leonardite HA measured at 45% and 98% rh (from Niederer et al. *Environ. Sci. Technol.* **2006**, 40, 5368-5373). Small highly polar compounds are: phenol, propanoic acid, and dimethyl succinate.

Figure SI-9 Suwannee River FA

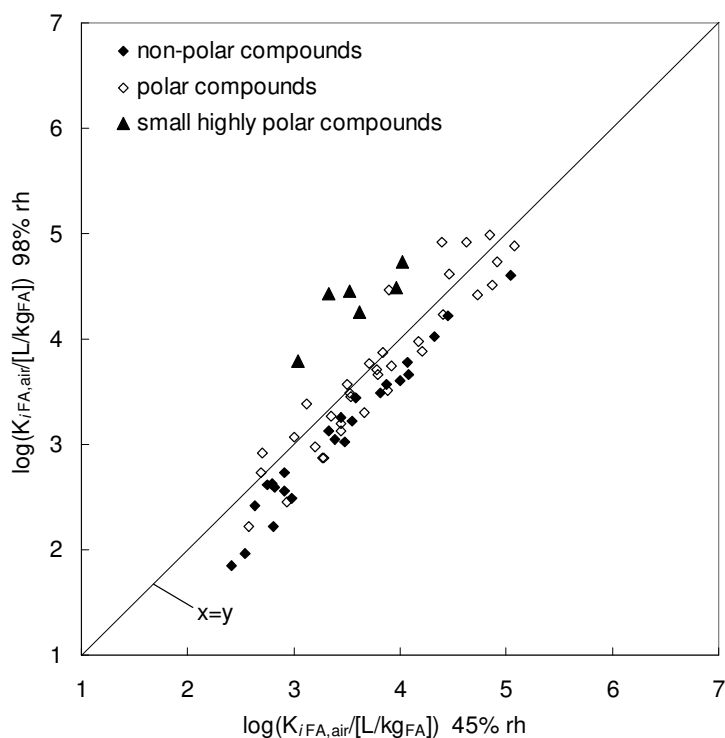
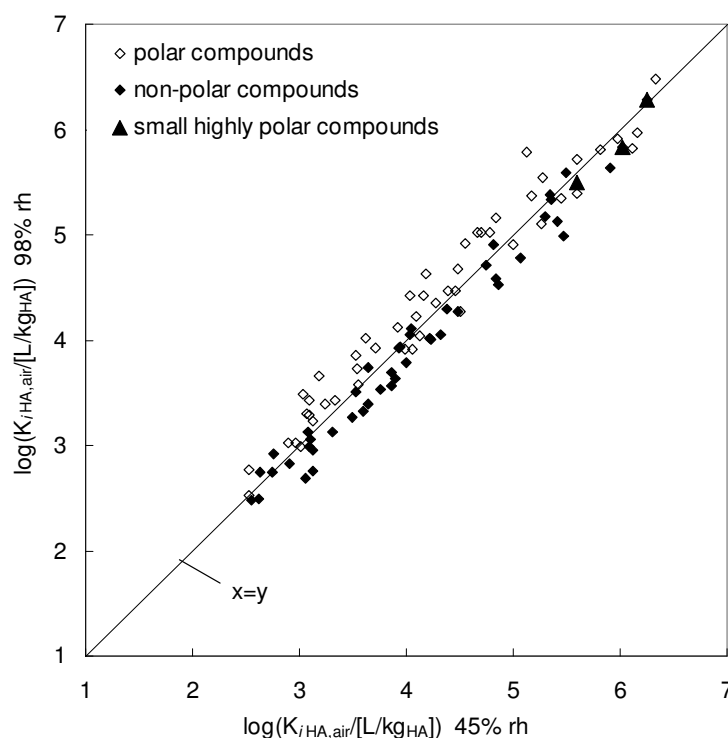


Figure SI-10 Leonardite HA



SI-12 Experimental partition coefficients of small highly polar compounds

experimental partition coefficients										
	Leonardite HA <i>reference</i> log(K _{HA,air})	Suw. River FA -1.06 log(K _{FA,air})	Waskish Peat HA -0.56 log(K _{HA,air})	Amherst HA -0.16 log(K _{HA,air})	Elliot Soil FA -0.97 log(K _{FA,air})	Suw. River HA -0.77 log(K _{HA,air})	Nordic Lake HA -0.74 log(K _{HA,air})	Waskish Peat FA -0.86 log(K _{FA,air})	Aldrich HA -0.50 log(K _{HA,air})	Suw. River NOM -0.82 log(K _{NOM,air})
mean average deviation ¹										
Hydroxyacetone	5.34	4.74	5.40	5.44	4.94	5.37	5.22	5.07	5.32	5.11
2-Methoxyethanol	5.00	4.43	5.05	5.26	4.53	5.07	4.91	4.66	5.10	4.79
2-Ethoxyethanol	4.94	4.46	4.96	5.23	4.31	<i>n.d.</i>	4.74	<i>n.d.</i>	<i>n.d.</i>	4.66
Dimethyl succinate	5.35	4.49	5.32	5.68	4.49	5.00	5.16	4.62	5.53	4.85
Dimethyl oxalate	4.71	3.79	4.59	4.87	3.97	4.38	4.41	4.52	4.87	4.30
Dimethyl malonate	5.02	4.25	5.04	5.36	4.27	4.70	4.80	4.29	5.24	4.62
2,5-Hexanedione	5.54	4.73	5.58	5.97	4.93	<i>n.d.</i>	5.47	5.26	5.85	5.20

predicted partition coefficients: (partition coefficient measured in Leonardite HA) - (mean average deviation)										
	Leonardite HA log(K _{HA,air})	Suw. River FA log(K _{FA,air})	Waskish Peat HA log(K _{HA,air})	Amherst HA log(K _{HA,air})	Elliot Soil FA log(K _{FA,air})	Suw. River HA log(K _{HA,air})	Nordic Lake HA log(K _{HA,air})	Waskish Peat FA log(K _{FA,air})	Aldrich HA log(K _{HA,air})	Suw. River NOM log(K _{NOM,air})
Hydroxyacetone		4.28	4.78	5.18	4.37	4.57	4.60	4.48	4.84	4.52
2-Methoxyethanol		3.94	4.44	4.84	4.03	4.23	4.26	4.14	4.50	4.18
2-Ethoxyethanol		3.88	4.38	4.78	3.97	<i>n.d.</i>	4.20	<i>n.d.</i>	<i>n.d.</i>	4.12
Dimethyl succinate		4.29	4.79	5.19	4.38	4.58	4.61	4.49	4.85	4.53
Dimethyl oxalate		3.65	4.15	4.55	3.74	3.94	3.97	3.85	4.21	3.89
Dimethyl malonate		3.96	4.46	4.86	4.05	4.25	4.28	4.16	4.52	4.20
2,5-Hexanedione		4.48	4.98	5.38	4.57	<i>n.d.</i>	4.80	4.68	5.04	4.72

(experimental partition coefficients) - (predicted partition coefficients)										
	Leonardite HA	Suw. River FA	Wask. Peat HA	Amherst HA	Elliot Soil FA	Suw. River HA	Nordic Lake HA	Wask. Peat FA	Aldrich HA	Suw. River NOM
Hydroxyacetone		-0.46	-0.62	-0.26	-0.57	-0.80	-0.62	-0.59	-0.48	-0.59
2-Methoxyethanol		-0.49	-0.61	-0.42	-0.50	-0.84	-0.65	-0.52	-0.60	-0.61
2-Ethoxyethanol		-0.58	-0.58	-0.45	-0.34	<i>n.d.</i>	-0.54	<i>n.d.</i>	<i>n.d.</i>	-0.54
Dimethyl succinate		-0.20	-0.53	-0.49	-0.11	-0.42	-0.55	-0.13	-0.68	-0.32
Dimethyl oxalate		-0.14	-0.44	-0.32	-0.23	-0.44	-0.44	-0.67	-0.66	-0.41
Dimethyl malonate		-0.29	-0.58	-0.50	-0.22	-0.45	-0.52	-0.13	-0.72	-0.42
2,5-Hexanedione		-0.25	-0.60	-0.59	-0.36	<i>n.d.</i>	-0.67	-0.58	-0.81	-0.48

¹please find more information in the article

SI-13 Temperature dependence study of partition coefficients in Suwannee River FA

Compound	20 °C	30 °C	40 °C	50 °C	60 °C	70 °C	75 °C	80 °C	90 °C	n	r ² van't Hoff Plot	<i>exp.</i> Δ _{abs} H	<i>exp.</i> Δ _{abs} H
	ln(K _{FA,air} /[L/kg _{FA}])											[kJ/mol] Suw. River FA	[kJ/mol] Leonardite HA
Phenol	10.88	10.27	9.18							3	0.970	-62.3	-65.1
p-Cresol	11.51	11.01	10.06	9.30	8.28					5	0.980	-63.6	-75.1
4-Chlorophenol		12.94	12.00	11.17	10.17					4	0.997	-74.2	-83.9
3,4-Dichlorophenol				13.05	12.26	11.39		10.54		4	0.998	-76.8	<i>n.d.</i>
1-Undecanol	13.68	12.52	11.26	10.43	9.43	8.65				6	0.998	-81.9	-73.8
1,2-Ethandiol			14.21	13.57		11.43		10.60		4	0.990	-83.2	-79.0
1,3-Propanediol			14.95	14.12	12.85	11.96		11.17	10.85	6	0.984	-79.3	-82.0
1,4-Butandiol						12.25	12.00	11.55	10.93	4	0.993	-67.3	<i>n.d.</i>
2-Butoxyethanol	10.12	9.61		8.57						3	0.999	-38.4	<i>n.d.</i>
1,4-Dinitrobenzene			12.39	11.54	10.87	9.54				4	0.970	-79.5	-64.7
1,2-Dihydroxybenz.						13.19	12.42	11.69		3	1.000	-147.8	<i>n.d.</i>
3-Nitrophenol						13.76		12.86	11.81	3	0.996	-97.8	<i>n.d.</i>
3-Hydroxybenzonitril						13.63	13.06	12.45	11.55	4	0.996	-104.9	-62.8
Hydroxyacetone	11.19	10.67	9.91	9.50	7.98					5	0.930	-58.7	-55.1
Chlorohexadecane		14.11	13.08			10.28				3	1.000	-80.4	-89.0
Chlorooctadecane			14.88	13.88	12.88	11.90		10.68		5	0.995	-92.3	<i>n.d.</i>
Anthracene		13.03	12.13	11.44	10.50					4	0.995	-66.8	-79.6
Phenanthrene		13.06	12.37	11.51	10.84	9.76				5	0.988	-67.4	-79.0
Fluoranthene			14.39	13.74	12.78	11.67		11.01		5	0.989	-78.2	<i>n.d.</i>
Lindane (γ-HCH)		13.35	12.49	11.52		9.49				4	0.995	-81.6	-89.0
Pyrene						11.77	11.34	10.84		3	0.997	-90.1	<i>n.d.</i>

Experimental partition coefficients before and after thermal treatment of Suwannee River FA

The table below shows experimental partition coefficients measured in Suwannee River FA at 20 °C and 98% rh before and after the thermal treatment (heating to 90 °C). The partition coefficients of phenol, p-cresol, pentachlorobenzene, 1-nonanol, 1-undecanol, and acenaphthene measured after the thermal treatment are between 50% and 100% higher compared to the coefficients measured before the treatment. The small highly polar compounds hydroxyacetone, dimethylsuccinate, and 2-ethoxyethanol show, however, comparable or even smaller partition coefficients. An interpretation of this effect is given in the article.

Compound	<i>before thermal treatment (th.t.) 20 °C log(K_{FA,air}/[L/kg_{FA}])</i>	<i>after thermal treatment 20 °C log(K_{FA,air}/[L/kg_{FA}])</i>	ratio K_{FA,air}(after th.t.) / K_{FA,air}(before th.t.)
p-Cresol	5.00	5.31	2.04
1-Nonanol	5.24	5.55	2.03
1-Undecanol	5.94	6.24	2.01
1-Decanol	5.67	5.95	1.92
Acenaphthene	4.80	5.05	1.81
Pentachlorobenzene	4.84	5.04	1.59
Phenol	4.73	4.91	1.51
Dimethylsuccinat	4.49	4.56	1.19
Hydroxyacetone	4.86	4.85	0.97
2-Ethoxyethanol	4.22	4.05	0.69
2,5-Hexanedione	4.67	4.36	0.50

SI-14 Mean absolute deviations compared to aromaticity

The table below shows the calculated mean absolute deviations of the partition coefficients from each NOM compared to the partition coefficients measured in Leonardite HA (for details see article). Figure SI-11 compares these absolute deviations with the aromaticity of the corresponding natural organic materials.

	average deviation	std. deviation	aromaticity [%]	f _{aromaticity}	$\Delta f_{\text{aromaticity}}$	[O/H]
Leonardite HA	0	-	58	0.58	0	8.45
Amherst HA	-0.16	0.31	45	0.45	0.13	8.89
Waskish Peat HA	-0.56	0.33	42	0.42	0.16	9.54
Nordic Lake HA	-0.74	0.31	38	0.38	0.2	10.85
Suwannee River HA	-0.77	0.31	31	0.31	0.27	9.82
Suwannee River NOM	-0.82	0.26	23	0.23	0.35	10.19
Waskish Peat FA	-0.86	0.30	36	0.36	0.22	9.86
Elliott Soil FA	-0.97	0.25	30	0.30	0.28	9.96
Suwannee River FA	-1.06	0.31	24	0.24	0.34	10.07

correlation with the aromaticity (see equation (3) in the article):

$$\log(K_{\text{NOM}}) = \log(K_{\text{Leonardite}}) - 3 \cdot (f_{\text{aromaticity, Leonardite}} - f_{\text{aromaticity, NOM}})$$

$$r^2 = 0.81$$

correlation with the aromaticity and the oxygen/hydrogen ratio [O/H]:

$$\log(K_{\text{NOM}}) = \log(K_{\text{Leonardite}}) - 2.1 \cdot (f_{\text{aromaticity, Leonardite}} - f_{\text{aromaticity, NOM}}) - 0.18 \cdot [\text{O/H}] + 1.52$$

$$r^2 = 0.86$$

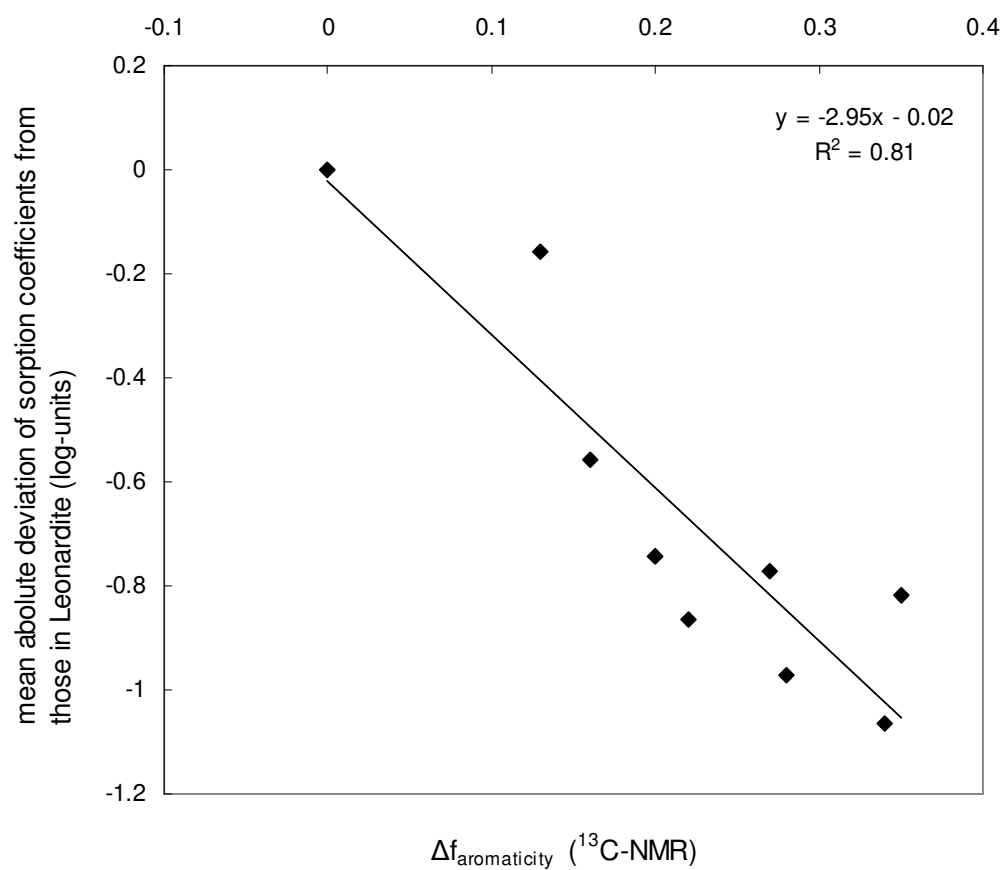


Figure SI-11 Correlation of the aromaticity with the *mean absolute deviations*

Conclusions and Outlook

A dataset containing more than 1000 natural organic matter/air partition coefficients of nonionic organic chemicals measured in 10 different natural organic matters (NOM) at different temperatures and different relative humidities is presented in this work. This dataset is by far the largest, most diverse and most consistent dataset for humic materials published so far. The conclusions that can be drawn from this dataset provide a deeper understanding of the mechanisms involved in the sorption of organic compounds in NOM. Further, this work makes an important contribution to practical applications of sorption coefficients, e.g., for environmental fate modeling of organic compounds. This chapter summarizes the major findings, shows implications for practical applications and identifies areas where future research is needed.

The study on the influence of relative humidity on NOM partitioning provided interesting mechanistical insights into this sorption process; however, the influence of relative humidity is only a secondary effect for practical applications except for small highly polar compounds. The differences in the sorption coefficients between dry and completely hydrated Leonardite HA were only up to a factor of three. Linear sorption isotherms over a wide sorbate concentration range were observed. According to the current consensus on sorption isotherms in humic materials, a nonlinear sorption isotherm goes along with the occurrence of glassy polymeric structures in the humic matrix. However, we did not observe any glass transitions in the range of 5-75 °C that would be relevant with respect to the sorption behavior of hydrated Leonardite HA.

It was found that specific interactions such as electron donor/acceptor interactions (including H-bonds) have a huge influence on the sorption of monopolar (i.e., electron donor or acceptor) and bipolar (i.e., electron donor and acceptor) compounds. This is an important conclusion for the

development of tools that predict NOM partition coefficients: these sorption processes can only be modeled correctly when the sorption process is understood on a mechanistical basis that accounts for the contribution of both specific and nonspecific molecular interactions (see below).

The large experimental data set allowed for a detailed study of the variability in the sorption properties of humic and fulvic acids from both aquatic and terrestrial origins. For a given chemical, the difference in sorption coefficients ranged more than one order of magnitude between NOM from different origins. The difference between any two types of NOM is mainly reflected by a constant shift in the partition coefficients that applies to all compounds in the same way. This indicates that it is the number of available sorption sites per mass of sorbents rather than the types of intermolecular interactions between the sorbate and the sorbent that governs the major differences between the sorption properties of various types of NOM. To find a sound mechanistical interpretation for these findings was not trivial; additional experiments such as temperature-dependent sorption studies in Suwannee River FA had to be conducted. Chapter 4 summarizes the results and provides possible interpretation approaches.

For the set of nine NOM an empirical correlation was found between aromaticity and the relative sorption capacity compared to Leonardite HA. The differences between the sorption characteristics of the different NOM were found to be related to the origin of the material, i.e., terrestrial or aquatic: The terrestrial HA exhibited substantially higher sorption coefficients compared to aquatic HA and FA. In agreement with other authors (4,5), the data in this study show that the commercial Aldrich HA is not an appropriate model for the sorption properties of NOM.

The extensive dataset of 200 experimental Leonardite HA/air partition coefficients allowed for the evaluation and development of predictive models (that have been published elsewhere) for NOM partitioning. This evaluation revealed that none of the regression models based on

partitioning into octanol yields satisfactory fits for polar compounds. In principle, the Karickhoff model ($K_{i\text{oc,air}}=0.41\cdot K_{i\text{octanol,air}}$; (1)) could be used for the prediction of partition coefficients for nonpolar compounds; however, reliable octanol partition data have to be available (see ref (2)). PcKocWIN, a model based on molecular connectivity indices, predicts organic-C/water partition coefficients exclusively from molecular structures. PcKocWIN did not provide reliable and consistent partition coefficients, neither for polar nor for nonpolar compounds. The evaluation of PcKocWIN showed some major shortcomings, such as the lack of a fragment correction term for aromatic hydroxy-groups, which resulted in an overestimation of the sorption of phenols and naphthols. The performance of SPARC, a web-based increment method that predicts thermodynamic data based on molecular structures, was also evaluated. SPARC predicted the experimental Leonardite HA partition coefficients with good accuracy using the molecular structure of Leonardite HA that has been proposed in this study. However, the disadvantage of increment methods such as SPARC and PcKocWIN is that their application domains are limited by their calibration dataset, which is often unknown to the user.

The models presented in the literature so far demand calibrations with experimental partition data and, for good accuracy, experimental compound descriptors. In contrast, the quantum-chemical model COSMOtherm predicts partition coefficients in various systems without calibration with experimental partition data. It only requires the 3-dimensional (3D) structures of the sorbates and the sorbent phase as its input. COSMOtherm predicted the experimental Leonardite HA partition coefficients within a factor of 3 to 5 using the suggested 3D structure of Leonardite HA. COSMOtherm may become a very promising tool for predicting the NOM sorption of compounds for which the molecular structure is the only reliable information available, such as compounds that have not yet been synthesized. Because of its fundamental nature COSMOtherm should be able to accurately predict partition coefficients for more complex compounds than tested in this study.

The best predictions of measured sorption coefficients in Leonardite HA was achieved with a polyparameter linear free energy relationship (pp-LFER) that explicitly accounts for cavity formation, nonspecific (vdW interactions) and specific (electron donor/acceptor interactions including H-bonds) interactions between the sorbate and the sorbent phase. This model predicted the 160 experimental Leonardite HA/air partition coefficients ranging over seven orders of magnitude within a factor of two.

No systematic approach has yet been developed to model the variability in the sorption properties of NOM besides a few studies that mainly focused on one single compound, e.g., pyrene in the study of Kopinke et al. (3). As mentioned above, the present study found that NOM vary mainly in their sorption capacities, i.e., the sorption variability can be explained by one single parameter that accounts for the sorption capacity. Therefore, the octanol and the PckocWIN model could principally be recalibrated for each NOM using the experimental data presented here. However, the same shortcomings discussed above would restrict the use of these newly calibrated models. The pp-LFER model evaluated with the large experimental dataset for Leonardite HA was successfully applied to all other NOM. The resulting ten pp-LFER equations currently present the most accurate way to account for the influence of the natural variability of NOM in chemical fate modeling. How the COSMOtherm model performs for other NOM is the focus of ongoing research.

Some important questions are still open. (a) In natural systems HA and FA often occur as coatings on various mineral surfaces. The influence of various minerals, e.g., Fe_2O_3 , Al_2O_3 , or SiO_2 , on the sorption capacity of humic materials has not yet been investigated. In the literature substantial differences in the sorption capacities of SOM coated on mineral surfaces compared to uncoated SOM are reported (6-8); (b) the influence of the pH, ionic strength and ionic composition on the partition process has not yet been systematically investigated; (c) almost no information is available on the sorption properties of humin; (d) there is

still not much known about the black carbon content of soils and sediments and its influence on sorption.

Nevertheless, despite these uncertainties, it is likely that the variability in the sorption properties of NOM from different origins is the most important error source in the prediction of sorption processes in NOM. Therefore, based on the knowledge gained in this study, a few recommendations for the practical handling of NOM sorption processes can be given: (a) if the aromaticity of the considered NOM is known then predictions should be conducted with the pp-LFER of that NOM that comes closest in aromaticity (Table 2 Chapter 4); alternatively, sorption data can be estimated in a NOM of interest using Equation 3 Chapter 4 and experimental partition coefficients measured in Leonardite HA or predicted partition coefficients with the pp-LFER fitted for Leonardite HA; (b) if a distinction between HA and FA can be made then Table 2 Chapter 4 also allows to choose a predictive equation for a similar material; (c) if no further characterization of the considered NOM is possible then the use of the pp-LFER equations for all HA and FA can at least serve to predict a range of values that can be represented by a mean value with a realistic standard deviation. It is important to note that this standard deviation (which will lie in the range of 0.3-0.6 log units) is not due to uncertainties in the prediction but it reflects the natural variability in NOM; (d) for sorption processes involving dissolved organic matter in aquatic systems, it is in principle possible to use only the equations for those materials. However, for sediment organic carbon or aquatic DOC that is dominated by scavenged NOM from agricultural soils again the use of all nine equations is recommended.

Although the experimental data and models in this study focus on NOM/gas phase partitioning, the NOM/water partitioning coefficients can be estimated by using the air/water partition coefficients. This expands the applicability of the results of this study because NOM/water sorption processes are of equal or even higher importance, e.g., sorption processes in water-saturated soils. Although the influences of factors such as pH, ionic strength, and ionic composition have not yet been investigated, several comparisons with NOM/water partition coefficients

indicate that partition coefficients calculated from the gas phase are precise enough for practical applications. This also suggests that such factors might be of minor importance for the sorption process.

Future Research

The investigation of the influence of various minerals, e.g., Fe_2O_3 , Al_2O_3 , or SiO_2 , on the sorption capacity of humic materials should be conducted. Preliminary experiments show that some minerals (e.g., Al_2O_3) have a significant impact. Compounds of actual environmental concern such as pharmaceuticals or pesticides are often acids or bases and hence the ionic form may dominate at ambient pH-values. Partition coefficients of ionic species are, however, not measurable using the presented methodology which involve the use of inverse gas chromatography. To measure partition coefficients from the aqueous phase an evaluation of a HPLC (high pressure liquid chromatography) system using NOM coated on a chromosorb support has been performed during this study (data not shown). The results are very promising and show that the thermodynamic cycle is indeed applicable in the NOM/water/air system. The combination of the used IGC system with such an HPLC system could provide a powerful tool to efficiently measure NOM partition coefficients of almost all nonionic as well as ionic organic compounds. Partition coefficients determined in the aqueous phase (e.g., very polar compounds) could be transferred to the gas phase using the air/water partition coefficients and vice versa. This HPLC system would also provide the possibility to study the influence of the pH, ionic strength, and ionic composition on sorption processes.

Pharmaceuticals, pesticides, and other compounds of environmental concern often exhibit one or several functional groups that may not interact independently from each other. Such complex compounds are challenging for predictive models such as those discussed in this study. Future work should focus on the measurement of polyfunctional compounds in order to understand the contribution of non-independently interacting groups to the overall sorption of the compound. The modeling of such complex compounds using the models

discussed in this study, i.e., pp-LFER, PcKocWIN, SPARC, and COSMOtherm, will reveal which of these models can successfully deal with such complex compounds.

References

- (1) Karickhoff, S. W. Semi-empirical estimation of sorption of hydrophobic pollutants on natural sediments and soils *Chemosphere* **1981**, *10*, 833-846.
- (2) Pontolillo, J., Eganhouse, R.P. "The search for reliable aqueous solubility (Sw) and octanol-water partitioning coefficient (Kow) data for hydrophobic organic compounds: DDT and DDE as a case study," U.S. Geological Survey, 2001.
- (3) Kopinke, F. D., Georgi, A., Mackenzie, K. Sorption of pyrene to dissolved humic substances and related model polymers. 1. Structure-property correlation *Environ. Sci. Technol.* **2001**, *35*, 2536-2542.
- (4) Malcolm, R. L., MacCarthy, P. Limitations in the use of commercial humic acids in water and soil research *Environ. Sci. Technol.* **1986**, *20*, 904-911.
- (5) Raber, B., Kögel-Knabner, I., Stein, C., Klem, D. Partitioning of polycyclic aromatic hydrocarbons to dissolved organic matter from different soils *Chemosphere* **1998**, *36*, 79-97.
- (6) Feng, X., Simpson, A.J., Simpson, M.J. Investigating the role of mineral-bound humic acid in phenanthrene sorption *Environ. Sci. Technol.* **2006**, *40*, 3260-3266.
- (7) Wang, K., Xing, B. Structural and sorption characteristics of adsorbed humic acid on clay minerals *J. Environ. Qual.* **2005**, *34*, 342-349.
- (8) Wang, K., Xing, B. Chemical extractions affect the structure and phenanthrene sorption of soil humin *Environ. Sci. Technol.* **2005**, *39*, 8333-8340.

Curriculum Vitae

Personal Data

Name Christian Niederer
Address Pflugstrasse 5, 8006 Zurich, Switzerland
e-mail cniederer@gmx.ch; christian.niederer@alumni.ethz.ch
Phone +41 79 7428344
Date of birth June 19, 1976; Swiss Citizen

Education and Studies

2003 until now Ph.D. Student at the Institute of Biogeochemistry and
Pollutant Dynamics, ETH Zurich
1997-2002 Studies in Environmental Sciences, Swiss Federal
Institute of Technology, ETH Zurich
Degree: Diploma (Master) in Environmental Natural
Sciences ETH
Major: Environmental Chemistry and Microbiology
Minor: Aquatic Systems
Diploma Thesis: *Toxicological Effects and Modes of Toxic
Actions of Reactive Chemicals with Chlorine and Epoxy
Functions in Green Algae*

Conferences and Presentations

2006 Meeting of the Intern. Humic Substances Society,
Karlsruhe, Germany (Keynote Speaker)
2006 World Congress of Soil Science, Philadelphia,
USA (Speaker)
2006 Gordon Research Conference: Water, NH, USA (Poster)
2005 IUSS Symposium: Advances of Molecular Modeling –
Perspectives for Soil Research, Vienna, Austria
(Speaker)
2004 Europ. Congress of Soil Sci., Freiburg, Germany
(Speaker)
2003 SETAC Meeting, Hamburg, Germany (Poster)

Professional Experience

- 2003/2004 Lecture Assistant „Environmental Organic Chemistry“,
ETH Zurich
- 11/2002-01/2003 Scientific Co-worker Dept. Microbiology and Molecular
Ecotoxicology at the Swiss Federal Institute of Aquatic
Sciences, EAWAG
- 2002/2003 Project Co-worker at the Academic Occupational
Counseling, Berne, Switzerland
- 10/2000-03/2001 Internship at the Credit Suisse Financial Services,
Environmental Risk Management (Industrial Sites)
-

Publications

Niederer, C., Schwarzenbach, R.P., Goss, K.-U. Variations in the Sorption Properties of Nine Humic and Fulvic Acids from Different Origins. *Environ. Sci. Technol.* Submitted May 2007.

Niederer, C., Goss, K.-U. Quantum-Chemical Modeling of Humic Acid/Air Equilibrium Partitioning of Organic Vapors. *Environ. Sci. Technol.* **2007**, 41, 3646-3652.

Arp, H.P., Niederer, C., Goss, K.-U. Predicting the Partition Behavior of Various Highly Fluorinated Compounds. *Environ. Sci. Technol.* **2006**, 40, 7298-7304.

Niederer, C., Goss, K.-U., Schwarzenbach, R.P. Sorption Equilibrium of a Wide Spectrum of Organic Vapors in Leonardite Humic Acid: Modeling of Experimental Data. *Environ. Sci. Technol.* **2006**, 40, 5374-5379.

Niederer, C., Goss, K.-U., Schwarzenbach, R.P. Sorption Equilibrium of a Wide Spectrum of Organic Vapors in Leonardite Humic Acid: Experimental Setup and Experimental Data. *Environ. Sci. Technol.* **2006**, 40, 5368-5373.

Niederer, C., Behra, R., Harder, A., Schwarzenbach, R.P., Escher, B.I. Mechanistic Approaches for Evaluating the Toxicity of Reactive Organochlorides and Epoxides in Green Algae. *Environ. Toxicol. Chem.* **2004**, 23, 697-704.
